DISSERTATION

BREAKING THE MF CURSE: THE REGULATORY ROLE OF THE METHYL FARNESOATE – MEKRE93 PATHWAY IN CRUSTACEAN MOLTING

Submitted by

Vanessa Leah Bentley

Department of Biology

In partial fulfillment of the requirements

For the Degree of Doctor of Philosophy

Colorado State University

Fort Collins, Colorado

Spring 2025

Doctoral Committee:

Advisor: Donald L. Mykles

Deborah M. Garrity
Taiowa Montgomery
Noreen Reist

ABSTRACT

BREAKING THE MF CURSE: THE REGULATORY ROLE OF THE METHYL FARNESOATE – MEKRE93 PATHWAY IN CRUSTACEAN MOLTING

Ecdysis, or the active shedding of the exoskeleton, is critical for arthropod growth, development, and/or regeneration of lost or damaged appendages. The antagonistic interaction between the steroid hormone 20-hydroxyecdysone (20-E) and the sesquiterpenoid juvenile hormone (JH) control insect molting and development, respectively. On the other hand, crustacean molting is primarily regulated through the endocrine crosstalk between 20-E and the neuropeptide molt-inhibiting hormone (MIH). MIH secretion by the X-organ, sinus gland complex (XO) inhibits Y-organ (YO) synthesis of 20-E. Molting is initiated by the decrease in MIH titers thereby allowing increasing 20-E concentrations in the hemolymph. The molting process is divided into different stages where the YO exhibits different phenotypic states: intermolt (IM)– basal, early premolt (EP)– activated, mid premolt (MP)– committed, late premolt (LP)– committed/repressed, ecdysis (E)– repressed, and postmolt (PM)– repressed/basal. The mechanistic target of rapamycin (mTOR) and transforming growth factor beta (TGF-β) signaling leads to YO activation and commitment, respectively. However, the YO transition to- and from- the repressed state is unknown.

Methyl farnesoate (MF), commonly referred to as the crustacean JH, is produced by the mandibular organ (MO) and is suppressed by the mandibular organ-inhibiting hormone (MOIH). MF regulates several physiological processes in crustaceans including metamorphosis, development, reproduction, morphogenesis, and molting; however, the underlying mechanism

remains unknown and thereby is considered to be “cursed”. The differential effects MF has on molting and ecdysteroidogenesis is hypothesized to be regulated through the Methoprene tolerant– Krüppel homolog 1– E93 (MEKRE93) transcriptional cascade.

Using bioinformatic approaches, the components of the MF signaling pathway were identified in the European green shore crab (*Carcinus maenas*) and the blackback land crab (*Gecarcinus lateralis*) YO transcriptomes, including the MF/JH receptor *Methoprene tolerant* (*Met*), the zinc finger transcription factor *Krüppel homolog 1* (*Kr-h1*), *Ecdysone response gene 93* (*E93*), *Steroid receptor coactivator* (*Src*), and transcription comediators *CREB–binding protein* (*CBP*) and *C-terminal–binding protein* (*CtBP*). Additionally, genes encoding for the MF synthetic pathway enzymes were also identified in the YO transcriptomes including *3-hydroxy-3-methylglutaryl-CoA reductase* (*HMGR*), *farnesoic acid O-methyltransferase* (*FAMeT*), and *FAMeT2*. Additionally, a *FAMeT2* transcript was also identified in the YO and contains an unconventional domain organization compared to annotated *FAMeT*. Nonetheless, phylogenetic analysis of each gene was overall highly conserved across pancrustaceans (and occaisionally panarthropodans).

Furthermore, *in vitro* assays showed that *C. maenas* and *G. lateralis* YOs were responsive to JH-mimics (e.g. pyriproxyfen, fenoxycarb, methoprene, and hydroprene), but not to MF. Taken altogether, these data suggest that the YO can respond to MF and may have its own MF-innate system serving as an autocrine factor to regulate the YO by acting through a MEKRE93 transcriptional network that can be mediated by coregulators.

ACKNOWLEDGEMENTS

First and foremost, I want to give my greatest thanks to my advisor Dr. Donald Mykles for providing me the opportunity to be part of his lab and pursue my passion of research. Thank you for your kindness and patience throughout the years; I am incredibly grateful for your support and understanding especially with everything thrown my way. I would also like to thank my committee Dr. Deborah Garrity, Dr. Tai Montgomery, and Dr. Noreen Reist for their time, support, and advice. I appreciate you all for your dedicated support pushing me to be a better scientist.

Additionally, thank you to past and present crab lab members especially Dr. Mihika Kozma, Dr. Jorge Pérez-Moreno, Talia Head, and Austin Ellingworth for their help. I want to thank all my CSU undergraduate mentees for motivating me to be the best mentor I can be along with assisting me with things around the lab. I want to thank Dr. Julie Adams, Dr. Carrie Milne-Zelman, and Dr. Sharon Miller for introducing me to the possibilities behind research from being part of a snake behavior project, to spending a day at turtle camp, and working with biomimetic materials. You have inspired me to embrace the concept research is not "weird" which ultimately was the start of my journey. Furthermore, thank you to my friends and colleagues I have met in Fargo at North Dakota State University (NDSU) and the USDA especially Dr. Bryan Helm, Dr. Kendra Greenlee, Dr. Julia Bowsher, Dr. Liz Kopco for your support, training, and mentoring inside and outside of the lab.

Additionally, I want to thank my family and friends for the constant encouragement, belief, faith, and prayers that have kept me going throughout the years regardless of time and distance. Thank you to my family who taught me since I was a little girl to always work hard for

what you want and persevere amid any situation even at times it may require a sacrifice. Although, I may not have been the person you all thought I would be, I hope I made you all proud on becoming a doctor and that my stubbornness served a purpose. I also want to thank my friends (including my gym family), for being there for me during my many breakdowns and giving me hope especially Zachary McCoy, Chase Tocco, Shawn Kalam, and Dr. Josh Malinis. You have never stopped pushing me to be better, strive for more, and stay hard. There are no words to truly express my gratitude for all the encouragement throughout the years from everyone; thank you!

Lastly, I want to acknowledge the National Science Foundation (NSF) for the funding that allowed me to conduct my experiments (IOS 1922701 and IOS 1922755) along with the travel support allowing me to go to Bodega Marine Lab to expand my investigation. Thank you all for being part of my journey and endeavors!

DEDICATION

To the people who have encouraged me to never give up and supported my “whole lot of hustle and ambition” mentality.

“You are capable of more than you know. Choose a goal that seems right for you and strive to be the best, however hard the path. Aim high. Behave honorably. Prepare to be alone at times, and to endure failure. Persist! The world needs all you can give.”
-E. O. Wilson

DEFINITION OF TERMS

Term	Definition
20-E	The most active form of ecdysteroid functioning as the molting hormone for insects and crustaceans. This steroid hormone is derived from a cholesterol precursor after undergoing a series of hydroxylation events by cytochrome p450 enzymes encoded by the Halloween genes.
bHLH-PAS	Proteins with a highly conserved 5' N-terminus consisting of the DNA-binding domain (basic helix-loop-helix or bHLH) followed by two Period- Aryl hydrocarbon receptor nuclear translocator- Single minded (Per-ARNT-Sim or PAS) domains (A and B respectively). The PAS-A domain ensures correct target gene activation by selecting the proper dimerization partner and is poorly linked to the PAS-B domain. The PAS-B domain, or the ligand binding domain is followed by a long, intrinsically disordered 3' C-terminus. The disordered region thereby allows these proteins to be dynamic in conformation upon ligand binding, thus ultimately affecting protein activity, interactions, and localization.
Br-C	Broad Complex is a transcription factor with several isoforms due to alternative splicing among duplicated exons each with one zinc finger (Zf) DNA-binding domain (Z1, Z2, Z3, or Z4). This early ecdysone response gene mediates ecdysone action essential for insect metamorphosis.
C2H2	A zinc finger (Znf) protein, generally associated with activation, that have two histidines (His) on the C-terminus of the α- helix and two cysteines (Cys) located on the β-strand which allow a zinc atom (Zn^{2+}) to bind. The binding of the Zn^{2+} with the Cys and His residues allow a tetrahedral structure contributing to the ability to bind to longer DNA sequences (~20-40 base pairs).
CA	The corpora allata is a pair of insect endocrine glands connected to the brain, located behind the corpora cardiaca (CC), that synthesize juvenile hormone (JH).
CC	The corpora cardiaca is a pair of insect neurohaemal organs that produce prothoracicotropic hormone (PTTH).
CBP	CREB (cAMP response element-binding protein)-binding protein is a transcriptional co-regulator with histone acetyl transferase (HAT) activity that affects gene expression by through different interactions with transcription machinery and DNA-binding proteins.

CHH	Crustacean hyperglycemic hormone is a family of neuropeptide hormones, such as molt-inhibiting hormone (MIH), mandibular organ-inhibiting hormone (MOIH), and gonad-inhibiting hormone (GIH). That regulate many crustacean physiological processes including metabolism, molting and reproduction.
E93	Ecdysone inducible protein (Eip93) or response gene 93 is a sequence specific, temporal transcription factor belonging to the helix-turn-helix, pipsqueak (HTH-Psq) class. Evidence suggests this ecdysone response gene, is repressed by expression of Krüppel homolog-1 (Kr-h1) despite being originally known for apoptosis in *Drosophila melanogaster.* It is hypothesized that E93 evolved from the mushroom body large-type Kenyon cell protein-1 (Mblk-1) considering its shared high homology.
EP	Early premolt, also referred to as D_0, is part of the crustacean molt cycle where the Y-organs (YO) are in an activated state due to the absence of molt inhibiting hormone (MIH). The absence of MIH allows hemolymph ecdysteroid titers to increase as it acts in a positive feedback manner through the mTOR pathway. During this stage, calcium is stored in gastroliths and/or in the hepatopancreas, the claw muscle atrophies, and the secondary limb regenerates grow (R-index= 12-16) . Throughout this stage the YO has MIH sensitivity but eventually loses this ability to delay molting at the "point of no return" before transitioning to mid premolt (MP).
FAMeT	Farnesoic acid O-methyl transferase is the enzyme responsible for methyl farnesoate (MF) synthesis from farnesoic acid (FA).
HMGR	3-hydroxy-3-methylglutaryl-coenzyme A reductase is a nicotinamide adenine dinucleotide phosphate (NADPH) and dithiothretitol/glutathione dependent microsomal enzyme that is the rate limiting step in the mevalonate pathway.
Hsp (83/90)	Heat shock proteins are a type of chaperone protein that regulates the cell cycle and signal transduction through managing specific target proteins and promoting cell maturation. This protein has been implicated in the nuclear import of Methoprene tolerant (Met) to regulate juvenile hormone (JH) signaling.
HTH-Psq	Helix-turn-helix, pipsqueak proteins is a transcription factor class within the larger helix-turn-helix (HTH) protein family which have two helices connected by a short loop. This transcription factor has a pipsqueak domain (Psq) consisting of four tandem repeats consisting of ~50 amino acids.
IM	The stage (also referred to as C_4) of the crustacean molt cycle where the Y-organ (YO) is in a basal state due to the presence of molt inhibiting hormone (MIH) and ecdysteroid titers in the hemolyph are low. During this stage, the animal has a fully formed, calcified exoskeleton and stores organic reserves in the hepatopancreas. Basal regenerates form at the autotomized limbs (R-index= 8-10).

JH	A group of acyclic sesquiterpenoid hormones produced by the corpora allata (CA), initially discovered by V. B. Wigglesworth, that regulate several insect physiological processes including reproduction and development. JH-III is the inhibitory hormone that inhibits insect metamorphosis/morphogenesis which bind to the Methoprene tolerant (Met) receptor.
JHAMT	Juvenile hormone acid methyltransferase is the enzyme responsible in juvenile hormone (JH) synthesis by transferring a methyl group to the carboxyl group of juvenile hormone acid or farnesoic acid (FA).
JHE	A juvenile hormone (JH) degradatory carboxylesterase, secreted in the hemolymph, that hydrolyzes the methyl ester of JH resulting in JH acid.
JHEH	Juvenile hormone epoxide hydrolase is a non-secretory, microsomal epoxide hydrolase (enzyme) responsible for catalyzing juvenile hormone (JH) degradation through hydrolysis of the epoxide ring thus resulting in the production of JH diol.
Kr-h1	Krüppel homolog 1 is a C2H2 zinc finger (Cys2-His2) transcription factor and a member of the Krüppel Like Family (KLF) containing many zinc finger (ZnF) motifs; insects have eight Znf motifs while crustaceans have seven. This transcription factor, sometimes referred to as the guardian of the juvenile status, is primarily associated with being the transducer of anti-metamorphic action in insects along with pancrustacean vitellogenesis. Kr-h1 works downstream of Methoprene tolerant (Met) and been shown to be strongly induced by juvenile hormone (JH) through the Met–Steroid receptor coactivator (Src) complex.
LP	Late premolt (or $D_{2\text{-}4}$) is the stage in the crustacean molt cycle where the Y-organs (YO) are still in the committed state and limb regenerates reach the maximum growth (R-index= ~24). Hemolymph ecdysteroid titers are high which peak in D_3 and subsequently decrease leading to ecdysis. Astaxanthin is reabsorbed from the exocuticle while the epicuticle and exocuticle are synthesized.
Mblk-1	Mushroom body large-type Kenyon cell protein-1 is the hypothesized ortholog to *Drosophila melanogaster* ecdysone response gene 93 (E93) that was initially isolated from mushroom bodies in the honeybee (*Apis mellifera*).
MEKRE93	The transcriptional cascade through the interaction of Methoprene tolerant (Met), Krüppel homolog-1 (Kr-h1), and ecdysone response gene 93 (E93) which regulates the ecdysteroid synthesis and ultimately insect metamorphosis.
Met	Methoprene tolerant (Met) is a basic helix-loop-helix, Period- Aryl hydrocarbon nuclear translocator- Single minded (Per- ARNT- Sim) or bHLH-PAS transcription factor that acts as the juvenile hormone (JH) and methyl farnesoate (MF) receptor.

MF	Methyl farnesoate is a sesquiterpenoid hormone synthesized by the crustacean mandibular organ (MO). Although this hormone is not fully understood it has been implicated in several physiological processes including reproduction, metamorphosis, and molting. This hormone is sometimes referred to as the crustacean juvenile hormone (JH) as it is the unepoxidated form of insect JH that binds to JH receptor Methoprene tolerant (Met).
MIH	Molt-inhibiting hormone is a neuropeptide produced by the X-organ, sinus gland complex (XO) that represses the Y-organ (YO) from synthesizing ecdysteroids.
MO	The mandibular organ is a pair of highly vascularized crustacean glands, located at the base of the mandibular tendon, that produce methyl farnesoate (MF). These glands are said to be "cursed" as the role they play in crustacean biology is not well established.
MOIH	Mandibular organ-inhibiting hormone is a neuropeptide produced by the X-organ, sinus gland complex (XO) that represses the mandibular organ (MO) from synthesizing methyl farnesoate (MF).
MP	Mid premolt (also referred to as D_1) is the stage of the crustacean molt cycle where the Y-organ (YO) transitions to a committed state through the TGF-β pathway. As hemolymph ecdysteroid titers continue to rise and the limb regenerates grow (R-index= 16-24), the YOs lose molt inhibiting hormone (MIH) sensitivity. The epidermis separates from the exoskeleton (apolysis) and the exoskeleton (beginning with the membranous layer) is degraded.
mTOR	The mechanistic target of rapamycin is signaling pathway part of the phosphatidylinositol 3-kinase (PI3K) network that is involved in growth and metabolism including Y-organ (YO) activation.
PG	The prothoracic glands are a pair of insect endocrine glands, ventrally located in the prothorax, that synthesize ecdysteroids– hormones playing various roles in several physiological functions including molting, metamorphosis, and reproduction.
PM	Post molt (also referred to as A, B, C_{1-3}) is the stage of the crustacean molt cycle where hemolymph ecdysteroid titers are extremely low and the Y-organs (YO) are in a repressed state. During this time the regenerates extend, and the animal continues to swallow air or water allowing the exoskeleton to expand. The endocuticle is synthesized, the membranous layer is formed, and eventually the endocuticle is calcified.
PTTH	Prothoracicotropic hormone is an insect hormone produced by the corpora cardiaca (CC) that is secreted after juvenile hormone (JH) is degraded. This hormone must be present to stimulate the prothoracic gland (PG) to produce ecdysteroids.
R-index	The R-index, or R-value, is ann external measurement of the regenerating limbs used to track the progress of proecdysial events; R-index= (length of limb regenerate in mm × 100)/carapace width in mm.

Src	Steroid receptor coactivator is a transcriptional co-regulator that acts part of the juvenile hormone (JH) and /or methyl farnesoate (MF) receptor complex with Methoprene tolerant (Met). This coregulator has a strongly association with steroid hormones as they transactivate the transcriptional potency of steroid hormone receptors.
TGF-β	Transforming growth factor-beta is a signaling pathway that acts upon phosphorylation of SMADS thereby regulating cell proliferation and differentiation including Y-organ (YO) commitment.
XO	The X-organ is the neurosecretory center located in the crustaceans' eyestalks where molt inhibiting hormone (MIH), mandibular organ inhibiting hormone (MOIH), crustacean hyperglycemic hormones (CHH), and other neuropeptide hormones are produced. XO in the present study implies to the XO-SG complex as the XO is part of the medulla terminalis and projects to the sinus gland (SG), a neurohemal organ.
YO	The Y-organ is a pair of crustacean glands, located in the anterior end of the cephalothorax in crabs and lobsters, that produce ecdysteroids. These glands are sometimes referred to as the crustacean molting organ as the function is analogous to the insect prothoracic gland (PG).

TABLE OF CONTENTS

CHAPTER 1

A MOLECULAR PERSPECTIVE ON THE REGULATION OF PANCRUSTAEAN MOLTING PHYSIOLOGY

Introduction

Having evolved over 485-541 million years ago during the Cambrian Period, arthropods are still the most diverse animal phyla today (Giribet and Edgecombe, 2019). Part of arthropods' success can be attributed to the chitin-based exoskeleton that is occasionally reinforced with calcium carbonate ($CaCO_3$). Although the exoskeleton aids in protection against external elements, predators and desiccation, being equipped with this rigid support system ultimately restricts growth, development, and/or regeneration. Therefore, to overcome this obstacle arthropods must shed the old exoskeleton through an event known as ecdysis. Ecdysis is energetically expensive, thus requiring arthropods to prepare for *and* recover from the exuviation. Consequently, the emergence leaves the animals in a temporary vulnerable state as the new exoskeleton is not fully formed. Continued synthesis and hardening of the exoskeleton during postmolt involves cross-linking of chitin polymers and in crustaceans, deposition of $CaCO_3$ (Roer and Dillaman, 1984; Abehsera et al., 2021; Mykles, 2024; Roer et al., 2024).

The entire process, including the preparation before and recovery after ecdysis, is known as molting. Molting is initiated by the continual increase of ecdysteroids, sterol-derived hormones, in the hemolymph. Therefore, molting—including ecdysteroid synthesis, metabolism, and regulation— must be highly regulated and synchronized to ensure this physiological process is not compromised, which could ultimately affect the animals' fitness. Through scientific and technological innovations, the incorporation of an 'omics perspective, along with the integration

of genetic and biochemical approaches, researching and enhancing the knowledge surrounding molting physiology are made feasible and greatly improved (Sagi et al., 2013; Ventura et al., 2018; Torson et al., 2020).

The Three E's– evolutionary, ecological, and economic impacts and significance

When it comes to molting physiology, the majority of the knowledge stems from a developmental and evolutionary context of the insect metamorphic molt in both hemimetabolous and holometabolous species (Belles, 2019; Jindra, 2019; Truman, 2019; Martín et al., 2021). Understanding the transition between the developmental stages in insects has been a topic of particular interest as it may be a way to control pests and/or manage vectors of human diseases (Gilbert et al., 2001; Minakuchi and Riddiford, 2006; Noriega and Nouzova, 2020). Although the information regarding the insect metamorphic molt is substantial, there is considerably less information regarding crustacean molting outside of a metamorphic context. Nonetheless, the investigation of understanding this conserved, yet plastic, process must progress and extend to their crustacean relatives— important organisms in evolutionary, ecological, and economic disciplines (Miura, 2019; Wolfe et al., 2019).

Evolutionary

Ecdysozoans (e.g. nematodes, tardigrades, onychophorans, and arthropods), as signified within their name, are invertebrates united by undergoing ecdysis. With regards to endocrine and genetic similarities, molting is viewed as an autapomorphy and thus would presumably be considered a highly conserved process. However, as research progresses and more evidence is discovered, the molting machinery appears to be plastic even within lower taxonomic ranks. For

instance, within Clade Pancrustacea, insects have a terminal molt upon reaching adulthood. By contrast, crustaceans not only undergo a metamorphic molt, but continue to molt as adults, enabling them to grow to larger sizes. Moreover, molting amongst Phylum Arthropoda is triggered by an increase of hemolymph ecdysteroid (or molting hormone) titers; however different versions of ecdysteroids are utilized for various individuals and in multiple physiological processes (e.g. metabolic, reproductive, and development). For example, Subphylum Chelicerata members primarily utilize ponasterone-A (25-deoxy-20E) whereas those in Subphylum Mandibulata (e.g. myriapods and pancrustaceans) primarily use 20-hydroxyecdysone (20-E) (Qu et al., 2015). It is hypothesized that chelicerate use of 25-deoxy-20-E is the result of the absence of *phantom* (*phm*), a cytochrome P450 family gene responsible for a hydroxylation of 5β-ketodiol to 5β-ketotriol (Mykles, 2011; Schumann et al., 2018). Evidence suggests that the genes that encode for cytochrome P450 enzymes (Halloween genes), the ecdysone receptor complex, and ecdysone signaling genes evolved stepwise across Clade Panarthropoda (Qu et al., 2015; Schumann et al., 2018).

Furthermore, the ecdysone pathway can be mediated in different ways including the interaction of other endocrine pathways such as by sesquiterpenoids. Sesquiterpenoids, a group of terpenes with three isoprene units, are biosynthesized through the mevalonate (MVA) pathway through the conversion of acetyl coenzyme A (acetyl-CoA) into mevalonate to then be transformed into farnesoic acid (FA), the byproduct used to biosynthesize juvenile hormone (JH) and methyl farnesoate (MF) (Bellés et al., 2005). The FA biosynthetic pathway is conserved overall; however, underlying mechanism and pathway afterwards is diverse, as the recruitment of specific enzymes result to different products (Tsang et al., 2020; So et al., 2022). For example, in insects, ecdysteroid secretion is stimulated by the absence juvenile hormone III (JH III), a

sesquiterpenoid produced as the result of juvenile hormone acid methyltransferase (JHAMT) and/or the P450 epoxidase CYP15 (Shinoda and Itoyama, 2003; Defelipe et al., 2011; Tsang et al., 2020; Tian et al., 2021; Orchard and Lange, 2024a). On the other hand, crustacean 20-E production is primarily prevented by the presence of molt-inhibiting hormone (MIH), a neuropeptide (Bliss and Welsh, 1952; Bliss et al., 1954; Techa and Chung, 2015). Nonetheless, methyl farnesoate (MF) has been identified and demonstrated to affect ecdysteroid synthesis and regulate other physiological functions in other arthropods, including crustaceans, myriapods, and chelicerates (Qu et al., 2015; Miura, 2019; Nicewicz et al., 2021). MF, nicknamed the crustacean juvenile hormone, is the unepoxidated form of JH III because of farnesoic acid *O*-methyltransferase (FAMeT) activity (Homola and Chang, 1997c). JH epoxidation is hypothesized to be an insect reproductive innovation; however, new data suggest that the evolution of sesquiterpenoid synthesis is more complex, as JH and/or MF signaling and synthetic genes have been identified in non-insect species (Hui et al., 2010; Xie et al., 2016a; Tsang et al., 2020; Nicewicz et al., 2021; Nouzova et al., 2021; So et al., 2022). Gaining perspectives on crustacean molting and regulation of ecdysteroidogenesis provide insight into the evolution underlying this physiological process, including the ecdysone and sesquiterpenoid pathways, that contributed to arthropod success (Tobe and Bendena, 1999; Cheong et al., 2015). A better understanding of the endocrine and neuromodulatory mechanisms driving and regulating ecdysis would result in new insights of molting physiology from behavioral, morphological, and evolutionary perspectives, while contributing evidence to sort out evolutionary relationships within Clade Panarthropoda and across ecdysozoans (Wolfe et al., 2019; Sullivan et al., 2022; Bernot et al., 2023).

Ecological

Measuring the ecological quality of an area links the environmental state to disturbed response(s), which then can be further applied to predict the effects on other organisms. Many insects act as bioindicators that assist with biomonitoring of an ecosystem; and nonetheless, crustaceans serve as bioindicators in aquatic systems (Rodríguez et al., 2007; Rodríguez, 2024). *Daphnia*, an aquatic crustacean with a critical role in aquatic food chains, is generally incorporated into ecotoxicological studies due to their high sensitivity to chemicals (e.g. endocrine disruptors and pesticides) (Ahmed, 2023). For example, bisphenol analogues and polystyrene beads disrupt ecdysteroid and JH signaling pathways that consequently lead to negative effects on reproduction in the brackish water flea (*Diaphanosoma celebensis*) (Cho et al., 2022). Polystyrene nanoplastics also are implicated in inducing oxidative stress in the Oriental river prawn (*Macrobrachium nipponense*) (Fan et al., 2022). Endocrine pathways regulate crustacean molting and thus are impacted by various compounds, such as antidepressants and opioids (LeBlanc, 2007; Mazurová et al., 2008; Hosamani et al., 2017; Knigge et al., 2021; Knigge, 2024). Perturbed endocrine systems, including ecdysteroid and sesquiterpenoid signaling, can impact the animals' fitness and cause further downstream affects as these hormones have various physiological roles.

Monitoring growth and molting can also determine an organisms' status, as it can be affected by abiotic and biotic factors, such as ocean acidification (Berger et al., 2021; McElhany and Busch, 2024; Thangal et al., 2024). A decrease in the seawater pH inhibits molting rate and frequency in the red king crab (*Paralithodes camtschaticus*), the giant mud crab (*Scylla serrata*), and the white spot wrist hermit crab (*Pagurus criniticornis*) (Long et al., 2019; Turra et al., 2020; Thangal et al., 2022). As a direct result of ocean acidification, $CaCO_3$ levels are reduced, which,

in turn, compromise postmolt by disrupting the synthesis and calcification of the exoskeleton in the blue crab (*Callinectes sapidus*) and the Dungeness crab (*Metacarcinus magister*) (Glandon et al., 2018; Bednaršek et al., 2020). Compromised molt rate, molt frequency, and exoskeleton integrity makes the animals more vulnerable to disease and predators. Interestingly, juvenile Dungeness crabs were smaller in size, but exhibited a higher survival in response to increased carbon dioxide levels (CO_2), suggesting that some species experience differential effects as a result of distinct mechanisms (McElhany et al., 2022). Overall, molting can be utilized as a parameter to observe changes in water chemistry and measure endocrine stability to assess an animal's physiological state.

Molting may also be used to manage certain invasive crustacean species. The European green shore crab (*Carcinus maenas*), a highly adaptable predator, was named one of the most damaging invasive species by the International Union for the Conservation of Nature (IUCN), as its spread has wreaked havoc on the non-native shores (Ens et al., 2022). In particular, the introduction of *C. maenas* devastated mollusk and decapod crustacean populations and demolished eelgrass (*Zostera marina*) habitats (Carlton and Cohen, 2003; Matheson et al., 2016; Ens et al., 2022). Eelgrass – a nursery and refuge for many organisms– have been shredded and/or displaced because of green crab foraging, thus diminishing biomass and functional biodiversity (Matheson et al., 2016; Ens et al., 2022). . Unfortunately, no long-term, cost-effective program has been successful in eliminating these invasive crabs. However, it has been shown that the embryonic growth and development may be influenced by abiotic factors (e.g. salinity and temperature) (Ens et al., 2022). Therefore, understanding developmental processes in provides strategies for managing this species prior to becoming a disruptive adult. Understanding crustacean molting and growth serve as a tool in ecological disciplines by incorporating it as a

parameter to monitor along with maintaining and managing the size and/or development of some species and thus protect endemic species.

Economic

Knowledge in crustacean physiology can extend beyond ecological applications and have a direct effect on the aquaculture industry and economics altogether. In 2018, aquatic animal global production reached a record 179 million tonnes, valued at $401 billion U.S. dollar (USD), where 156 million tonnes were for direct human consumption (FAO, 2021). The annual global average of seafood consumption, from 1961 to 2017, increased at an annual rate of 3.1%, a rate nearly doubled the 1.6% population growth and 2.1% non-aquatic protein foods (FAO, 2021). Seafood is a fundamental food source for millions of people globally with a per capita annual consumption average of 20.21 kilograms (kg) (Garlock et al., 2022). According to data and statistics drawn from the Food and Agriculture Organization of the United Nations (FAO) and the State of World Fisheries and Aquaculture (SOFIA), aquaculture and fisheries accounted for 15.7% in 2007, 16.6% in 2009, and 17% in 2017 of total animal-source protein consumption (Bondad-Reantaso et al., 2012; Kobayashi et al., 2015; Boyd et al., 2022).

In 2021, seafood provided 3.2 billion people a minimum 20% of the per capita all-animal source protein supply (FAO, 2024). With a continually growing demand and changing climate, capture fisheries alone are not sustainable; however, aquaculture has helped accommodate this need by producing almost half of aquatic animal food destined for human consumption (Bondad-Reantaso et al., 2012; Kobayashi et al., 2015; Boenish et al., 2022; Manfrini et al., 2024). Aquaculture has increased the overall total yield; from 2019 to 2020 aquatic animal production grew by 2.7%, resulting in 87.5 million tonnes (FAO, 2022). Of those, 87.5 million tonnes in

2020, 11.2 million tonnes were from crustacean species alone – valued at $81.5 billion USD (FAO, 2022)! As of 2022, since 2020 overall aquaculture production has grown by 6.6%, of which the aquatic animals yielded 94.4 million tonnes – the first occasion where aquaculture yields exceeded capture fisheries (FAO, 2024). Moreover, within the aquaculture industry, the crustacean sector was reported to be a fast-growing division in comparison to others (e.g. finfish and mollusks) along with being a significant contributor due to the faster production rate (Bondad-Reantaso et al., 2012; FAO, 2012; Boenish et al., 2022; Boyd et al., 2022). Besides protein, seafood provides quality nutritional value to individuals and thus is integral to global food security, as it contains a high level of nutrients, essential amino acids, and protein (Nanda et al., 2021; Boyd et al., 2022). One example of the nutrient dense food is the red king crab (*Paralithodes camtschaticus*) leg meat. Red king crab leg meat contains 43 fatty acids (including saturated or SFA, mono-unsaturated or MUFA, and polyunsaturated or PUFA), a low proportion of cholesterol to muscle protein, and high quantities of amino acids (e.g. tyrosine, histidine, arginine, tryptophan and cysteine) (Dvoretsky et al., 2021). Several other studies have analyzed the nutritional composition of various edible tissues from different crustaceans, including factors that may impact these elements; various research studies of the nutritional value from top crab food commodities are presented in Table 1.1 (Nanda et al., 2021).

In addition to being good food sources, crustaceans are important assets and commodities for market sustainability. According to the FAO, the fisheries and aquaculture sectors employed 61.8 million people with most jobs in Asia at 85% and Africa at 10%, followed by Latin America and the Caribbean at 4%; combined employment in Europe, Oceania, and North America is at 1% (FAO, 2024). Furthermore, the international trade value of aquatic products was assessed at $195 billion USD with China, Norway, Vietnam, Ecuador, and Chile being the top exporters and

the United States of America, China, Japan, Spain, and France being the top importers (FAO, 2024). Seafood has a high-value chain as it creates employment opportunities while providing means to evaluate a country's productivity through assessing the gross domestic product (GDP). GDP gauges the economy by measuring the gross total market value of *domestic* goods and products of which is affected by export and import activity. An increase in imports and trade deficit could lead to a negative effect on the exchange rate and consequently the inflation rate. Therefore, an understanding of the fisheries and aquaculture markets and projections is important to evaluate a nation's economic health (Bondad-Reantaso et al., 2012; He, 2015; Kobayashi et al., 2015). In Bangladesh, for instance, the Bangladesh Department of Fisheries (DoF) reported the crab exportation value in 1977 was $2,000 USD but has increased to $27 million USD in 2018 with a volume of 11,435 metric tons (Lahiri et al., 2021). In Norway, the red king crab and snow crab have high market value and are significant sources of revenue to which the Norwegian Seafood Council stated that in 2016, 3952 metric tons of frozen snow crab clusters were exported at a value of 331 Norwegian Kroner (NOK) (Lorentzen et al., 2018). Additionally, soft-shell rearing swimming crabs, specifically of portunids and mud cabs, is a multimillion-dollar activity involved the international market at the both the artisanal and industrial level (Hungria et al., 2017). With the demand for soft-shell crabs higher than the supply and the market value of reducing as the exoskeleton hardens, optimizing molt-inducing methods and lengthening the time elapsed after molting is an important issue to address in commercial production and trade (Hungria et al., 2017; Rahman et al., 2020; Voldnes et al., 2020; Lahiri et al., 2021; Tavares et al., 2021; Waiho et al., 2021; Zhang et al., 2024). Additionally, the tropical rock lobster (*Panulirus ornatus*) is an overall good commercialization candidate as it is valued at $75-100 USD per kilogram, but, unfortunately, is difficult to rear due to its high cannibalistic nature (Sutherland et

al., 2023). Monitoring pre-ecdysis events is then critical as it allows for intervention and cannibalism prevention. Thus molt-monitoring techniques, including integument ultrasounds and suture algorithm recognition, are being assessed (Sutherland et al., 2023). Optimization of the knowledge in crustacean fisheries and the aquaculture industry is important for global food security, as well as economic stimulation worldwide (Jung et al., 2013; Reddy, 2017; Abdullah-Zawawi et al., 2021; Waiho et al., 2022; Yuan et al., 2023; Wang et al., 2024).

Crustacean molting and mediation through the neuroendocrine system

Molting is a unidirectional progression of changes in the exoskeleton that involve preparation, shedding (ecdysis), and recovery from ecdysis. The crustacean molt cycle, as further described subsequent sections, is divided into major stages: intermolt (IM), premolt, ecdysis (E), and postmolt (PM), of which premolt consists of early (EP), mid (MP), and late (LP) substages. Although molting may be mediated through various signaling pathways and/or factors, crustacean molting is coordinated primarily through neuroendocrine interaction of ecdysteroids and the neuropeptide molt-inhibiting hormone (MIH) as reviewed by several others (Chang, 1985, 1993; Skinner, 1985b; Lachaise et al., 1993; Covi et al., 2012; Webster, 2015; Mykles and Chang, 2020; Mykles, 2021).

The molting gland (Y-organ) and hormone

Ecdysteroids are a class of polyhydroxylated steroid hormones present in plants, fungi, and animals involved in important biological processes (Spindler et al., 2009; Wen et al., 2023). More specifically, ecdysteroids have critical roles in arthropod growth, development, molting, regeneration, and reproduction (Subramoniam, 2000; Spindler et al., 2009). 20-Hydroxyecdsone

(20-E) is the most active form of ecdysteroid (or molting hormone) that is primarily produced and secreted by the Y-organ (YO), analogous to the insect 20-E production by the prothoracic gland (PG) (Chang, 1993; Mykles et al., 2010). The YOs, also referred to as the molting or ecdysial glands, are a pair of ectodermally-derived glands located at the anterior end of the cephalothorax in decapod crustaceans (Chang et al., 1993; Lachaise et al., 1993). As first described by Gabe in 1953, the surface of the YOs is covered with capillaries despite other surface features, such as texture, varying across species (Gabe, 1953; Achdiat et al., 2024). In brachyurans, the YO cells possess numerous mitochondria with tubular cristae, smooth endoplasmic reticulum, a basophilic nucleus, scarce cytoplasm, and varying sized vacuoles (Buchholz and Adelung, 1980; Taketomi and Hyodo, 1986; Taketomi and Nakano, 2007). Nonetheless, changes of the YO histomorphology have been reported during the transitions between the molt cycle stages (Taketomi and Nakano, 2007; Ayanath and Raghavan, 2021).

Ecdysteroidogenesis depends on the sequential enzymatic activity of Cytochrome P450s (CYP450s) monooxygenase enzymes which, in turn, are encoded by the Halloween genes (Schumann et al., 2018; Kamiyama and Niwa, 2022; Lewis et al., 2024). As thoroughly described in the Mykles (2011) review, ecdysteroid production is divided into two main stages. Due to the inability of arthropods to biosynthesize cholesterol from acetate (*de novo*), dietary cholesterol serves as the precursor for ecdysteroid production (Zhu et al., 2022; Wen et al., 2023). Initially, dietary cholesterol is converted by the monooxygenase neverland to 7-dehydrocholesterol and later processed into 25-deoxyecdysone (25dE) through a “black box” involving *Non-moltng glossy* (*Nm-G*), *Shroud* (*Sro*), along with *Spook* (*Spo*) (CYP307A1) and its paralogs *Spookier* (*Spok*) (CYP307A2) and *Spookiest* (*Spot*) (CYP307B1) (Mykles, 2011). In the subsequent phase, the Halloween genes *Phantom* (*Phm*) (CYP306A1), *Disembodied* (*Dib*)

(CYP302A1), and *Shadow* (*Sad*) (CYP315A1) convert the ketodiol to ecdysone (Mykles, 2011; Niwa and Niwa, 2014). Ecdysone is eventually converted to the active 20-E in peripheral tissues by the hydroxylation through *Shed* or *Shade* (CYP314A1) in decapods and insects, respectively (Ventura et al., 2017; Hyde et al., 2019a). Remarkably, 28 transcripts of 42 CYP450s were annotated in the ornate spiny lobster (*Panulirus ornatus*), of which four *Shed* transcripts exhibited overlapping expression across adult and metamorphic tissues (Lewis et al., 2024). Even in the blackback land crab (*Gecarcinus lateralis)*, six *Shed* orthologs were identified in the YO alone (Swall et al., 2021). Suppression of the ecdysteroid synthetic genes have been experimentally shown to affect 20-E concentrations in the hemolymph. For instance, independent RNA-interference (RNAi) experiments in the Oriental river prawn (*Macrobrachium nipponense*) showed that the introduction of double-stranded RNA (dsRNA) of *Spo* and *Phm* decreased 20-E titers, inhibited the molting frequency, and reduced body weight (Yuan et al., 2021a; Pan et al., 2022). Zheng et al. (2023b) also demonstrated that silencing CYP302A1, or *Dib*, in female *M. nipponense* decreased ecdysteroid concentrations, thus delaying ovarian development and molting.

The X-organ (XO) and neuropeptides– the neuroendocrine inhibitor

20-E secretion is inhibited by molt-inhibiting hormone (MIH), a neuropeptide produced by the X-organ/sinus gland complex (XO) located within the eyestalk ganglia (Bliss and Welsh, 1952; Bliss et al., 1954; Techa and Chung, 2015). MIH is classified within the crustacean hyperglycemic hormone (CHH) superfamily and is a Type II peptide member (along with gonad-inhibiting hormone or GIH and mandibular organ-inhibiting hormone or MOIH), as it contains the diagnostic six cysteine residues that form three intramolecular disulfide bridges (Nakatsuji et

al., 2009). Although CHH has some ability to repress, MIH is the primary antagonist for YO ecdysteroidogenesis (Webster, 1986, 1993; Webster and Keller, 1986; Chung and Webster, 2005; Lee et al., 2007; Chung et al., 2010; Webster et al., 2012; Chen et al., 2020; Mykles and Chang, 2020). After the kuruma prawn (*Marsupenaeus japonicus*) YOs were exposed to MIH *in vitro*, expression of *Phm* (one of the Halloween genes) is downregulated (Asazuma et al., 2009). Techa and Chung (2015) further described the feedback mechanism of the neuroendocrine system between MIH and 20-E in the blue crab (*Callinectes sapidus*) through dsRNA-mediated knockdown of *Cs-MIH*. Knocking out *Ec-MIH* with CRISPR/Cas9 in the ridge tail white prawn (*Exopalaemon carinicauda*) further supported its effect on 20-E, as it shortened the larval metamorphosis time (Zhang et al., 2018a). Therefore, YO production of 20-E can be stimulated through the removal of the XO by eyestalk ablation (ESA), which is effective method utilized in lab and aquaculture settings to induce molting in some crustacean species (Hopkins, 2012). Despite the efforts attempted by Asazuma et al. (2005) and others, the MIH receptor has yet to be confidently identified. It is hypothesized that the MIH receptor is a Class A Rhodopsin-like G protein-coupled receptor (GPCR) with an extended extracellular loop-2 with an additional two-stranded β-sheet, which putatively assists with ligand binding affinity and specificity (Tran et al., 2019; Kozma et al., 2024). Nonetheless, MIH activity upon binding with a putative GPCR receptor, is proposed to be coordinated between cyclic adenosine monophosphate (cAMP)/Ca^{2+} and nitric oxide (NO)/cyclic guanosine monophosphate (cGMP) phases, or the triggering and summation phase as depicted in Figure 1.1 (Spaziani et al., 1999; Covi et al., 2009, 2012; Mykles et al., 2010; Pitts and Mykles, 2017; Pitts et al., 2017; Mykles, 2024).

The crustacean molt cycle

The molt cycle was initially described by Drach who divided the entire process into five stages (A-E) and further divided the stages into substages based on the structural features of the epidermis and exoskeleton (Drach, 1939). As Skinner elaborated to greater detail, there are several biochemical and physiological changes that occur not only to the exoskeleton itself but to other tissues during the molt cycle (Skinner, 1962, 1985b; Chang, 1995). Throughout the progression of the molt stages, the properties of the YO change and is correlated with hemolymph 20-E titers (Skinner, 1985b; Okumura and Aida, 2000). Stage C_4 is the longest period of the molt cycle commonly referred to as intermolt (IM). In IM, the YO is in a basal phenotypic state, as the presence of MIH in the hemolymph prevents an increase in 20-E synthesis. Once MIH clears from the hemolymph, the YO becomes activated. Molt induction, accordingly YO activation, can be experimentally initiated by ESA or by removal of five or more legs, referred to as multiple leg autotomy (MLA) (Skinner and Graham, 1972). YO activation leads to an increase in hemolymph 20-E levels, thus allowing the crab to enter premolt or stage D. Shyamal et al. (2018) reported that YO activation is controlled by the positive-feedback mechanistic target of rapamycin (mTOR) signaling pathway, causing an upregulation of ecdysteroid synthetic genes and a continued rise of 20-E titers. Hou et al. 2021) supported claim further this by silencing mTOR through RNAi in the Chinese mitten crab (*Eriocheir sinensis*). As a result of RNAi to *Es-mTOR*, several genes were downregulated, including *Es-Rheb,* a molecular marker for tissue growth, and delaying molting (Hou et al., 2021). During this period, limb the regenerates grow; however, molting can be delayed if the regenerates are autotomized (Mykles, 2001; Yu et al., 2002). More specifically, the ability to postpone molting indicates the YO has MIH sensitivity and that the animal is in the early onset of early premolt (EP or D_0).

During this period, the claw muscle atrophies, while gastroliths start to form. At this point of the molt cycle, 20-E titers increase and may be correlated with increased expression of certain ecdysteroid synthetic genes, such as *Gl-Shadow* and *Gl-Shed5A* (Swall et al., 2021; Benrabaa et al., 2023). In the blue crab (*Callinectes sapidus*) YO, increased expression of *Cs-Neverland* and *Cs-Spook* is correlated with increased ecdysteroidogenesis (Legrand et al., 2021). Progression into mid-premolt (MP), or stage D_1, serves as a molt commitment checkpoint that is regulated through transforming growth factor-beta (TGF-β) signaling. At this phase, the YO loses MIH sensitivity and becomes fixed into a committed phenotypic state consequently not allowing molting to be delayed (Abuhagr et al., 2016; Das et al., 2016). Apolysis, from which the epidermis separates from the exoskeleton, thickens, and starts secreting the outer layers (epicuticle and exocuticle) of the new exoskeleton in stage D_1 and continues in stage D_2. Astaxanthin from the old exocuticle is reabsorbed thereby turning the hemolymph pink in hue in late premolt (LP or stages $D_{2\text{-}4}$). During D_2, ecdysteroid levels drastically increase eventually reaching a peak and subsequently dropping. The decrease in ecdysteroid concentration triggers the YO repression to, which, leads up to ecdysis (E). During postmolt (PM or A, B, $C_{1\text{-}3}$), the two inner layers of the exoskeleton (endocuticle and membranous layer) are synthesized and hardened by sclerotization and calcification of the exocuticle and endocuticle (Figure 1.2) (Chang and Mykles, 2011; Mykles and Chang, 2020). The YO is in the repressed state, resulting the lowest hemolymph 20-E titers of the entire molt cycle. After the membranous layer is deposited at the end of PM, the YO transitions back to the basal state and the animal returns to the intermolt stage. Figure 1.3 illustrates the molt cycle in the blackback land crab (*Gecarcinus lateralis*) (Skinner, 1962; Chang, 1995; Yu et al., 2002; Mykles and Chang, 2020). The signaling mechanisms controlling the transition of the YO from the committed to repressed state and the

transition of the YO from the repressed to basal states are unknown (Figure 1.4). As it occurs at the end of PM when synthesis and hardening of the exoskeleton is completed, it may involve an insulin-like peptide (ILP) from the integument that restores MIH control of ecdysteroid synthesis in the basal YO. The committed to repressed transition may involve interactions between ecdysteroid and methyl farnesoate (MF) signaling, as the transition coincides with the peak in 20-E titer at the end of LP; however, the repressed to basal transition remains a mystery (Figure 1.2).

The ecdysteroid receptor and ecdysone response genes

The ecdysteroid receptor is a nuclear receptor heterodimer of ecdysone receptor (EcR) and Ultraspiracle (USP) or the retinoid X receptor (RXR) in insects and crustaceans, respectively (Abdullah-Zawawi et al., 2021). Nuclear receptors (NRs) are ligand-activated proteins with a single polypeptide chain containing several domains that recognize hormone response elements (HREs) to mediate extracellular signaling and transcriptional responses (Kumar and Thompson, 1999; Bain et al., 2007; Taubenheim et al., 2021). The N-terminal region contains the A and B domain; this region varies between nuclear receptors but encompasses an activation function 1 (AF-1) motif that can drive ligand-independent transcription (Wärnmark et al., 2003; Fahrbach et al., 2012). As a result, this region is likely a site for phosphorylation and post-translational modifications that can consequently lead to differentially-regulated isoforms (Bain et al., 2007). The C domain, a highly conserved DNA-binding domain (DBD), contains conserved cysteine residues for the binding of two zinc fingers (Zf) (Cys2-Cys2) (Fahrbach et al., 2012). The E domain is the ligand binding domain (LBD) that is flanked by the activation function 2 (AF-2) subdomain at the C-terminus. Similar to AF1, AF2 enhances the ligand-dependent transcription

by binding to coactivation factors (Wärnmark et al., 2003; Fahrbach et al., 2012). The D domain is also referred to as the hinge region as this area links DBD and the LBD. This hinge domain contains amino acid residues that bind to the DNA minor groove, thus assisting with protein flexibility (Fahrbach et al., 2012). The binding of ecdysone to the ecdysteroid receptor complex increases the expression of EcR–RXR/USP itself, along with the expression of downstream transcription factors: the ecdysone response genes (Abdullah-Zawawi et al., 2021).

The expression of ecdysone response genes is initiated upon binding of ecdysone to the receptor complex. As proposed by the Ashberner model, with the observations made from puffing patterns of the polytene chromosomes in the *Drosophila* salivary glands, the expression of genes in early puff regions represses the expression of those in the late puff regions and thus has led to the general categorization as early, early-late, and late genes (Ashburner et al., 1974). Although this paradigm supports temporal gene expression, it cannot be applied in every context (e.g. types of tissues, across different species, and the response to the timing of the pulsatile releases). Thus, categorizing these genes in this manner cannot provide a full explanation of the diverse roles these genes have, including the interactions outside of a developmental context (Ou and King-Jones, 2013). Moreso, for many of these genes, different isoforms have been identified that have distinct promoter regions.

Early genes, such as the NR5 subfamily member hormone receptor 39 (HR39), ecdysone-induced protein 23 (Eip23 or E23), ecdysone-induced protein 75 (Eip75 or E75), ecdysone-induced protein 74 (Eip74 or E74), ecdysone-induced protein 93 (Eip93 or E93), and Broad-complex (Br-C), are directly induced by ecdysone. Ecdysone binding activates the early genes but can repress their own transcription, depending on hormone level, and nonetheless activate downstream (early-late and late) genes (Thummel, 1990, 2002). E23 encodes an ATP-binding

cassette (ABC) transporter protein, a major transmembrane protein family, that modulates ecdysone response by interfering with other ecdysone response genes (Hock et al., 2000). Broad complex (Br-C) is a Bric-a-brac, Tramtrack, Broad – zinc finger (BTB–Zf) transcription factor with multiple isoforms as result of alternative splicing (Karim et al., 1993; Spokony and Restifo, 2007; Siggs and Beutler, 2012). Br-C was identified in the ovaries of the giant tiger prawn (*Penaeus monodon*), in which *Pm–Br-C* expression increased after treatment with 20-E (Buaklin et al., 2013). E74, an Ets transcription factor homologue, is required for stage- and tissue-specific transcription of ecdysone secondary response genes (Fletcher et al., 1995; Sharrocks, 2001; Sun et al., 2002, 2005). Silencing the E74 ortholog in the *P. monodon* (*Pm-E74*) affected the expression of other ecdysone response genes (Si et al., 2022). E75, a member of the NR1 subfamily, contains a heme in the ligand pocket, thereby allowing gases [e.g. nitric oxide (NO) and carbon monoxide (CO)] to modify interactions with other components (Reinking et al., 2005; Nakagawa and Henrich, 2009; Cáceres et al., 2011; Ou and King-Jones, 2013). Nonetheless, E75 has been shown to be required in molting and metamorphosis in insects (Segraves and Hogness, 1990; Segraves and Woldin, 1993; Bialecki et al., 2002; Niwa and Niwa, 2016).

The early-late genes include the NR4 subfamily member hormone receptor 38 (HR38), ecdysone-induced protein 78 (Eip78 or E78), hormone receptor 3 (HR3), and hormone receptor 4 (HR4). Like the early genes, they are directly induced by ecdysone but require protein synthesis for maximal induction (Stone and Thummel, 1993; Nakagawa and Henrich, 2009). E78, a NR1 subfamily member, is required for development of the somatic germline stem cell niche, follicle survival, and lipid homeostasis in *Drosophila*, but also is reported to interact with other components of the ecdysone signaling pathway (Ables et al., 2015; Praggastis et al., 2021). HR3,

a member of the NR1 subfamily, acts an activator upon binding to the retinoid orphan receptor element (RORE) motif in response genes (Swevers et al., 2002; Reinking et al., 2005). *Mr-HR3* expression in the giant freshwater prawn (*Macrobrachium rosenbergii*) was shown to be directly correlated to *E75* levels, in which both these genes can be affected by titanium dioxide–graphene oxide (TiO2–GO) (Guo et al., 2023). HR3 action can be suppressed by E75 through direct binding with HR3, or competition for the binding site; however, this inhibition can be alleviated through NO–E75 binding (Swevers et al., 2002; Reinking et al., 2005). *HR3* expression for the water flea (*Daphnia magna*) increased 30-fold within 48 hours into the molt cycle due to increased ecdysteroid concentrations, in contrast to E75 transcript levels that varied depending in context (Hannas and LeBlanc, 2010). Hannas et al. (2010) additionally reported that E75 likely interacts directly with HR3, and not the response element, to mediate its activity in *Daphnia pulex.* Increasing ecdysteroid concentrations in the Oriental river prawn (*Macrobrachium nipponense*) and the blue crab (*Callinectes sapidus*), either through 20-E injections or through ESA respectively, resulted in the increase expression of HR4, a member of the NR6 subfamily (Legrand et al., 2021; Yuan et al., 2022). Furthermore, by knocking down *Mn-HR4* the molting frequency significantly decreased (Yuan et al., 2022).

Both HR3 and HR4 repress early genes and induce the expression of the NR5 nuclear receptor subfamily late gene *Fushi tarazu transcription factor 1* (*Ftz-f1*) (King-Jones and Thummel, 2005; Nakagawa and Henrich, 2009; Ou and King-Jones, 2013). Ftz-f1 mediates ecdysteroidogenesis in the cigarette beetle (*Lasioderma serricorne*) and the cotton bollworm (*Helicoverpa armigera*), as the expression of other ecdysone synthetic and signaling genes was downregulated and prevented the larva-to-pupa metamorphic molt (Zhang et al., 2021; Yan et al., 2023b). Additionally, two Ftz-F1 isoforms were identified in the salmon louse (*Lepeophtheirus*

salmonis), in which the knockdown of *FTZ-F1β* in nauplius larvae and in pre-adult males resulted in molting arrest (Brunet et al., 2021). Silencing *Mn-Ftz-f1* in the *M. nipponense* through double stranded RNA (dsRNA) inhibited the expression of Halloween genes *Mn-Spook* and *Mn-Phantom* and consequently reduced molting and ovulation frequency (Yuan et al., 2021b).

Ecdysone response genes have been identified and characterized in many insect species and within various tissues, while crustacean ecdysone response genes have not been investigated not nearly as intensively in comparison. Table 1.2 summarizes the ecdysone response genes identified and characterized in various decapod crustaceans to, which, the putative E93 ortholog having been recently identified in one species in addition to current study (as further described in a subsequent section) (Ge et al., 2024). Nonetheless, Benrabaa et al. (2024) provided a collective insight on the expression of ecdysteroid response genes with respect to molting, in which *Gl–EcR*, *Gl–BrC, Gl–E74, Gl–Hr3, Gl–Hr4, Gl–FOXO, and Gl– Ftz-f1* were identified in the blackback land crab (*Gecarcinus lateralis*) YO transcriptome. MLA-molt induced crabs increased expression of *Gl–Hr3* and *Gl–FOXO* in premolt, with small effects on expression of *Gl–EcR, Gl–E75,* and *Gl–Hr4,* and no effect on *Gl–Br-C, Gl–E74,* and *Gl–Ftz-f1* (Benrabaa et al., 2024). On the other hand, the expression of these ecdysone response genes were not correlated to the hemolymph concentration of 20-E in ESA-molt induced individuals, thereby suggesting that ecdysteroid synthesis is regulated through both transcriptional and translational mechanisms (Benrabaa et al., 2024).

Methyl farnesoate (MF)

Methyl farnesoate (MF) is a hydrophobic sesquiterpenoid hormone that was initially discovered by Laufer et al. (1987) in the spider crab (*Libinia emarginata*). MF is produced by the

crustacean mandibular organ (MO), a pair of ectodermally-derived glands homologous to the insect corpora allata (CA) (Borst et al., 1987a; Tobe et al., 1989a). The MO is located at the base of the mandibular tendon for many decapod crustaceans and was first identified by Le Roux (1968). These highly vascularized, ductless endocrine glands are composed of large cells generally arranged into clusters (Gopal et al., 2018). The MO contains an unfolded and folded region to which the unfolded region contains C-type cells, large cells with numerous mitochondria and large vacuoles (Borst et al., 1994). On the other hand, fan-fold region contains A and B cells of which A cells are undifferentiated while the B cells contained numerous vacuoles and thus B cells are likely the site of MF synthesis (Borst et al., 1994). In comparison to the Y-organ (YO), which consist of small cells with peripherally located nuclei arranged in a densely packed fashion, the MO cells are larger with centrally located nuclei and contain a substantial amount cytoplasm (Buchholz and Adelung, 1980; Gopal et al., 2018). On the other hand, both MO and YO cells contain numerous mitochondria and an extensive smooth endoplasmic reticulum (Buchholz and Adelung, 1980). Additionally, both the MO and YO experience phenotypic and histological alterations when undergoing a physiological event, such as molting and reproduction (Aoto et al., 1974; Taketomi and Nakano, 2007; Smija and Sudha Devi, 2016; Ayanath and Raghavan, 2021). These endocrines glands, previously described in various species as presented in Table 1.3, have been often confused for another with regards to similarities in anatomical proximity and features, but nonetheless are distinguished biochemically as the MO and YO synthesizes MF and ecdysteroids, respectively (Borst and Tsukimura, 1991; Fingerman, 1997).

The MO production of MF is suppressed by the mandibular organ-inhibiting hormone (MOIH), a neuropeptide produced by the X-organ, sinus gland complex (XO/SG) located within

the eyestalk ganglia (Tsukimura and Borst, 1992; Borst et al., 2001). MOIH is a type II peptide hormone, along with gonad-inhibiting hormone (GIH) and molt-inhibiting hormone (MIH), classified within the crustacean hyperglycemic hormone (CHH) superfamily, as it contains the diagnostic six cysteine residues that form three intramolecular disulfide bridges (Böcking et al., 2002; Nakatsuji et al., 2009; Chung et al., 2010; Webster et al., 2012; Katayama et al., 2013; Chen et al., 2020). Therefore, the MO can be stimulated to secrete MF by removing the XO, and thus the source of MOIH, such as through eyestalk ablation (ESA) (Tsukimura and Borst, 1992; Borst et al., 2001; Paran et al., 2010; Alnawafleh et al., 2014). Moreso, Tsukimura et al. (1993) have shown that the XO inhibition of MF production is regulated by cyclic guanosine monophosphate (cGMP), a second messenger molecule. Besides cyclic nucleotides, it has been reported that MF synthesis may be mediated by biogenic amines, such as serotonin, as seen in the giant mud crab (*Scylla serrata*) and the narrow-clawed crayfish (*Pontatacus leptodactylus*) (Girish et al., 2017; Farhadi et al., 2020). Allatostatin C (ASTC), sometimes referred to as PISCF/AST, is a neuropeptide that has been reported to inhibit JH biosynthesis in the Chinese white pine beetle (*Dendrovtonus armandi*) by inhibiting juvenile hormone O-methyltransferase (JHAMT), they key enzyme for JH production (Sun et al., 2022). ASTC has also been shown to inhibit MF biosynthesis in the green mud crab (*Scylla paramamosain*) MO along with inhibiting the YO production of 20-E (Liu et al., 2021a). Altogether, the MO and MF serve as important regulators of various biological processes as reviewed by Nagaraju (2007) and Homola and Chang (1997). However, Fingerman (1997) designated this endocrine complex (MO-MF) as cursed due to MF actions on various physiological processes. More specifically, how MF regulates YO ecdysteroidogenesis and molting remains a mystery.

MF anabolism

MF biosynthesis is divided into two phases: 1) the mevalonate pathway (MVA) and the 2) farnesyl diphosphate/isopentenoid pathway (Tobe and Bendena, 1999; Bellés et al., 2005; Hui et al., 2010). Within the MVA pathway, acetyl coenzyme A (acetyl-CoA) is converted to hydroxymethylglutharyl-CoA (HMG-CoA) and later is reduced into mevalonate by HMG-CoA reductase, or 3-hydroxy-3-methylglutaryl coenzyme A (HMGR), a rate-limiting step (Goldstein and Brown, 1990; Bellés et al., 2005). Through the series of enzymatic steps, mevalonate is eventually converted to farnesyl pyrophosphate (FPP), an important intermediate in the synthesis of cholesterol and other bioactive terpenoids, by the specific action of farnesyl diphosphate synthase or FPPS (Bellés et al., 2005; Liu et al., 2022a). During the later phase, FPP is hydrolyzed to farnesol, subsequently oxidized into farnesal, and then through the removal of hydrogen atoms becomes farnesoic acid (FA) (Bellés et al., 2005; Hui et al., 2010). Independent studies have demonstrated that RNA interference (RNAi)-mediated knockdown of *HMGR* and *FPPS* have consequences on MF regulated physiological processes, including vitellogenesis in the Chinese mitten crab (*Eriocheir sinensis*) and vitellogenesis and the gene responses involved in ovary and metabolic response in the red cherry shrimp (*Neocaridina denticulta sinensis*) (Chen et al., 2022b; Liu et al., 2022a). FA is transformed into MF through the methylation by farnesoic acid *O*-methyltransferase (FAMeT) in the presence of a P450 monooxygenase and S-adenosyl-L-methionine (SAM) (Tobe et al., 1989b; Wainwright et al., 1998; Borst et al., 2001; Holford et al., 2004). MOs have been shown to secrete (*in vitro*) both FA and MF with the FA secretion rate 10-fold higher than of MF; however, hemolymph analyses detected the presence of only MF and not FA (Tobe et al., 1989b). As suggested by these results, although FA may potentially serve a biological importance itself, FA is likely to be quickly metabolized,

sequestered, and/or taken up by other target tissues (Tobe et al., 1989b). These actions are aided through the action of MF-binding proteins (MFBP), as identified and characterized in various decapod species including *L. emarginata*, the Dungeness crab (*Cancer magister*), the green mud crab (*Scylla paramamosain)*, and the American lobster (*Homarus americanus*) (Tobe et al., 1989a; Prestwich et al., 1990, 1996; Li and Borst, 1991; King et al., 1995; Tamone et al., 1997; Takáč et al., 1998; Zhao et al., 2020). Single and multiple FAMeT transcripts have been identified and localized in various pancrustacean tissues, including decapod crustaceans as summarized in Table 1.4. With the wide distribution of FAMeT transcripts in an assortment of tissues, it is speculated that the tissues have cellular machinery required for MF biosynthesis (Claerhout et al., 1996; Wainwright et al., 1998; Holford et al., 2004). Furthermore, it has been postulated that that target tissues may have an inactive FAMeT enzyme that becomes activated in the appropriate setting in time and place (Homola and Chang, 1997c). FAMeT orthologs contain two methyltransferase (Methyltransf_FA) domains with an overall high similarity between the two regions and thus is hypothesized to have arisen by tandem duplication of a single copy of the domain (Holford et al., 2004; Kuballa et al., 2007; Hui et al., 2008; Saikrithi et al., 2019). Generally, those individuals with multiple isoforms just vary in length with slight, but distinct, variation (Kuballa et al., 2007; Hui et al., 2008; Buaklin et al., 2015). It is speculated that the multiple FAMeT isoforms are members of a multi-gene family; however, some genomic data suggests only one gene exists (Kuballa et al., 2007; Hui et al., 2010; Yang et al., 2012; Qian and Liu, 2019). Moreover, elucidating the origins of FAMeT, including its isoforms, remains largely unknown. Several studies have shown that decapod FAMeT orthologs, including those in the brown crab (*Cancer pagarus*), the greasyback shrimp (*Metapenaeus ensis*), and the whiteleg

shrimp (*Litopenaeus vannamei*), lack the typical SAM binding motif and therefore are classified as SAM-independent (Gunawardene et al., 2001; Ruddell et al., 2003; Hui et al., 2008, 2010).

Additionally, Zhao et al. (2018) identified a FAMeT sequence in *S. paramamosain* (*Sp-FAMeT2*) that contained one Methyltransf_FA domain and one domain of unknown function (DUF) with a DM9 repeat, an uncharacterized protein domain that is originally discovered in *Drosophila melanogaster* (Ponting et al., 2001). An additional FAMeT2 sequence was identified that contained two DM9 repeats, similar to insect FAMeT orthologs, suggesting *Sp-FAMeT2* may have alternative splice sites (Zhao et al., 2018). A DM9-containing protein (DM9CP-1) was also identified in *E. sinensis* that encompassed the Methyltransf_FA domain, followed by two consecutive DM9 repeats (Li et al., 2024). In *S. paramamosain* individuals, *FAMeT2* expression followed a similar expression to that of *HMGR*, varied across different tissue types, and fluctuated at different developmental stages (Zhao et al., 2018). The provided evidence supports the novel crustacean FAMeT2 and its role implicated in MF biosynthesis, signaling, and/or regulation, despite the sequence and structural differences with conventional FAMeT.

MF metabolism

MF is converted to FA through ester hydrolysis catalyzed by carboxylesterases (CXEs), such as MF esterase (MFE) and/or JHE-like esterase (sometimes simply referred to as CXE) (Homola and Chang, 1997b). CXEs are a family of enzymes classified on their physiological and biochemical functions in insects, which possess a catalytic site (e.g., Ser-His-Glu triad) coupled to the oxyanion hole and the acyl pocket for substrate stabilization (Satoh and Hosokawa, 2006; Yu et al., 2009). It has been shown that the level of degradative activity, which can be assayed with different methods, may be impacted by seasonality for some species and varies in different

tissues as reported in *L. emarginata* and the red swamp crayfish (*Procambarus clarkii*) (Laufer and Albrecht, 1990; King et al., 1995; Homola and Chang, 1997a; Takac et al., 1997). For example, CXE5 regulates MF degradation in the *E. sinensis* hepatopancreas, but not in the ovary (Li et al., 2021d). Genes encoding MF-degrading enzymes were downregulated after the terminal molt in the snow crab (*Chionecetes opilio*), thereby leading to an increase in MF levels (Toyota et al., 2023).

JHE-like enzymes, as identified in the gazami crab (*Portunus trituberculatus*), putatively can hydrolyze MF (Tao et al., 2017). CXEs have been identified in several crustacean species including the morotoge shrimp (*Pandalopsis japonica*), *E. sinensis*, and the giant freshwater prawn (*Macrobrachium rosenbergii*) (Lee et al., 2011; Xu et al., 2017; Zhu et al., 2018; Li et al., 2021d). Twenty-one CXEs with complete open reading frames (ORFs) were identified in the whiteleg shrimp (*L. vannamei*) with proteins ranging from 488 to 669 amino acids in length and molecular weight from 54.3 to 74.5 kDa (Zhang et al., 2020). Phylogenetic analysis of the CXEs revealed that despite *Lv-CXE5* containing the GQSAG motif, a diagnostic feature of the ability of JHE to degrade JH in most insects, it is not orthologous to insect JHE (Kamita et al., 2003, 2011; Kamita and Hammock, 2010; Zhang et al., 2020). However, the GESAG motif, which is hypothesized to be associated for specific MF esterase activity, was identified in 14 CXEs in *L. vannamei* (Tao et al., 2017; Xu et al., 2017; Zhang et al., 2020). Furthermore, juvenile hormone epoxide hydrolase-like (JHEH-like) has recently been identified in *E. sinensis*, *M. rosenbergii*, and *P. trituberculatus* and is hypothesized to have putative roles in MF catabolism (Chen et al., 2021b, 2022a; Tu et al., 2022).

The mysterious MF and its many physiological roles

MF is implicated in several physiological processes including morphogenesis, reproduction, metamorphosis/development, and molting (Borst et al., 1987b; Chang, 1993; Chang et al., 1993; Fingerman, 1997; Homola and Chang, 1997c; Laufer and Biggers, 2001; Tiu et al., 2012). In the spider crab (*Libinia emarginata*), Laufer et al. (2002) reported that males in the penultimate stage before differential molt MF prevented allometric growth of the claw propodus. Additionally, Rotllant et al. (2000) reported that MF controlled the morphogenesis in the small-claw unabraded small-carapace (SUM) polymorph. Morphogenesis in the red swamp crayfish (*Procambarus clarkii)* is affected by MF, as primary reproductives (Form Is) depend on a low level of MF prior to the molt, in contrast to Form IIs that developed in high levels of MF (Laufer et al., 2005). Interestingly, exogenous MF and 20-E on the kuruma prawn (*Marsupenaeus japonicus*) decreased the survival rate and slowed larval development and metamorphosis (Toyota et al., 2020a). More specifically, the metamorphic effects were correlated in a dose-dependent manner and were stage specific; nauplius exhibited a stronger resistance to MF and 20-E in comparison to zoea and mysis stages (Toyota et al., 2020a). MF has also been reported to affect metamorphosis in the barnacle larva (*Balanas amphitrite*) and the giant freshwater prawn (*Macrobachium rosenbergii)* (Abdu et al., 1998; Smith et al., 2000). Dietary MF to *M. rosenbergii)* resulted in altered metamorphic patterns and consequent larval intermediates (Abdu et al., 1998).

MF has been shown to affect molting in various crustacean species. The duration of the molt cycle was reduced in intermolt (IM) *O. senex senex*, when MF was administered either by injections or through dietary means (Reddy et al., 2004; Reddy and Arifullah, 2021). The stimulatory effect of MF in regard to the onset of proecdysis and ecdysis and a shortened molt

cycle duration in the orange mud crab (*Scylla olivacea*) and *T. schirnerae* (Tahya et al., 2016b; Raghavan and Ayanath, 2019). MF injections reduced the interval period in intermolt and premolt in *T. schirnerae* individuals in which, premolt crabs required a higher concentration than intermolt crabs (Raghavan and Ayanath, 2019). Upon MF injection, molting was accelerated and induced in *P. monodon* and the Japanese swamp shrimp (*Caridina denticulata*), respectively (Taketomi et al., 1989; Suneetha et al., 2010). Despite these data of the ability of MF to stimulate crustacean molting, the mechanism regulating YO ecdysteroidogenesis, specifically molting outside of a developmental context, is not well-understood. Tamone and Chang (1993) showed that MF stimulates ecdysteroid production in the Dungeness crab (*Metacarinus magister*) YO *in vitro*.

The emphasis of MF research has been focused on reproduction. Although MF has been shown to stimulate testicular growth in the Indian freshwater rice field crab *Oziotelphusa senex senex*), the giant tiger prawn (*Penaeus monodon*), and in European green shore crab (*Carcinus maenas*) under certain environmental conditions, the focus has been on oocyte maturation in the ovary and vitellogenesis in the hepatopancreas (Kalavathy et al., 1999; Nagaraju and Borst, 2008; Suneetha et al., 2010). MF administration enhances ovarian growth and maturation in several crustacean species, including the orange mud crab (*Scylla olivacea*), brown crab (*Cancer pagurus*), *P. monodon*, freshwater crab *Travancoriana schirnerae*, and *O. senex senex* (Wainwright et al., 1996; Reddy and Ramamurthi, 1998; Reddy et al., 2004; Paran et al., 2010; Suneetha et al., 2010; Devi et al., 2018; Muhd-Farouk et al., 2019). Moreso, MF stimulates the uptake of vitellogenin (Vg, the yolk protein precursor) by ovaries in the gazami crab (*Portunus trituberculatus*), crucifix crab (*Charybidis feriatus*), greasyback shrimp (*Metapenaeus ensis*), and

the American lobster (*Homarus americanus*) (Mak et al., 2005; Tiu et al., 2006, 2010; Xie et al., 2015).

RNA-seq data from the red cherry shrimp (*Neocaridina denticulata sinensis*) ovary revealed that ovarian development associated genes were down regulated as a result of the knockdown of farnesyl pyrophosphate synthase (FPPS), an enzyme in the MF biosynthetic pathway (Liu et al., 2022a). Silencing *3-hydroxy-3-methylglutaryal coenzyme a reductase* (*HMGR*), another MF biosynthetic enzyme, inhibited vitellogenesis in the Chinese mitten crab (*Eriocheir sinensis*) (Chen et al., 2022b). MF exposure to female Australian red-claw crayfish (*Cherax quadricarinatus*) during their winter reproductive arrest period had no effect on reproduction, accelerated molted, and increased mortality (Abdu et al., 2001). MF in the whiteleg shrimp (*Litopenaeus vannamei*) stimulated both ovarian maturation and molting (Alnawafleh et al., 2014). It is hypothesized that MF operates in a similar fashion in terms of the transcriptional cascade to regulate different physiological processes; however, MF is considered 'cursed' as the mechanism is unelucidated (Fingerman, 1997).

MF/JH and the MEKRE93 transcriptional cascade

MF is the unepoxidated form of the insect juvenile hormone III (JH III) and plays similar physiological roles in reproduction, metamorphosis, and development. JH-III, discovered by Wigglesworth in 1934, is an acyclic sesquiterpenoid hormone synthesized by the corpora allata (CA) and represses the 20-E production in the insect prothoracic gland (PG) (Riddiford et al., 2003; Li et al., 2018a). 20-E secretion in insects is further mediated by prothoracicotropic hormone (PTTH), a neuropeptide hormone produced by the corpora cardiaca (CC) (Nijhout and Williams, 1974; Jindra et al., 2013; Nijhout et al., 2014). JH III was nicknamed the *status quo*

hormone as it has been shown to prevent development and maintain larval/nymphal status when present in the hemolymph. In terms of reproductive physiology, JH III has been shown to regulate reproductive diapause in the grassland leaf beetle (*Galeruca daurica*) and the cabbage beetle (*Colaphellus bowringi*); vitellogenesis in the book louse *Liposcelis entomophila*, the striped rice stemborer (*Chilo suppressalis*), and the Asian lady beetle (*Harmonia axyridis*); oocyte development the kissing bug (*Dipetalogaster maxima*) and the brown plant hopper (*Nilaparvata lugens*); and the development of male accessory glands in dark sword-grass moth (*Agrotis ipsilon*) (Mao et al., 2019; Tang et al., 2020; Gassias et al., 2021; Ma et al., 2021b, 2021a; Tian et al., 2021; Han et al., 2022; Ramos et al., 2022; Yang et al., 2023). JH action has also been reported to have overlapping physiological roles, such as oocyte maturation/vitellogenesis and metamorphosis in the cotton bollworm (*Helicoverpa armigera*), the oriental fruit moth (*Grapholita molesta*), and the bean bug (*Riptortus pedestris*) (Ma et al., 2018; Zhang et al., 2018b, 2019a; Dong et al., 2022). JH III induces a mechanistic transcriptional cascade: the Methopene tolernant (Met)– Krüppel homolog 1 (Kr-h1)– Ecdysone response gene 93 (E93) or collectively referred to as the MEKRE93 signaling cascade (Belles and Santos, 2014). In brief (as later described in further detail), JH signaling regulates 20-E signaling through the induction of Kr-h1 to inhibit E93, an ecdysone response gene (Belles, 2019).

In insects, in the presence of JH, Met associates with Heat shock protein 83 (Hsp83) to allow a conformational change in Met and promote JH binding (He et al., 2014). Hsp83 interacts with the tetatricopeptide repeat (TPR) domain of a 358-kDA nucleoporin (Nup358), which leads to nuclear import of the complex, as transport receptor importin β recognizes the Met nuclear localization signal (NLS) (He et al., 2017b). Importin β binds with RanGTP upon nuclear import, thus dissociating the receptor complex and allowing cofactor binding (e.g., Steroid receptor

coactivator or Src), leading to the binding on JH response elements (JHRE) in the promoters of response genes, such as Kr-h1 (Zhang et al., 2011; He et al., 2017b). Figure 1.5 illustrates the proposed model of the Met molecular mechanism in insect JH signaling (He et al., 2017b).

The MEKRE93 cascade has adopted the new name "Metamorphic Gene Network" (or MGN), as it likely that the transcription factors behave in a non-linear fashion with different factors. The interaction and orchestration of these components influence the plasticity of the network itself across taxa in different physiological contexts (Martín et al., 2021). Several heat shock proteins have been identified in crustaceans, specifically in immunity context; however, none have been directly shown in crustacean Met nuclear transport (Junprung et al., 2021). Before addressing the downstream implications, it is first necessary to describe the various types of transcription factors that compose the network.

Methoprene tolerant (Met) and Steroid receptor coactivator (Src)

Met and Src are bHLH-PAS transcription factors with an intrinsically disordered C-terminus (Kolonko et al., 2016). The basic helix-loop-helix (bHLH) transcription factor superfamily consists of members that have two conserved domains: the basic DNA-binding domain (containing a consensus sequence referred to as the E-box) and the helix–loop–helix (HLH) dimerization domain (Jones, 2004). Genome-wide analyses suggest that the expansion of bHLHs in the water flea (*Daphnia magna*) and the copepod (*Paracyclopina nana)* is the result of lineage-specific duplications, as other crustaceans have fewer (Chang and Lai, 2018). It is hypothesized that the expansion of these proteins in these lower crustaceans, provides an adaptive mechanism to address adverse environment conditions considering that many bHLH proteins acts as environmental sensors (Chang and Lai, 2018).

The bHLH superfamily is furthermore divided into six groups (A-F) in regard to distinct structural features (Atchley and Fitch, 1997; Massari and Murre, 2000; Ledent and Vervoort, 2001; Jones, 2004). Within the bHLH superfamily, proteins classified within Group C bind to ACGTG/GCGTG and contain a PAS domain, or Period (Per)-Aryl Hydrocarbon Receptor Nuclear Translocator (ARNT)-Single minded (SIM) domain (Jones, 2004; Daffern and Radhakrishnan, 2024). The PAS domain is divided into the PAS-A and PAS-B regions and are linked by a poorly conserved region (Ponting and Aravind, 1997). The PAS domain serves as a dimerization motif that allows binding to other proteins, small molecules, and hormones (Coumailleau et al., 1995; Crews and Fan, 1999; Kewley et al., 2004). The bHLH–PAS transcription factors have roles in various physiological processes including organogenesis, morphogenesis, and development, and signal transduction processes (Crews, 1998; Greb-Markiewicz and Kolonko, 2019; Tumova et al., 2024). The bHLH-PAS family is also divided into Class 1 and Class 2. Class 1 proteins, including single-minded (SIM), hypoxia-inducible factors (HIF, HIF-1α, HIF-2α, HIF-3α), neuronal PAS domain proteins (NPAS), aryl hydrocarbon receptor (repressor) (AHR and AHRR), circadian locomotor output cycles protein kaput (CLOCK), and Methoprene tolerant (Met), serve as archetypal sensors of tissue specific or environmental signals (Crews, 1998; Kewley et al., 2004; Wu and Rastinejad, 2017; Kolonko and Greb-Markiewicz, 2019). Class 1 proteins require a Class 2 member, including Aryl Hydrocarbon Receptor Nuclear Translocator (ARNT) and BMAL, for dimerization (Hoffman et al., 1983; Andreasen et al., 2002; Fribourgh and Partch, 2017; Wu and Rastinejad, 2017; Kolonko and Greb-Markiewicz, 2019). Phylogenetic analysis of crustacean bHLH-PAS orthologs show a clear demarcation between Class 1 and Class 2 with the ARNT proteins forming a well-supported monophyletic group (Chang and Lai, 2018). Class 1, on the other hand,

are paraphyletic with HIF and SIM members cluster together while Met and Clock form separate monophyletic groups (Chang and Lai, 2018). It is hypothesized that bHLH and PAS domain association occurred multiple times independently through domain duplication or insertion as a result of modular evolution (Chang and Lai, 2018).

Steroid receptor coactivators (Srcs) are a group of transcription-regulating nuclear proteins that were first discovered as auxiliary factors recruited by a nuclear receptor (NR) (Pecenova and Farkas, 2016). Src is structurally homologous to the p160 coactivator family, in which it encompasses a bHLH–PAS domain at the N-terminus and has a serine/threonine rich center and phosphorylation site that can regulate its activity (Pecenova and Farkas, 2016). Src-1 was reported to be a general co-activator for several steroid receptors and thus enhanced the transactivation of steroid hormone-dependent target genes (Oñate et al., 1995). Interestingly, Src-1 has been shown to synergistically interact with CREB-binding protein (CBP), a transcriptional comediator to enhance transcriptional activity (Leo and Chen, 2000). Nonetheless, Src may be recruited for the assembly of bHLH-PAS heterodimer (Zhang et al., 2011; Pecenova and Farkas, 2016).

Krüppel homolog 1 (Kr-h1)

Krüppel (Kr), translated from the German word for “cripple”, was identified as a gap gene in *Drosophila melanogaster*, as mutants resulted in the failure to develop the appropriate thoracic and anterior segments due to the inability to regulate segment polarity genes (Nüsslein and Wieschaus, 1980; Preiss et al., 1984; Wieschaus et al., 1984; Licht et al., 1990; Hoshizaki, 1994). Krüppel is a member of the Krüppel-like factor (Klf) family, a group of zinc finger (Zf) transcription factors associated with several physiological processes, including proliferation,

apoptosis, differentiation and development (Pearson et al., 2008). The characterization of a *Drosophila* transposable element, or P-element, led to the discovery of Krüppel homolog 1 (Kr-h1), in which the mutant died during the prepupal period and failed to complete head eversion (Schuh et al., 1986; Pecasse et al., 2000a). Additional studies have reported two, or sometimes three major transcripts, (e.g. Kr-h1α and Kr-h1β) that are derived from distinct promoters from the Kr-h1 locus (Pecasse et al., 2000a). Kr-h1 is a C2H2 (Cys2-His2) zinc finger (Zf) transcription factor, the most common type of zinc finger containing protein, with insects having eight ZF repeats (Schuh et al., 1986; Pecasse et al., 2000a; Fedotova et al., 2017; Bonchuk and Georgiev, 2024). C2H2 zinc fingers are independently folded proteins, with a hydrophobic core, consisting of an α-helix and β-hairpin (Laity et al., 2001; Fedotova et al., 2017). Each zinc finger has two cysteine and two histidine residues that bind a zinc ion that aid in specific DNA-binding (Fedotova et al., 2017). Unlike most transcription factors that bind relatively short DNA sequences (i.e. 6–12 base pairs), C2H2 proteins bind to longer DNA sequences (i.e. 20–40 base pairs). In addition to DNA binding, they are involved in protein–protein and protein–RNA interactions (Fedotova et al., 2017; Krieger et al., 2022).

Ecdysone response gene 93 (E93)

Ecdysone response gene 93 (E93), also referred to as ecdysone inducible factor 93 (Eip93*),* is a helix-turn-helix (HTH) transcription factor containing of two α-helices connected by a β-turn (Baehrecke and Thummel, 1995; Siegmund and Lehmann, 2002). E93 is a member of the Pipsqueak (Psq) family, as it contains a Psq DNA-binding domain consisting of a 50 amino acid tandem repeat (Siegmund and Lehmann, 2002). E93 was discovered to direct larval cell apoptosis and morphogenesis, as it promotes the expression of apoptosis and autophagy genes

(e.g. *RHG* genes), along with repressing PI3K-TORC1 signaling genes (Baehrecke and Thummel, 1995; Liu et al., 2014; Zhang et al., 2023).

E93 has also been linked to changes in chromatin accessibility, in which it can activate late-acting enhancers and represses early-acting enhancers (Uyehara et al., 2017; Nystrom et al., 2020; Ling et al., 2023). In the red flour beetle (*Tribolium castaneum*), E93 is essential in reproductive physiology, as double-stranded RNA (dsRNA)-mediated knockdown of *Tc-E93* decreases vitellogenin (Vg) synthesis, oocyte development, and egg-laying (Eid et al., 2020). In locust, E93 has critical roles in cuticle, wing, and ovary development and metamorphosis (Gijbels et al., 2020; Liu et al., 2021b). According to the Ashburner model, E93 is classified as an early gene; however, unlike other ecdysone response genes E93 exhibits complex spatial and temporal regulation (Baehrecke and Thummel, 1995; Lam et al., 2022; Zhang et al., 2023). As an early ecdysone response gene, E93 expression responds directly to ecdysone, as studies on the yellow fever mosquito (*Aedes aegypti*) have shown that 20-E upregulates *E93* expression, and knockdown of *Aa-EcR* downregulates *E93* expression (He et al., 2021; Wang et al., 2021). Additionally, *E93* suppression in *A. aegypti* results in the loss of 20-E responsiveness of other genes and demonstrates its critical role in regulating blood meal digestion and gonadotrophic cycles (He et al., 2021; Martín, 2021; Wang et al., 2021). RNAi-mediated knockdown in *A. aegypti* of *Aa–E93* disrupts *HR3* expression (Wang et al., 2021). In the brown planthopper (*Nilaparavata lugens*), immunofluorescence showed that both E93 and E78 proteins are located in the nucleus and co-immunoprecipitation confirmed interaction between the two ecdysone response genes (Zheng et al., 2023a). In the gazami crab (*Portunus trituberculatus*), 20-E increases *Pt-E93* expression *in vivo* and *in vitro*; however, RNAi-mediated knockdown of *Pt-E93* increases expression of Halloween genes *Spo* and *Sad* (Ge et al., 2024). Recently, an E93

ortholog was identified in *P. trituberculatus* (*Pt-E93*) and was reported to exhibit responsiveness to 20-E and methyl farnesoate (MF), as administration of exogenous 20-E increased *Pt-E93* expression, while MF suppressed *Pt-E93* expression in juvenile crabs (Ge et al., 2024). Interestingly, *Pt-E93* exhibited a negative correlation in ecdysteroidogenesis as silencing of *Pt-E93* induced the expression of *Spook* (*Spo*) and *Shadow* (*Sad*) ecdysteroid biosynthetic genes (Ge et al., 2024).

E93 is hypothesized to be the Mushroom body large-type Kenyon cell-specific protein-1 (Mblk-1) ortholog (Mou et al., 2012). For example, *Drosophila melanogaster E93* (*Dm-E93*) and the honeybee Mblk-1 have low sequence identity overall, despite the domains share a higher sequence identity (Takeuchi et al., 2001). Mblk-1 was identified in the honeybee brain specifically in the large-type Kenyon cells of mushroom bodies, a region generally associated for higher-order processing in insects (Farris, 2005; Yasugi and Nishimura, 2016) (Takeuchi et al., 2001). In the honeybee increased Mblk-1 transcriptional activity is attributable to phosphorylation through the Ras/MAPK pathway and shown to be involved in ecdysteroid signaling with stage-specific functions (Kumagai et al., 2020). Mushroom bodies are nitric oxide (NO) containing neuronal centers hypothesized to have independently risen multiple times in the invertebrate lineage, thus contributing to phenotypic variation across pancrustaceans (O'Shea et al., 1998; Strausfeld et al., 2020; Strausfeld, 2021). Crustacean mushroom bodies, first discovered by Wolff et al. (2017) in mantis shrimps, are primarily investigated with research pursuits focusing in the neuroscience discipline (Strausfeld et al., 2020; Strausfeld, 2021). It has been reported that mushroom bodies express *Chinmo*, or Chronologically inappropriate morphogenesis (Farris, 2005; Yasugi and Nishimura, 2016). Chinmo is a Bric-a-brac, Tramtrack, Broad zinc finger (BTB–Zf) transcription factor (Narbonne-Reveau and Maurange, 2019).

Although serving as a neuron specifier, Chinmo also acts a repressor of both *Br-C* and *E93* and may serve as a pro-oncogene to these ecdysone response genes (Zhu et al., 2006; Marchetti and Tavosanis, 2017; Narbonne-Reveau and Maurange, 2019; Truman and Riddiford, 2022). It is hypothesized that *Chinmo* may serve as master regulatory gene for *Br-C* and *E93*, critical ecdysone response genes for metamorphosis (Reynolds, 2022; Truman and Riddiford, 2022; Chafino et al., 2023; Khong et al., 2024).

Building the MEKRE93 network

Structural and functional evidence suggests that Met is the receptor for JH III and MF (along with other juvenoids) and subsequently induce the same downstream targets in crustaceans and insects (Miura et al., 2005; Bernardo and Dubrovsky, 2012; Miyakawa et al., 2013; Kakaley et al., 2017; Jindra and Bittova, 2020). In the presence of MF/JH, the Met homodimer (or the germ cell-expressed (GCE) *Drosophila* paralog) dissociates and upon ligand binding Met binds to Src, orthologs to *Aedes* FISC and *Drosophila* Taiman (Tai) (Bernardo and Dubrovsky, 2012; Kakaley et al., 2017). Juvenoids specifically bind to the Met PAS-B domain encompassing several amino acid residues that form a ligand-binding pocket; however amino acid substitutions can affect ligand binding due to steric hindrance (Charles et al., 2011). Mutations of these specific amino acid residues associate with the ligand-binding pocket has been reported to affect juvenoid sensitivity and receptor dimerization in *Daphnia* (Miyakawa et al., 2013; Hirano et al., 2020). Juvenoid binding to the PAS-B domain can affect the conformation of the intrinsically disordered C-terminus of Met and interact with Ftz-F1 (Kolonko et al., 2016). Additionally, Met interacts with the ultraspiracle (USP) protein and, in turn, inhibits the ecdysone receptor complex binding to ecdysone response elements in the cotton

bollworm (*Helicoverpa armigera*) (Zhao et al., 2014). The Met ortholog was identified in various tissues of female gazami crabs (*Portunus trituberculatus*) with *Pt-Met* highly expressed in the hepatopancreas, the primary site for vitellogenesis (Liu et al., 2016). Liu et al. (2016) also reported that administration of MF (*in vivo* and *in vitro*) stimulated *Pt-Met and Pt-Vg* expression in the hepatopancreas.

The interaction between Met and Src is dependent on JH, in order to induce downstream *Kr-h1* expression in the domestic silk moth (*Bombyx mori*) (Kayukawa et al., 2012). Kr-h1 is nicknamed the 'guardian of juvenile status' or the 'metamorphosis doorkeeper,' as it mediates the anti-metamorphic action of JH (Minakuchi et al., 2009; Lozano and Belles, 2011; Ojani et al., 2018; Belles, 2019; Jindra, 2019). Zhang et al. (2018b) and Kayukawa et al. (2014) reported that Kr-h1 inhibits steroidogenic enzymes in *Drosophila* and *Bombyx ex vivo* prothoracic glands (PG), thus repressing ecdysone biosynthesis. The *Kr-h1* ortholog has been identified in *P. trituberculatus* (*Pt-Kr-h1*) with a high expression in the hepatopancreas (Xie et al., 2018). Treatment of *Pt-Met* dsRNA consequently led to a decrease in *Pt-Kr-h1* expression, suggesting *Pt-Kr-h1* is downstream of *Pt-Met* (Xie et al., 2018). Xie et al. (2018) also reported that RNAi knockdown of *Pt-Kr-h1 and Pt-Met* led to a decreased expression of *Pt-Vg*, thereby supporting the role of MF in reproduction by means of Met and Kr-h1. The Met ortholog (*Es-Met*) along with Kr-h1 (*Es-Kr-h1*) were also identified in the Chinese mitten crab (*Eriocheir sinensis*) (Li et al., 2021b, 2021c). Similar to *P. trituberculatus*, *Es-Met* was largely expressed in the hepatopancreas and injections of MF increased *Es-Met* and *Es-Vg* expression (Li et al., 2021b). *Es-Kr-h1* was also highly expressed in the hepatopancreas and increased after MF injections (*in vivo* and *in vitro*) (Li et al., 2021c).

Kr-h1 inhibits *E93,*in addition to *E93* inhibiting *Kr-h1,* to ensure proper metamorphosis in brown planthopper (*Nilaparvata lugens*) and the common bed bug (*Cimex lectularius*) (Gujar and Palli, 2016; Li et al., 2018b). In *T. castaneum*, *E93* is a vital temporal factor that triggers metamorphosis (Chafino et al., 2019). *E93* is known as the "universal adult specifier gene," as various studies have demonstrated that silencing of *E93* resulted in supernumerary pupal or nymphal stages, thereby preventing the transition from pupa-to-adult or nymph-to-adult (Ureña et al., 2014; Gijbels et al., 2020; Kamsoi and Belles, 2020; He and Zhang, 2022; Fernandez-Nicolas et al., 2023). However, Kr-h1also has been shown to interact with *Br-C* and have ecdysteroidogenic effects (Minakuchi et al., 2008, 2011; Kayukawa et al., 2016; Ureña et al., 2016; Okude et al., 2022). Overall, this transcriptional network is plastic, as the molecular mechanisms of activation and downstream effects vary depending on contexts (Mazina and Vorobyeva, 2019).

Other transcriptional effectors

Forkhead Box O (FOXO) is a transcription factor in the Forkhead (FH) transcription family, which belong to the larger Winged Helix Protein superfamily (Obsil and Obsilova, 2008). FOX proteins encompass a forkhead DNA-binding domain that folds into three α-helices and three β-sheets with two wing-like loops that flank the third β-sheet (Huang and Tindall, 2007). FOX proteins within the 'O', or other, class are the most divergent subfamily because of sequence differences within their DNA-binding domain (Kaestner et al., 2000; Barthel et al., 2005). FOXO is reported to be critical for growth, as it negatively regulates the insulin/insulin growth factor signaling pathway (IlS) and regulates many physiological processes, including development, metabolism, cell cycle control, and lifespan (Huang and Tindall, 2007). Gene

silencing of FOXO in the red flour beetle (*Tribolium castaneum*) affects the expression of insulin and ecdysone signaling genes, such as hormone receptor 3 (HR3), causing to in a decrease in ecdysteroid titers and a delay in pupation (Lin et al., 2018). Interestingly, FOXO-like was identified in the Chinese mitten crab (*Eriocheir sinensis*). *Es-FOXO-like* was largely expressed in premolt and inhibited ecdysteroid signaling via mTOR (Li et al., 2023). FOXO may also affect 20-E signaling via the juvenile hormone (JH) signaling. Although FOXO expression levels in the red flour beetle (*Tribolium castaneum*) were not affected after the downregulation of the downstream effector of TORC1 S6 kinase (S6K), FOXO nuclear translocation was promoted after the downregulation of S6K and FOXO negatively regulated farnesol dehydrogenase, a JH biosynthetic gene (Jiang et al., 2022). On the other hand, FOXO is reported to regulate JH degradation, rather than the production, in the domestic silk moth (*Bombyx mori*) (Zeng et al., 2017). Furthermore, *in vitro* and *in vivo* studies revealed that FOXO physically and genetically interacts with Krüppel homolog 1 (Kr-h1), the transcription factor inhibiting E93, to regulate the insulin receptor (InR) activation (Kang et al., 2017).

The recruitment of co-activators or repressors to specific DNA sequences influences transcriptional activation and repression (respectively), thereby regulating gene expression. CREB (cAMP response element binding protein)-binding protein (CREB-binding protein or CBP) and C-terminal-binding protein (CtBP) are two commonly known transcription mediators associated with various transcription factors.

CtBP is a transcriptional corepressor that was initially discovered as a protein that interacted with the C-terminal motif (PLDLS) of adenovirus E1A oncoprotein (Boyd et al., 1993; Schaeper et al., 1995). CtBP has critical roles in development, tumorigenesis, and cell fate through the repression of transcription factors including Krüppel, Knirps, and Snail (Nibu et al.,

1998; Chinnadurai, 2007). Despite recognized as a transcriptional corepressor across many organisms, CtBP directly activates transcription of particular Wnt genes in *Drosophila* embryos, while repressing other target genes (Fang et al., 2006). Structurally, CtBP has a conserved D2 hydroxyacid dehydrogenase (D2-HDH) domain to, which, binding of nicotinamide adenine dinucleotide, or NAD(H), can facilitate functionality (Kumar et al., 2002). Although dimer and oligomeric forms of CtBP associates with other factors to regulate transcriptional activity, the tetrameric form is more active; thus, NAD(H) binding affirms oligomerization of larger protein complex and accordingly transcriptional repression (Kumar et al., 2002; Raicu et al., 2023). The deyhydrogenase domain contains the "Rossmann Fold" with the GXGXXG (17x) motif for NAD(H) binding, along with the catalytic Arginine- Glutamic acid- Histidine (Arg-Glu-His or REH) triad motif (Kumar et al., 2002). In addition to the dehydrogenase domain, CtBP has an N-terminal substrate binding domain (NTD) and the C-terminal domain (CTD). The NTD is responsible for substrate (transcription factor) binding by the recognition of and binding to the consensus sequence (e.g. PxDLS). Bilaterian CtBP orthologs exhibit high conservation in length of the NTD (approximately 100 amino acids) and contains putative post-translational modifications sites (e.g., phosphorylation and SUMOylation) (Schaeper et al., 1995; Nardini et al., 2006; Raicu et al., 2023, 2024). CtBP CTD is a proline/glycine-rich intrinsically disordered region (IDR) that contributes to its unstructured configuration, the distinguishing feature of CtBP from other HDHs (Schaeper et al., 1995; Nardini et al., 2006). Interestingly, different CtBP forms that contain and lack the CTD have been identified and have functionality (Raicu et al., 2023, 2024). In *Drosophila*, for instance, Raicu et al. (2024) reported that different CtBP isoforms had differential severity effects on wing phenotype thus selective modulation of gene targets. In the vertebrate lineage, CtBP has undergone gene duplications that produce two or more paralogs

(Raicu et al., 2023). By contrast, invertebrates have one CtBP gene but due to alternative splicing and alternative promoters may express several isoforms (Raicu et al., 2023).

CBP, the mammalian paralog of p300 or Nejire in *Drosophila*, is a promiscuous transcriptional coactivator with over 400 interaction partners (McManus and Hendzel, 2001). CBP is an important player in facilitating growth and developmental processes (McManus and Hendzel, 2001). CBP has histone acetyltransferase (HAT) activity involved in chromatin remodeling (McManus and Hendzel, 2001). Moreover, CBP has three cysteine-histidine-rich (CH) regions are flanked by transactivation domains (e.g., transcriptional adaptor zinc finger domains or TAZ) at the N and C termini; within these regions are a series of functional domains with zinc-binding motifs (McManus and Hendzel, 2001). CH1 incorporates the TAZ1 domain; followed directly after is the kinase-inducible interacting domain (KIX). The KIX domain is comprised of three α and two α -3_{10} helices that form two distinct binding surfaces and is critical for the magnitude of the transcriptional response (Shaywitz et al., 2000). The CBP catalytic core consists of the (1) Bromodomain (BROMO), followed by the (2) CH2 domain which encompasses the Really Interesting New Gene (RING) and Plant Homeodomain (PHD), (3) the histone acetyltransferase (HAT) domain, and the (4) CH3 domain that contains the ZZ zinc finger (ZZ) and TAZ2 domain (Legge et al., 2004; Dyson and Wright, 2016). Interactions with and binding to the TAZ2 domain brings the transcriptional factor closer in proximity to the HAT domain thereby contributing acetylation regulation (Dancy and Cole, 2015). In the N-terminus contains the CREB-binding region, which has the coactivator binding sites located within the nuclear coactivator binding domain (NCBD). The NCBD binds to various protein partners , such as steroid receptor coactivator (Src) and thyroid and retinoid receptors (Dyson and Wright, 2016). The C-terminus has a glutamine- and proline-rich region.

CBP affects the expression of transcription factors in the JH and ecdysteroid signaling cascade. In the yellow fever mosquito (*Aedes aegypti*), RNA-interference (RNAi)–mediated knockdown of *CBP* downregulated *Kr-h1* and upregulated *E93* in the JH and ecdysteroid pathway (respectively), thus consequently resulting in premature metamorphosis, larval-pupal intermediate formation, improper eye development, and increased mortality (Gaddelapati et al., 2020). In the presence of JH, acetylation of core histones at the Kr-h1 promoter region increased *Aa–Kr-h1* expression, while CBP inhibited E75a-dependent expression of *Aa–EcR, Aa–USP, Aa–Br-C,* and *Aa–E93* (Gaddelapati et al., 2020). Moreover, CBP knockdown in the red flour beetle (*Tribolium castaneum*) decreased JH signaling genes, including *Kr-h1*, while a histone deacetylase (HDAC) inhibitor increased the *Kr-h1* expression (Xu et al., 2018). Roy et al. (2017) confirmed the decreased expression of JH responsive genes (e.g., *Kr-h1* and *Hairy*) and ecdysone response genes (e.g., *EcR, E74, E75,* and *Br-C*) resulting from RNAi–mediated knockdown of CBP in *T. castaneum*. Molting was delayed in pre-metamorphic German cockroaches (*Blatella germanica*) treated with double-stranded CBP (dsCBP); they experienced a reduced food intake and downregulation of *E75a/b* and *HR3* (Fernandez-Nicolas and Belles, 2016). Although CBP could be affecting molting directly via ecdysone response genes, it is plausible that the delay resulted from CBP acting indirectly through TGF-β and/or JH signaling. Fernandez-Nicolas and Belles (2016) reported that the downregulation of CBP disrupted the normal *Kr-h1* decline and increase of *E93*. When dsCBP- treated *B*. *germanica* individuals were treated with JH, the abrogated the normal increase in *Kr-h1* expression and reduced the expression of *E93*, suggesting that CBP may be an activator to *Kr-h1*, *E93*, or both (Fernandez-Nicolas and Belles, 2016). Furthermore, Wu et al. (2021) showed that PKCα phosphorylation of Kr-h1 in juveniles

can recruit CtBP, thereby repressing E93. while in adults, phosphorylation recruits CBP and enhances vitellogenesis-related genes.

Research rationale

Research objective, specific aims, and hypothesis

The goal of this research project is to examine the role of MF in the regulation of the YO. More specifically, how does the MF–MEKRE93 transcriptional cascade affect ecdysteroid production thus contributing to the YO transition from the committed-to-repressed state and the repressed-to-basal state? It is hypothesized that MF acts through the Met receptor, but the effects of MF on YO ecdysteroid synthesis are determined by hemolymph titers of 20-E. At low levels 20-E, such as in IM animals, MF stimulates ecdysteroidogenesis and contributes to YO activation. At high levels of 20-E when the YO is committed, such as in MP and LP animals, MF inhibits ecdysteroidogenesis and contributes to YO repression. MF binding to Met is hypothesized to translocate to the nucleus and thereby bind to a response element in the promoter region of the *Kr-h1* gene. At high hemolymph 20-E levels *Kr-h1* inhibits *E93* transcription, resulting in the downregulation of ecdysone response genes and the Halloween genes. *Kr-h1* expression also may be enhanced by *CBP*, thereby further downregulating ecdysone response genes. At low hemolymph 20-E levels, *Kr-h1* is downregulated as a result of *CtBP* expression. Suppression of *Kr-h1* stimulates *E93* transcription, resulting in upregulation of ecdysone response genes and Halloween genes. The different interaction between *Kr-h1* and *E93*, and/or with other ecdysone-response genes may be due to the presence of other transcription factors or/and comediators (e.g. *CtBP* and *CBP)* (Figure 1.6).

To address this objective, the components of the MF–MEKRE93 transcriptional cascade and associated transcriptional comediators were identified and characterized (Aim 1; Chapter 2). Additionally, the YO responsiveness to MF and JH analogs was determined through *in vitro* cultures (Aim 2; Chapter 2). In the last aim, components involved in the MF synthetic pathway were identified and characterized (Aim 3; Chapter 3).

Meet the model organisms

Adult male crabs from two brachyuran crab species, the blackback land crab (*Gecarcinus lateralis*) and the European green shore crab (*Carcinus maenas*) were used for these studies. The similarities and differences between the two brachyuran species are compared in Figure 1.7.

The blackback land crab (*Gecarcinus lateralis*), a terrestrial species that inhabits tropical, habitats native to the shorelines of Caribbean islands and Bermuda, molts once annually as adult (Bliss, 1968, 1979; Skinner, 1985b). An advantage of using a terrestrial species is that it does not require an aquatic environment and thus is relatively easy to maintain in the lab (Bliss, 1968, 1979; Skinner, 1985b, 1985a). In particular, *G. lateralis* serves as an excellent model species to study molt regulation, as molting can be experimentally induced. Eyestalk ablation (ESA) is an effective molt induction method, as the removal of the eyestalks eliminates the primary source of MIH, which is synthesized in the XO (Hopkins, 2012; Mykles, 2024). An alternative, a more natural, method to induce molting is through multiple leg autotomy (MLA), which involves removal of five to eight walking legs (Skinner and Graham, 1972; Skinner, 1985b, 1985a; Mykles, 2001, 2024). The molt stage can be determined by measuring the regeneration index (R-index or value), which is calculated by the [limb regenerate length (mm) x 100]/carapace width

(mm)] (Skinner, 1962, 1985b; Skinner and Graham, 1972; Holland and Skinner, 1976; Hopkins, 1982; Yu et al., 2002; Covi et al., 2010).

G. lateralis were collected in the Dominican Republic and shipped by air freight to Colorado State University (CSU) in Fort Collins, Colorado. Animals were kept in an environmental chamber at 27 °C and 75-80% relative humidity under a twelve-hour: light-dark cycle (Bliss and Boyer, 1964; Bliss et al., 1966b; Bliss, 1968; Covi et al., 2010). The land crabs were housed in large, plastic communal enclosures with Tekland Envigo Aspen Bedding Laboratory Grade #7093 shavings saturated with 5 parts per thousand (ppt) Instant Ocean®. Animals were fed twice a week on a diet consisting of lettuce, carrots, and calcium-coated raisins. Before any experimental testing or tissue harvesting was conducted, the blackback land crabs were acclimated to the lab setting for one month while the third right leg was autotomized to monitor any potential spontaneous molting (Covi et al., 2009).

Carcinus maenas is a marine species native in the eastern North Atlantic and has invaded temperate coastal and estuarine habitats all over the world (Ens et al., 2022). . Unlike *G. lateralis*, both ESA and MLA do not induce molting in *C. maenas.* In some *C. maenas* populations, green color morphs invest more energy towards molting, whereas red morphs invest more energy in reproduction (Abuhagr et al., 2014; Mykles, 2024). There is a large, well-established green crab population in Bodega Harbor (Bodega Bay, California), which provided a large number of animals for determining the effects of MF and JH-mimics on YO ecdysteroid secretion *in vitro* (Aim 2; Chapter 2). *C. maenas* were trapped in Bodega Harbor and maintained at the UC Davis Bodega Marine Laboratory (BML) in a flowing sea water system at ambient water temperatures (12–15 ˚C). For both brachyuran species, the molt stage was determined using the R-value, presence or absence of the membranous layer of the exoskeleton, and the

concentration of 20-E quantified with a competitive enzyme-linked immunosorbent assay (ELISA) as described and modified by Kingan (1989) and Abuhagr et al. (2014), respectively.

Summary

The main purpose of this research is to provide a greater understanding of the physiological transitions of the crustacean molting gland (Y-organ) by the endocrine crosstalk between the MF and ecdysone signaling pathways. The role of MF in ecdysteroid production depend on the level of ecdysteroids present in the hemolymph (Figure 1.6). Although the MO is believed to be the primary source of MF, the identification and expression of transcripts of the MF-synthetic pathway in the YO suggests that these organs can also synthesize MF. The identification and expression of transcripts of the MF signaling (MEKRE93) pathway in the YO suggests that the function of this pathway extends beyond development and metamorphosis (as established in insects), but, also acts as a regulator of molting and growth. The interactions between these two endocrine pathways can reveal the underlying mechanisms that drive ecdysteroid synthesis and insight into how the YO enters and exits the repressed state.

Table 1.1. Top decapod crab, food commodity species and relevant nutritional studies.

Food commodity	Species	References
King crab	*Paralithodes camtschaticus*	Dvoretsky et al., 2021 Ermolenko et al., 2023 Krzeczkowski et al., 1971 Latyshev et al., 2009
	Paralithodes platypus	Latyshev et al., 2009
	Lithodes santolla	Risso and Carelli, 2012
Snow crab	*Chionoecetes opilio*	Vilasoa-Martínez et al., 2007 Lauer et al., 1974 Addison et al., 1972 Latyshev et al., 2009
	Chionoecetes angulatus	Latyshev et al., 2009
	Chionoecetes japonicus	Latyshev et al., 2009
	Chionoecetes bairdi	Krzeczkowski and Stone, 1974
Soft shell crab	*Portunus sanguinolentus*	Wilson et al., 2017 Sudhakar et al., 2009
	Portunus pelagicus	Wu et al., 2010 Pathak et al., 2021 Lu et al., 2020
	Portunus trituberculatus	Lu et al., 2020 Chen et al., 2022 Yan et al., 2023a Huo et al., 2014 He et al., 2017a
	Scylla paramamosain	Wan Yusof et al., 2020 Gao et al., 2023
	Scylla tranquebarica	Sreelakshmi et al., 2016
	Scylla olivacea	Ullah et al., 2020 Azra et al., 2020 Karim et al., 2024
	Scylla serrata	Sreelakshmi et al., 2016 Sarower et al., 2013 Anas et al., 2009 Catacutan, 2002 Islam et al., 2022
	Callinectes sapidus	Çelik et al., 2004 Zotti et al., 2016 Kuley et al., 2008 Tsai et al., 1984 Küçükgülmez et al., 2006
Other crabs	*Eriocheir sinensis*	Wang et al., 2018 Wang et al., 2020 Chen et al., 2007 Wu et al., 2020 Shao et al., 2013 Guo et al., 2015 Kong et al., 2012
	Eriocheir japonica	Ermolenko et al., 2023 Wang et al., 2020
	Cancer borealis	Lauer et al., 1974
	Cancer pagurus	Barrento et al., 2009 Barrento et al., 2010 Zotti et al., 2016
	Carcinus mediterraneus	Cherif et al., 2008
	Carcinus maenas	Fulton and Fairchild, 2013 Skonberg and Perkins, 2002 Naczk et al., 2004
	Metacarcinus magister	Allen, 1971

Table 1.2. Ecdysteroid response genes in decapod crustaceans.

Infraorder	Scientific name	Early	Early–late	Late	References
Anomura	*Paralithodes camtschaticus*	Br-C, E75	HR3	Ftz-f1	Andersen et al., 2022
Brachyura	*Callinectes sapidus*		HR4		Legrand et al., 2021
	Chionoecetes opilio	Br-C, E75	HR3	Ftz-f1	Andersen et al., 2022
	Eriocheir sinensis	E75			Chen et al., 2023
	Gecarcinus laterallis	Br-C, E74, E75	HR3, HR4	Ftz-f1	Kim et al., 2005; Benrabaa et al., 2024
	Oziothelphusa senex senex	E75			Girish et al., 2015
	Portunus trituberculatus	E75, E93			Xie et al., 2016b; Ge et al., 2024
	Scylla paramamosain	E75			Gong et al., 2019
	Scylla serrata	E75			Girish et al., 2017
Astacidea	*Panulirus ornatus*	E75	E78, HR3, HR4, HR38	Ftz-f1	Hyde et al., 2019b
Achelata	*Homarus americanus*		HR3		Haj et al., 1997
	Procambarus clarkii	E74, E75			Zhu et al., 2017a, 2017b
Dendrobranchiata	*Fenneropenaeus chinensus*	E75			Priya et al., 2009, 2010
	Litopenaeus vannamei	Br-C, E74, E75	E78	Ftz-f1	Qian et al., 2014; Wei et al., 2014; Gao et al., 2015
	Metapenaeus ensis	E75		Ftz-f1	Chan, 1998; Chan and Chan, 1999
	Penaeus monodon	Br-C, E74, E75		Ftz-f1	Buaklin et al., 2011, 2013; Zhou et al., 2019; Si et al., 2022
Caridea	*Macrobrachium nipponense*		HR4	Ftz-f1	Yuan et al., 2021b, 2022
	Macrobrachium rosenbergii	E75	HR3		Guo et al., 2023
	Neocaridina denticulata	Br-C			Sin et al., 2015

Table 1.3. Comparison of the histology and ultrastructure of the crustacean mandibular organ (MO) and the Y-organ (YO).

	Mandibular organ (MO)	Both MO and YO	Y-organ (YO)
Characteristics	▪ Large cell size, with centered nuclei containing ample cytoplasm, generally arranged in clusters ▪ Site of MF production ▪ Identified by Le Roux (1968)	▪ Vascularized endocrine glands ▪ Contains an extensive smooth endoplasmic reticulum and abundant in mitochondria ▪ Located in the cephalothorax ▪ Experiences ultrastructural changes (e.g. hypertrophy) throughout the molt cycle and/or reproductive cycles	▪ Relatively small cell size, with peripherally located nuclei, tightly packed together ▪ Site of ecdysteroid production ▪ Identified by Gabe (1953)
Species & References	▪ *Barytelphusa cunicularis* (Gopal et al., 2018) ▪ *Callinectes sapidus* (Yudin et al., 1980) ▪ *Libinia emargnata* (Hinsch, 1977) ▪ *Homarus americanus* (Byard et al., 1975) (Borst et al., 1994) ▪ *Penaeus japonicus* (Taketomi and Kawano, 1985)	▪ *Carcinus maenas* (Buchholz and Adelung, 1980) ▪ *Hemigrapsus nudus* (Buchholz and Adelung, 1980) ▪ *Procambarus clarkii* (Taketomi and Nakano, 2007) ▪ *Palaemon paucidens* (Aoto et al., 1974)	▪ *Scylla olivacea* (Achdiat et al., 2024) ▪ *Portunus trituberculatus* (Taketomi and Hyodo, 1986) ▪ *Cancer antennarius* (Hinsch et al., 1980) ▪ *Travancoriana schirnerae* (Ayanath and Raghavan, 2021) (Smija and Sudha Devi, 2016) ▪ *Libinia emargnata* (Hinsch and Hajj, 1975)

Table 1.4. Tissue distribution of farnesoic acid O-methyl transferase (FAMeT) transcripts identified in decapod crustaceans. Abbreviations: Br, brain; CNS, central nervous system; Ep, epidermis; EG, eyestalk ganglia; Gi, gill; Hc, hemocytes; Hp, hepatopancreas; Ht, heart; In, intestine; MO, mandibular organ; Mu, muscle; NC, nerve cord; Ov, ovary; St, stomach; Te, testis; TG, thoracic ganglion, and YO, Y-organ.[1]

Species	Gene #	Br	CNS	Ep	EG	Gi	Hc	Hp	Ht	In	MO	Mu	NC	Ov	St	Te	TG	YO
Brachyura																		
Cancer pagurus[a]	1			X	X	X		X	X	X	X	X		X				
Eriocheir sinensis[b]	1					X		X	X	X				X	X			
Portunus pelagicus[c]	3	X		X	X						X	X						X
Portunus trituberculatus[d]	1					X		X	X		X	X		X		X	X	X
Scylla olivacea[e]	1										X							
Scylla paramamosain[f]	3	X			X	X		X	X		X	X		X	X		X	
	1*	X		X		X	X	X	X		X	X		X			X	
Astacidea																		
Homarus americanus[g]	1										X	X						
Procambarus clarkii[h]	1				X				X		X	X	X					
Dendrobranchiata																		
Litopenaeus vannamei[i]	2				X			X	X			X	X					
Metapenaeus ensis[h, j]	1			X	X			X	X		X	X	X	X		X		
Penaeus chinensis[k]	1				X	X	X	X	X			X		X		X		
Penaeus indicus[l]	1		X		X			X	X	X		X		X				
Penaeus monodon[m]	2													X				
Caridea																		
Exopalaemon carinicauda[n]	1				X	X	X	X		X		X		X	X			
Macrobrachium rosenbergii[o]	1			X	X	X	X	X	X	X		X			X	X		
Neocaridina denticulata[p]	1				X	X		X	X	X		X		X		X		

[1] Asterisk (*) indicates the FAMeT containing one methyltransferase domain and one DM9-repeat containing domain of unknown function (DUF) that differs from the conventional FAMeT with two methyltransferase domains. The presence of the FAMeT transcript in which gonadal tissue in *P. chinensis* was not specified and thereby both Ov and Te are denoted. References: [a]Ruddell et al., 2003; [b]Chen et al., 2021; [c]Kuballa et al., 2007; [d]Xie et al., 2013, 2015; [e]Sunarti et al., 2016; Tahya et al., 2016; [f]Yang et al., 2012; Zhao et al., 2018; [g]Holford et al., 2004; [h]Gunawardene et al., 2003; [i]Hui et al., 2008; [j]Gunawardene et al., 2001, 2002; [k]Li et al., 2013; [l]Saikrithi et al., 2019; [m]Buaklin et al., 2015; [n]Duan et al., 2014; [o]Qian and Liu, 2019; [p]Liu et al., 2022.

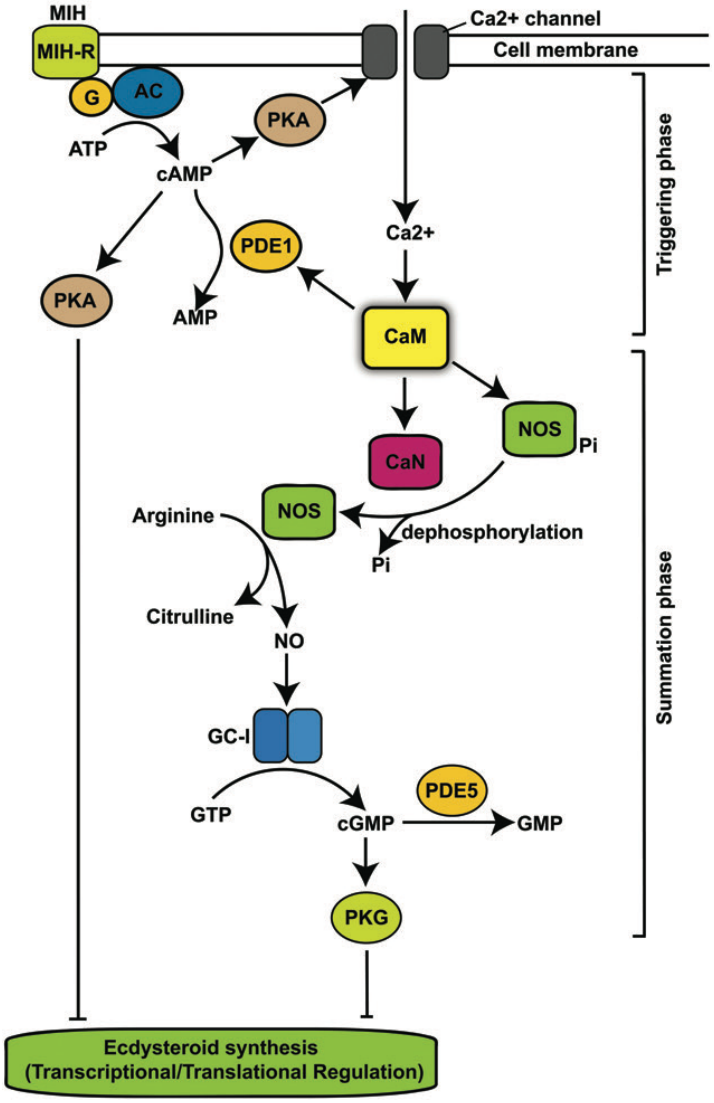

Figure 1.1. Proposed molt-inhibiting hormone (MIH) signaling pathway mediating the crustacean molting gland and ecdysteroidogenesis. The "triggering phase" is initiated by binding of MIH to its receptor (MIH–R), a hypothesized GPCR. Activation of adenylyl cyclase (AC)/cAMP increases intracellular Ca2+ via cAMP-dependent protein kinase (PKA) phosphorylation of Ca2+ channels. MIH sensitivity differs across the molt cycle and is determined by phosphodiesterase 1 (PDE1) activity. Calmodulin (CaM) connects the "triggering phase" to the "summation phase". The summation phase is mediated by NO and cGMP through the activation of NO synthase (NOS) by calcineurin (CaN), both directly and indirectly. CaN dephosphorylates NOS which can prolong the MIH response. Additionally, CaM can activate PDE1 to inhibit the triggering phase; PDE1 can hydrolyze cGMP and thereby inhibiting the "summation phase". cGMP-dependent protein kinase (PKG) inhibits ecdysteroidogenesis. From Covi et al. (2012).

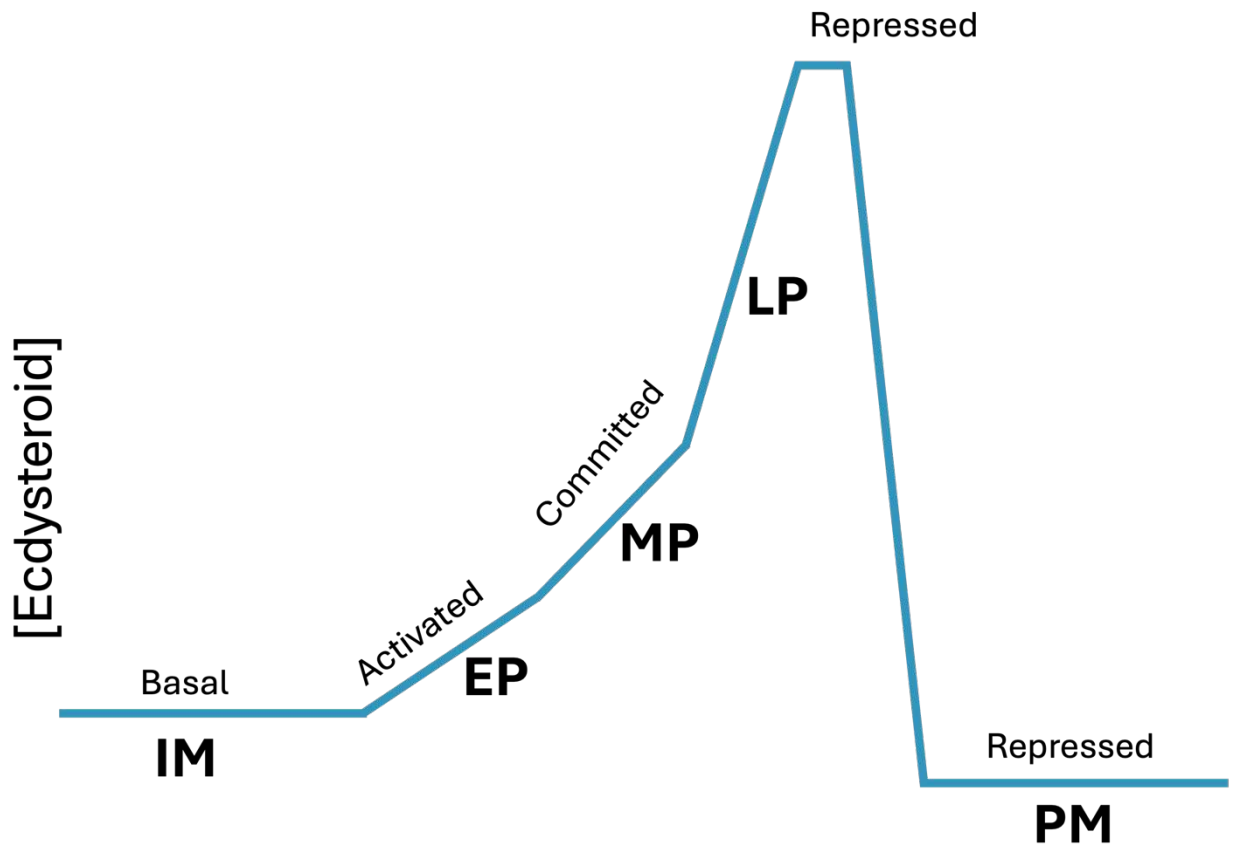

Figure 1.2. Schematic illustration of the Y-organ (YO) phenotypic status and hemolymph ecdysteroid concentration throughout the molt cycle. As ecdysteroid levels increase throughout the progression of molting, the YO transitions through four physiological states: basal in intermolt (IM), activated in early premolt (EP), committed in mid premolt (MP) and late premolt (LP), and repressed in the later phases of LP and post molt (PM). Modified from Chang and Mykles (2011).

Figure 1.3.

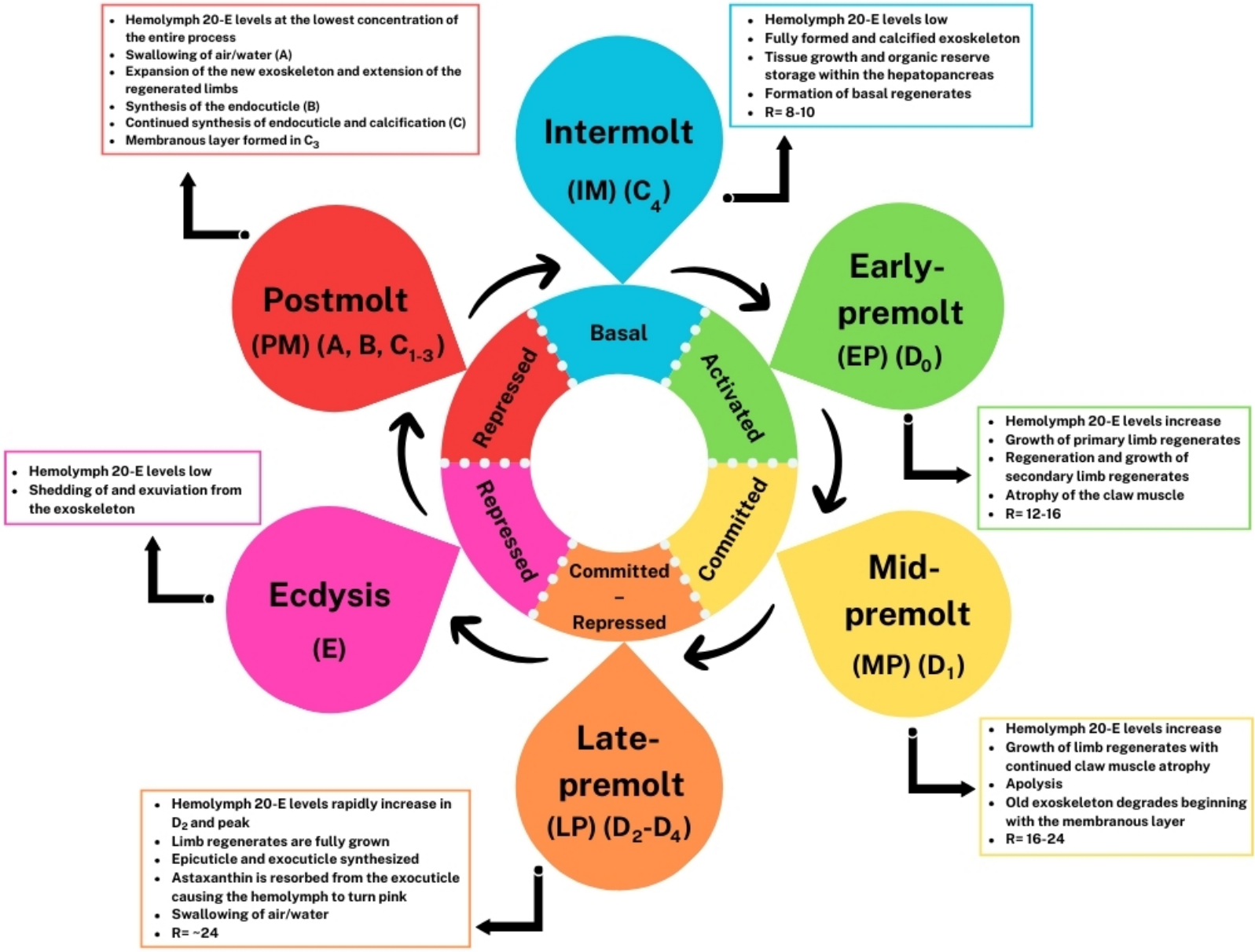
Hemolymph 20-E levels at the lowest concentration of the entire process
Swallowing of air/water (A)
Expansion of the new exoskeleton and extension of the regenerated limbs
Synthesis of the endocuticle (B)
Continued synthesis of endocuticle and calcification (C)
Membranous layer formed in C3
Intermolt (IM) (C4)
Hemolymph 20-E levels low
Fully formed and calcified exoskeleton
Tissue growth and organic reserve storage within the hepatopancreas
Formation of basal regenerates
R= 8-10
Postmolt (PM) (A, B, C1-3)
Early-premolt (EP) (D0)
Basal
Activated
Committed
Committed – Repressed
Repressed
Repressed
Hemolymph 20-E levels increase
Growth of primary limb regenerates
Regeneration and growth of secondary limb regenerates
Atrophy of the claw muscle
R= 12-16
Hemolymph 20-E levels low
Shedding of and exuviation from the exoskeleton
Ecdysis (E)
Mid-premolt (MP) (D1)
Late-premolt (LP) (D2-D4)
Hemolymph 20-E levels increase
Growth of limb regenerates with continued claw muscle atrophy
Apolysis
Old exoskeleton degrades beginning with the membranous layer
R= 16-24
Hemolymph 20-E levels rapidly increase in D2 and peak
Limb regenerates are fully grown
Epicuticle and exocuticle synthesized
Astaxanthin is resorbed from the exocuticle causing the hemolymph to turn pink
Swallowing of air/water
R= ~24

Figure 1.3. The general molt cycle and description of events as described in *G. lateralis* (Skinner, 1962; Mykles and Chang, 2020). Progression throughout the molt stages can be tracked by measuring the growth of the limb regenerates, or regeneration index (R-index) (Holland and Skinner, 1976; Yu et al., 2002).

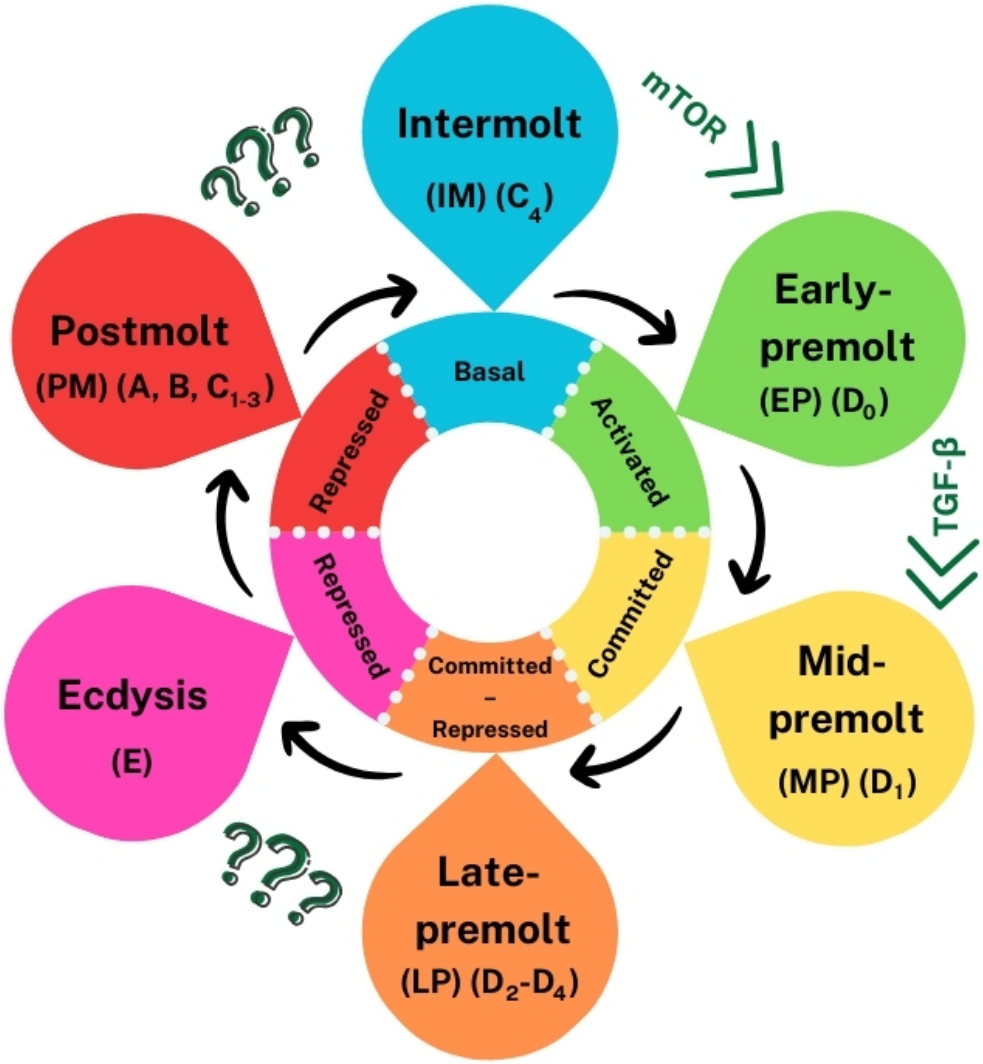

Figure 1.4. Signaling pathways associated with different stages of the crustacean molt cycle. The activation of the Y-organ (YO) is regulated through the mechanistic target of rapamycin complex 1 (mTORC1) signaling, while YO commitment is driven by the Transforming growth factor beta (TGF-β)/activin-myostatin pathway. The YO transition from the committed-to-repressed state coincides with the peak in hemolymph 20-E titer in late premolt (LP). The YO transition from the repressed back to the basal state is proposed to occur at the end of postmolt (PM), when the synthesis and calcification of the new exoskeleton is complete.

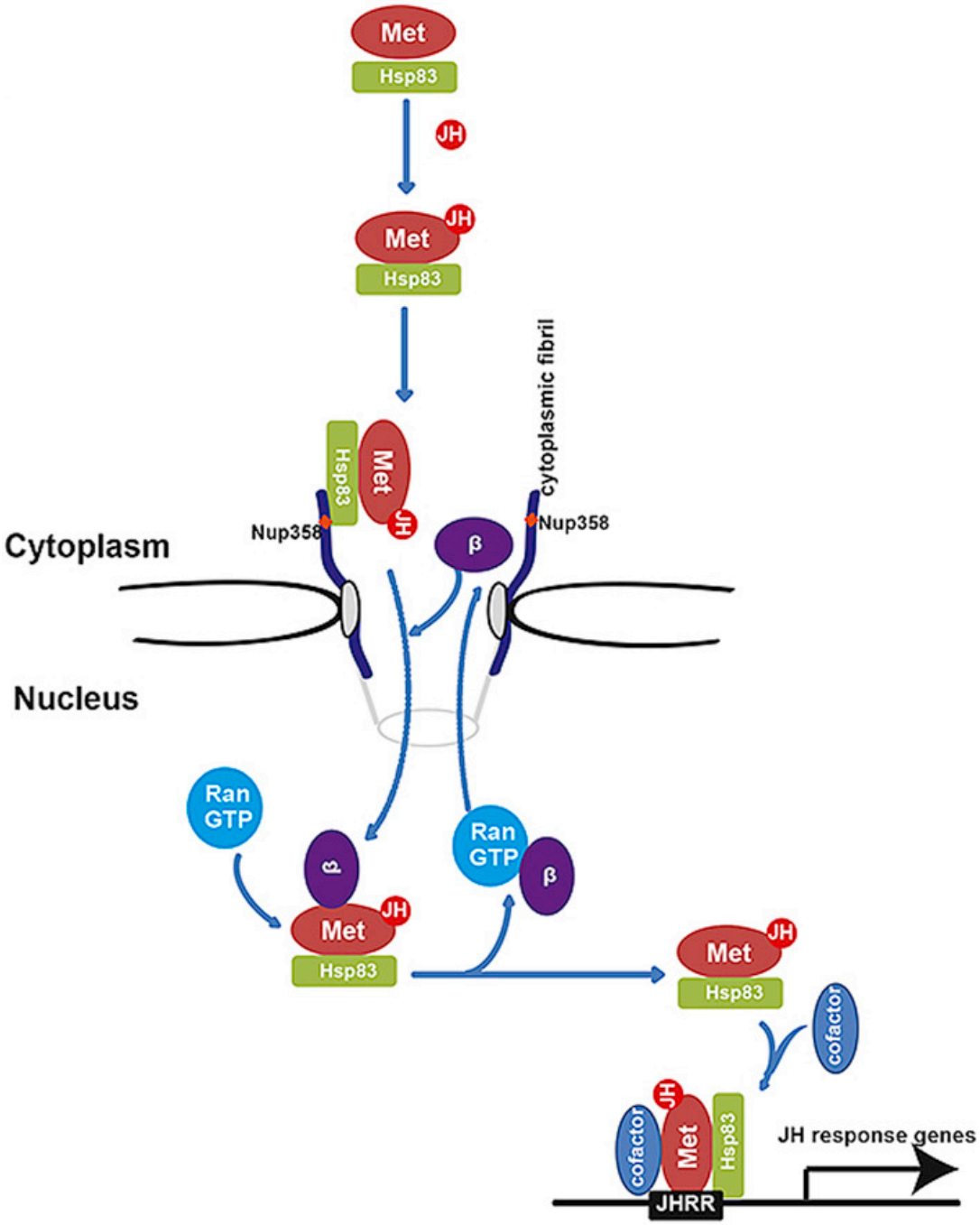

Figure 1.5. Proposed model of juvenile hormone (JH) signaling through Methoprene tolerant (Met) nuclear import. Importin β transports the Met receptor complex as a result of heat shock protein 83 (Hsp83) binding to the Nucleoporin 358 (Nup358) and the recognition of the nuclear localization signal (NLS). RanGTP binding to importin β dissociates the receptor complex thereby allowing Met to bind to JH primary response genes, such as Krüppel homolog 1 (Kr-h1). From He et al. (2017).

Figure 1.6

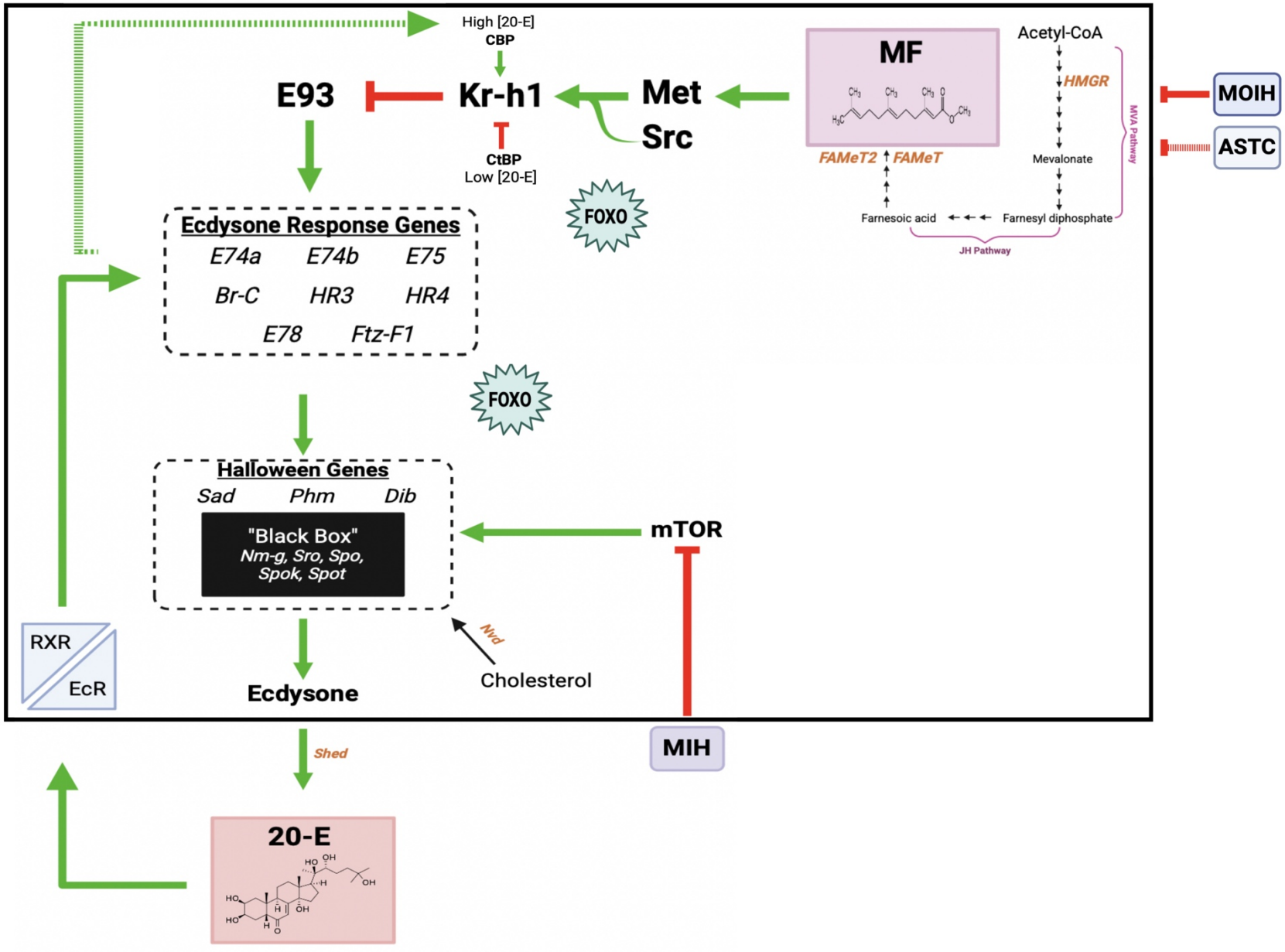
High [20-E]
CBP
E93
Kr-h1
CtBP
Low [20-E]
Met
Src
MF
Acetyl-CoA
HMGR
MVA Pathway
FAMeT2
FAMeT
Mevalonate
Farnesoic acid
Farnesyl diphosphate
JH Pathway
MOIH
ASTC
FOXO
Ecdysone Response Genes
E74a
E74b
E75
Br-C
HR3
HR4
E78
Ftz-F1
FOXO
Halloween Genes
Sad
Phm
Dib
"Black Box"
Nm-g, Sro, Spo, Spok, Spot
mTOR
Nvd
Cholesterol
RXR
EcR
Ecdysone
MIH
Shed
20-E

Figure 1.6. Mediation of ecdysteroidogenesis through the methyl farnesoate (MF) transcriptional cascade of Methoprene tolerant (Met) – Krüppel homolog 1 (Kr-h1) – Ecdysone response gene 93 (E93) in the Y-organ (YO). MF is proposed to act as an autocrine factor to regulate the endocrine cross talk with 20-E as the genes encoding for the synthetic enzymes were identified including *3-hydroxy-3-methylglutaryl-CoA reductase* (*HMGR*) and *farnesoic acid O-methyltransferase* (*FAMeT*). MF biosynthesis is inhibited by mandibular-organ inhibiting hormone (MOIH) and potentially Allatostatin C (ASTC). High hemolymph titers of 20-E, such as in mid and/or late premolt (MP and/or LP) inhibit 20-E synthesis thus leading to the transition from a committed to repressed state. By contrast, low 20-E titers in the hemolymph, such as in intermolt (IM) when the YO is in a basal or repressed state, stimulate the YO ecdysteroid production. Although molt-inhibiting hormone (MIH) inhibits ecdysteroid synthesis through the mechanistic target of rapamycin complex 1 (mTORC1), MF is proposed to act as an autocrine factor acting through the action of Kr-h1, mediated by transcriptional corepressor C-terminal-binding protein (CtBP) and/or CREB-binding protein (CBP), facilitating the expression of the ecdysone response genes and in turn the ecdysteroid biosynthetic genes. Ecdysteroidogenesis may further be impacted at a transcriptional level with the consideration to the transcription factor forkhead box O (FOXO) which has been implicated in both MF and 20-E pathways.

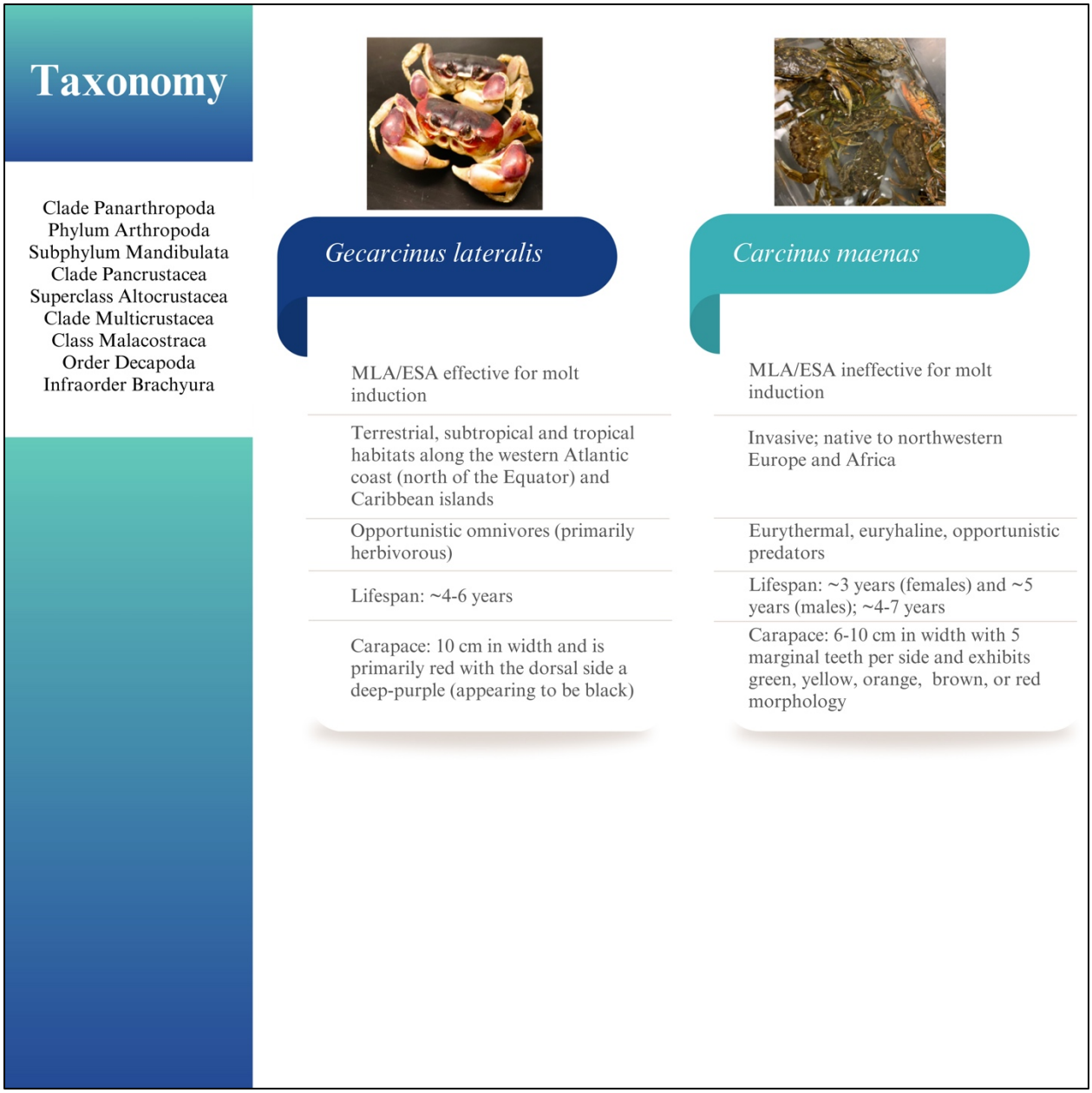

Figure 1.7. Characteristics of the two model organisms, the blackback land crab (*Gecarcinus lateralis*) and the European green shore crab (*Carcinus maenas*), incorporated in the following research studies

REFERENCES

Abdu, U., Barki, A., Karplus, I., Barel, S., Takac, P., Yehezkel, G., Laufer, H., and Sagi, A. (2001). Physiological effects of methyl farnesoate and pyriproxyfen on wintering female crayfish *Cherax quadricarinatus*. *Aquaculture*. **202**, 163–175.

Abdu, U., Takac, P., Laufer, H., and Sagi, A. (1998). Effect of Methyl Farnesoate on Late Larval Development and Metamorphosis in the Prawn *Macrobrachium rosenbergii* (Decapoda, Palaemonidae): A Juvenoid-like Effect? *Reference: Biol. Bull.* **195**, 112–119.

Abdullah-Zawawi, M. R., Afiqah-Aleng, N., Ikhwanuddin, M., Sung, Y. Y., Tola, S., Fazhan, H., and Waiho, K. (2021). Recent development in ecdysone receptor of crustaceans: current knowledge and future applications in crustacean aquaculture. *Reviews in Aquaculture.* **13**, 1938–1957.

Abehsera, S., Bentov, S., Li, X., Weil, S., Manor, R., Sagi, S., Li, S, Li, F., Khalaila, I., Aflalo, E. D., and Sagi, A. (2021). Genes encoding putative bicarbonate transporters as a missing molecular link between molt and mineralization in crustaceans. *Scientific Reports.* **11**, 11722.

Ables, E. T., Bois, K. E., Garcia, C. A., and Drummond-Barbosa, D. (2015). Ecdysone response gene E78 controls ovarian germline stem cell niche formation and follicle survival in *Drosophila*. *Dev Biol.* **400** (1), 33–42.

Abuhagr, A. M., Blindert, J. L., Nimitkul, S., Zander, I. A., LaBere, S. M., Chang, S. A., MacLea, K. S., Chang, E. S. (2014). Molt regulation in green and red color morphs of the crab *Carcinus maenas*: gene expression of molt-inhibiting hormone signaling components. *Journal of Experimental Biology.* **217** (5), 796–808.

Abuhagr, A. M., MacLea, K. S., Mudron, M. R., Chang, S. A., Chang, E. S., and Mykles, D. L. (2016). Roles of mechanistic target of rapamycin and transforming growth factor-β signaling in the molting gland (Y-organ) of the blackback land crab, *Gecarcinus lateralis*. *Comp Biochem Physiol A Mol Integr Physiol.* **198**, 15–21.

Achdiat, M., Fujaya, Y., Fazhan, H., Rozaimi, R., Chung, J. S., Wang, Y., Tan, K., Shu-Chien, A. C., Maulidiani, M., and Waiho, K. (2024). Identification and Characterization of the Y-Organ of Orange Mud Crab *Scylla Olivacea*. *Microscopy Research and Technique*. **0**, 1–12.

Addison, R. F., Ackman, R. G., and Hingley, J. (1972). Lipid Composition of the Queen Crab (*Chionoecetes opilio*). *Canadian Journal of Fisheries and Aquatic Sciences.* **29** (4), 407–411.

Ahmed, S. (2023). Applications of *Daphnia Magna* in Ecotoxicological Studies: A Review. *J. Adv. Res. Biology*. **6** (2), 16–35.

Allen, W. V. (1971). Amino Acid and Fatty Acid Composition of Tissues of the Dungeness crab (*Cancer magister*). *J. Fish. Res. Bd. Canada.* **28** (8), 1191–1195.

Alnawafleh, T., Kim, B. K., Kang, H. E., Yoon, T. H., and Kim, H. W. (2014). Stimulation of Molting and Ovarian Maturation by Methyl Farnesoate in the Pacific White Shrimp *Litopenaeus vannamei* (Boone, 1931). *Fish. Aquat. Sci*. **17** (1), 115–121.

Anas, M. U. M., Edirisinghe, E. M. R. K. B., and Jayasinghe, J. M. P. K. (2009). Lipid composition and fatty acid profiles of wild caught and fattened mud crab, Scylla serrata, in Sri Lanka. *Sri Lanka J. Aquat. Sci*. **14**, 75-85.

Andersen, Ø., Johnsen, H., Wittmann, A. C., Harms, L., Thesslund, T., Berg, R. S., Siikavuopio, and Mykles, D. L. (2022). *De novo* transcriptome assemblies of red king crab (*Paralithodes camtschaticus*) and snow crab (*Chionoecetes opilio*) molting gland and eyestalk ganglia - Temperature effects on expression of molting and growth regulatory genes in adult red king crab. *Comp. Biochem. Physiol. B: Biochem. Mol. Biol.* **257**.

Andreasen, E. A., Spitsbergen, J. M., Tanguay, R. L., Stegeman, J. J., Heideman, W., and Peterson, R. E. (2002). Tissue-Specific Expression of AHR2, ARNT2, and CYP1A in Zebrafish Embryos and Larvae: Effects of Developmental Stage and 2,3,7,8-Tetrachlorodibenzo-*p*-dioxin Exposure. *Toxicological Sciences*. **68**, 403–419.

Aoto, T., Kamiguchi, Y., and Hisano, S. (1974). Histological and Ultrastructural Studies on the Y Organ and the Mandibular Organ of the Freshwater Prawn, *Palaemon paucidens,* with Special Reference to Their Relation with the Molting Cycle. *Jour. Fac. Sci. Hokkaido Univ. Ser. VI, Zool.* **19** (2).

Asazuma, H., Nagata, S., Katayama, H., Ohira, T., and Nagasawa, H. (2005). Characterization of a Molt-Inhibiting Hormone (MIH) Receptor in the Y-Organ of the Kuruma Prawn, *Marsupenaeus japonicus*. *Ann. N.Y. Acad. Sci.* **1040**, 215–218.

Asazuma, H., Nagata, S., and Nagasawa, H. (2009). Inhibitory Effect of Molt-Inhibiting Hormone on *Phantom* Expression in the Y-Organ of the Kuruma Prawn, *Marsupenaeus japonicus*. *Arch. Insect Biochem. Physiol.* **72**, 220–233.

Ashburner, M., Chihara, C., Meltzer, P., and Richards, G. (1974). Temporal Control of Puffing Activity in Polytene Chromosomes. *Cold Spring Harb. Symp. Quant. Biol.* **38**, 655–662.

Atchley, W. R. and Fitch, W. M. (1997). A natural classification of the basic helix-loop-helix class of transcription factors. *Proc. Natl. Acad. Sci.* **94** (10), 5172–5176.

Ayanath, A. and Raghavan, S. D. A. (2021). Effect of 20-OH ecdysone and methyl farnesoate on histomorphology of the Y-organ during late intermoult and postmoult stages in the freshwater crab *Travancoriana schirnerae* Bott, 1969 (Crustacea: Gecarcinucidae). *Nauplius.* **29**, e2021037.

Azra, M. N., Tavares, C. P. D. S., Abol-Munafi, A. B., and Ikhwanuddin, M. (2020). Growth rate and fatty acid composition of orange mud crab instars, *Scylla olivacea*, reared at different temperatures. *Egypt J. Aquat. Res.* **46**, 97–102.

Baehrecke, E. H. and Thummel, C. S. (1995). The *Drosophila* E93 gene from the 93F early puff displays stage- and tissue-specific regulation by 20-hydroxyecdysone. *Dev. Biol.* **171** (1), 85–97.

Bain, D. L., Heneghan, A. F., Connaghan-Jones, K. D., and Miura, M. T. (2007). Nuclear receptor structure: implications for function. *Annu. Rev. Physiol.* **69**, 201–220.

Barrento, S., Marques, A., Teixeira, B., Anacleto, P., Vaz-Pires, P., and Nunes, M. L. (2009). Effect of season on the chemical composition and nutritional quality of the edible crab *Cancer pagurus*. *J. Agric. Food Chem.* **57** (22), 10814–10824.

Barrento, S., Marques, A., Teixeira, B., Mendes, R., Bandarra, N., Vaz-Pires, P., and Nunes, M. L. (2010). Chemical composition, cholesterol, fatty acid and amino acid in two populations of brown crab *Cancer pagurus*: Ecological and human health implications. *Journal of Food Composition and Analysis.* **23**, 716–725.

Barthel, A., Schmoll, D., and Unterman, T. G. (2005). FoxO proteins in insulin action and metabolism. *TRENDS in Endocrinology and Metabolism.* **16** (4), 183–189.

Bednaršek, N., Feely, R. A., Beck, M. W., Alin, S. R., Siedlecki, S. A., Calosi, P., Norton, E. L., Saenger, C., Štrus, J., Greeley, D., Nezlin, N. P., Roethler, M., and Spicer, J. I. (2020). Exoskeleton dissolution with mechanoreceptor damage in larval Dungeness crab related to severity of present-day ocean acidification vertical gradients. *Science of the Total Environment*. **716**, 136610.

Belles, X. (2019). The innovation of the final moult and the origin of insect metamorphosis. *Phil. Trans. R. Soc. B.* **374**, 20180415.

Bellés, X., Martín, D., and Piulachs, M. D. (2005). The Mevalonate Pathway and the Synthesis of Juvenile Hormone in Insects. *Annu. Rev. Entomol.* **50**, 181–199.

Belles, X. and Santos, C. G. (2014). The MEKRE93 (Methoprene tolerant-Krüppel homolog 1-E93) pathway in the regulation of insect metamorphosis, and the homology of the pupal stage. *Insect Biochemistry and Molecular Biology.* **52**, 60–68.

Benrabaa, S. A. M., Chang, S. A., Chang, E. S., and Mykles, D. L. (2023). Effects of molting on the expression of ecdysteroid biosynthesis genes in the Y-organ of the blackback land crab, *Gecarcinus lateralis*. *General and Comparative Endocrinology.* **340**, 114304.

Benrabaa, S. A. M., Chang, S. A., Chang, E. S., and Mykles, D. L. (2024). Effects of molting on the expression of ecdysteroid responsive genes in the crustacean molting gland (Y-organ). *General and Comparative Endocrinology.* **355**, 114548.

Berger, H. M., Siedlecki, S. A., Matassa, C. M., Alin, S. R., Kaplan, I. C., Hodgson, E. E., Pilcher, D. L., Norton, E. L., andNewton, J. A. (2021). Seasonality and Life History Complexity Determine Vulnerability of Dungeness Crab to Multiple Climate Stressors. *AGU Advances.* **2**, e2021AV000456.

Bernardo, T. J. and Dubrovsky, E. B. (2012). Molecular Mechanisms of Transcription Activation by Juvenile Hormone: A Critical Role for bHLH-PAS and Nuclear Receptor Proteins. *Insects* **3**, 324–338.

Bernot, J. P., Owen, C. L., Wolfe, J. M., Meland, K., Olesen, J., and Crandall, K. A. (2023). Major Revisions in Pancrustacean Phylogeny and Evidence of Sensitivity to Taxon Sampling. *Mol. Biol. Evol.* **40** (8).

Bialecki, M., Shilton, A., Fichtenberg, C., Segraves, W. A., and Thummel, C. S. (2002). Loss of the ecdysteroid-inducible E75A orphan nuclear receptor uncouples molting from metamorphosis in *Drosophila*. *Dev Cell.* **3** (2), 209–220.

Bliss, D. E. (1968). Transition from Water to Land in Decapod Crustaceans. *Am. Zool.* **8** (3), 355–392.

Bliss, D. E. (1979). From Sea to Tree: Saga of a Land Crab. *Am. Zool.* **19** (2), 385–410.

Bliss, D. E. and Boyer, J. R. (1964). Environmental Regulation of Growth in the Decapod Crustacean *Gecarcinus lateralis*. *General and Comparative Endocrinology.* **4** (1), 15–41.

Bliss, D. E., Durand, J. B., and Welsh, J. H. (1954). Neurosecretory Systems in Decapod Crustacea. *Zeitschrift für Zellforschung, Bd.* **39**, 520–536.

Bliss, D. E., Wang, S. M. E., and Martinez, E. A. (1966a). Water balance in the land crab, *Gecarcinus lateralis*, during the intermolt cycle. *Am. Zool.* **6** (2), 197–212.

Bliss, D. E. and Welsh, J. H. (1952). The Neurosecretory System of Brachyuran Crustacea. *Biological Bulletin.* **103** (2), 157–169.

Böcking, D., Dircksen, H., and Keller, R. (2002). "The Crustacean Neuropeptides of the CHH/MIH/GIH Family: Structures and Biological Activities," in *The Crustacean Nervous System*, (Springer), 84–97.

Boenish, R., Kritzer, J. P., Kleisner, K., Steneck, R. S., Werner, K. M., Zhu, W., Schram, F., Rader, D., Cheung, W., Ingles, J., Tian, Y., Mimikakis J. (2022). The global rise of crustacean fisheries. *Front. Ecol. Environ.* **20** (2), 102–110.

Bonchuk, A. N. and Georgiev, P. G. (2024). C2H2 proteins: Evolutionary aspects of domain architecture and diversification. *BioEssays.* **46**, 2400052.

Bondad-Reantaso, M. G., Subasinghe, R. P., Josupeit, H., Cai, J., and Zhou, X. (2012). The role of crustacean fisheries and aquaculture in global food security: Past, present and future. *Journal of Invertebrate Pathology.* **110**, 158–165.

Borst, D. W., Laufer, H., Landau, M., Chang, E. S., Hertz, W. A., Baker, F. C., and Schooley, D. A. (1987). Methyl farnesoate and its role in crustacean reproduction and development. *Insect Biochemistry.* **17** (7) 1123–1127.

Borst, D. W., Ogan, J., Tsukimura, B., Claerhout, T., and Holford, K. C. (2001). Regulation of the Crustacean Mandibular Organ. *Amer. Zool.* **41** (3), 430–441.

Borst, D. W. and Tsukimura, B. (1991). Quantification of methyl farnesoate levels in hemolymph by high-performance liquid chromatography. *Journal of Chromatography.* **545**, 71–78.

Borst, D. W., Tsukimura, B., Laufer, H., and Couch, E. F. (1994). Regional Differences in Methyl Farnesoate Production by the Lobster Mandibular Organ. *Biol. Bull.* **186** (1), 9–16.

Boyd, C. E., McNevin, A. A., and Davis, R. P. (2022). The contribution of fisheries and aquaculture to the global protein supply. *Food Sec.* **14**, 805–827.

Boyd, J. M., Subramanian, T., Schaeper, U., La Regina, M., Bayley, S., and Chinnadurai, G. (1993). A region in the C-terminus of adenovirus 2/5 E1a protein is required for association with a cellular phosphoprotein and important for the negative modulation of T24-ras mediated transformation, tumorigenesis and metastasis. *EMBO J.* **12** (2), 469–478.

Brunet, J., Eichner, C., and Male, R. (2021). The FTZ-F1 gene encodes two functionally distinct nuclear receptor isoforms in the ectoparasitic copepod salmon louse (*Lepeophtheirus salmonis*). *PLoS One.* **16** (5), e0251575.

Buaklin, A., Jantee, N., Sittikankaew, K., Chumtong, P., Janpoom, S., Menasveta, P., Klinbunga, S., and Khamnamtong, B. (2015). Expression and polymorphism of farnesoic acid *O*-methyltransferase (FAMeT) and association between its SNPs and reproduction-related parameters of the giant tiger shrimp *Penaeus monodon*. *Aquaculture.* **441**, 106–117.

Buaklin, A., Klinbunga, S., and Mensveta, P. (2011). Identification and expression analysis of the *Broad-Complex core protein isoform 6* (*BR-C Z6*) gene in the giant tiger shrimp *Penaeus monodon* (Penaeidae: Decapoda). *Genet, and Mol. Res.* **10** (4), 2290–2306.

Buaklin, A., Sittikankaew, K., Khamnamtong, B., Menasveta, P., and Klinbunga, S. (2013). Characterization and expression analysis of the *Broad-complex* (*Br-c*) gene of the giant tiger shrimp *Penaeus monodon*. *Comparative Biochemistry and Physiology - B Biochemistry and Molecular Biology.* **164** (4), 280–289.

Buchholz, C. and Adelung, D. (1980). The ultrastructural basis of steroid production in the Y-organ and the mandibular organ of the crabs Hemigrapsus nudus (Dana) and *Carcinus maenas* L. *Cell and Tissue Res*. **206** (1), 83–94.

Byard, E. H., Shivers, R. R., and Aiken, D. E. (1975). The mandibular organ of the lobster, *Homarus americanus*. *Cell and Tissue Res*. **162** (1), 13–22.

Cáceres, L., Necakov, A. S., Schwartz, C., Kimber, S., Roberts, I. J. H., and Krause, H. M. (2011). Nitric oxide coordinates metabolism, growth, and development via the nuclear receptor E75. *Genes Dev.* **25** (14), 1476–1485.

Carlton, J. T. and Cohen, A. N. (2003). Episodic global dispersal in shallow water marine organisms: The case history of the European shore crabs *Carcinus maenas* and *C. aestuarii*. *Journal of Biogeography.* **30** (12), 1809–1820.

Catacutan, M. R. (2002). Growth and body composition of juvenile mud crab, Scylla serrata, fed different dietary protein and lipid levels and protein to energy ratios. *Aquaculture.* **208**, 113–123.

Çelik, M., Türeli, C., Çelik, M., Yanar, Y., Erdem, Ü., and Küçükgülmez, A. (2004). Fatty acid composition of the blue crab (*Callinectes sapidus* Rathbun, 1896) in the north eastern Mediterranean. *Food Chem.* **88** (2), 271–273.

Chafino, S., Giannios, P., Casanova, J., Martín, D., and Franch-Marro, X. (2023). Antagonistic role of the BTB-zinc finger transcription factors Chinmo and Broad-Complex in the juvenile/pupal transition and in growth control. *Elife*. **12**, e84648.

Chafino, S., Ureña, E., Casanova, J., Casacuberta, E., Franch-Marro, X., and Martín, D. (2019). Upregulation of E93 Gene Expression Acts as the Trigger for Metamorphosis Independently of the Threshold Size in the Beetle *Tribolium castaneum*. *Cell Rep.* **27** (4), 1039-1049.e2.

Chan, S.M. (1998). Cloning of a shrimp (*Metapenaeus ensis*) cDNA encoding a nuclear receptor superfamily member: an insect homologue of E75 gene. *FEBS Lett.* **436** (3), 395–400.

Chan, S.M. and Chan, K.M. (1999). Characterization of the shrimp eyestalk cDNA encoding a novel fushi tarazu-factor 1 (FTZ-F1). *FEBS Lett.* **454**, 109–114.

Chang, E. S. (1985). Hormonal Control of Molting in Decapod Crustacea. *Amer. Zool.* **25** (1), 179–185.

Chang, E. S. (1993). Comparative Endocrinology of Molting and Reproduction: Insects and Crustaceans. *Annu. Rev. Entomol.* **38**, 161–180.

Chang, E. S. (1995). Physiological and biochemical changes during the molt cycle in decapod crustaceans: an overview. *Journal of Experimental Marine Biology and Ecology.* **193**, 1–14.

Chang, E. S., Bruce, M. J., and Tamone, S. L. (1993). Regulation of Crustacean Molting: A Multi-Hormonal System. *American Zoologist*. **33** (3), 324–329.

Chang, E. S. and Mykles, D. L. (2011). Regulation of crustacean molting: A review and our perspectives. *Gen. Comp. Endocrinol.* **172** (3), 323–330.

Chang, W. H. and Lai, A. G. (2018). Genome-wide analyses of the bHLH superfamily in crustaceans: reappraisal of higher-order groupings and evidence for lineage-specific duplications. *R. Soc. Open Sci.* **5** (3), 172433.

Charles, J. P., Iwema, T., Epa, V. C., Takaki, K., Rynes, J., and Jindra, M. (2011). Ligand-binding properties of a juvenile hormone receptor, Methoprene-tolerant. *Proc. Natl. Acad. Sci. U. S. A.* **108** (52), 21128–21133.

Chen, D. W., Zhang, M., and Shrestha, S. (2007). Compositional characteristics and nutritional quality of Chinese mitten crab (*Eriocheir sinensis*). *Food Chem.* **103** (4), 1343–1349.

Chen, H. Y., Toullec, J. Y., and Lee, C. Y. (2020). The Crustacean Hyperglycemic Hormone Superfamily: Progress Made in the Past Decade. *Front. Endocrinol.* **11**, 578958.

Chen, T., Diao, Y., Xu, R., Sheng, N., Liu, F., Xie, Q., Su, S., Ma, K., and Li, X. (2022a). Cloning and expression analysis of juvenile hormone epoxide hydrolase-like (*EsJHEH-like*) from *Eriocheir sinensis*, and its potential roles in methyl farnesoate metabolism. *Invertebrate Reproduction & Development*. **66** (1), 23–32.

Chen, T., Xu, R., Sheng, N., Che, S., Zhu, L., Liu, F., Su, S., Ding, S., and Li, X. (2021a). Molecular evidence for farnesoic acid *O*-methyltransferase (FAMeT) involved in the biosynthesis of vitellogenin in the Chinese mitten crab *Eriocheir sinensis*. *Animal Reproduction Science.* **234**, 106868.

Chen, T., Xu, R., Sheng, N., Che, S., Zhu, L., Liu, F., Su, S., Ding, S., and Li, X. (2022b). RNAi silencing of the 3-hydroxy-3-methylglutaryl coenzyme A reductase (*HMGR*) gene inhibits vitellogenesis in Chinese mitten crab *Eriocheir sinensis*. *Comp. Biochem. Physiol. A Mol. Integr. Physiol.* **263**, 111078.

Chen, W., Li, X., Qin, K., Gao, T., Wang, C., and Wang, H. (2022c). Effects of low salinity on fatty acid and free amino acid composition of muscle tissues in *Portunus trituberculatus*. *Aquaculture Research.* **53** (5), 1627–1635.

Chen, X., Gao, Q., Cheng, H., Peng, F., Wang, C., and Xu, B. (2021b). Molecular cloning and expression pattern of the juvenile hormone epoxide hydrolase gene from the giant freshwater prawn *Macrobrachium rosenbergii* during larval development and the moult cycle. *Aquac. Res.* **52**, 3890–3899.

Chen, X., Hou, X., Yang, H., Liu, H., Wang, J., and Wang, C. (2023). Molecular interplay between ecdysone receptor and retinoid X receptor in regulating the molting of the Chinese mitten crab, *Eriocheir sinensis*. *Front Endocrinol.* **14**.

Cheong, S. P. S., Huang, J., Bendena, W. G., Tobe, S. S., and Hui, J. H. L. (2015). Evolution of Ecdysis and Metamorphosis in Arthropods: The Rise of Regulation of Juvenile Hormone. *Integr. Comp. Biol*. **55** (5), 878–890.

Cherif, S., Frikha, F., Gargouri, Y., and Miled, N. (2008). Fatty acid composition of green crab (*Carcinus mediterraneus*) from the Tunisian mediterranean coasts. *Food Chem.* **111** (4), 930–933.

Chinnadurai, G. (2007). Transcriptional regulation by C-terminal binding proteins. *Int. J. Biochem. Cell Biol.* **39** (9), 1593–1607.

Cho, H., Jeong, C. B., and Lee, Y. M. (2022). Modulation of ecdysteroid and juvenile hormone signaling pathways by bisphenol analogues and polystyrene beads in the brackish water flea *Diaphanosoma celebensis*. *Comparative Biochemistry and Physiology Part - C: Toxicology and Pharmacology.* **262**, 109462.

Chung, J. S. and Webster, S. G. (2005). Dynamics of in Vivo release of Molt-Inhibiting Hormone and Crustacean Hyperglycemic Hormone in the Shore Crab, *Carcinus maenas*. *Endocrinology.* **146** (12), 5545–5551.

Chung, J. S., Zmora, N., Katayama, H., and Tsutsui, N. (2010). Crustacean hyperglycemic hormone (CHH) neuropeptides family: Functions, titer, and binding to target tissues. *Gen. Comp. Endocrinol.* **166** (3), 447–454.

Claerhout, T., Bendena, W., Tobe, S. S., and Borst, D. W. (1996). Characterization of methyl transferase activity in the mandibular organ of the American lobster, *Homarus americanus*. *Biol. Bull.* **191** (2), 304–304.

Coumailleau, P., Poellinger, L., Gustafsson, J.-Å., and Whitelaw, M. L. (1995). Definition of a Minimal Domain of the Dioxin Receptor That Is Associated with Hsp90 and Maintains Wild Type Ligand Binding Affinity and Specificity. *J. Biol. Chem.* **270** (42), 25291–25300.

Covi, J. A., Bader, B. D., Chang, E. S., and Mykles, D. L. (2010). Molt cycle regulation of protein synthesis in skeletal muscle of the blackback land crab, *Gecarcinus lateralis*, and the differential expression of a myostatin-like factor during atrophy induced by molting or unweighting. *J. Exp. Biol.* **213** (1), 172–183.

Covi, J. A., Chang, E. S., and Mykles, D. L. (2009). Conserved role of cyclic nucleotides in the regulation of ecdysteroidogenesis by the crustacean molting gland. *Comp. Biochem. Physiol. A Mol. Integr. Physiol.* **152** (4), 470–477.

Covi, J. A., Chang, E. S., and Mykles, D. L. (2012). Neuropeptide signaling mechanisms in crustacean and insect molting glands. *Invertebrate Reproduction and Development*. **56** (1), 33–49.

Crews, S. T. (1998). Control of cell lineage-specific development and transcription by bHLH-PAS proteins. *Genes Dev.* **12** (5), 607–620.

Crews, S. T. and Fan, C.M. (1999). Remembrance of things PAS: regulation of development by bHLH-PAS proteins. *Current Opinion in Genetics & Development.* **9** (5), 580–587.

Daffern, N. and Radhakrishnan, I. (2024). Per-ARNT-Sim (PAS) Domains in Basic Helix-Loop-Helix (bHLH)-PAS Transcription Factors and Coactivators: Structures and Mechanisms. *J. Mol. Biol.* **436** (3), 168370.

Dancy, B. M. and Cole, P. A. (2015). Protein lysine acetylation by p300/CBP. *Chem. Rev.* **115** (6), 2419–2452.

Das, S., Pitts, N. L., Mudron, M. R., Durica, D. S., and Mykles, D. L. (2016). Transcriptome analysis of the molting gland (Y-organ) from the blackback land crab, *Gecarcinus lateralis*. *Comp. Biochem. Physiol. Part D Genomics Proteomics.* **17**, 26–40.

Defelipe, L. A., Dolghih, E., Roitberg, A. E., Nouzova, M., Mayoral, J. G., Noriega, F. G., and Turjanski, A. G. (2011). Juvenile hormone synthesis: "esterify then epoxidize" or " epoxidize then esterify" ? Insights from the structural characterization of juvenile hormone acid methyltransferase. *Insect Biochem. Mol. Biol.* **41** (4), 228–235.

Devi, S., Raghavan, A., and Ayanath, A. (2018). Effect of Methyl Farnesoate Administration on Ovarian Growth and Maturation in the Freshwater Crab *Travancoriana schirnerae*. *Egypt J. Aquat. Biol. Fish.* **22** (5), 257–271.

Dong, L., Muramatsu, N., Numata, H., and Ito, C. (2022). Functional Analysis of a Juvenile Hormone Inducible Transcription Factor, Krüppel homolog 1, in the Bean Bug, *Riptortus pedestris*. *Zoolog. Sci.* **39**, 562–569.

Drach, P. (1939). Mue et cycle d' intermue chez les Crustaces Decapodes. *Ann. Inst. Oceanogr.* **19**, 103–391.

Duan, Y., Liu, P., Li, J., Wang, Y., Li, J., and Chen, P. (2014). A farnesoic acid *O*-methyltransferase (FAMeT) from *Exopalaemon carinicauda* is responsive to Vibrio anguillarum and WSSV challenge. *Cell Stress Chaperones.* **19** (3), 367–377.

Dvoretsky, A. G., Bichkaeva, F. A., Baranova, N. F., and Dvoretsky, V. G. (2021). Fatty acid composition of the Barents Sea red king crab (*Paralithodes camtschaticus*) leg meat. *Journal of Food Composition and Analysis.* **98** (3), 103826.

Dyson, H. J., and Wright, P. E. (2016). Role of Intrinsic Protein Disorder in the Function and Interactions of the Transcriptional Coactivators CREB-binding Protein (CBP) and p300. *Journal of Biological Chemistry.* **291** (13), 6714–6722.

Eid, D. M., Chereddy, S. C. R. R., and Palli, S. R. (2020). The effect of E93 knockdown on female reproduction in the red flour beetle, *Tribolium castaneum*. *Arch. Insect Biochem. Physiol.* **104**, e21688.

Ens, N. J., Harvey, B., Davies, M. M., Thomson, H. M., Meyers, K. J., Yakimishyn, J., Lee, L. C., McCord, M.E., and Gerwing, T. G. (2022). The Green Wave: reviewing the environmental impacts of the invasive European green crab (*Carcinus maenas*) and potential management approaches. *Environmental Reviews.* **30** (2), 306–322.

Ermolenko, E. V., Sikorskaya, T. V., and Grigorchuk, V. P. (2023). Crabs *Eriocheir japonica* and *Paralithodes camtschaticus* Are a Rich Source of Lipid Molecular Species with High Nutritional Value. *Foods.* **12** (18), 3359.

Fahrbach, S. E., Smagghe, G., and Velarde, R. A. (2012). Insect nuclear receptors. *Annu. Rev. Entomol.* **57**, 83–106.

Fan, W., Yang, P., Qiao, Y., Su, M., and Zhang, G. (2022). Polystyrene nanoplastics decrease molting and induce oxidative stress in adult *Macrobrachium nipponense*. *Fish & Shellfish Immunol.* **122**, 419–425.

Fang, M., Li, J., Blauwkamp, T., Bhambhani, C., Campbell, N., and Cadigan, K. M. (2006). C-terminal-binding protein directly activates and represses Wnt transcriptional targets in *Drosophila*. *EMBO Journal.* **25** (12), 2735–2745.

FAO. (2012). The State of World Fisheries and Aquaculture 2012. Rome: Food and Agriculture Organization of the United Nations.

FAO. (2021). The State of World Fisheries and Aquaculture 2020. Sustainability in Action. Rome: American Oil Chemists Society.

FAO. (2022). The State of World Fisheries and Aquaculture 2022. Towards Blue Transformation. Rome: FAO.

FAO. (2024). In Brief to The State of World Fisheries and Aquaculture 2024. Blue Transformation in Action. Rome.

Farhadi, A., Harlıoğlu, M. M., and Yılmaz, Ö. (2020). Effect of serotonin injection on the reproductive parameters and haemolymph methyl farnesoate level in the narrow-clawed crayfish *Pontastacus leptodactylus* (Eschscholtz, 1823). *Aquaculture Research.* **51** (1), 155–163.

Farris, S. M. (2005). Evolution of insect mushroom bodies: Old clues, new insights. *Arthropod Structure & Development.* **34** (3), 211–234.

Fedotova, A. A., Bonchuk, A. N., Mogila, V. A., and Georgiev, P. G. (2017). C2H2 Zinc Finger Proteins: The Largest but Poorly Explored Family of Higher Eukaryotic Transcription Factors. *Acta Naturae.* **9** (2), 47–58.

Fernandez-Nicolas, A. and Belles, X. (2016). CREB-binding protein contributes to the regulation of endocrine and developmental pathways in insect hemimetabolan pre-metamorphosis. *Biochim. Biophys. Acta.* **1860** (3), 508–515.

Fernandez-Nicolas, A., Machaj, G., Ventos-Alfonso, A., Pagone, V., Minemura, T., Ohde, T., Ylla, G. and Belles, X. (2023). Reduction of embryonic E93 expression as a hypothetical driver of the evolution of insect metamorphosis. *Proc. Natl. Acad. Sci. U. S. A.* **120** (7), e2216640120.

Fingerman, M. (1997). Crustacean endocrinology: a retrospective, prospective, and introspective analysis. *Physiol. Zool.* **70** (3), 257–269.

Fletcher, J. C., Burtis, K. C., Hogness, D. S., and Thummel, C. S. (1995). The *Drosophila* E74 gene is required for metamorphosis and plays a role in the polytene chromosome puffing response to ecdysone. *Development.* **121** (5), 1455–1465.

Fribourgh, J. L. and Partch, C. L. (2017). Assembly and function of bHLH-PAS complexes. *Proc. Natl. Acad. Sci. U. S. A.* **114** (21), 5330–5332.

Fulton, B. A. and Fairchild, E. A. (2013). Nutritional Analysis of Whole Green Crab, *Carcinus maenas*, for Application as a Fishmeal Replacer in Agrifeeds. *Sustainable Agriculture Research.* **2**, 126–135.

Gabe, M. (1953). Sur l'existence, chez quelques crustacés Malacostraces, d'un organe comparable a la glande de la mue des Insects. *Comptes Rendus Hebdomadaires de l'Academie des Sciences.* **327**, 1111–1113.

Gaddelapati, S. C., Dhandapani, R. K., and Palli, S. R. (2020). CREB-binding protein regulates metamorphosis and compound eye development in the yellow fever mosquito, *Aedes aegypti*. *Biochim. Biophys. Acta Gene Regul. Mech.* **1863** (8), 194576.

Gao, W., Yuan, Y., Huang, Z., Chen, Y., Cui, W., Zhang, Y., Saqib, H. S. A., Ye, S., Li, S., Zheng, H., Zhang, Y., Ikhwanuddin, M., and Ma, H. (2023). Evaluation of the Feasibility of Harvest Optimisation of Soft-Shell Mud Crab (*Scylla paramamosain*) from the Perspective of Nutritional Values. *Foods.* **12** (3), 583.

Gao, Y., Zhang, X., Wei, J., Sun, X., Yuan, J., Li, F., and Xiang, J. (2015). Whole Transcriptome Analysis Provides Insights into Molecular Mechanisms for Molting in *Litopenaeus vannamei*. *PLoS One*. **10** (12), e0144350.

Garlock, T., Asche, F., Anderson, J., Ceballos-Concha, A., Love, D. C., Osmundsen, T. C., and Pincinato, R. B. M. (2022). Aquaculture: The missing contributor in the food security agenda. *Glob. Food Sec.* **32**, 100620.

Gassias, E., Maria, A., Couzi, P., Demondion, E., Durand, N., Bozzolan, F., Aguliar, P., and Debernard, S. (2021). Involvement of Methoprene-tolerant and Krüppel homolog 1 in juvenile hormone-signaling regulating the maturation of male accessory glands in the moth *Agrotis ipsilon*. *Insect Biochem. Mol. Biol.* **132**, 103566.

Ge, F., Yu, Q., Zhang, J., Han, Y., Zhu, D., and Xie, X. (2024). E93 gene in the swimming crab, *Portunus trituberculatus*: Responsiveness to 20-hydroxyecdysone and methyl farnesoate and role on regulating ecdysteroid synthesis. *Comp. Biochem. Physiol. B Biochem. Mol. Biol.* **270**, 110910.

Gijbels, M., Marchal, E., Verdonckt, T. W., Bruyninckx, E., and Broeck, J. Vanden (2020). RNAi-Mediated Knockdown of Transcription Factor E93 in Nymphs of the Desert Locust (*Schistocerca gregaria*) Inhibits Adult Morphogenesis and Results in Supernumerary Juvenile Stages. *Int. J. Mol. Sci.* **21** (20), 7518.

Gilbert, L. I., Rybczynski, R., and Warren, J. T. (2001). Control and biochemical nature of the ecdysteroidogenic pathway. *Annu. Rev. Entomol.* **47**, 883–916.

Giribet, G. and Edgecombe, G. D. (2019). The Phylogeny and Evolutionary History of Arthropods. *Current Biology.* **29** (12), R592–R602.

Girish, B. P., Swetha, C. H., and Reddy, P. S. (2015). Expression of RXR, EcR, E75 and VtG mRNA levels in the hepatopancreas and ovary of the freshwater edible crab, *Oziothelphusa senex senex* (Fabricius, 1798) during different vitellogenic stages. *Naturwissenschaften*. **102**, 20.

Girish, B. P., Swetha, C. H., and Reddy, P. S. (2017). Serotonin induces ecdysteroidogenesis and methyl farnesoate synthesis in the mud crab, *Scylla serrata*. *Biochemical and Biophysical Researach Communications.* **490** (4), 1340–1345.

Glandon, H. L., Kilbourne, K. H., Schijf, J., and Miller, T. J. (2018). Counteractive effects of increased temperature and *p*CO2 on the thickness and chemistry of the carapace of juvenile blue crab, *Callinectes sapidus*, from the Patuxent River, Chesapeake Bay. *Journal of Experimental Marine Biology and Ecology.* **498**, 39–45.

Goldstein, J. L. and Brown, M. S. (1990). Regulation of the mevalonate pathway. *Nature.* **343** (6257), 425–430.

Gopal, N. and Devi, A. R. S. (2018). Morphology and Histology of Mandibular Organ in Relation to Growth and Reproduction in the Freshwater Crab *Barytelphusa cunicularis*. *International Journal of Oceans and Oceanography.* **12** (2), 93–109.

Greb-Markiewicz, B. and Kolonko, M. (2019). Subcellular localization signals of bHLH-PAS proteins: Their significance, current state of knowledge and future perspectives. *Int. J. Mol. Sci.* **20** (19), 4746.

Gujar, H. and Palli, S. R. (2016). Krüppel homolog 1 and E93 mediate Juvenile hormone regulation of metamorphosis in the common bed bug, *Cimex lectularius*. *Sci. Rep.* **6**, 26092.

Gunawardene, S. Y. I. N., Chow, B. K. C., He, J. G., and Chan, S. M. (2001). The shrimp FAMeT cDNA is encoded for a putative enzyme involved in the methylfarnesoate (MF) biosynthetic pathway and is temporally expressed in the eyestalk of different sexes. *Insect Biochem. Mol. Biol.* **31** (11), 1115–1124.

Gunawardene, S. Y. I. N., Tobe, S. S., Bendena, W. G., Chow, B. K. C., Yagi, K. J., and Chan, S. M. (2002). Function and cellular localization of farnesoic acid *O*-methyltransferase (FAMeT) in the shrimp, *Metapenaeus ensis*. *Eur. J. Biochem.* **269** (14), 3587–3595.

Gunawardene, Y. I. N. S., Bendena, W. G., Tobe, S. S., and Chan, S. M. (2003). Comparative immunohistochemistry and cellular distribution of farnesoic acid *O*-methyltransferase in the shrimp and the crayfish. *Peptides*. **24** (10), 1591–1597.

Guo, Y. R., Gu, S. Q., Wang, X. C., Zhuang, K. J., Wang, S., and Shi, J. (2015). Nutrients and non-volatile taste compounds in Chinese mitten crab by-products. *Fisheries Science.* **81**, 193–203.

Guo, Z., Xu, L., Wang, W., Chen, W., Ma, C., Zhang, F., Ma, L., Liu, Z., and Ma, K. (2023). Molecular characterization and transcriptional response to TiO2–GO nanomaterial exposure of two molt-related genes in the juvenile prawn, *Macrobrachium rosenbergii*. *Sci. Rep.* **13** (1).

Han, H., Feng, Z., Han, S., Chen, J., Wang, D., and He, Y. (2022). Molecular Identification and Functional Characterization of Methoprene-Tolerant (Met) and Krüppel-Homolog 1 (Kr-h1) in *Harmonia axyridis* (Coleoptera: Coccinellidae). *J. Econ. Entomol.* **115** (1), 334–343.

Hannas, B. R. and LeBlanc, G. A. (2010). Expression and ecdysteroid responsiveness of the nuclear receptors HR3 and E75 in the crustacean *Daphnia magna*. *Mol. Cell Endocrinol.* **315**, 208–218.

Hannas, B. R., Wang, Y. H., Baldwin, W. S., Li, Y., Wallace, A. D., and LeBlanc, G. A. (2010). Interactions of the crustacean nuclear receptors HR3 and E75 in the regulation of gene transcription. *Gen. Comp. Endocrinol.* **167** (2), 268–278.

He, J. (2015). Chinese public policy on fisheries subsidies: Reconciling trade, environmental and food security stakes. *Marine Policy* **56**, 106–116.

He, J., Xuan, F., Shi, H., Xie, J., Wang, W., Wang, G., and Xu, W. (2017a). Comparison of nutritional quality of three edible tissues of the wild-caught and pond-reared swimming crab (*Portunus trituberculatus*) females. *LWT.* **75**, 624–630.

He, Q., Wen, D., Jia, Q., Cui, C., Wang, J., Pallii, S. R., and Li, S. (2014). Heat shock protein 83 (Hsp83) facilitates methoprene-tolerant (Met) nuclear import to modulate juvenile hormone signaling. *Journal of Biological Chemistry.* **289** (40), 27874–27885.

He, Q. and Zhang, Y. (2022). Kr-h1, a Cornerstone Gene in Insect Life History. *Front. Physiol.* **13**, 905441.

He, Q., Zhang, Y., Zhang, X., Xu, D. D., Dong, W., Li, S., and Wu, R. (2017b). Nucleoporin Nup358 facilitates nuclear import of Methoprene-tolerant (Met) in an importin β- and Hsp83-dependent manner. *Insect Biochem. Mol. Biol.* **81**, 10–18.

He, Y. Z., Ding, Y., Wang, X., Zou, Z., and Raikhel, A. S. (2021). E93 confers steroid hormone responsiveness of digestive enzymes to promote blood meal digestion in the midgut of the mosquito *Aedes aegypti*. *Insect Biochem. Mol. Biol.* **134**, 103580.

Hinsch, G. W. (1977). Fine structural changes in the mandibular gland of the male spider crab, *Libinia emarginata* (L). Following eyestalk ablation. *J. Morphol.* **154** (2), 307–315.

Hinsch, G. W. and Hajj, H. Al (1975). The ecdysial gland of the spider crab, *Libinia emarginata* (L). Ultrastructure of the gland in the male. *J. Morphol.* **145** (2), 179–187.

Hinsch, G. W., Spaziani, E., and Vensel, W. H. (1980). Ultrastructure of the y-organs *of Cancer antennarius* in normal and de-eyestalked crabs. *J. Morphol.* **163** (2), 167–174.

Hirano, M., Toyota, K., Ishibashi, H., Tominaga, N., Sato, T., Tatarazako, N., and Iguchi, T. (2020). Molecular Insights into Structural and Ligand Binding Features of Methoprene-Tolerant in Daphnids. *Chem. Res. Toxicol.* **33** (11), 2785–2792.

Hock, T., Cottrill, T., Keegan, J., and Garza, D. (2000). The E23 early gene of *Drosophila* encodes an ecdysone-inducible ATP-binding cassette transporter capable of repressing ecdysone-mediated gene activation. *PNAS.* **97** (17), 9519–9524.

Hoffman, E. C., Reyes, Her., Chu, F., Sander, F., Conley, L. H., Brooks, B. A., and Hankinson, O. (1983). Cloning of a Factor Required for Activity of the Ah (Dioxin) Receptor. *Science.* **252** (5008), 954–958.

Holford, K. C., Edwards, K. A., Bendena, W. G., Tobe, S. S., Wang, Z., and Borst, D. W. (2004). Purification and characterization of a mandibular organ protein from the American lobster, *Homarus americanus*: A putative farnesoic acid *O*-methyltransferase. *Insect Biochem. Mol. Biol.* **34** (8), 785–798.

Holland, C. A. and Skinner, D. M. (1976). Interactions Between Molting and Regeneration in the Land Crab. *Biol. Bull.* **150** (2), 222–240.

Homola, E. and Chang, E. S. (1997a). Assay Methods for Methyl Farnesoate Esterases in Crustaceans. *Arch. Insect Biochem. Physiol.* **36** (2), 115–128.

Homola, E. and Chang, E. S. (1997b). Distribution and Regulation of Esterases That Hydrolyze Methyl Farnesoate in *Homarus americanus* and Other Crustaceans. *General and Comparative Endocrinoology.* **106**, (1) 62–72.

Homola, E. and Chang, E. S. (1997c). Methyl Farnesoate: Crustacean Juvenile Hormone in Search of Functions. *Comparative Biochemistry and Physiology Part B: Biochemistry and Molecular Biology.* **117** (3), 347–356.

Hopkins, P. M. (1982). Growth and Regeneration Patterns in the Fiddler Crab, *Uca pugilator*. *Biol. Bull.* **163** (2), 301–319.

Hopkins, P. M. (2012). The eyes have it: A brief history of crustacean neuroendocrinology. *Gen. Comp. Endocrinol.* **175**, 357–366.

Hosamani, N., Reddy B, S., and Reddy P, R. (2017). Crustacean Molting: Regulation and Effects of Environmental Toxicants. *Journal of Marine Science: Research & Development.* **07** (5).

Hoshizaki, D. K. (1994). Krüppel Expression during Postembryonic Development of *Drosophila*. *Dev. Biol.* **163**, 133–140.

Hou, X., Yang, H., Chen, X., Wang, J., and Wang, C. (2021). RNA interference of mTOR gene delays molting process in *Eriocheir sinensis*. *Comp. Biochem. Physiol. B Biochem. Mol. Biol.* **256**, 110651.

Huang, H. and Tindall, D. J. (2007). Dynamic FoxO transcription factors. *J. Cell Sci.* **120**, 2479–2487.

Hui, J. H. L., Hayward, A., Bendena, W. G., Takahashi, T., and Tobe, S. S. (2010). Evolution and functional divergence of enzymes involved in sesquiterpenoid hormone biosynthesis in crustaceans and insects. *Peptides.* **31** (3), 451–455.

Hui, J. H. L., Tobe, S. S., and Chan, S. M. (2008). Characterization of the putative farnesoic acid O-methyltransferase (LvFAMeT) cDNA from white shrimp, *Litopenaeus vannamei*: Evidence for its role in molting. *Peptides.* **29** (2), 252–260.

Hungria, D. B., dos Santos Tavares, C. P., Pereira, L. Â., de Assis Teixeira da Silva, U., and Ostrensky, A. (2017). Global status of production and commercialization of soft-shell crabs. *Aquaculture International.* **25**, 2213–2226.

Huo, Y. W., Jin, M., Zhou, P. P., Li, M., Mai, K. Sen, and Zhou, Q. C. (2014). Effects of dietary protein and lipid levels on growth, feed utilization and body composition of juvenile swimming crab, *Portunus trituberculatus*. *Aquaculture.* **434**, 151–158.

Hyde, C. J., Elizur, A., and Ventura, T. (2019a). The crustacean ecdysone cassette: A gatekeeper for molt and metamorphosis. *Journal of Steroid Biochemistry and Molecular Biology.* **185**, 172–183.

Hyde, C. J., Fitzgibbon, Q. P., Elizur, A., Smith, G. G., and Ventura, T. (2019b). Transcriptional profiling of spiny lobster metamorphosis reveals three new additions to the nuclear receptor superfamily. *BMC Genomics.* **20**, 531.

Islam, T., Saha, D., Bhowmik, S., Nordin, N., Islam, S., Ujjaman Nur, A. A., and Begum, M. (2022). Nutritional properties of wild and fattening mud crab (*Scylla serrata*) in the south-eastern district of Bangladesh. *Heliyon*. **8** (6), e09696.

Jiang, H., Zhang, N., Ge, H., Wei, J., Xu, X., Meng, X., Qian, K., Zheng, Y., and Wang, J. (2022). S6K1 acts through FOXO to regulate juvenile hormone biosynthesis in the red flour beetle, *Tribolium castaneum*. *J Insect Physiol.* **140**, 104405.

Jindra, M. (2019). Where did the pupa come from? The timing of juvenile hormone signalling supports homology between stages of hemimetabolous and holometabolous insects. *Phil. Trans. R. Soc. B*. **374**, 20190064.

Jindra, M. and Bittova, L. (2020). The juvenile hormone receptor as a target of juvenoid "insect growth regulators." *Arch. Insect Biochem. Physiol.* **103** (3), e21615.

Jindra, M., Palli, S. R., and Riddiford, L. M. (2013). The juvenile hormone signaling pathway in insect development. *Annu. Rev. Entomol.* **58**, 181–204.

Jones, S. (2004). An overview of the basic helix-loop-helix proteins. *Genome Biol.* **5**, 226.

Jung, H., Lyons, R. E., Hurwood, D. A., and Mather, P. B. (2013). Genes and growth performance in crustacean species: A review of relevant genomic studies in crustaceans and other taxa. *Rev. Aquac.* **5**, 77–110.

Junprung, W., Supungul, P., and Tassanakajon, A. (2021). Structure, gene expression, and putative functions of crustacean heat shock proteins in innate immunity. *Dev. Comp. Immunol.* **115**, 103875.

Kaestner, K. H., Knö, W., and Martínez, D. E. (2000). Unified nomenclature for the winged helix/forkhead transcription factors. *Genes Dev.* **14** (2), 142–146.

Kakaley, E. K. M., Wang, H. Y., and LeBlanc, G. A. (2017). Agonist-mediated assembly of the crustacean methyl farnesoate receptor. *Sci. Rep.* **7**, 45071.

Kalavathy, Y., Mamatha, P., and Reddy, P. S. (1999). Methyl farnesoate stimulates testicular growth in the freshwater crab *Oziotelphusa senex sene*x fabricius. *Naturwissenschaften.* **86**, 394–395.

Kamita, S. G. and Hammock, B. D. (2010). Juvenile hormone esterase: biochemistry and structure. *J. Pestic. Sci.* **35** (3), 265–274.

Kamita, S. G., Hintona, A. C., Wheelock, C. E., Wogulis, M. D., Wilson, D. K., Wolf, N. M., Stok, J. E., Hock, B., and Hammock, B. D. (2003). Juvenile hormone (JH) esterase: Why are you so JH specific? *Insect Biochem. Mol. Biol.* **33** (12), 1261–1273.

Kamita, S. G., Samra, A. I., Liu, J. Y., Cornel, A. J., and Hammock, B. D. (2011). Juvenile hormone (JH) esterase of the mosquito *Culex quinquefasciatus* is not a target of the JH analog insecticide methoprene. *PLoS One.* **6**. (12), e28392.

Kamiyama, T. and Niwa, R. (2022). Transcriptional Regulators of Ecdysteroid Biosynthetic Enzymes and Their Roles in Insect Development. *Front. Physiol.* **13**.

Kamsoi, O. and Belles, X. (2020). E93-depleted adult insects preserve the prothoracic gland and molt again. *Development.* **147** (22), dev190066.

Kang, P., Chang, K., Liu, Y., Bouska, M., Birnbaum, A., Karashchuk, G., Thakore, R., Zheng, W., Post, S., Brent, C. S., Li, S., Tatar, M, and Bai, H. (2017). *Drosophila* Kruppel homolog 1 represses lipolysis through interaction with dFOXO. *Sci. Rep.* **7**, 16369.

Karim, F. D., Guild, G. M., and Thummel, C. S. (1993). The *Drosophila* Broad-Complex plays a key role in controlling ecdyonse-regulated gene expression at the onset of metamorphosis. *Development.* **118** (3), 977–988.

Karim, N. U., Mohd Noor, N. S., Sofian, M. F., Hassan, M., Ikhwanuddin, M., and Nirmal, N. P. (2024). Lipid profile and antioxidant activities of mud crab (*Scylla olivacea*) extract obtained from muscle and hepatopancreas. *CyTA - Journal of Food* **22** (1).

Katayama, H., Ohira, T., and Nagasawa, H. (2013). Crustacean Peptide Hormones: Structure, Gene Expression and Function. *Aqua-BioScience Monographs.* **6** (2), 49–90.

Kayukawa, T., Minakuchi, C., Namiki, T., Togawa, T., Yoshiyama, M., Kamimura, M., Mita, K., Imanishi, S., Kiuchi, M., Ishikawa, Y., and Shinoda, T. (2012). Transcriptional regulation of juvenile hormone-mediated induction of Krüppel homolog 1, a repressor of insect metamorphosis. *Proc. Natl. Acad. Sci. U. S. A.* **109** (29), 11729–11734.

Kayukawa, T., Murata, M., Kobayashi, I., Muramatsu, D., Okada, C., Uchino, K., Sezutsu, H., Kiuchi, M., Tamura, T., Hiruma, K., Ishikawa, Y., and Shinoda, T. (2014). Hormonal regulation and developmental role of Krüppel homolog 1, a repressor of metamorphosis, in the silkworm *Bombyx mori*. *Dev. Biol.* **388** (1), 48–56.

Kayukawa, T., Nagamine, K., Ito, Y., Nishita, Y., Ishikawa, Y., and Shinoda, T. (2016). Krüppel Homolog 1 Inhibits Insect Metamorphosis via Direct Transcriptional Repression of Broad-Complex, a Pupal Specifier Gene. *Journal of Biological Chemistry.* **291** (4), 1751–1762.

Kewley, R. J., Whitelaw, M. L., and Chapman-Smith, A. (2004). The mammalian basic helix-loop-helix/PAS family of transcriptional regulators. *International Journal of Biochemistry and Cell Biology.* **36** (2), 189–204.

Khong, H., Hattley, K. B., and Suzuki, Y. (2024). The BTB transcription factor, Abrupt, acts cooperatively with Chronologically inappropriate morphogenesis (Chinmo) to repress metamorphosis and promotes leg regeneration. *Dev. Biol.* **509**, 70–84.

Kim, H. W., Sung, G. L., and Mykles, D. L. (2005). Ecdysteroid-responsive genes, RXR and E75, in the tropical land crab, *Gecarcinus lateralis*: differential tissue expression of multiple RXR isoforms generated at three alternative splicing sites in the hinge and ligand-binding domains. *Mol. Cell Endocrinol.* **242**, 80–95.

King, L. E., Ding, Q., Prestwtch, G. D., and Tobe, S. S. (1995). The Characterization of a Haemolymph Methyl Farnesoate Binding Protein and the Assessment of Methyl Farnesoate Metabolism by the Haemolymph and Other Tissues from *Procambrus clarkii*. *Insect Biochem. Mol. Biol.* **25** (4), 495–501.

Kingan, T. G. (1989). A Competitive Enzyme-Linked Immunosorbent Assay: Applications in the assay of peptides, steroids, and cyclic nucleotides. *Analytical Biochemistry.* **183** (2), 283–289.

King-Jones, K. and Thummel, C. S. (2005). Nuclear receptors - a perspective from *Drosophila*. *Nat. Rev. Genet.* **6**, 311–323.

Knigge, T. (2024). Antidepressants – The new endocrine disruptors? The case of crustaceans. *Mol. Cell Endocrinol.* **583**, 112155.

Knigge, T., LeBlanc, G. A., and Ford, A. T. (2021). A Crab Is Not a Fish: Unique Aspects of the Crustacean Endocrine System and Considerations for Endocrine Toxicology. *Front. Endocrinol.* **12**.

Kobayashi, M., Msangi, S., Batka, M., Vannuccini, S., Dey, M. M., and Anderson, J. L. (2015). Fish to 2030: The Role and Opportunity for Aquaculture. *Aquaculture Economics and Management.* **19**, 282–300.

Kolonko, M. and Greb-Markiewicz, B. (2019). bHLH–PAS proteins: Their structure and intrinsic disorder. *Int. J. Mol. Sci.* **20** (15), 3653.

Kolonko, M., Ozga, K., Hołubowicz, R., Taube, M., Kozak, M., Ozyhar, A., and Greb-Markieqicz, B. (2016). Intrinsic Disorder of the C-terminal Domain of *Drosophila* Methoprene-Tolerant Protein. *PLoS One.* **11** (9), e0162950.

Kong, L., Cai, C., Ye, Y., Chen, D., Wu, P., Li, E., Chen, L., and Song, L. (2012). Comparison of non-volatile compounds and sensory characteristics of Chinese mitten crabs (*Eriocheir sinensis*) reared in lakes and ponds: Potential environmental factors. *Aquaculture.* **364–365**, 96–102.

Kozma, M. T., Pérez-Moreno, J. L., Gandhi, N. S., Hernandez Jeppesen, L., Durica, D. S., Ventura, T., and Mykles, D. L. (2024). *In silico* analysis of crustacean hyperglycemic hormone family G protein-coupled receptor candidates. *Front. Endocrinol.* **14**.

Krieger, G., Lupo, O., Wittkopp, P., and Barkai, N. (2022). Evolution of transcription factor binding through sequence variations and turnover of binding sites. *Genome Res.* **32** (6), 1099–1111.

Krzeczkowski, R. A. and Stone, F. E. (1974). Amino Acid, Fatty Acid, and Proximate Composition of Snow Crab (*Chionoecetes bairdi*). *J. Food Sci.* **39** (2), 386–388.

Krzeczkowski, R. A., Tenney, R. D., and Kelley, C. (1971). Alaska King Crab: Fatty Acid Composition, Carotenoid Index, and Proximate Analysis. *J. Food Sci.* **36** (4), 604–606.

Kuballa, A. V., Guyatt, K., Dixon, B., Thaggard, H., Ashton, A. R., Paterson, B., Merritt, D. J., and Elizur, A. (2007). Isolation and expression analysis of multiple isoforms of putative farnesoic acid *O*-methyltransferase in several crustacean species. *Gen. Comp. Endocrinol.* **150** (1), 48–58.

Küçükgülmez, A., Çelik, M., Yanar, Y., Ersoy, B., and Çikrikçi, M. (2006). Proximate composition and mineral contents of the blue crab (*Callinectes sapidus*) breast meat, claw meat and hepatopancreas. *Int. J. Food Sci. Technol.* **41** (9), 1023–1026.

Kuley, E., Özoğul, F., Özogul, Y., and Olgunoglu, A. I. (2008). Comparison of fatty acid and proximate compositions of the body and claw of male and female blue crabs (*Callinectes sapidus*) from different regions of the Mediterranean coast. *Int. J. Food Sci. Nutr.* **59**, 573–580.

Kumagai, H., Kunieda, T., Nakamura, K., Matsumura, Y., Namiki, M., Kohno, H., and Kubo, T. (2020). Developmental stage-specific distribution and phosphorylation of Mblk-1, a transcription factor involved in ecdysteroid-signaling in the honey bee brain. *Sci. Rep.* **10**, 8735.

Kumar, R. and Thompson, E. B. (1999). The structure of the nuclear hormone receptors. *Steroids*. **64 (**5), 310–319.

Kumar, V., Carlson, J. E., Ohgi, K. A., Edwards, T. A., Rose, D. W., Escalante, C. R., Rosenfeld, M. G., and Aggarwal, A. K. (2002). Transcription Corepressor CtBP is an NAD- Regulated Dehydrogenase. *Mol. Cell.* **10**, 857–869.

Lachaise, F., Le Roux, A., Hubert, M., and Lafont, R. (1993). The Molting Gland of Crustaceans: Localization, Activity, and Endocrine Control (A Review). *Journal of Crustacean Biology.* **13** (2), 198–234.

Lahiri, T., Nazrul, K. M. S., Rahman, M. A., Saha, D., Egna, H., Wahab, M. A., and Mamun, A. A. (2021). Boom and bust: Soft-shell mud crab farming in south-east coastal Bangladesh. *Aquac. Res.* **52** (2), 5056–5068.

Laity, J. H., Lee, B. M., and Wright, P. E. (2001). Zinc finger proteins: new insights into structural and functional diversity. *Curr. Opin. Struct. Biol.* **11** (1), 39–46.

Lam, G., Nam, H. J., Velentzas, P. D., Baehrecke, E. H., and Thummel, C. S. (2022). *Drosophila* E93 promotes adult development and suppresses larval responses to ecdysone during metamorphosis. *Dev. Biol.* **481**, 104–115.

Latyshev, N. A., Kasyanov, S. P., Kharlamenko, V. I., and Svetashev, V. I. (2009). Lipids and of fatty acids of edible crabs of the north-western Pacific. *Food Chem.* **116** (3), 657–661.

Lauer, B. H., Murray, M. C., Anderson, W. E., and Guptill, E. B. (1974). Atlantic queen crab (*Chionoecetes opilio*), Jonah crab (*Cancer borealis*), and red crab (*Geryon quinquedens*). Proximate Composition of Crabmeat from Edible Tissues and Concentrations of Some Major Mineral Constituents in the Ash. *J. Food Sci.* **39** (2), 383–385.

Laufer, H., Ahl, J., Rotllant, G., and Baclaski, B. (2002). Evidence that ecdysteroids and methyl farnesoate control allometric growth and differentiation in a crustacean. *Insect Biochem. Mol. Biol.* **32** (2), 205–210.

Laufer, H. and Biggers, W. J. (2001). Unifying Concepts Learned from Methyl Farnesoate for Invertebrate Reproduction and Post-Embryonic Development. *Amer. Zool.* **41** (3), 4–8.

Laufer, H., Demir, N., Pan, X., Stuart, J. D., and Ahl, J. S. B. (2005). Methyl farnesoate controls adult male morphogenesis in the crayfish, *Procambarus clarkii*. *Journal of Insect Physiology*. **51** (4), 379–384.

Laufer, H., Borst, D., Baker, F. C., Reuter, C. C., Tsai, L. W., Schooley, D. A., Carrasco, C., and Sinkus, M. (1987a). Identification of a Juvenile Hormone-Like Compound in a Crustacean. *Science.* **235** (4785), 202–205.

Le Roux, A. (1968). Description d'organes mandibulaires nouveaux chez les crustaces decapods. *CR Acad. Sci. Paris.* **266**, 1414–14717.

LeBlanc, G. A. (2007). Crustacean endocrine toxicology: A review. *Ecotoxicology.* **16** (1), 61–81.

Ledent, V. and Vervoort, M. (2001). The basic helix-loop-helix protein family: comparative genomics and phylogenetic analysis. *Genome Res.* **11** (5), 754–770.

Lee, K. J., Kim, H. W., Gomez, A. M., Chang, E. S., Covi, J. A., and Mykles, D. L. (2007). Molt-inhibiting hormone from the tropical land crab, *Gecarcinus lateralis*: Cloning, tissue expression, and expression of biologically active recombinant peptide in yeast. *Gen. Comp. Endocrinol.* **150** (3), 505–513.

Lee, S. O., Jeon, J. M., Oh, C. W., Kim, Y. M., Kang, C. K., Lee, D. S., Mykles, D. L., and Kim, H. W. (2011). Two juvenile hormone esterase-like carboxylesterase cDNAs from a Pandalus shrimp (*Pandalopsis japonica*): Cloning, tissue expression, and effects of eyestalk ablation. *Comparative Biochemistry and Physiology - B Biochemistry and Molecular Biology.* **159** (3), 148–156.

Legge, G. B., Martinez-Yamout, M. A., Hambly, D. M., Trinh, T., Lee, B. M., Dyson, H. J., and Wright, P. E. (2004). ZZ domain of CBP: an unusual zinc finger fold in a protein interaction module. *J. Mol. Biol.* **343** (4), 1081–1093.

Legrand, E., Bachvaroff, T., Schock, T. B., and Chung, J. S. (2021). Understanding molt control switches: Transcriptomic and expression analysis of the genes involved in ecdysteroidogenesis and cholesterol uptake pathways in the Y-organ of the blue crab, *Callinectes sapidus*. *PLoS One.* **16** (9), e0256735.

Leo, C. and Chen, J. D. (2000). The SRC family of nuclear receptor coactivators. *Gene.* **245** (1), 1–11.

Lewis, C. L., Fitzgibbon, Q. P., Smith, G. G., Elizur, A., and Ventura, T. (2024). Ontogeny of the Cytochrome P450 Superfamily in the Ornate Spiny Lobster (*Panulirus ornatus*). *Int. J. Mol. Sci.* **25** (2), 1070.

Li, H. and Borst, D. W. (1991). Characterization of a Methyl Farnesoate Binding Protein in Hemolymph from *Libinia emarginata*. *Gen. Comp. Endocrinol.* **81** (3), 335–342.

Li, K., Jia, Q. Q., and Li, S. (2018a). Juvenile hormone signaling – a mini review. *Insect Sci*. **26** (4), 600–606.

Li, K. L., Yuan, S. Y., Nanda, S., Wang, W. X., Lai, F. X., Fu, Q., and Wan, P. J. (2018b). The Roles of E93 and Kr-h1 in Metamorphosis of *Nilaparvata lugens*. *Front. Physiol.* **9**, 1677.

Li, X., Chen, T., Han, Y., Huang, M., Jiang, H., Huang, J., Tao, M., Xu, R., Xie, Q., and Su, S. (2021b). Potential role of Methoprene-tolerant (Met) in methyl farnesoate-mediated vitellogenesis in the Chinese mitten crab (*Eriocheir sinensis*). *Comp. Biochem. Physiol. B Biochem. Mol. Biol.* **252**, 110524.

Li, X., Chen, T., Jiang, H., Huang, J., Huang, M., Xu, R., Xie., Q., Zhu, H., and Su, S. (2021c). Effects of methyl farnesoate on Krüppel homolog 1 (Kr-h1) during vitellogenesis in the Chinese mitten crab (*Eriocheir sinensis*). *Anim. Reprod. Sci.* **224**, 106653.

Li, X., Chen, T., Xu, R., Huang, M., Huang, J., Xie, Q., Liu, F., Su, S., and Ma, K. (2021d). Identification, characterization and mRNA transcript abundance profiles of the carboxylesterase (CXE5) gene in *Eriocheir sinensis* suggest that it may play a role in methyl farnesoate degradation. *Comp. Biochem. Physiol. B Biochem. Mol. Biol.* **256**, 110630.

Li, Y., Yang, W., Sun, J., Lian, X., Li, X., Zhao, X., Liu, Y., Wang, L., and Song, L. (2024). A DM9-containing protein from crab *Eriocheir sinensis* functions as a novel multipotent pattern recognition receptor. *Fish Shellfish Immunol.* **145**, 109356.

Li, Z., Xu, X., Wang, J., and Wang, C. (2013). Possible Roles of Farnesoic Acid *O*-Methyltransferase in Regulation of Molting in the Shrimp, *Penaeus Chinensis*. *J. World Aquac. Soc.* **44** (6), 826–834.

Licht, J. D., Grossel, M. J., Figge, J., and Hansen, U. M. (1990). *Drosophila* Krüppel protein is a transcriptional repressor. *Nature.* **346** (6279), 76–79.

Lin, X., Yu, N., and Smagghe, G. (2018). FoxO mediates the timing of pupation through regulating ecdysteroid biosynthesis in the red flour beetle, *Tribolium castaneum*. *Gen Comp Endocrinol.* **258**, 149–156.

Ling, L., Mühling, B., Jaenichen, R., and Gompel, N. (2023). Increased chromatin accessibility promotes the evolution of a transcriptional silencer in *Drosophila*. *Sci Adv.* **9**, 1–10.

Liu, A., Shi, W., Lin, D., and Ye, H. (2021a). A Possible Role of Allatostatin C in Inhibiting Ecdysone Biosynthesis Revealed in the Mud Crab *Scylla paramamosain*. *Front. Mar. Sci.* **8**.

Liu, H., Wang, J., and Li, S. (2014). E93 predominantly transduces 20-hydroxyecdysone signaling to induce autophagy and caspase activity in *Drosophila* fat body. *Insect Biochem. Mol. Biol.* **45**, 30–39.

Liu, M., Wu, Z., Yan, C., Liu, Y., Xing, K., Zhang, J., and Sun, Y. (2022a). Ovarian transcriptome and metabolic responses of RNAi-mediated farnesyl pyrophosphate synthase knockdown in *Neocaridina denticulata sinensis*. *Genomics.* **114** (6), 110484.

Liu, M., Xie, X., Tao, T., Jiang, Q., Shao, J., and Zhu, D. (2016). Molecular characterization of methoprene-tolerant gene (Met) in the swimming crab *Portunus trituberculatus*: Its putative role in methyl farnesoate-mediated vitellogenin transcriptional activation. *Anim. Reprod. Sci.* **174**, 132–142.

Liu, M., Yan, C., Liu, Y., Wu, Z., Zhang, J., and Sun, Y. (2022b). Cloning, expression analysis and RNAi of farnesoic acid O-methylransferase gene from *Neocaridina denticulata sinensis*. *Comp. Biochem. Physiol. B Biochem. Mol. Biol.* **259**, 110719.

Liu, X. J., Jun, G., Liang, X. Y., Zhang, X. Y., Zhang, T. T., Liu, W. M., Zhang, J. Z., and Zhang, M. (2021b). Silencing of transcription factor E93 inhibits adult morphogenesis and disrupts cuticle, wing and ovary development in *Locusta migratoria*. *Insect Sci.* **29** (2), 33–343.

Long, W. C., Pruisner, P., Swiney, K. M., Foy, R. J., and Woodson, C. B. (2019). Effects of ocean acidification on the respiration and feeding of juvenile red and blue king crabs (*Paralithodes camtchaticus* and *P. platypus*). *ICES Journal of Marine Science*. **76** (5), 1335–1343.

Lorentzen, G., Voldnes, G., Whitaker, R. D., Kvalvik, I., Vang, B., Gjerp Solstad, R., Thomassen, M. R., and Siikavuopio, S. I. (2018). Current Status of the Red King Crab (*Paralithodes camtchaticus*) and Snow Crab (*Chionoecetes opilio*) Industries in Norway. *Reviews in Fisheries Science and Aquaculture* **26**, 42–54.

Lozano, J. and Belles, X. (2011). Conserved repressive function of Krüppel homolog 1 on insect metamorphosis in hemimetabolous and holometabolous species. *Sci. Rep.* **1**, 163.

Lu, T., Shen, Y., Cui, G. X., Yin, F. W., Yu, Z. L., and Zhou, D. Y. (2020). Detailed Analysis of Lipids in Edible Viscera and Muscles of Cooked Crabs *Portunus trituberculatus* and *Portunus pelagicus*. *Journal of Aquatic Food Product Technology.* **29** (4), 391–406.

Ma, H. Y., Li, Y. Y., Li, L., Tan, Y., and Pang, B. P. (2021a). Juvenile hormone regulates the reproductive diapause through Methoprene-tolerant gene in *Galeruca daurica*. *Insect Mol. Biol.* **30**, 446–458.

Ma, H. Y., Li, Y. Y., Li, L., Tan, Y., and Pang, B. P. (2021b). Regulation of juvenile hormone on summer diapause of *Galeruca daurica* and its pathway analysis. *Insects.* **12** (3), 237.

Ma, L., Zhang, W., Liu, C., Chen, L., Xu, Y., Xiao, H., and Liang, G. (2018). Methoprene-tolerant (Met) is indispensable for larval metamorphosis and female reproduction in the cotton bollworm helicoverpa armigera. *Front. Physiol.* **9**

Mak, A. S. C., Choi, C. L., Tiu, S. H. K., Hui, J. H. L., He, J. G., Tobe, S. S., and Chan, S. M. (2005). Vitellogenesis in the red crab *Charybdis feriatus*: Hepatopancreas-specific expression and farnesoic acid stimulation of vitellogenin gene expression. *Mol. Reprod. Dev.* **70** (3), 288–300.

Manfrini, E., Courchamp, F., and Leroy, B. (2024). Mitigating the role of aquaculture in crustacean invasions. *Rev Aquac*. **17** (1).

Mao, Y., Li, Y., Gao, H., and Lin, X. (2019). The Direct Interaction between E93 and Kr-h1 Mediated Their Antagonistic Effect on Ovary Development of the Brown Planthopper. *Int. J. Mol. Sci.* **20** (10), 2431.

Marchetti, G. and Tavosanis, G. (2017). Steroid Hormone Ecdysone Signaling Specifies Mushroom Body Neuron Sequential Fate via Chinmo. *Current Biology.* **27**, 3017-3024.e4.

Martín, D. (2021). Adult specifier E93 takes control of reproductive cyclicity in mosquitoes. *Proc. Natl. Acad. Sci. U S A.* **118**, 1–3.

Martín, D., Chafino, S., and Franch-Marro, X. (2021). How stage identity is established in insects: the role of the Metamorphic Gene Network. *Curr. Opin. Insect Sci.* **43**, 29–38.

Massari, M. E. and Murre, C. (2000). Helix-Loop-Helix Proteins: Regulators of Transcription in Eucaryotic Organisms. *Mol. Cell. Biol.* **20** (2), 429–440.

Matheson, K., McKenzie, C. H., Gregory, R. S., Robichaud, D. A., Bradbury, I. R., Snelgrove, P. V. R., and Rose, G. A. (2016). Linking eelgrass decline and impacts on associated fish communities to European green crab *Carcinus maenas* invasion. *Mar. Ecol. Prog. Ser.* **548**, 31–45.

Mazina, M. Y. and Vorobyeva, N. E. (2019). Mechanisms of transcriptional regulation of ecdysone response. *Vavilovskii Zhurnal Genet Selektsii.* **23** (2), 212–218.

Mazurová, E., Hilscherová, K., Triebskorn, R., Köhler, H. R., Maršálek, B., and Bláha, L. (2008). Endocrine regulation of the reproduction in crustaceans: Identification of potential targets for toxicants and environmental contaminants. *Biologia.* **63**, 139–150.

McElhany, P. and Busch, D. S. (2024). Ocean acidification thresholds for decapods are unresolved. *Front. Mar. Sci.* **11**.

McElhany, P., Busch, D. S., Lawrence, A., Maher, M., Perez, D., Reinhardt, E. M., Rovinski, K., and Tully, E. M. (2022). Higher survival but smaller size of juvenile Dungeness crab (*Metacarcinus magister*) in high CO_2. *J. Exp. Mar. Biol. Ecol.* **555**, 151781.

McKenney, C. L., Cripe, G. M., Foss, S. S., Tuberty, S. R., and Hoglund, M. (2004). Comparative embryonic and larval developmental responses of estuarine shrimp (*Palaemonetes pugio*) to the juvenile hormone agonist fenoxycarb. *Arch. Environ. Contam. Toxicol.* **47**, 463–470.

McManus, K. J. and Hendzel, M. J. (2001). CBP, a transcriptional coactivator and acetyltransferase. *Biochemistry and Cell Biology.* **79**, 253–266.

Minakuchi, C., Namiki, T., and Shinoda, T. (2009). Krüppel homolog 1, an early juvenile hormone-response gene downstream of Methoprene-tolerant, mediates its anti-metamorphic action in the red flour beetle *Tribolium castaneum*. *Dev. Biol.* **325**, 341–350.

Minakuchi, C. and Riddiford, L. M. (2006). Insect juvenile hormone action as a potential target of pest management. *J. Pestic. Sci.* **31**, 77–84.

Minakuchi, C., Tanaka, M., Miura, K., and Tanaka, T. (2011). Developmental profile and hormonal regulation of the transcription factors broad and Krüppel homolog 1 in hemimetabolous thrips. *Insect Biochem. Mol. Biol.* **41**, 125–134.

Minakuchi, C., Zhao, X., and Riddiford, L. M. (2008). Krüppel homolog 1 (Kr-h1) mediates juvenile hormone action during metamorphosis of *Drosophila melanogaster*. *Mech. Dev.* **125**, 91–105.

Miura, K., Oda, M., Makita, S., and Chinzei, Y. (2005). Characterization of the *Drosophila* Methoprene-tolerant gene product: Juvenile hormone binding and ligand-dependent gene regulation. *FEBS Journal.* **272**, 1169–1178.

Miura, T. (2019). Juvenile hormone as a physiological regulator mediating phenotypic plasticity in pancrustaceans. *Dev. Growth Differ.* **61**, 85–96.

Miyakawa, H., Toyota, K., Hirakawa, I., Ogino, Y., Miyagawa, S., Oda, S., Tatarazako, N. Miura, T. Colbourne, J, K., and Iguchi, T. (2013). A mutation in the receptor Methoprene-tolerant alters juvenile hormone response in insects and crustaceans. *Nat. Commun.* **4**, 1856.

Mou, X., Duncan, D. M., Baehrecke, E. H., and Duncan, I. (2012). Control of target gene specificity during metamorphosis by the steroid response gene E93. *Proc. Natl. Acad. Sci. U. S. A.* **109**, 2949–2954.

Muhd-Farouk, H., Nurul, H. A., Abol-Munafi, A. B., Mardhiyyah, M. P., Hasyima-Ismail, N., Manan, H., Fatihah, S. N., Amin-Safwan, A., and Ikhwanuddin, M. (2019). Development of ovarian maturations in orange mud crab, *Scylla olivacea* (Herbst, 1796) through induction of eyestalk ablation and methyl farnesoate. *Arab J. Basic Appl. Sci.* **26** (1), 171–181.

Mykles, D. L. (2001). Interactions Between Limb Regeneration and Molting in Decapod Crustaceans. *American Zoologist.* **41** (3), 399–406.

Mykles, D. L. (2011). Ecdysteroid metabolism in crustaceans. *Journal of Steroid Biochemistry and Molecular Biology.* **127**, 196–203.

Mykles, D. L. (2021). Signaling Pathways That Regulate the Crustacean Molting Gland. *Front Endocrinol.* **12**.

Mykles, D. L. (2024). "Molting Physiology," in *Frontiers in Invertebrate Physiology A Collection of Review*, eds. S. Saleuddin, S. P. Leys, R. D. Roer, and I. C. Wilkie (Apple Academic Press). **229**.

Mykles, D. L., Adams, M. E., Gäde, G., Lange, A. B., Marco, H. G., and Orchard, I. (2010). Neuropeptide action in insects and crustaceans. *Physiological and Biochemical Zoology.* **83**, 836–846.

Mykles, D. L. and Chang, E. S. (2020). Hormonal control of the crustacean molting gland: Insights from transcriptomics and proteomics. *Gen. Comp. Endocrinol.* **294**.

Naczk, M., Williams, J., Brennan, K., Liyanapathirana, C., and Shahidi, F. (2004). Compositional characteristics of green crab (*Carcinus maenas*). *Food Chem.* **88**, 429–434.

Nagaraju, G. P. C. (2007). Is methyl farnesoate a crustacean hormone? *Aquaculture.* **272**, 39–54.

Nagaraju, G. P. C. and Borst, D. W. (2008). Methyl farnesoate couples environmental changes to testicular development in the crab *Carcinus maenas. Journal of Experimental Biology.* **211**, 2773–2778.

Nakagawa, Y. and Henrich, V. C. (2009). Arthropod nuclear receptors and their role in molting. *FEBS Journal.* **276**, 6128–6157.

Nakatsuji, T., Lee, C. Y., and Watson, R. D. (2009). Crustacean molt-inhibiting hormone: Structure, function, and cellular mode of action. *Comparative Biochemistry and Physiology - A Molecular and Integrative Physiology.* **152**, 139–148.

Nanda, P. K., Das, A. K., Dandapat, P., Dhar, P., Bandyopadhyay, S., Dib, A. L., Lorenzo, J. M., and Gagaoua, M. (2021). Nutritional aspects, flavour profile and health benefits of crab meat based novel food products and valorisation of processing waste to wealth: A review. *Trends Food Sci. Technol.* **112**, 252–267.

Narbonne-Reveau, K. and Maurange, C. (2019). Developmental regulation of regenerative potential in *Drosophila* by ecdysone through a bistable loop of ZBTB transcription factors. *PLoS Biol.* **17** (2), e3000149.

Nardini, M., Svergun, D., Konarev, P. V., Spanò, S., Fasano, M., Bracco, Pesce, A. Donadini, A., Cericola, C., Secundo, F., Luini, A., Corda, D., and Bolognesi, M. (2006). The C-terminal domain of the transcriptional corepressor CtBP is intrinsically unstructured. *Protein Science.* **15** (15), 1042–1050.

Nibu, Y., Zhang, H., Bajor, E., Barolo, S., Small, S., and Levine, M. (1998). dCtBP mediates transcriptional repression by Knirps, Krüppel and Snail in the *Drosophila* embryo. *EMBO J.* **17** (23), 7009– 7020.

Nicewicz, A. W., Sawadro, M. K., Nicewicz, Ł., and Babczyńska, A. I. (2021). Juvenile hormone in spiders. Is this the solution to a mystery? *Gen. Comp. Endocrinol.* **308**.

Nijhout, H. F., Riddiford, L. M., Mirth, C., Shingleton, A. W., Suzuki, Y., and Callier, V. (2014). The developmental control of size in insects. *Wiley Interdiscip. Rev. Dev. Biol.* **3** (1), 113–134.

Nijhout, H. F. and Williams, C. M. (1974). Control of Moulting and Metamorphosis in the Tobacco Hornworm, *Manduca sexta* (L.): Growth of the Last-Instar Larva and the Decision to Pupate. *J. Exp. Biol.* **61** (2), 481–491.

Niwa, R. and Niwa, Y. S. (2014). Enzymes for ecdysteroid biosynthesis: Their biological functions in insects and beyond. *Biosci. Biotechnol. Biochem.* **78**, 1283–1292.

Niwa, Y. S. and Niwa, R. (2016). Transcriptional regulation of insect steroid hormone biosynthesis and its role in controlling timing of molting and metamorphosis. *Dev. Growth. Differ.* **58**, 94–105.

Noriega, F. G. and Nouzova, M. (2020). Approaches and tools to study the roles of juvenile hormones in controlling insect biology. *Insects.* **11**, 1–9.

Nouzova, M., Edwards, M. J., Michalkova, V., Ramirez, C. E., Ruiz, M., Areiza, M., DeGennaro, M., Fernandez-Lima, F., Feyereisen, R., Jindra, M. and Noriega, F. G. (2021). Epoxidation of juvenile hormone was a key innovation improving insect reproductive fitness. *PNAS.* **118**, 1–9.

Nüsslein, C. and Wieschaus, E. (1980). Mutations affecting segment number and polarity in *Drosophila*. *Nature.* **287**, 795–801.

Nystrom, S. L., Niederhuber, M. J., and McKay, D. J. (2020). Expression of E93 provides an instructive cue to control dynamic enhancer activity and chromatin accessibility during development. *Development.* **147**.

Obsil, T. and Obsilova, V. (2008). Structure/function relationships underlying regulation of FOXO transcription factors. *Oncogene.* **27**, 2263–2275.

Ojani, R., Fu, X., Ahmed, T., Liu, P., and Zhu, J. (2018). Krüppel homologue 1 acts as a repressor and an activator in the transcriptional response to juvenile hormone in adult mosquitoes. *Insect Mol. Biol.* **27**, 268–278.

Okude, G., Moriyama, M., Kawahara-Miki, R., Yajima, S., Fukatsu, T., and Futahashi, R. (2022). Molecular mechanisms underlying metamorphosis in the most-ancestral winged insect. *PNAS.* **119**, 1–12.

Okumura, T. and Aida, K. (2000). Fluctuations in hemolymph ecdysteroid levels during the reproductive and non-reproductive molt cycles in the giant freshwater prawn *Macrobrachium rosenbergii*. *Fisheries Science.* **66**, 876–883.

Oñate, S. A., Tsai, S. Y., Tsai, M.J., and O'Malley, B. W. (1995). Sequence and Characterization of a Coactivator for the Steroid Hormone Receptor Superfamily. *Science Reports.* **270**, 1354–1357.

Orchard, I. and Lange, A. B. (2024a). The neuroendocrine and endocrine systems in insect – Historical perspective and overview. *Mol. Cell Endocrinol.* **580**.

O'Shea, M., Colbert, R., Williams, L., and Dunn, S. (1998). Nitric oxide compartments in the mushroom bodies of the locust brain. *Neuroreport.* **9** (2), 333–336.

Ou, Q. and King-Jones, K. (2013). "What Goes Up Must Come Down. Transcription Factors Have Their Say in Making Ecdysone Pulses," in *Current Topics in Developmental Biology*, (Academic Press Inc.), 35–71.

Pan, F., Fu, Y., Zhang, W., Jiang, S., Xiong, Y., Yan, Y., Gong, Y., Qiao, H., and Fu, H. (2022). Characterization, expression and functional analysis of CYP306a1 in the oriental river prawn, *Macrobrachium nipponense*. *Aquac. Rep.* **22**, 101009.

Paran, B. C., Fierro, I. J., and Tsukimura, B. (2010). Stimulation of ovarian growth by methyl farnesoate and eyestalk ablation in penaeoidean model shrimp, *Sicyonia ingentis* Burkenroad, 1938. *Aquac. Res.* **41**, 1887–1897.

Pathak, N., Shakila, R. J., Jeyasekaran, G., Padmavathy, P., Neethiselvan, N., Shalini, R., Arisekar, U., Patel, A., Kumar, U., Malini, A. H., and Mayilvahnan, R. (2021). Variation in the Nutritional Composition of Soft and Hard Blue Swimming Crabs (*Portunus pelagicus*) Having Good Export Potential. *Journal of Aquatic Food Product Technology.* **30**, 706–719.

Pearson, R., Fleetwood, J., Eaton, S., Crossley, M., and Bao, S. (2008). Krüppel-like transcription factors: A functional family. *International Journal of Biochemistry and Cell Biology.* **40**, 1996–2001.

Pecasse, F., Beck, Y., Ruiz, C., and Richards, G. (2000a). Krüppel-homolog, a stage-specific modulator of the prepupal ecdysone response, is essential for *Drosophila* metamorphosis. *Dev. Biol.* **221** (1), 53–67.

Pecenova, L. and Farkas, R. (2016). Multiple functions and essential roles of nuclear receptor coactivators of bHLH-PAS family. *Endocr. Regul.* **50**, 165–181.

Pitts, N. L. and Mykles, D. L. (2017). Localization and expression of molt-inhibiting hormone and nitric oxide synthase in the central nervous system of the green shore crab, *Carcinus maenas*, and the blackback land crab, *Gecarcinus lateralis*. *Comp. Biochem. Physiol. A Mol Integr. Physiol*. **203**, 328–340.

Pitts, N. L., Schulz, H. M., Oatman, S. R., and Mykles, D. L. (2017). Elevated expression of neuropeptide signaling genes in the eyestalk ganglia and Y-organ of *Gecarcinus lateralis* individuals that are refractory to molt induction. *Comp. Biochem. Physiol. A Mol Integr. Physiol.* **214**, 66–78.

Ponting, C. P. and Aravind, L. (1997). PAS: a multifunctional domain comes to light. *Current Biology.* **7**, R674–R677.

Ponting, C. P., Mott, R., Bork, P., and Copley, R. R. (2001). Novel protein domains and repeats in *Drosophila melanogaster*: Insights into structure, function, and evolution. *Genome Res.* **11**, 1996–2008.

Praggastis, S. A., Lam, G., Horner, M. A., Nam, H. J., and Thummel, C. S. (2021). The *Drosophila* E78 nuclear receptor regulates dietary triglyceride uptake and systemic lipid levels. *Developmental Dynamics.* **250**, 640–651.

Preiss, A., Rosenberg, U. B., Kienlin, A., Seifert, E., and Jackie, H. (1984). Molecular genetics of Krüppel, a gene required for segmentation of the *Drosophila* embryo. *Nature.* **313**, 520–528.

Prestwich, G. D., Bruce, M. J., Ujvary, I., and Chang, E. S. (1990). Binding Proteins for Methyl Farnesoate in Lobster Tissues: Detection by Photoaffinity Labeling. *Gen Comp Endocrinol* **80**, 232–237.

Prestwich, G. D., Wojtasek, H., Lentz, A. J., and Rabinovich, J. M. (1996). Biochemistry of Proteins That Bind and Metabolize Juvenile Hormones. *Arch. Insect Biochem. Physiol.* **32**, 407–419.

Priya, T. A. J., Li, F., Zhang, J., Wang, B., Zhao, C., and Xiang, J. (2009). Molecular characterization and effect of RNA interference of retinoid X receptor (RXR) on E75 and chitinase gene expression in Chinese shrimp *Fenneropenaeus chinensis*. *Comparative Biochemistry and Physiology - B Biochemistry and Molecular Biology.* **153**, 121–129.

Priya, T. A. J., Li, F., Zhang, J., Yang, C., and Xiang, J. (2010). Molecular characterization of an ecdysone inducible gene E75 of Chinese shrimp *Fenneropenaeus chinensis* and elucidation of its role in molting by RNA interference. *Comparative Biochemistry and Physiology - B Biochemistry and Molecular Biology.* **156**, 149–157.

Qian, Z., He, S., Liu, T., Liu, Y., Hou, F., Liu, Q., Wang, X. Mi, X., Wang, P. and Liu, X. (2014). Identification of ecdysteroid signaling late-response genes from different tissues of the Pacific white shrimp, *Litopenaeus vannamei*. *Comparative Biochemistry and Physiology - A Molecular and Integrative Physiology.* **172**, 10–30.

Qian, Z. and Liu, X. (2019). Elucidation of the role of farnesoic acid *O*-methyltransferase (FAMeT) in the giant freshwater prawn, *Macrobrachium rosenbergii*: Possible functional correlation with ecdysteroid signaling. *Comp. Biochem. Physiol. A Mol. Integr. Physiol.* **232**, 1–12.

Qu, Z., Kenny, N. J., Lam, H. M., Chan, T. F., Chu, K. H., Bendena, W. G., Tobe, S. S., and Hui J. H. L. (2015). How Did Arthropod Sesquiterpenoids and Ecdysteroids Arise? Comparison of Hormonal Pathway Genes in Noninsect Arthropod Genomes. *Genome Biol. Evol.* **7**, 1951–1959.

Raghavan, S. D. A. and Ayanath, A. (2019). Effect of 20-OH ecdysone and methyl farnesoate on moulting in the freshwater crab *Travancoriana schirnerae*. *Invertebr. Reprod. Dev.* **63**, 309–318.

Rahman, M. R., Asaduzzaman, M., Zahangir, M. M., Islam, S. R., Nahid, S. A. Al, Jahan, D. A., Mahmud, Y., and Khan, M. N. A. (2020). Evaluation of limb autotomy as a promising strategy to improve production performances of mud crab (*Scylla olivacea*) in the soft-shell farming system. *Aquac. Res.* **51**, 2555–2572.

Raicu, A. M., Kadiyala, D., Niblock, M., Jain, A., Yang, Y., Bird, K. M., Bertholf, K., Seenivasan, A., Siddiq, M., and Arnosti, D. N. (2023). The Cynosure of CtBP: Evolution of a Bilaterian Transcriptional Corepressor. *Mol. Biol. Evol.* **40**.

Raicu, A. M., Suresh, M., and Arnosti, D. N. (2024). A regulatory role for the unstructured C-terminal domain of the CtBP transcriptional corepressor. *Journal of Biological Chemistry.* **300**.

Ramos, F. O., Nouzova, M., Fruttero, L. L., Leyria, J., Ligabue-Braun, R., Noriega, F. G., and Canavoso, L.E. (2022). Role of Methoprene-tolerant in the regulation of oogenesis in *Dipetalogaster maxima*. *Sci. Rep.* **12**.

Reddy, P, R. (2017). Crustacean Endocrinology: Intriguing Towards Quality Protein Production. *J. Endocrinol. Thyroid. Res.* **1**.

Reddy, P. R. and Arifullah, M. (2021). Dietary methyl farnesoate, a potential growth inducer in male crab *Oziothelphusa senex senex*. *IOP Conference Series: Earth and Environmental Science*. **756** (1), 012062.

Reddy, P. R., Purna, G., Nagaraju, C., and Reddy, P. S. (2004). Involvement of Methyl Farnesoate in the Regulation of Molting and Reproduction in the Freshwater Crab *Oziotelphusa senex senex*. *Journal of Crustacean Biology.* **24**, 511–515.

Reddy, P. S. and Ramamurthi, R. (1998). Methyl farnesoate stimulates ovarian maturation in the freshwater crab *Oziotelphusa senex senex* Fabricius. *Current Science.* **74**, 68–70.

Reinking, J., Lam, M. M. S., Pardee, K., Sampson, H. M., Liu, S., Yang, P., Williams, S. White, W., Lajoie, G., Edwards, A., and Krause, H. M. (2005). The *Drosophila* nuclear receptor E75 contains heme and is gas responsive. *Cell.* **122**, 195–207.

Reynolds, S. E. (2022). A transcription factor enables metamorphosis. *Proc. Natl. Acad. Sci. U. S. A.* **119** (22), e2204972119.

Riddiford, L. M., Hiruma, K., Zhou, X., and Nelson, C. A. (2003). Insights into the molecular basis of the hormonal control of molting and metamorphosis from *Manduca sexta* and *Drosophila melanogaster. Insect Biochem. Mol. Biol.* **33**, 1327–1338.

Risso, S. J. and Carelli, A. A. (2012). Nutrient composition of raw and cooked meat of male southern king crab (*Lithodes santolla* Molina, 1782). *Journal of Aquatic Food Product Technology.* **21**, 433–444.

Rodríguez, E. M. (2024). Endocrine disruption in crustaceans: New findings and perspectives. *Mol. Cell Endocrinol.* **585**.

Rodríguez, E. M., Medesani, D. A., and Fingerman, M. (2007). Endocrine disruption in crustaceans due to pollutants: A review. *Comparative Biochemistry and Physiology - A Molecular and Integrative Physiology.* **146**, 661–671.

Roer, R. D. , Shaked, S., and Sagi, A. (2024). "Biomineralization: Ion Transport and Control Processes," in *Frontiers in invertebrate physiology : a collection of reviews*, eds. S. Saleuddin, S. P. Leys, R. Roer, and I. C. Wilkie (Apple Academic Press), 275.

Roer, R. and Dillaman, R. (1984). The Structure and Calcification of the Crustacean Cuticle. *Amer. Zool.* **24**, 893–909.

Roy, A., George, S., and Palli, S. R. (2017). Multiple functions of CREB-binding protein during postembryonic development: Identification of target genes. *BMC Genomics.* **18**.

Ruddell, C. J., Wainwright, G., Geffen, A., White, M. R. H., Webster, S. G., and Rees, H. H. (2003). Cloning, Characterization, and Developmental Expression of a Putative Farnesoic Acid *O*-Methyl Transferase in the Female Edible Crab *Cancer pagurus*. *Biol. Bull.* **205** (3), 308–318.

Sagi, A., Manor, R., and Ventura, T. (2013). Gene Silencing in Crustaceans: From Basic Research to Biotechnologies. *Genes.* **4**, 620–645.

Saikrithi, P., Balasubramanian, C. P., Otta, S. K., and Tomy, S. (2019). Characterization and expression profile of farnesoic acid *O*-methyltransferase gene from Indian white shrimp, *Penaeus indicus*. *Comp. Biochem. Physiol. B Biochem. Mol. Biol.* **232**, 79–86.

Sarower, M. G., Bilkis, S., Rauf, M. A., Khanom, M., and Islam, M. S. (2013). Comparative Biochemical Composition of Natural and Fattened Mud Crab *Scylla serrata*. *Journal of Scientific Research.* **5**, 545–553.

Satoh, T. and Hosokawa, M. (2006). Structure, function and regulation of carboxylesterases. *Chem. Biol. Interact.* **162**, 195–211.

Schaeper, U., Boyd, J. M., Verma, S., Uhlmann, E., Subramanian, T., and Chinnadurai, G. (1995). Molecular cloning and characterization of a cellular phosphoprotein that interacts with a conserved C-terminal domain of adenovirus ElA involved in negative modulation of oncogenic transformation. *Proc. Natl. Acad. Sci. U S A.* **92** .

Schuh, R., Aicher, W., Gaul, U., Cime, S., Preiss, A., Maier, D., Seifer, E. Nauber, U., Schröder, C., Kemler, R., and Jäckle, H. (1986). A Conserved Family of Nuclear Proteins Containing Structural Elements of the Finger Protein Encoded by Krüppel, a *Drosophila* Segmentation Gene. *Cell.* **47**, 1025–1032.

Schumann, I., Kenny, N., Hui, J., Hering, L., and Mayer, G. (2018). Halloween genes in panarthropods and the evolution of the early moulting pathway in Ecdysozoa. *R. Soc. Open Sci.* **5**.

Segraves, W. A. and Hogness, D. S. (1990). The E75 ecdysone-inducible gene responsible for the 75B early puff in *Drosophila* encodes two new members of the steroid receptor superfamily. *Genes Dev.* **4**, 204–219.

Segraves, W. A. and Woldin, C. (1993). The E75 Gene of *Manduca* sexta and Comparison with its *Drosophila* Homolog. *Insect Biochem. Molec. Biol.* **23**, 91–97.

Shao, L., Wang, C., He, J., Wu, X., and Cheng, Y. (2013). Hepatopancreas and gonad quality of Chinese mitten crabs fattened with natural and formulated diets. *J. Food Qual.* **36**, 217–227.

Sharrocks, A. D. (2001). The ETS-Domain Transcription Factor Family. *Nat. Rev. Mol. Cell Biol.* **2**, 827–837.

Shaywitz, A. J., Dove, S. L., Kornhauser, J. M., Hochschild, A., and Greenberg, M. E. (2000). Magnitude of the CREB-Dependent Transcriptional Response Is Determined by the Strength of the Interaction between the Kinase-Inducible Domain of CREB and the KIX Domain of CREB-Binding Protein. *Mol. Cell Biol.* **20** (24), 9409–9422.

Shinoda, T. and Itoyama, K. (2003). Juvenile hormone acid methyltransferase: A key regulatory enzyme for insect metamorphosis. *PNAS.* **100**, 11986–11991.

Shyamal, S., Das, S., Guruacharya, A., Mykles, D. L., and Durica, D. S. (2018). Transcriptomic analysis of crustacean molting gland (Y-organ) regulation via the mTOR signaling pathway. *Sci Rep.* **8**.

Si, M. R., Li, Y. D., Jiang, S. G., Yang, Q. Bin, Jiang, S., Yang, L. S., Huang, J. H., Chen, X., and Zhou, F. L. (2022). Identification of multifunctionality of the PmE74 gene and development of SNPs associated with low salt tolerance in *Penaeus monodon*. *Fish Shellfish Immunol.* **128**, 7–18.

Siegmund, T. and Lehmann, M. (2002). The *Drosophila* Pipsqueak protein defines a new family of helix-turn-helix DNA-binding proteins. *Dev. Genes Evol.* **212**, 152–157.

Siggs, O. M. and Beutler, B. (2012). The BTB-ZF transcription factors. *Cell Cycle.* **11**, 3358–3369.

Sin, Y. W., Kenny, N. J., Qu, Z., Chan, K. W., Chan, K. W. S., Cheong, S. P. S., Leung, R. W. T., Chan, T. F., Bendena, W. G., Chu, K. H., Tobe, S. S., and Hui., J. H. L. (2015). Identification of putative ecdysteroid and juvenile hormone pathway genes in the shrimp *Neocaridina denticulata*. *Gen. Comp. Endocrinol.* **214**, 167–176.

Skinner, D. M. (1962). The Structure and Metabolism of a Crustacean Integumentary Tissue During a Molt Cycle. *Biol. Bull.* **123** (3), 635–647.

Skinner, D. M. (1985a). Interacting Factors in the Control of the Crustacean Molt Cycle. *American Zool.* **25**, 275–284.

Skinner, D. M. (1985b). "Molting and Regeneration," in *Biology of Crustacea*, (Academic Press), 550.

Skinner, D. M. and Graham, D. E. (1972). Loss of Limbs as a Stimulus to Ecdysis in Brachyura (True Crabs). *Biol. Bull.* **143**, 222–233.

Skonberg, D. I. and Perkins, B. L. (2002). Nutrient composition of green crab (*Carcinus maenus*) leg meat and claw meat. *Food Chem.* **77**, 401–404.

Smija, M. K. and Sudha Devi, A. R. (2016). Histological changes of Y organ in *Travancoriana schirnerae* during moult cycle and in de-eyestalked crabs. *Turk. J. Fish. Aquat. Sci.* **16**, 533–544.

Smith, P. A., Clare, A. S., Rees, H. H., Prescott, M. C., Wainwright, G., and Thorndyke, M. C. (2000). Identification of methyl farnesoate in the cypris larva of the barnacle, *Balanus amphitrite*, and its role as a juvenile hormone. *Insect Biochem. Mol. Biol.* **30**, 885–890.

So, W. L., Kai, Z., Qu, Z., Bendena, W. G., and Hui, J. H. L. (2022). Rethinking Sesquiterpenoids: A Widespread Hormone in Animals. *Int. J. Mol. Sci.* **23**.

Spaziani, E., Mattson, M. P., Wang, W. L., and Mcdougall, H. E. (1999). Signaling Pathways for Ecdysteroid Hormone Synthesis in Crustacean Y-organs. *American Zoologist*. **39** (3), 496–512.

Spindler, K. D., Hönl, C., Tremmel, C., Braun, S., Ruff, H., and Spindler-Barth, M. (2009). Ecdysteroid hormone action. *Cellular and Molecular Life Sciences.* **66**, 3837–3850.

Spokony, R. F. and Restifo, L. L. (2007). Anciently duplicated Broad Complex exons have distinct temporal functions during tissue morphogenesis. *Dev. Genes Evol.* **217**, 499–513.

Sreelakshmi, K. R., Manjusha, L., Vartak, V. R., and Venkateshwarlu, G. (2016). Variation in proximate composition and fatty acid profiles of mud crab meat with regard to sex and body parts. *Indian Journal of Fisheries.* **63**, 147–150.

Stone, B. L. and Thummel, C. S. (1993). The *Drosophila* 78C Early Late Puff Contains E78, an Ecdysone-lnducible Gene That Encodes a Novel Member of the Nuclear Hormone Receptor Superfamily. *Cell.* **75**, 307–320.

Strausfeld, N. J. (2021). Mushroom bodies and reniform bodies coexisting in crabs cannot both be homologs of the insect mushroom body. *Journal of Comparative Neurology.* **529**, 3265–3271.

Strausfeld, N. J., Wolff, G. H., and Sayre, M. E. (2020). Mushroom body evolution demonstrates homology and divergence across Pancrustacea. *Elife*. **9**.

Subramoniam, T. (2000). Crustacean ecdysteriods in reproduction and embryogenesis. *Comparative Biochemistry and Physiology Part C.* **125**.

Sudhakar, M., Manivannan, K., and Soundrapandian, P. (2009). Nutritive Value of Hard and Soft Shell Crabs of *Portunus sanguinolentus* (Herbst). *Int. J. Anim. Vet. Adv.* **1**, 44–48.

Sullivan, L. F., Barker, M. S., Felix, P. C., Vuong, R. Q., and White, B. H. (2022). Neuromodulation and the toolkit for behavioural evolution: can ecdysis shed light on an old problem? *FEBS Journal.* **291**, 1049–1079.

Sun, G., Zhu, J., Chen, L., and Raikhel, A. S. (2005). Synergistic action of E74B and ecdysteroid receptor in activating a 20-hydroxyecdysone effector gene. *PNAS.* **102**, 15506–15511.

Sun, G., Zhu, J., Li, C., Tu, Z., and Raikhel, A. S. (2002). Two isoforms of the early E74 gene, an Ets transcription factor homologue, are implicated in the ecdysteroid hierarchy governing vitellogenesis of the mosquito *Aedes aegypti*. *Mol. Cell Endocrinol.* **2002**, 147157.

Sun, Y., Fu, D., Liu, B., Wang, L., and Chen, H. (2022). Functional Characterization of Allatostatin C (PISCF/AST) and Juvenile Hormone Acid *O*-Methyltransferase in *Dendroctonus armandi*. *Int. J. Mol. Sci.* **23**.

Sunarti, Y., Soejoedono, R. D., Mayasari, N. L. P. I., and Tahya, A. M. (2016). RNA expression of farnesoic acid O-methyl transferase in mandibular organ of intermolt and premolt mud crabs *Scylla olivacea*. *AACL Bioflux.* **9** (2), 270–275.

Suneetha, Y., Naga Jyothi, P., and Srinivasulu Reddy, M. (2010). Impact of Methyl Farnesoate in the regulation of Molting and Reproduction in the Tropical Penaeid Prawn *Penaeus monodon*. *Global Journal of Biotecnology & Biochemistry.* **5**, 75–70.

Sutherland, C., Henderson, A., Trotter, A. J., Giosio, D., and Smith, G. (2023). Assessing sensing techniques for detecting markers of approaching ecdysis in juvenile tropical rock lobsters, *Panulirus ornatus*. *Aquac. Eng.* **102**.

Swall, M. E., Benrabaa, S. A. M., Tran, N. M., Tran, T. D., Ventura, T., and Mykles, D. L. (2021). Characterization of Shed genes encoding ecdysone 20-monooxygenase (CYP314A1) in the Y-organ of the blackback land crab, *Gecarcinus lateralis*. *Gen. Comp. Endocrinol.* **301**.

Swevers, L., Ito, K., and Iatrou, K. (2002). The BmE75 nuclear receptors function as dominant repressors of the nuclear receptor BmHR3A. *Journal of Biological Chemistry.* **277**, 41637–41644.

Tahya, A. M., Zairin Junior, M., Boediono, A., Artika, I. M., and Suprayudi, M. A. (2016a). Expression of RNA encode FAMeT in mandibular organ of mud crabs *Scylla olivacea*. *Int. J. Pharmtech Res.* **9**, 219–223.

Tahya, A. M., Zairin, M. J., Artika, A. B. I. M., and Suprayudi, M. A. (2016b). Important role of mandibular organ in molting, growth, and survival of mud crab *Scylla olivacea*. *Int. J. Chemtech. Res.* **9**, 529–533.

Takac, P., Ahl, J. S. B., and Laufer, H. (1997). Seasonal differences in methyl farnesoate esterase activity in tissues of the spider crab *Libinia emarginata*. *Invertebr. Reprod. Dev.* **31**, 211–216.

Takác, **P.**, Ahl, J. S. B., and Laufer, H. (1998). Methyl farnesoate binding proteins in tissues of the spider crab, *Libinia emarginata*. *Comparative Biochemistry and Physiology Part B.* **120**, 769–775.

Taketomi, T., Motono, M., and Miyakawi, M. (1989). On the biological function of the mandibular gland of decapod crustacea. *Cell Biol. Int. Rep.* **13**, 463.

Taketomi, Y. and Hyodo, M. (1986). The Y Organ of the Crab, *Portunus trituberculatus*: Effects of Ecdysterone on the Ultrastructure. *Cell Biol. Int. Rep.* **70**, 367–374.

Taketomi, Y. and Kawano, Y. (1985). Ultrastructure of the mandibular organ of the shrimp, *Penaeus japonicus*, in untreated and experimentally manipulated individuals. *Cell Biol. Int. Rep.* **9**, 1069–1074.

Taketomi, Y. and Nakano, Y. (2007). Y-organ and mandibular organ of the crayfish *Procambarus clarkii* during the molt cycle. *Crustacean Research* 36, 25–36.

Takeuchi, H., Kage, E., Sawata, M., Kamikouchi, A., Ohashi, K., Ohara, M., Fujiyuki, T., Kunieda, T., Sekimizu, K., Natori, S., and Kubo, T. (2001). Identification of a novel gene, Mblk-1, that encodes a putative transcription factor expressed preferentially in the large-type Kenyon cells of the honeybee brain. *Insect Mol. Biol.* **10** (5), 487–494.

Tamone, S. L. and Chang, E. S. (1993). Methyl farnesoate stimulates Ecdysteroid Secretion from Crab Y-organs *in Vitro*. *General and Comparative Endocrinology.* **89** (3), 425–432.

Tamone, S. L., Prestwich, G. D., and Chang, E. S. (1997). Identification and Characterization of Methyl Farnesoate Binding Proteins from the Crab, *Cancer magister*. *Gen. Comp. Endocrinol.* **105**, 168–175.

Tang, Y., He, H., Qu, X., Cai, Y., Ding, W., Qiu, L., and Li, Y. (2020). RNA interference-mediated knockdown of the transcription factor Krüppel homologue 1 suppresses vitellogenesis in *Chilo suppressalis*. *Insect Mol. Biol.* **29** (2), 183–192.

Tao, T., Xie, X., Liu, M., Jiang, Q., and Zhu, D. (2017). Cloning of two carboxylesterase cDNAs from the swimming crab *Portunus trituberculatus*: Molecular evidences for their putative roles in methyl farnesoate degradation. *Comp. Biochem. Physiol. B Biochem. Mol. Biol.* **203**, 100–107.

Taubenheim, J., Kortmann, C., and Fraune, S. (2021). Function and Evolution of Nuclear Receptors in Environmental-Dependent Postembryonic Development. *Front. Cell Dev. Biol.* **9**.

Tavares, C. P. S., Da Silva, U. A. T., Pereira, L. Â., and Ostrensky, A. (2021). Evaluation of different induced molting methods in *Callinectes ornatus* (Crustacea, Decapoda, Portunidae) as a tool for the commercial production of soft-shell crabs. *An. Acad. Bras. Cienc.* **93** (2), e20190580.

Techa, S. and Chung, J. S. (2015). Ecdysteroids regulate the levels of molt- inhibiting hormone (MIH) expression in the blue crab, *Callinectes sapidus*. *PLoS One.* **10**.

Thangal, S. H., Muralisankar, T., Anandhan, K., Gayathri, V., and Yogeshwaran, A. (2022). Effect of CO_2 driven ocean acidification on the mud crab *Scylla serrata* instars. *Environmental Pollution.* **31**2.

Thangal, S. H., Muralisankar, T., Mohan, K., Santhanam, P., and Venmathi Maran, B. A. (2024). Biological and physiological responses of marine crabs to ocean acidification: A review. *Environ. Res.* **248**.

Thummel, C. S. (1990). Puffs and gene regulation — molecular insights into the *Drosophila* ecdysone regulatory hierarchy. *BioEssays.* **12**, 561–568.

Thummel, C. S. (2002). Ecdysone-regulated puff genes 2000. *Insect Biochem. Mol. Biol.* **32**, 113–120.

Tian, Z., Guo, S., Li, J. X., Zhu, F., Liu, W., and Wang, X. P. (2021). Juvenile hormone biosynthetic genes are critical for regulating reproductive diapause in the cabbage beetle. *Insect Biochem. Mol. Biol.* **139**.

Tiu, S. H. K., Hui, J. H. L., He, J. G., Tobe, S. S., and Chan, S. M. (2006). Characterization of vitellogenin in the shrimp *Metapenaeus ensis*: Expression studies and hormonal regulation of MeVg1 transcription in vitro. *Mol. Reprod. Dev.* **73**, 424–436.

Tiu, S. H. K., Hult, E. F., Yagi, K. J., and Tobe, S. S. (2012). Farnesoic acid and methyl farnesoate production during lobster reproduction: Possible functional correlation with retinoid X receptor expression. *Gen. Comp. Endocrinol.* **175**, 259–269.

Tobe, S. S. and Bendena, W. G. (1999). The regulation of juvenile hormone production in arthropods. Functional and evolutionary perspectives. *Ann N Y Acad. Sci.* **897**, 300–310.

Tobe, S. S., Young, D. A., and Khoo, H. W. (1989a). Production of Methyl Farnesoate by the Mandibular Organs of the Mud Crab, *Scylla serrata*: Validation of a Radiochemical Assay. *General and Comparative Endocrinology.* **73**, 342–353.

Tobe, S. S., Young, D. A., Khoo, H. W., and Baker, F. C. (1989b). Farnesoic acid as a major product of release from crustacean mandibular organs in vitro. *Journal of Experimental Zoology.* **249**, 165–171.

Torson, A. S., Dong, Y. W., and Sinclair, B. J. (2020). Help, there are “omics” in my comparative physiology! *Journal of Experimental Biology.* **223** (24), jeb191262.

Toyota, K., Yamamoto, T., Mori, T., Mekuchi, M., Miyagawa, S., Ihara, M., Shigenobu, S., and Ohira, T. (2023). Eyestalk transcriptome and methyl farnesoate titers provide insight into the physiological changes in the male snow crab, *Chionoecetes opilio*, after its terminal molt. *Sci. Rep.* **13**, 7204.

Toyota, K., Yamane, F., and Ohira, T. (2020). Impacts of Methyl Farnesoate and 20-Hydroxyecdysone on Larval Mortality and Metamorphosis in the Kuruma Prawn *Marsupenaeus japonicus*. *Front. Endocrinol.* **11**.

Tran, N. M., Mykles, D. L., Elizur, A., and Ventura, T. (2019). Characterization of G-protein coupled receptors from the blackback land crab *Gecarcinus lateralis* Y organ transcriptome over the molt cycle. *BMC Genomics.* **20**, 74.

Truman, J. W. (2019). The Evolution of Insect Metamorphosis. *Current Biology.* **29**, R1252–R1268.

Truman, J. W. and Riddiford, L. M. (2022). Chinmo is the larval member of the molecular trinity that directs *Drosophila* metamorphosis. *Proc. Natl. Acad. Sci. U. S. A.* **119** (15), e2201071119.

Tsai, D. E., Chen, H.C., and Tsai, C.F. (1984). Total lipid and cholesterol content in the blue crab, *Callinectes sapidus* Rathbun. *Comparative Biochemistry and Physiology Part B: Comparative Biochemistry.* **78** (1), 27–31.

Tsang, S. S. K., Law, S. T. S., Li, C., Qu, Z., Bendena, W. G., Tobe, S. S., and Hui, J. H. L. (2020). Diversity of Insect Sesquiterpenoid Regulation. *Front. Genet.* **11**.

Tsukimura, B. and Borst, D. W. (1992). Regulation of Methyl Farnesoate in the Hemolymph and Mandibular Organ of the Lobster, *Homarus americanus*. *Gen. Comp. Endocrinol.* **86**, 297–303.

Tsukimura, B., Kamemoto, F. I., and Borst, D. W. (1993). Cyclic nucleotide regulation of methyl farnesoate synthesis by the mandibular organ of the lobster, *Homarus americanus*. *Journal of Experimental Zoology.* **265**, 427–431.

Tu, S., Tuo, P., Xu, D., Wang, Z., Wang, M., Xie, X., and Zhu, D. (2022). Molecular Characterization of the Cytochrome P450 Epoxidase (CYP15) in the Swimming Crab *Portunus trituberculatus* and Its Putative Roles in Methyl Farnesoate Metabolism. *Biological Bulletin.* **242**, 75–86.

Tumova, S., Dolezel, D., and Jindra, M. (2024). Conserved and Unique Roles of bHLH-PAS Transcription Factors in Insects – From Clock to Hormone Reception. *J. Mol. Biol.* **436** (3), 168332.

Turra, A., Ragagnin, M. N., McCarthy, I. D., and Fernandez, W. S. (2020). The effect of ocean acidification on the intertidal hermit crab *Pagurus criniticornis* is not modulated by cheliped amputation and sex. *Mar. Environ. Res.* **153**, 104794.

Ullah, A. Md., Hossain, M. I., Hasan, T., Sultana, M., Babu, N. H. B. Md., and Hasan, R. Md. (2020). Biochemical composition and caloric values of different body segments of the female mangrove crab (*Scylla olivacea*). **24** (7), 817–823.

Ureña, E., Chafino, S., Manjón, C., Franch-Marro, X., and Martín, D. (2016). The Occurrence of the Holometabolous Pupal Stage Requires the Interaction between E93, Krüppel-Homolog 1 and Broad-Complex. *PLoS Genet.* **12** (5), e1006020.

Ureña, E., Manjón, C., Franch-Marro, X., and Martín, D. (2014). Transcription factor E93 specifies adult metamorphosis in hemimetabolous and holometabolous insects. *Proc. Natl. Acad. Sci. U. S. A.* **111** (19), 7024–7029.

Uyehara, C. M., Nystrom, S. L., Niederhuber, M. J., Leatham-Jensen, M., Ma, Y., Buttitta, L. A., and McKay, D. J. (2017). Hormone-dependent control of developmental timing through regulation of chromatin accessibility. *Genes Dev.* **31** (9), 862–875.

Ventura, T., Bose, U., Fitzgibbon, Q. P., Smith, G. G., Shaw, P. N., Cummins, S. F., and Elizur, A. (2017). CYP450s analysis across spiny lobster metamorphosis identifies a long sought missing link in crustacean development. *Journal of Steroid Biochemistry and Molecular Biology.* **171**, 262–269.

Ventura, T., Palero, F., Rotllant, G., and Fitzgibbon, Q. P. (2018). Crustacean metamorphosis: an omics perspective. *Hydrobiologia.* **825**, 47–60.

Vilasoa-Martínez, M., López-Hernández, J., and Lage-Yusty, M. A. (2007). Protein and amino acid contents in the crab, *Chionoecetes opilio*. *Food Chem.* **103** (4), 1330–1336.

Voldnes, G., Kvalvik, I., and Nøstvold, B. (2020). Taking care of a highly valuable resource throughout the value chain - Lack of market orientation in red king crab export? *Marine Policy.* **117** (1), 103965.

Waiho, K., Ikhwanuddin, M., Afiqah-Aleng, N., Shu-Chien, A. C., Wang, Y., Ma, H., and Fazhan, H. (2022). Transcriptomics in advancing portunid aquaculture: A systematic review. *Rev. Aquac.* **14** (4), 2064–2088.

Waiho, K., Ikhwanuddin, M., Baylon, J. C., Jalilah, M., Rukminasari, N., Fujaya, Y., and Fazhan, H. (2021). Moult induction methods in soft-shell crab production. *Aquac. Res.* **52**, 4026–4042.

Wainwright, G., Prescott, M. C., Rees, H. H., and Webster, S. G. (1996). Mass spectrometric determination of methyl farnesoate profiles and correlation with ovarian development in the edible crab, *Cancer pagurus*. *Journal of Mass Spectrometry.* **31**, 1338–1344.

Wainwright, G., Webster, S. G., and Rees, H. H. (1998). Neuropeptide regulation of biosynthesis of the juvenoid, methyl farnesoate, in the edible crab, *Cancer pagurus*. *Biochem. J.* **334**, 651–657.

Wan Yusof, W. R., Ahmad, N. M., Zailani, M. A., Shahabuddin, M. M., Sing, N. N., and Husaini, A. A. S. (2020). Nutritional Composition, Antioxidants and Antimicrobial Activities in Muscle Tissues of Mud Crab, *Scylla paramamosain*. *Res. J. Biotechnol.* **15** (4), 86–92.

Wang, J., Cheng, Y., Su, B., and Dunham, R. A. (2024). Genome Manipulation Advances in Selected Aquaculture Organisms. *Rev Aquac*. **17** (1).

Wang, Q., Wu, X., Long, X., Zhu, W., Ma, T., and Cheng, Y. (2018). Nutritional quality of different grades of adult male Chinese mitten crab, *Eriocheir sinensis*. *J. Food Sci. Technol.* **55** (3), 944–955.

Wang, X., Ding, Y., Lu, X., Geng, D., Li, S., Raikhel, A. S., and Zou, Z. (2021). The ecdysone-induced protein 93 is a key factor regulating gonadotrophic cycles in the adult female mosquito *Aedes aegypti*. *Proc. Natl. Acad. Sci. U. S. A.* **118**, (8) e2021910118.

Wang, Z., Zu, L. U., Li, Q., Jiang, X., Xu, W., Soyano, K., Cheng, Y., and Wu, X. (2020). A comparative evaluation of the nutritional quality of *Eriocheir sinensis* and *Eriocheir japonica* (Brachyura, Varunidae). *Crustaceana.* **93**, 567–585.

Wärnmark, A., Treuter, E., Wright, A. P. H., and Gustafsson, J. Å. (2003). Activation Functions 1 and 2 of Nuclear Receptors: Molecular Strategies for Transcriptional Activation. *Molecular Endocrinology.* **17** (10), 1901–1909.

Webster, S. G. (1986). Neurohormonal control of ecdysteroid biosynthesis by *Carcinus maenas* Y-organs *in vitro*, and preliminary characterization of the putative molt-inhibiting hormone (MIH). *Gen. Comp. Endocrinol.* **61** (2), 237–247.

Webster, S. G. (1993). High-affinity binding of putative moult-inhibiting hormone (MIH) and crustacean hyperglycaemic hormone (CHH) to membrane-bound receptors on the Y-organ of the shore crab *Carcinus maenas*. *Pro. R. Soc. Lond. B*. **251**, 53–59.

Webster, S. G. (2015). "Endocrinology of Molting," in *The Natural History of Crustacea: Physiology*, eds. E. Chang and M. Thiel.

Webster, S. G. and Keller, R. (1986). Purification, characterization and amino acid composition of the putative moult-inhibiting hormone (MIH) of *Carcinus maenas* (Crustacea, Decapoda). *J. Comp. Physiol. B.* **156**, 617–624.

Webster, S. G., Keller, R., and Dircksen, H. (2012). The CHH-superfamily of multifunctional peptide hormones controlling crustacean metabolism, osmoregulation, moulting, and reproduction. *Gen. Comp. Endocrinol.* **175** (2), 217–233.

Wei, J., Zhang, X., Yu, Y., Huang, H., Li, F., and Xiang, J. (2014). Comparative Transcriptomic Characterization of the Early Development in Pacific White Shrimp *Litopenaeus vannamei*. *PLoS One.* **9** (9), e106201.

Wen, D., Chen, Z., Wen, J., and Jia, Q. (2023). Sterol Regulation of Development and 20-Hydroxyecdysone Biosynthetic and Signaling Genes in *Drosophila melanogaster*. *Cells.* **12** (13), 1739.

Wieschaus, E., Nusslein-Volhard, C., and Kluding, H. (1984). Krüppel, a Gene Whose Activity Is Required Early in the Zygotic Genome for Normal Embryonic Segmentation. *Dev. Biol.* **104**, 172–186.

Wilson, S., Jeyasanta, I., and Patterson, J. (2017). Nutritional Status of Swimming Crab *Portunus sanguinolentus* (Herbst, 1783). *Kerala Journal of Aquatic Biology & Fisheries.* **5**, 191–202.

Wolfe, J. M., Breinholt, J. W., Crandall, K. A., Lemmon, A. R., Lemmon, E. M., Timm, L. E., Siddall, M. E., Bracken-Grissom, H. D. (2019). A phylogenomic framework, evolutionary timeline and genomic resources for comparative studies of decapod crustaceans. *Proceedings of the Royal Society B: Biological Sciences.* **286** (1901).

Wolff, G. H., Thoen, H. H., Marshall, J., Sayre, M. E., and Strausfeld, N. J. (2017). An insect-like mushroom body in a crustacean brain. *Elife*. **6**, e29889.

Wu, D. and Rastinejad, F. (2017). Structural characterization of mammalian bHLH-PAS transcription factors. *Curr. Opin. Struct. Biol.* **43**, 1–9.

Wu, H., Ge, M., Chen, H., Jiang, S., Lin, L., and Lu, J. (2020). Comparison between the nutritional qualities of wild-caught and rice-field male Chinese mitten crabs (*Eriocheir sinensis*). *LWT*. 117 (4), 108663.

Wu, X., Zhou, B., Cheng, Y., Zeng, C., Wang, C., and Feng, L. (2010). Comparison of gender differences in biochemical composition and nutritional value of various edible parts of the blue swimmer crab. *Journal of Food Composition and Analysis.* **23** (2), 154–159.

Wu, Z., Yang, L., Li, H., and Zhou, S. (2021). Krüppel-homolog 1 exerts anti-metamorphic and vitellogenic functions in insects via phosphorylation-mediated recruitment of specific cofactors. *BMC Biol.* **19**, 222.

Xie, X. I., Zhu, D., Li, Y., Qiu, X., Cui, X., and Tang, J. (2015). Hemolymph Levels of Methyl Farnesoate During Ovarian Development of the Swimming Crab *Portunus trituberculatus*, and Its Relation to Transcript Levels of HMG-CoA Reductase and Farnesoic Acid O-Methyltransferase. *Biol. Bull.* **228** (2), 118–124.

Xie, X., Liu, M., Jiang, Q., Zheng, H., Zheng, L., and Zhu, D. (2018). Role of Kruppel homolog 1 (Kr-h1) in methyl farnesoate-mediated vitellogenesis in the swimming crab *Portunus trituberculatus*. *Gene.* **679**, 260–265.

Xie, X., Tao, T., Liu, M., Zhou, Y., Liu, Z., and Zhu, D. (2016a). The potential role of juvenile hormone acid methyltransferase in methyl farnesoate (MF) biosynthesis in the swimming crab, *Portunus trituberculatus*. *Anim. Reprod. Sci.* **168**, 40–49.

Xie, X., Zhou, Y., Liu, M., Tao, T., Jiang, Q., and Zhu, D. (2016b). The nuclear receptor E75 from the swimming crab, *Portunus trituberculatus*: cDNA cloning, transcriptional analysis, and putative roles on expression of ecdysteroid-related genes. *Comp. Biochem. Physiol. B Biochem. Mol. Biol.* **200**, 69–77.

Xie, X., Zhu, D., Cui, X., Tang, J., and Qiu, X. (2013). Cloning and expression analysis of farnesoic acid O-methyl transferase (FAMeT) during molting in *Portunus trituberculatus*. *Journal of Fisheries of China.* **37**, 994–1001.

Xu, J., Roy, A., and Palli, S. R. (2018). CREB-binding protein plays key roles in juvenile hormone action in the red flour beetle, *Tribolium Castaneum*. *Sci. Rep.* **8**, 1426.

Xu, Y., Zhao, M., Deng, Y., Yang, Y., Li, X., Lu, Q., Ge, J., Pan, J., and Xu, Z. (2017). Molecular cloning, characterization and expression analysis of two juvenile hormone esterase-like carboxylesterase cDNAs in Chinese mitten crab, *Eriocheir sinensis*. *Comp. Biochem. Physiol. B Biochem. Mol. Biol.* **205**, 46–53.

Yan, S., Mao, S., Xia, Q., Cui, Z., Duan, H., Ren, G., Li, X., Ge, H., Liu, M., and Dong, Z. (2023a). Effects of Different Habitat Space on Growth Performance and Nutritional Composition of Swimming Crabs (*Portunus trituberculatus*). *Aquac. Res.* **2023** (1), 1307590.

Yan, S. Y., Ma, L. X., Xu, K. kang, Li, C., and Yang, W. J. (2023b). Nuclear receptor FTZ-F1 is required for larval-pupal molting by regulating ecdysteroidogenesis and chitin metabolism in *Lasioderma serricorne*. *J. Stored. Prod. Res.* **101**, 102096.

Yang, B. B., Miao, S. Y., Lu, Y. J., Wang, S. S., Wang, Z. Y., and Zhao, Y. R. (2023). Involvement of Methoprene-tolerant and Krüppel homolog 1 in juvenile hormone-mediated vitellogenesis of female *Liposcelis entomophila* (End.) (Psocoptera: Liposcelididae). *Arch. Insect Biochem. Physiol* **112** (1), e21973.

Yang, Y., Ye, H., Huang, H., Jin, Z., and Li, S. (2012). Cloning, expression and functional analysis of farnesoic acid *O*-methyltransferase (FAMeT) in the mud crab, *Scylla paramamosain*. *Mar. Freshw. Behav. Physiol.* **45**, 209–222.

Yasugi, T. and Nishimura, T. (2016). Temporal regulation of the generation of neuronal diversity in *Drosophila*. *Dev. Growth Differ.* **58** (1), 73–87.

Yu, Q. Y., Lu, C., Li, W. Le, Xiang, Z. H., and Zhang, Z. (2009). Annotation and expression of carboxylesterases in the silkworm, *Bombyx mori*. *BMC Genomics.* **10**, 553.

Yu, X., Chang, E. S., and Mykles, D. L. (2002). Characterization of Limb Autotomy Factor-Proecdysis (LAF_{pro}), Isolated From Limb Regenerates, That Suspends Molting in the Land Crab *Gecarcinus lateralis*. *Bio. Bull.* **202** (3), 204–212.

Yuan, H., Qiao, H., Fu, Y., Fu, H., Zhang, W., Jin, S., Gong, Y., Jiang, S., Xiong, Y., Hu, Y., and Wu. (2021a). RNA interference shows that *Spook*, the precursor gene of 20-hydroxyecdysone (20E), regulates the molting of *Macrobrachium nipponense*. *Journal of Steroid Biochemistry and Molecular Biology.* **213**, 105976.

Yuan, H., Zhang, W., Fu, Y., Jiang, S., Xiong, Y., Zhai, S., Gong, Y., Qiao, H., Fu, H., and Wu, Y. (2021b). *MnFtz-f1* Is Required for Molting and Ovulation of the Oriental River Prawn *Macrobrachium nipponense*. *Front. Endocrinol.* **12**, 798577.

Yuan, H., Zhang, W., Qiao, H., Jin, S., Jiang, S., Xiong, Y., Gong, Y., and Fu, H. (2022). *MnHR4* Functions during Molting of *Macrobrachium nipponense* by Regulating 20E Synthesis and Mediating 20E Signaling. *Int. J. Mol. Sci.* **23** (10), 12528.

Yuan, J., Yu, Y., Zhang, X., Li, S., Xiang, J., and Li, F. (2023). Recent advances in crustacean genomics and their potential application in aquaculture. *Rev. Aquac.* **15** (4), 1501–1521.

Yudin, A. I., Diener, R. A., Clark, W. H., and Chang, E. S. (1980). Mandibular Gland of the Blue Crab *Callinectes sapidus*. *Biol. Bull.* **159** (3), 760–772.

Zeng, B., Huang, Y., Xu, J., Shiotsuki, T., Bai, H., Palli, S. R., Huang, Y., and Tan, A. (2017). The FOXO transcription factor controls insect growth and development by regulating juvenile hormone degradation in the silkworm, *Bombyx mori*. *Journal of Biological Chemistry.* **292** (28), 11659–11669.

Zhang, J., Liu, X., Liu, Y., An, Y., Fang, H., Michaud, J. P., Zhang, H., Li, Y., Zhang, Q., and Li, Z. (2019a). Molecular Characterization of Primary Juvenile Hormone Responders Methoprene-Tolerant (Met) and Krüppel Homolog 1 (Kr-h1) in *Grapholita molesta* (Lepidoptera: Tortricidae) with Clarification of Their Roles in Metamorphosis and Reproduction. *J. Econ. Entomol.* **112** (5), 2369–2380.

Zhang, J., Song, F., Sun, Y., Yu, K., and Xiang, J. (2018a). CRISPR/Cas9-mediated deletion of EcMIH shortens metamorphosis time from mysis larva to postlarva of *Exopalaemon carinicauda*. *Fish Shellfish Immunol.* **77**, 244–251.

Zhang, J., Zhang, W., Wei, L., Zhang, L., Liu, J., Huang, S., Li, S., Yang, W. and Li, K. (2023). E93 promotes transcription of RHG genes to initiate apoptosis during *Drosophila* salivary gland metamorphosis. *Insect Sci.* **30** (3), 588–598.

Zhang, W., Ma, L., Liu, X., Peng, Y., Liang, G., and Xiao, H. (2021). Dissecting the roles of FTZ-F1 in larval molting and pupation, and the sublethal effects of methoxyfenozide on *Helicoverpa armigera*. *Pest Manag. Sci.* **77** (3), 1328–1338.

Zhang, W. N., Ma, L., Liu, C., Chen, L., Xiao, H. J., and Liang, G. M. (2018b). Dissecting the role of Krüppel homolog 1 in the metamorphosis and female reproduction of the cotton bollworm, *Helicoverpa armigera*. *Insect Mol. Biol.* **27** (4), 492–504.

Zhang, X., Yuan, J., Zhang, X., Xiang, J., and Li, F. (2020). Genomic Characterization and Expression of Juvenile Hormone Esterase-Like Carboxylesterase Genes in Pacific White Shrimp, *Litopenaeus vannamei*. *Int. J. Mol. Sci.* **21** (15), 5444.

Zhang, Y., Gao, W., Yuan, Y., Cui, W., Xiang, Z., Ye, S., Ikhwanuddin, M., and Ma, H. (2024). Impact and accumulation of calcium on soft-shell mud crab *Scylla paramamosain* in recirculating aquaculture system. *Aquaculture.* **593**, 741323.

Zhang, Z., Xu, J., Sheng, Z., Sui, Y., and Palli, S. R. (2011). Steroid receptor co-activator is required for juvenile hormone signal transduction through a bHLH-PAS transcription factor, methoprene tolerant. *Journal of Biological Chemistry.* **286** (10), 8437–8447.

Zhao, M., Wang, W., Ma, C., Zhang, F., and Ma, L. (2020). Characterization and expression analysis of seven putative JHBPs in the mud crab *Scylla paramamosain*: Putative relationship with methyl farnesoate. *Comp. Biochem. Physiol. B Biochem. Mol. Biol.* **241**, 110390.

Zhao, M., Zhang, F., Jiang, K., Wang, W., Chen, W., Ma, C., Song, W., and Ma, L. (2018). Cloning, characterization, and expression profile of an insect farnesoic acid *O*-methyltransferase orthologue from the mud crab *Scylla paramamosain* Estampador, 1950 (Brachyura: Portunidae): Putative relationship with methyl farnesoate. *Journal of Crustacean Biology.* **38** (4), 443–450.

Zhao, W. L., Liu, C. Y., Liu, W., Wang, D., Wang, J. X., and Zhao, X. F. (2014). Methoprene-tolerant 1 regulates gene transcription to maintain insect larval status. *J. Mol. Endocrinol.* **53** (1), 93–104.

Zheng, S. W., Jiang, X. J., Mao, Y. W., Li, Y., Gao, H., and Lin, X. D. (2023a). Brown planthopper E78 regulates moulting and ovarian development by interacting with E93. *J. Integr. Agric.* **22** (5), 1455–1464.

Zheng, Y., Zhang, W., Xiong, Y., Wang, J., Jin, S., Qiao, H., Jiang S., and Fu, H. (2023b). Dual roles of CYP302A1 in regulating ovarian maturation and molting in *Macrobrachium nipponense*. *Journal of Steroid Biochemistry and Molecular Biology.* **232**, 106336.

Zhou, K., Zhou, F., Jiang, S., Huang, J., Yang, Q., Yang, L., and Jiang, S. (2019). Ecdysone inducible gene E75 from black tiger shrimp *Penaeus monodon*: Characterization and elucidation of its role in molting. *Mol. Reprod. Dev.* **86** (3), 265–277.

Zhu, B. J., Tang, L., Yu, Y. Y., Wang, D. J., and Liu, C. L. (2017a). Identification and expression patterns of 20-hydroxyecdysone-responsive genes from *Procambarus clarkii*. *Genes & Genomics.* **39**, 601–609.

Zhu, B., Tang, L., Yu, Y., Yu, H., Wang, L., Qian, C., Wei, G., and Liu, C. (2017b). Identification of ecdysteroid receptor-mediated signaling pathways in the hepatopancreas of the red swamp crayfish, *Procambarus clarkii*. *Gen. Comp. Endocrinol.* **246**, 372–381.

Zhu, S., Lin, S., Kao, C. F., Awasaki, T., Chiang, A. S., and Lee, T. (2006). Gradients of the *Drosophil*a Chinmo BTB-Zinc Finger Protein Govern Neuronal Temporal Identity. *Cell.* **127** (2), 409–422.

Zhu, T., Zhou, Q., Yang, Z., Zhang, Y., Luo, J., Zhang, X., Shen, Y., Jiao, L., Tocher, D. R., and Jin, M. (2022). Dietary cholesterol promotes growth and ecdysone signalling pathway by modulating cholesterol transport in swimming crabs (*Portunus trituberculatus*). *Animal Nutrition.* **10**, 249–260.

Zhu, X. J., Xiong, Y., He, W., Jin, Y., Qian, Y. Q., Liu, J., and Dai, Z. M. (2018). Molecular cloning and expression analysis of a prawn (*Macrobrachium rosenbergii*) juvenile hormone esterase-like carboxylesterase following immune challenge. *Fish Shellfish Immunol.* **80**, 10–14.

Zotti, M., Coco, L. Del, Pascali, S. A. De, Migoni, D., Vizzini, S., Mancinelli, G., and Fanizzi, F. P. (2016). Comparative analysis of the proximate and elemental composition of the blue crab *Callinectes sapidus*, the warty crab *Eriphia verrucosa*, and the edible crab *Cancer pagurus*. *Heliyon.* **2** (2), e00075.

CHAPTER 2

METHYL FARNESOATE SIGNALING GENE NETWORK AS A TRANSCRIPTIONAL REGULATOR OF ECDYSTEROIDOGENESIS IN THE DECAPOD MOLTING GLAND (Y-ORGAN)

Abstract

In insects, the Methoprene tolerant–Krüppel homolog 1– E93 (MEKRE93) transcriptional cascade is induced by juvenile hormone (JH) to repress ecdysteroid synthesis in the prothoracic gland (PG). Methyl farnesoate (MF) is acknowledged as the crustacean JH with various physiological roles, including morphogenesis, metamorphosis, reproduction, and molting. Previous reports have demonstrated that MF stimulates ecdysteroid production in the Y-organ (YO) and therby accelerates molting. It is hypothesized that MF acting on the MEKRE93 signaling genes regulate YO ecdysteroidogenesis.

MF signaling genes, consisting of *Methoprene tolerant* (*Met*), *Steroid receptor coactivator* (*Src*), *Krüppel homolog 1* (*Kr-h1*), and *Ecdysone response gene 93* (*E93*), and transcriptional comediators *CREB-binding protein* (*CBP*) and *C-terminal–binding protein* (*CtBP*) were identified in the European green shore crab (*Carcinus maenas*) and the blackback land crab (*Gecarcinus lateralis*) YO transcriptomes. Phylogenetic and sequence analysis showed that this transcriptional cascade was highly conserved across pancrustacean species. Met and Src were classified as basic helix-loop-helix, Period- Aryl hydrocarbon nuclear translocator, Single minded protein (bHLH–PAS) transcription factors (TFs); Kr-h1 was classified as a C2H2 zinc finger TF with seven zinc finger motifs; and E93 was classified as a helix-turn-helix, pipsqueak (HTH_Psq) TF. Analysis of *C. maenas* YO RNA-seq data showed that *Met, Src, Kr-h1, E93,*

CBP, CtBP were expressed at all the molt stages. Analysis of *G. lateralis* YO RNA-seq data showed that expression of *Met, Src, Kr-h1, E93, CBP, CtBP* was upregulated in intermolt (IM) and decreased during premolt, with little to no expression by postmolt. *In vitro* assays revealed that exposure to JH-mimics affected the ability of the YO to respond to produce ecdysteroids. These cultures indicated that the YOs *in vitro* required a high concentration to elicit a response and after 48-hours ecdysteroid secretion is complete. These cultures also revealed that even within the same infraorder, the YOs from two brachyuran species exhibited differential effects to the same compound treatment and the sensitivity may change over time. Molt stage is also a factor that was shown to impact YO responsiveness to the compounds.

These data show that the YO has a functional MEKRE93 signaling system. A model is proposed that links MF signaling with ecdysteroid synthesis. Transcriptional control of Kr-h1 is mediated by co-activator CBP and co-repressor CtBP under high and low 20-hydroxyecdysone conditions, respectively.

Introduction

Crustacean molting is driven by the increase hemolymph titers of 20-hydroxyecdysone (20-E), a steroid hormone produced by the Y-organs (YO) (Skinner, 1985b; Chang, 1993; Mykles, 2024). The binding of 20-E to the ecdysone receptor/retinoid X receptor (EcR/RXR) complex activates a transcriptional cascade of ecdysone response genes in target tissues (Spindler et al., 2009; Hyde et al., 2019a; Mazina and Vorobyeva, 2019; Benrabaa et al., 2024; Mykles, 2024). Numerous studies have shown that ecdysone-directed physiological processes, such as reproduction, development, and metamorphosis, in pancrustaceans are regulated by the crosstalk between the ecdysteroid and juvenile hormone (JH) signaling pathways (Mu and LeBlanc, 2004; Jindra et al., 2013; Li et al., 2018a; Liu et al., 2018; Adhitama et al., 2020).

Methyl farnesoate (MF) is a sesquiterpenoid hormone, identified by Laufer et al. (1987a) produced by the crustacean mandibular organ (MO) (Laufer et al., 1987b; Tobe et al., 1989a). MF is nicknamed 'the crustacean JH' as it is structurally the unepoxidated form of JH III and shares similar physiological roles in crustaceans as JH does in insects (Borst et al., 1987a; Homola and Chang, 1997c; Laufer and Biggers, 2001; Nagaraju, 2007). MF has been shown to stimulate gonad growth and maturation in the ridgeback shrimp (*Sicyonia ingentis*), the whiteleg shrimp (*Litopenaeus vannamei*), the orange mud crab (*Scylla* olivacea), the freshwater crab *Travancoriana schirnerae*, and the Indian rice field crab (*Oziotelphusa senex senex*) (Reddy and Ramamurthi, 1998; Kalavathy et al., 1999; Reddy et al., 2004; Paran et al., 2010; Alnawafleh et al., 2014; Devi et al., 2018; Muhd-Farouk et al., 2019). In the case of the Australian freshwater crayfish (*Cherax quadricarinatus*), MF had no reproductive effect on wintering females (Abdu et al., 2001). MF has also been reported to impacts morphogenesis in some species such as in the red swamp crayfish (*Procambarus clarkii*) and spider crabs (*Libinia emarginata*) (Rotllant et al., 2000; Laufer et al., 2005). Laufer et al. (2002) revealed that the balance between MF ecdysteroids determine the morphogenetic effects in allometric growth. Allometric growth in the spider crab was stimulated with ecdysteroids and a low MF concentration but allometric growth was inhibited when ecdysteroid and MF was high (Laufer et al., 2002). In context the development and metamorphosis, MF delayed larval development and metamorphosis in the giant freshwater prawn (*Macrobrachium rosenbergii*) and the kuruma prawn (*Marsupenaeus japonicus*) while induced precocious metamorphosis in the acorn barnacle *Balanus amphitrite* (Yamamoto et al., 1997; Abdu et al., 1998; Smith et al., 2000; Toyota et al., 2020b). As adults, MF accelerated molting in wintering *C. quadicarinatus* and stimulated molting in *L. vannamei* and *T. schirnerae* (Abdu et al., 2001; Alnawafleh et al., 2014; Raghavan and Ayanath, 2019).

Tamone and Chang (1993) demonstrated that MF stimulates the Dungeness crab (*Metacarcinus magister*) YO ecdysteroidogenesis *in vitro* at high concentrations (e.g., 1.0 μM and 10.0 μM) primarily after 24-hours of exposure. These results suggest MF mediates the YO secretion of 20-E (Tamone and Chang, 1993b). Despite these reported accounts, the underlying mechanism of MF remains unknown and thereby is "cursed" (Fingerman, 1997).

In insects, JH induces the Methoprene tolerant (Met)– Krüppel homolog 1 (Kr-h1)– Ecdysone response gene 93 (E93), or MEKRE93, transcriptional cascade to inhibit ecdysone response gene expression, and consequently ecdysteroid synthesis, to regulate insect development metamorphosis (Belles and Santos, 2014; Li et al., 2018a; Belles, 2019; Martín et al., 2021). Methoprene tolerant (Met) is a basic helix-loop-helix (bHLH), Period (Per)- Aryl hydrocarbon receptor nuclear translocator (ARNT)- Single minded (Sim) (bHLH–PAS) transcription factor and is the accepted JH (and MF) recptor (Miura et al., 2005; Charles et al., 2011; Bernardo and Dubrovsky, 2012; Zhao et al., 2014; Kolonko et al., 2016). Heat shock protein 83 (Hsp83) is a chaperone protein that assists in JH binding to the PAS-B domain of Met, or the ligand binding domain (LBD) (He et al., 2014, 2017b). The interaction between Hsp83 and nucleoporin 358 (Nup358) tetratricopeptide repeat (TPR) domains tethers the Met receptor complex to the nuclear pore complex (NPC) (He et al., 2014, 2017b). Upon recognition, the transport receptor importin β binds to the Met nuclear localization signal (NLS) thereby transporting the entire Met receptor complex through the NPC (He et al., 2014, 2017b). In the nucleus, the receptor complex dissociates due to a high concentration of RanGRP binding to importin β thus allowing the Met receptor complex, along with recruited cofactors such as steroid receptor coactivator (Src), to bind to JH response regions on the promoter region of Kr-h1 (Zhang et al., 2011; He et al., 2014, 2017b). Kr-h1 is a C2H2 zinc finger (Zf) transcription factor

encompassing seven or eight Zf repeats in crustaceans and insects, respectively (Pecasse et al., 2000b; Xie et al., 2018; Zhang et al., 2019a; Li et al., 2021c; He and Zhang, 2022). E93 is a helix-turn-helix, pipsqueak (HTH_Psq) transcription factor and is conventionally classified as an early ecdysone response gene (Baehrecke and Thummel, 1995; Siegmund and Lehmann, 2002; Mou et al., 2012; Lam et al., 2022). *Kr-h1* has been reported to repress *E93* expression and/or other ecdysone response targets, such as Broad Complex (Br-C) (Minakuchi et al., 2008; Lozano and Belles, 2011; Kayukawa et al., 2012, 2017; Ureña et al., 2014, 2016; Liu et al., 2015b; Li et al., 2018b; Chafino et al., 2019; Kamsoi and Belles, 2020; Suzuki et al., 2021; He and Zhang, 2022; Fernandez-Nicolas et al., 2023). Although Kr-h1 is a transcriptional repressor, its effect on E93 expression may be impacted by the transcriptional comediators CBP, or CREB (cyclic adenosine monophosphate response element-binding protein)–binding protein, and C-terminal-binding protein (CtBP) (Wu et al., 2021).

Nonetheless, Met is also acknowledged to be the crustacean MF receptor (Miyakawa et al., 2013; Kakaley et al., 2017; Hirano et al., 2020). In the Chinese mitten crab (*Eriocheir sinensis*) and the gazami crab (*Portunus trituberculatus*), Kr-h1 is downstream of Met and MF stimulates vitellogenenin synthesis in the hepatopancreas by upregulating the expression of *Met* and *Kr-h1* (Liu et al., 2016; Xie et al., 2018; Li et al., 2021c, 2021b). Additionally, the *E93* ortholog was identified in *P, trituberculatus* was shown to be induced by 20-E and suppressed by MF (Ge et al., 2024).

To better understand the role of MF in regulating YO ecdysteroidogenesis, the MF-MEKRE93 cascade in crustaceans was investigated. *Met*, *Src*, *Kr-h1*, *E93*, *CBP*, and *CtBP* were characterized in the European green shore crab (*Carcinus maenas*) and the blackback land crab (*Gecarcinus lateralis*) YO transcriptomes. The mRNA transcript levels were profiled for each

MF-MEKRE93 signaling gene across the different stages of the molt cycle. *In vitro* assays determined the effects of MF and JH-mimics on YO ecdysteroid secretion. The results show that the YO expresses a functional MEKRE93 signaling cascade that is linked to ecdysteroid synthesis.

Materials and Methods

Animals

Adult male green shore crabs (*Carcinus maenas*) were collected from Bodega Harbor, Bodega Bay, California and housed at the UC Davis Bodega Marine Laboratory in a flowing seawater system at ambient temperature (11 to 14 °C) (Abuhagr et al., 2014). The YOs were harvested from the animals for *in vitro* YO assays within two weeks from collection.

Adult male blackback land crabs (*Gecarcinus lateralis*) were collected from the Dominican Republic and shipped by air cargo to Fort Collins, Colorado. Animals were housed at Colorado State University (CSU) in an environmental chamber maintained at 27 °C at 75-80% relative humidity under a 12-hour dark:12-hour light cycle (Bliss and Boyer, 1964; Bliss, 1968). The crabs were communally kept in plastic cages with Tekland Envigo Aspen Bedding Laboratory Grade #7093 shavings saturated with 5 parts per thousand (ppt) Instant Ocean® deionized water. Crabs were fed twice a week on a diet consisting of lettuce, carrots, and raisins coated with calcium powder. The third right walking leg was autotomized to monitor for spontaneous molting (Covi et al., 2009). The animals were acclimated for one month before experiments or tissue harvesting were conducted. Molting was induced by autotomy of eight walking legs, also referred to as multiple leg autotomy (MLA) or through eyestalk ablation (ESA) (Skinner, 1962, 1985b, 1985a; Skinner and Graham, 1972; Chang, 1985, 1993, 1995;

Chang et al., 1993; Lachaise et al., 1993). Progression through premolt was monitored by measuring the limb regenerate growth as determined by the regeneration index (R-index = [mm limb regenerate length x 100]/mm carapace width) (Bliss et al., 1966a; Hopkins, 1982). Molt stage was determined by the R-index; hemolymph 20-hydroxyecdysone (20-E) titer; presence of the membranous layer, the innermost layer of the exoskeleton; and the presence of gastroliths (Skinner, 1962, 1985a, 1985b; Hopkins, 1982; Chang, 1995; Yu et al., 2002).

On the day of tissue harvesting, 100 µL of hemolymph was drawn using 22-gauge sterile, hypodermic needles from the randomly sampled individuals (e.g. color morph, size, presence of fungus/barnacles, and/or the number of limbs present). The hemolymph was combined with 300 µL 100% methanol (MeOH) in O-ring microcentrifuge tubes, and vortexed to prevent coagulation (Gianazza et al., 2021). The 20-E concentration in the hemolymph and media samples were quantified with a competitive enzyme-linked immunosorbent assay (ELISA) as described by Kingan (1989) and modified by Abuhagr et al. (2014). The reagents used in the ELISA were AffiniPure™ Goat Anti-Rabbit IgG, Fc fragment-specific secondary antibody (Jackson ImmunoResearch Inc. 111-005-008), and the SeraCare TMB Peroxidase Kit (Yu et al., 2002; Abuhagr et al., 2014).

Identification and characterization of MEKRE93 sequences

Previously identified and/or annotated protein sequences of MEKRE93 components were used as queries in the National Center for Biotechnology Information Basic Local Alignment Search Tool (NCBI BLAST) program to search for candidate genes in CrusTome, CrustyBase, CrusTF (crustacean transcription factor), CAT (a crustacean annotated transcriptome), and GenBank databases; identities were verified through a reciprocal BLAST search (Qin et al.,

2017; Zhang et al., 2019b; Hyde et al., 2020; Nong et al., 2020; Pérez-Moreno et al., 2023; Hyde and Ventura, 2024). Reference sequences and the BLAST hit queries were aligned with Multiple Alignment using Fast Fourier Transform (MAFFT) (v.7.490) including the *dash* parameter to refine the multiple sequence alignment (MSA) from the Database of Aligned Structural Homologs (DASH) (Katoh and Toh, 2008; Yamada et al., 2016; Rozewicki et al., 2019). The MSAs were trimmed with ClipKIT using the *smart-gap* parameter to remove gaps, while preserving informative sites (Steenwyk et al., 2020). Phylogenetic analyses were inferred from the aligned protein sequences with the suitable model, as determined by ModelFinder following the Baeysian Information Criteria (BIC) (Kalyaanamoorthy et al., 2017; Guindon, 2018). Maximum likelihood phylogenetic trees were constructed using IQ-Tree with the degree of branch support evaluated with 1,000 ultrafast bootstrap iterations (UFBoot=1,000) (Hoang et al., 2017; Minh et al., 2020). The phylogenetic trees were then rooted and visualized in FigTree (v1.4.4) and Inkscape (Rambaut, 2010).

Conserved domains and residues were identified with the NCBI Conserved Domain Database (CDD) platform. Additional MSAs were executed using Mafft EINSI with default vacancy penalty scores and parameters on the Jalview (v.2.11) platform and subsequently trimmed with ClipKIT (Clamp et al., 2004; Katoh and Toh, 2008; Waterhouse et al., 2009; Yamada et al., 2016; Steenwyk et al., 2020). Domain organizations were illustrated and annotated using Illustrator for Biological Sequences 2.0 (IBS 2.0) (Xie et al., 2022). Species taxonomic ranks were annotated according to the classifications defined by Giribet and Edgecombe (2019).

Differential gene expression (DGE)

C. maenas relative gene expression was acquired from the YO RNA-seq data generated by Oliphant et al. (2018) and assembled in the CrusTome database (v.0.1.0) (n = 5 biological replicates of paired YOs per molt stage) (Pérez-Moreno et al., 2023). Relative gene expression in the YOs was determined for *G. lateralis* using RNA-seq data from animals induced to molt by multiple leg autotomy (MLA) (n = pooled replicates of 3 animals each) (Das et al., 2018). Gene expression, measured as transcripts per million reads (TPM), was quantified using Salmon (v.1.7.0) with the "*--seqBias --gcBias –validateMappings*" parameters for quantitative accuracy and mitigation of possible biases. Transcript expression was graphed as mean TPM ± standard error of the mean (SEM). Statistical differences were analyzed with Analysis of Variance (ANOVA) and post-hoc Tukey's HSD test ($p < 0.05$).

YO *in vitro* assays

YOs from *C. maenas* and *G. lateralis* were used to determine the effects of MF and JH-mimics on ecdysteroid secretion *in vitro*. One YO of each pair received the control to which the right and left YO were alternated in receiving the experimental or control treatment to minimize potential asymmetrical bias. Each YO was incubated in 500 µL Medium 199 (M199) (Sigma M0393; Lot 083K83201) that was modified with the appropriate crab saline solution to maintain proper osmotic pressure [*G. lateralis* saline with a sodium phosphate buffer: 316 mM sodium chloride (NaCl), 5.4mM potassium chloride (KCl), 10 mM HEPES, 6.8 mM magnesium sulfate heptahydrate ($MgSO_4 \cdot 7H_2O$), and 8.8 mM calcium chloride dihydrate ($CaCl_2 \cdot 2H_2O$); *C. maenas* saline: 430 mM NaCl, 5 mM potassium chloride (K_2SO_4), 10 mM HEPES, 7 mM magnesium sulfate hexahydrate ($MgSO_4 \cdot 6H_2O$), and 4.5 mM calcium chloride dihydrate ($CaCl_2 \cdot 2H_2O$)]. The

media was adjusted with 5 M sodium hydroxide (NaOH) achieve a pH of 7.4 and 7.2 in *G. lateralis* and *C. maenas*, respectively. The culture media was filtered through a sterile Corning Filter System Low Protein Binding, 0.22 μm cellulose acetate membrane (SKU#: 430626). The M199 was supplemented with 10 i.u./mL Penicillin (Calbiochem Penicillin G, potassium B grade; Lot 700844) and 10 μg/mL Streptomycin (Calbiochem Streptomycin, sulfate B grade; Lot 701865), to minimize bacterial growth (Tamone and Chang, 1993b; Covi et al., 2010). MF and the JH-mimics were solubilized in dimethyl sulfoxide (DMSO) and added to the culture media with a 0.1% DMSO final concentration (Table A1).

Various concentrations of the JH-mimics were tested on *C. maenas* YOs to determine the effects of concentration and incubation time on 20-E secretion (Tamone and Chang, 1993b). Relatively high concentrations compensated for the absence of MF binding proteins naturally found in the hemolymph (Prestwich et al., 1990, 1996; Li and Borst, 1991; King et al., 1995; Tamone et al., 1997; Takác et al., 1998; Zhao et al., 2020). Initially, *C. maenas* intermolt (IM) YOs in the experimental treatment were exposed to media containing 0.1 μM, 1.0 μM, or 10.0 μM MF or a JH-mimic (pyriproxyfen, fenoxycarb, hydroprene, or methoprene), while the control YOs were incubated in media with vehicle alone (0.1 % DMSO final concentration) (n = 10 IM crabs per tested compound at each concentration). The YOs were incubated at room temperature in 18 flat-well sterile culture plates sealed with parafilm and shaken on an orbital shaker at 100 rotations per minute (rpm). Throughout the 48-hour incubation period, the YOs were transferred to a new sterile culture plate with fresh media for each eight-hour interval while the media from the previous plate was transferred to O-ring microcentrifuge tubes. Media samples were stored at -20°C until the competitive ELISA analyses for 20-E secretion were performed.

The same experimental design was used on the *G. lateralis* YOs with modifications necessitated by the limited number of animals available (n = 10 IM crabs per tested compound and n = 6 MP crabs induced by multiple leg autotomy, or MLA, per tested compound). The modifications were informed by the results from the *C. maenas* experiments. Incubations used 10.0 µM MF and JH-mimics, as this concentration yielded the largest and most significant effects on YO ecdysteroid secretion. Pyriproxyfen was excluded, as this compound had no effect on *C. maenas* YO secretion. Furthermore, the MF media was supplemented with a 0.1% bovine serum albumin (BSA) heat shock fraction, pH 7 (Sigma-Aldrich; Lot: SLCH3830), which facilitates transport and delivery of lipophilic molecules (Riley et al., 1998; Paran et al., 2010).

Statistical analyses

Two tailed paired *t*-tests were applied independently for each chemical compound (fenoxycarb, hydroprene, methoprene, MF, and pyriproxyfen) at every combination of concentration (0.1 μM, 1 μM, and 10.0 μM) and time point (8, 16 , 24, 32, and 48 hours) to examine the difference in the cumulative amount of 20-E synthesized for control and treated YOs in the same subject. For comparisons between the two species, as well as between intermolt (IM) and mid-premolt (MP) stages in *G. lateralis*, the data were analyzed using a linear model. The paired difference in the total amount of 20-E synthesized by a control and treated YO from the same individual crab was considered as the response variable and the chemical compound was the covariate of interest in the formula $Y_{ij1} - Y_{ij0} = \beta_j + \epsilon_{ij}$. In this setting, Y_{ijk} is the cumulative 20-E synthesized for the YO from the i^{th} crab within treatment status $k \in \{0,1\}$ and chemical status $j \in \{1, 2, 3, 4\}$, referring to fenoxycarb, hydroprene, methoprene, and MF respectively. Thus, it follows that the response $Y_{ij1} - Y_{ij0}$, is the difference in 20-E synthesized

by the treated YO and the control YO from the same individual; β_j is the fixed effect for chemical j; and ϵ_{ij} is the random variation in the paired difference in 20-E synthesized from the i^{th} crab in chemical group j. All visualizations were created using the ggplot2 package and arranged using the ggpubr and gridExtra packages in R.

Results

Identification of the MEKRE93 signaling genes

To investigate crustacean MF MEKRE93 signaling genes, BLAST inquiry analyses of YO transcriptomes and databases were performed using candidate genes, as indicated by the asterisk in the corresponding spreadsheet (found in the supplementary data on the online repository). Each contig identity was verified through reciprocal BLAST searches and included in supplementary data spreadsheet on the online repository. MEKRE93 signaling genes *Met*, *Src*, *Kr-h1*, and *E93* along with transcriptional coregulators *CBP* and *CtBP* were identified across Clade Panarthropoda (Table 2.1). Contigs encoding MEKRE93 genes were identified in brachyuran YO transcriptomes accessed from the CrusTome database. In *G. lateralis*, complete sequences of *Gl-Met*, *Gl-Kr-h1*, *Gl-CBP*, and *Gl-CtBP* contigs and partial sequences of *Gl-Src* and *Gl-E93* contigs were identified in the YO transcriptome (Table 2.2). In *C. maenas*, complete *Cm-Kr-h1* and *Cm-E93* contigs and partial *Cm-Met*, *Cm-Src*, *Cm-CBP*, and *Cm-CtBP* contigs were identified in both YO and central nervous system (CNS) transcriptomes (Table 2.3).

Characterization of the MEKRE93 signaling genes

Phylogenetic trees were constructed and analyzed to validate and corroborate the BLAST results, while determining the evolutionary relationship of the MEKRE93 signaling genes in

panarthropod taxa. MEKRE93 protein sequences were further characterized by multiple sequence alignments (MSA) and annotation of conserved functional domains, motifs, and residues.

Methoprene tolerant (Met)

Met protein sequences were used to construct a maximum likelihood tree with the common house spider (*Parasteatoda tepidarum*) Met sequence as the outgroup. Phylogenetic analysis showed that the arthropod sequences were separated into the insect and crustacean divisions (Figure 2.1). Within each division, the sequences sorted along hierarchical taxonomic ranking of class, order, and infraorder. The only exceptions were the Met proteins from the two *Daphnia* species, crustaceans within Clade Allotriocarida, that were grouped amongst the insects (other members of Clade Allotriocarida) (Figure 2.1). The amphipod Met proteins were more phylogenetically divergent when compared to the other malacostracan orders, such as isopods and decapods (Figure 2.1). Decapod Met sequences segregated into two groups with one containing anomuran and brachyuran infraorders and the other containing astacuran and shrimp infraorders (Figure 2.1).

The domain organization of Met proteins in 18 decapod species is compared in Figure 2.2. This includes a full-length sequence from *G. lateralis* (Table 2.2; Figure A1) and a partial sequence from *C. maenas* (Table 2.3; Figure A2). Although the Met sequences varied across taxa, the N-terminal region had the same arrangement of three conserved domains: an N-terminal basic helix–loop–helix (bHLH) domain followed by two Period (Per)–Aryl hydrocarbon receptor nuclear transporter (Arnt)–Single-minded (Sim) A and B, or PAS-A and PAS-B domains, respectively (Figure 2.2). Decapod and amphipod Met orthologs were ~1K amino acids

in length, whereas the cladoceran and isopod Met orthologs were shorter in length (~690 amino acids and 766 amino acids, respectively; Figure A3). The lengths of decapod Met sequences were double that in some beetle species (Order Coleoptera) and *Bombyx mori* (Order Lepidoptera), while similar in length to some hemipterans (Figure A3).

MSAs of the decapod Met sequences showed that the three domains were highly conserved. The 55-amino acid bHLH domain had high amino acid identity among 19 species, including 10 residues involved in DNA binding (Figure 2.3). The PAS-A domain also had high sequence identity, including seven active site residues (Figure 2.4). By contrast, the PAS-B domain sequences varied among the decapod taxa, including substitutions at the fifth and eighth residues involved in JH binding in insects (Figure 2.5). The C-terminal region was less conserved, varying in length and amino acid sequence (Figure 2.2; supplementary data).

Steroid receptor complex (*Src*)

As shown in the strongly supported maximum likelihood phylogenetic tree, Src proteins segregated into insect and crustacean groups, with subclades organized along lower taxonomic hierarchy (Figure 2.6). In crustaceans, the Src proteins diverged at Class Branchiopoda (Orders Cladocera and Anostraca) and Class Malacostraca. No amphipod Src orthologs were identified. Multiple Src variants were identified in some decapod species, such as *Paratya australiensis* and *Bathypalaemonella serratipalma*, *Gastroptychus formosus*, and *Leptuca pugilator* (Figure 2.6; supplementary data). A Src sequence was only identified in one penaeid shrimp (*Litopenaeus vannamei*) (Figure 2.6; supplementary data). Decapod Src sequences were further divided between the crab infraorders (Infraorders Anomura and Brachyura) and the lobster and shrimp infraorders (Figure 2.6). One partial transcript was identified in the *G. lateralis* YO

transcriptome (*Gl-Src*; Table 2.2; Figure A4), while two partial *Src* sequences were identified in *C. maenas* (*Cm-Src*; Table 2.3; Figure A5).

The domain organization of the Src proteins is conserved among the 14 decapod species, which included sequences from *G. lateralis* and *C. maenas* (Tables 2.2 and 2.3). The N-terminal region encompassed the bHLH, PAS-A, and PAS-B domains (Figure 2.7). Src sequences showed high sequence identity in the three domains; the C-terminal region varied in length and amino acid sequence (Figure A6; supplementary data).

Krüppel homolog 1 (*Kr-h1*)

A midpoint-rooted, maximum likelihood tree segregated pancrustacean Kr-h1 proteins into insect and crustacean groups (Figure 2.8). Further division of Kr-h1 orthologs followed taxonomic ranks, which were supported by strong bootstrap values. Generally, insect Kr-h1 orthologs were more closely related, as indicated by short branch lengths across the various orders (Figure 2.8). By contrast, the crustacean orthologs had longer branch lengths across the different subclades (Figure 2.8). The Kr-h1 sequences in two copepod species, which are members of Clade Multicrustacea, did not cluster with other the orders within this clade, including krill and decapod species (Figure 2.8). Instead, the copepod species were positioned adjacent to Clade Allotriocarida, which includes *Daphnia*. Within the Multicrustacea, decapod Kr-h1 sequences were segregated from the Kr-h1 sequences in Orders Euphausiacea (krill), Amphipoda, and Isopoda, as indicated by highly supported, long branch lengths (Figure 2.8).

The domain organization of decapod Kr-h1 orthologs was highly conserved in 22 species (Figure 2.9). These included full-length sequences from *G. lateralis* and *C. maenas* (Tables 2.2 and 2.3; Figures A7 and A8). The N-terminal region had a series of DNA-binding domains

consisting of seven C2H2 zinc finger (Znf) repeats of ~21 amino acids in length (Figure 2.9). MSA analysis of pancrustacean Kr-h1 orthologs showed high sequence identity of the Znf repeats, with insect Kr-h1 having eight repeats and crustacean Kr-h1 having seven repeats (Figure 2.10; Figures A9 and A10). Although classified within Clade Allotriocarida along with the insects, *Daphnia* Kr-h1 sequence (781-860 amino acids) had seven Znf repeats as in other crustaceans, but was similar in length (791 amino acids) to *Drosophila melanogaster* Kr-h1 (Figure 2.10; Figures A9 and A10). Thus, the difference in the number of Znf repeats was distinguishing feature between insect and crustacean Kr-h1 orthologs.

Ecdysone response gene 93 (*E93*)

Annotated E93 amino acid sequences were used to construct a maximum likelihood phylogenetic tree that included E93 orthologs annotated as Mushroom body large-type Kenyon cell protein-1 (Mblk-1). The phylogenetic analysis showed segregation of pancrustacean E93 proteins into insect and crustacean clades with chelicerate species as the outgroup (Figure 2.11). No E93 orthologs were identified in copepod, *Daphnia*, and isopod species. Within each clade, the grouping of E93 orthologs followed taxonomic hierarchy. A fish louse crustacean (*Argulus siamensis*), member of Superclass Oligostraca, sequence was positioned between chelicerate and malacostracan E93 sequences (Figure 2.11). Within Class Malacostraca, E93 sequences were partitioned between amphipod, krill, shrimp/prawn, lobster/crayfish, and crab taxa (Figure 2.11).

Decapod E93 sequences had two helix-turn-helix, pipsqueak (HTH_Psq) domains (Figure 2.12). These included one full-length E93 sequence from *G. lateralis* and two full-length sequences from *C. maenas* (Tables 2.2 and 2.3; Figures A11 and12). The only exception was *L. vannamei* E93, which had one HTH_Psq domain (Figure 2.12). Besides the HTH_Psq domains,

the pancrustacean E93/Mblk-1 orthologs varied in length and amino acid sequence including within taxonomic orders (Figure 2.12; Figures A13-A15).

CREB-binding protein (CBP)

CBP protein sequences were used for the construction of a maximum likelihood phylogenetic tree that was rooted with two tardigrade CBPs. The three major clades did not always follow taxonomic groupings, as the pancrustacean sequences did not group together. Copepod CBPs formed a separate group from other malacostracans, such as the isopods, krill, and decapods (Figure 2.13). At the copepod branchpoint, the Pancrustacea partitioned into insect and crustacean groups with *Daphni*a positioned with the insects, as both are members of Clade Allotriocarida. Two spider CBPs were positioned between *Daphnia* and the insect orders (Figure 2.13). However, Class Malacostraca followed taxonomic order, with decapod CBPs grouping with infraorder hierarchy (Figure 2.13).

CBP proteins of 15 decapod species, including *G. lateralis* (Figure A.16) and *C. maenas* (Figure A17), were over 2K amino acids in length and had the same domain organization (Figure A14). The domain arrangement included several Zf binding regions, including the Transcription Adaptor Zinc Finger 1 (TAZ1) and 2 (TAZ2), Really Interesting New Gene (RING), Plant homeodomain (PHD), and Z-type zinc finger (ZZ) domains. CBPs contained additional domains such as the transcription factor docking site Kinase-inducible Domain Interacting (KIX), the acetylated lysine recognition and binding Bromodomain (BROMO) site, and Histone acetyltransferase (HAT) domains. The CREB binding region, located near the C-terminus, contained a nuclear receptor coactivator binding domain (NCBD) with coactivator binding sites (Figure 2.14). Across infraorders, the length varied after the NCBD, with the HAT domain the

longest in length. Within Infraorder Astacidea, the CBP ortholog in *Homarus americanus* was 2623 amino acids, in *Procambarus clarkii* was 2636 amino acids, and in *Cherax quadricarinatus* was 2175 amino acids. The CBP orthologs within Infraorder Caridea, specifically in *Macrobrachium nipponense* and *Neocaridina denticulata* were 2178 and 2585 amino acids in length, respectively (Figure 2.14). The majority of crustacean CBP orthologs, except *Daphnia*, were shorter than the dipteran CBPs (Figures A18 and A19).

C-terminal-binding protein (*CtBP*)

CtBP protein sequences were identified in many species in Clade Panarthropoda. A maximum likelihood phylogenetic tree showed a distinct separation of arthropods from tardigrades (Figure 2.15). Furthermore, the division between the chelicerates and mandibulates was supported with strong bootstrap values, except for the barnacles (Order Thecostraca). Class Branchiopoda (Orders Cladocera and Notostraca) CtBPs were more closely related to other crustaceans, even though they are classified with insects in Clade Allotriocarida (Figure 2.15). Within Class Malacostraca, CtBP sequences followed taxonomic order and infraorder hierarchy. Caridean shrimp had long and short CtBP transcripts. Only one CtBP variant was identified in the other decapod infraorders (Brachyura, Anomura, Achelata, Astacidea, and Dendrobranchiata).

Moreso, a full-length CtBP transcript was identified in the *G. lateralis* YO transcriptome (*Gl-CtBP*) (Table 2.2; Figure A20) but only partials sequences were obtained from the *C. maenas* CNS and YO assemblies (*Cm-CtBP*) (Table 2.3; Figure A21). All CtBP sequences contained the dehydrogenase domain (CtBP_dh) flanked by the N-terminal domain (NTD) and the C-terminal domain (CTD) (Figure 2.16; Figures A22 and A23). The N-terminal region of CtBP exhibited

high conservation especially within the CtBP_dh domain with regards to the dehydrogenase diagnostic features of NAD(H) binding sites and the catalytic triad, arginine (Arg)- glutamic acid (Glu)- histidine (His) (Figure 2.16; Figures A22 and A23). Opposed to the NTD the C-terminal domain (CTD), the site of posttranslational modification such as sumolyation and phosphorylation, exhibits more variability (Figures 2.17 and 2.18). While most decapod crustaceans had one CtBP transcript containing a CTD, caridean shrimp had two isoforms with one containing a CTD and one lacking a CTD (Figure 2.18). The crustacean CTD contains the conserved the CVNKEY, NGGYY/GLNG-–YY central block, and AHSTT motifs with polyproline repeats following the central block (Table 2.4). Only barnacles had the ancestral SEVH motif (Table 2.4; Figure A24). In amphipods and the tadpole shrimp, polyalanine stretches replaced the proline repeats, which also occurred in CTDs in tardigrades and *Drosophila* (Figure A25).

Gene expression over the molt cycle

The relative gene expression of MEKRE93 signaling components and transcription coregulators were determined in the *G. lateralis* and *C. maenas* YO across the different molt stages. In the *C. maenas* YO, *Cm-Met*, *Cm-Src*, *Cm-Kr-h1,* and *Cm-E93* were expressed at all stages of the molt cycle (Figure 2.19). *Cm-Met* was highly expressed at all stages, with no significant differences between the means (Figure 2.19a). Expression of *Cm-Src* was significantly higher in mid-premolt (MP) and significantly lower in intermolt (IM), late premolt (LP), and postmolt (PM); IM–MP: $p = 0.0471$; LP–MP: $p = 0.047$; MP–PM: $p = 0.0346$ (Figure 2.19b). *Cm-Kr-h1* and *Cm-E93* were expressed at all molt stages with no significant differences between the means (Figure 2.19c, d). *Cm-CBP* and *Cm-CtBP* were constitutively expressed

throughout the different molt cycle stages, with the mean at MP significantly higher than that at IM; *Cm-CBP* IM–MP: $p = 0.022$; *Cm-CtBP* IM–MP: $p = 0.035$ (Figure 2.20). In the *G. lateralis* YO, *Gl-Met* and *Gl-Kr-h1* were largely expressed in IM, decreased throughout premolt, and not expressed in PM (Figure 2.21a, c). *Gl-Src* and *Gl-E93* was also upregulated in IM, lower throughout premolt, but had low expression in PM (Figure 2.21 b, d). *Gl-CBP* and *Gl-CtBP* were constitutively expressed throughout the different stages of the molt cycle (except PM) with the mean at IM significantly higher in comparison (Figure 2.22).

Effects of MF and JH-mimics on YO ecdysteroid secretion

Experiments on YOs from intermolt (IM) *C. maenas* determined the effects of three concentrations of MF and JH-mimics on ecdysteroid secretion over a 48-hour incubation period. The results from paired *t*-tests applied to the differences in the quantity of 20-E equivalents secreted were greater at 10.0 µM with secretion rates slowing by 24 hours (Table A2, Figure 2.23). Consequently, 10.0 µM of each compound and 48 hours incubation were used on YOs from IM *G. lateralis* and 10.0 µM of each compound and 24 hours incubation were used on YOs from mid-premolt (MP) *G. lateralis*. A linear model applied to these data and the associated data for YOs from IM and MP *G. lateralis* summed and aggregated the amount of 20-E secreted at each eight-hour interval to obtain the cumulative amount of 20-E secreted at 24 and 48-hours *for C. maenas* and at 24 hours for *G. lateralis* (see Materials and Methods).

After 24-hours, *C. maenas* YO ecdysteroid secretion was inhibited by fenoxycarb ($t = -1.9$, $p = 0.060$), in which YOs secreted, on average, 19.8 pg/µL less 20-E (95% confidence interval or CI: -40.6, 0.6) than untreated paired YOs (Figure 2.24a; Figures A26 and A27). By contrast, ecdysteroid secretion was stimulated by S-hydroprene ($t = 2.2$, $p = 0.033$) or

methoprene (t = 3.8, p < 0.001) treatments (Figure 2.24a; Figures A26 and A27). It is estimated that S-hydroprene stimulated the YOs to secrete 22.6 pg/μL more 20-E (95% CI: 1.9, 43.3) and methoprene stimulated the YOs to secrete 38.6 pg/μL more 20-E (95% CI: 17.9, 59.3) relative to untreated paired YOs. On average, the YOs exposed to MF produced 10.5 pg/μL less 20-E (95% CI: -31.2, 10.2); however, there was no statistically significant difference in the means between treated and control YOs (t = -1.0, p = 0.310) (Figure 2.24a; Figures A26 and A27).

After 48 hours, fenoxycarb continued to inhibit the ecdysteroid secretion and gained statistical significance (t = 2.1, p = 0.039) (Figure 2.24a; Figures A26 and A27). Moreover, the estimated inhibiting effect increased in magnitude, as the estimated average difference in 20-E secreted at 48-hours was 51.4 pg/μL less 20-E secreted (95% CI: -100.2, -2.7) than that by paired untreated YOs. However, the stimulation of ecdysteroid secretion by S-hydroprene lost significance at 48 hours (t = 1.0, p = 0.313), even though, on average, the treatment of S-hydroprene increased 20-E secretion by 24.6 pg/μL 20-E (95% CI: -24.1, 73.4) control YOs (Figure 2.24b; Figures A26 and A27). The difference between treated and untreated YOs at 48-hours was similar magnitude at 24-hours, indicating that the stimulatory effect of S-hydroprene occurred in the first 24-hours of incubation. By contrast, the stimulation of methoprene on ecdysteroid secretion continued after 48-hours (t = 2.4, p = 0.0194). The estimated average 20-E equivalents secreted was 58.9 pg/μL more that of paired untreated YOs (95% CI: 10.1, 107.6), a quantity greater in magnitude compared to 24-hours (Figure 2.24b; Figures A26 and A27). MF had no effect on YO ecdysteroid secretion at 48-hours (t = -0.0, p = 0.986). There was no significant difference between the means of MF treated and untreated paired YOs ($\bar{x}$ = 0.4 pg/µL; 95% CI: -49.2, 48.3) (Figure 2.24a; Figures A26 and A27).

At 24-hours, intermolt *G. lateralis* YO ecdysteroid secretion was inhibited by fenoxycarb (t = -2.9, p = 0.005) or S-hydroprene (t = -4.7, p < 0.001) (Figure 2.24c; Figures A25 and A28). On average, 17.0 pg/μL less 20-E was secreted with fenoxycarb treatment (95% CI: -28.7, -5.2) and 27.9 pg/μL less 20-E was secreted with S-hydroprene treatment (95% CI: -39.6, -16.2) compared to untreated paired YOs. Neither methoprene (t = -0.4, p = 0.712) nor MF (t = -1.2, p = 0.221) had a significant effect on ecdysteroid secretion. YOs treated with methoprene secreted 2.2 pg/μL less 20-E (95% CI: -13.9, 9.5), while treated with MF secreted 7.3 pg/μL less 20-E (95% CI: -19.0, 4.5), which were not significantly different from untreated paired YOs (Figure 2.24c; Figures A25 and A28).

At 48-hours, fenoxycarb (t = -2.7, p = 0.001) and S-hydroprene (t = -4.5, p < 0.001,) continued to inhibit ecdysteroid secretion by IM *G. lateralis* YOs (Figure 2.24d; Figures A25 and A28). Fenoxycarb-treated YOs secreted 17.2 pg/μL less 20-E (95% CI: -30.1, -4.3), while S-hydroprene-treated YOs secreted 28.9 pg/μL less 20-E (95% CI: -41.8, -16.0), than untreated paired YOs. The magnitudes of the inhibiting effects for both compounds were similar at 24 and 48-hours, indicating the maximal effects of these compounds occurred by 24-hours. Neither methoprene (t = 0.2, p = 0.816) nor MF (t = -0.3, p = 0.750) had a significant effect on YO ecdysteroid secretion (Figure 2.24d; Figures A25 and A28). 20-E secretion of YOs treated with MF was only 2.1 pg/μL less (95% CI: -15.0, 10.8) than untreated controls, while 20-E secretion of YOs treated methoprene was only 1.5 pg/μL more (95% CI: -11.4, 14.4) than that of the untreated paired YO.

The effects of MF and JH-mimics on YOs from MP *G. lateralis* were determined after 24-hours incubation. Fenoxycarb (t = -2.9, p = 0.009) significantly inhibited YO secretion (Figures A25 and A28). Fenoxycarb-treated YOs secreted 17.0 pg/μL less 20-E equivalents than

the untreated paired YOs (95% CI: -27.2, -4.6) (Figure 2.24e). By contrast, methoprene (t = -1.7, p = 0.107) and S-hydroprene (t = -0.6, p = 0.489) had no significant effect on YO ecdysteroid secretion (Figure 2.24e; Figures A25 and A28). YOs treated with methoprene secreted 9.1 pg/μL less 20-E, which was not significantly different from the control (95% CI: -20.4, 2.2). S-Hydroprene showed no effect on the YO 20-E secretion (95% CI: -15, 7.5) (Figure 2.24e). A comparison of the effects of MF and JH-mimics on YO secretion in *C. maenas* and *G. lateralis* is summarized in Table 2.5.

Discussion

Ecdysteroid signaling is essential for molting thereby regulating pancrustaean growth, development, and/or regeneration (Chang, 1993; Chang et al., 1993; Fingerman, 1997; Subramoniam, 2000; Gilbert et al., 2001; Mykles, 2024; Orchard and Lange, 2024b). Ecdysteroid binding to the EcR/RXR receptor activates the ecdysone response gene cascade, which, can be affected by the MF MEKRE93 transcriptional cascade (Mu and LeBlanc, 2004; Liu et al., 2018; Mazina and Vorobyeva, 2019; Adhitama et al., 2020). The CrusTome database, along with other published repositories, was used to identify *Met*, *Src*, *Kr-h1*, and *E93* genes in pancrustacean taxa (Table 2.1). Transcriptional comediators *CBP* and *CtBP* were also identified. The contig sequences were obtained from *C. maenas* and *G. lateralis* YO transcriptomes and characterized (Tables 2.2 and 2.3). This study constitutes the most comprehensive analysis of the crustacean MF MEKRE93 signaling genes. Phylogenetic and sequence analysis revealed high conservation of the domain organization and functional motifs, which will aid in the identification and annotation of new sequences as transcriptomes and genomes are added to GenBank and other repositories.

The MEKRE93 and comediator genes were expressed in the *G. lateralis* and *C. maen*as YO at all molt stages. However, expression patterns were not consistent between species for each gene. Post-translation modifications of Methoprene tolerant (Met) and Krüppel homolog 1 (Kr-h1) have been reported to affect transcription activity. In the yellow fever mosquito (*Aedes aegypti*) within the presence of JH, *Aa-Met* Serine residue 77 (Ser-77) and Serine 710 (Ser-710) were phosphorylated, phosphoserine residues 73 and 747 were dephosphorylated, and a transient but reversible phosphorylation of Thr-664 and Ser723 (Kim et al., 2021). Additionally, in the presence of JH *Aa-Kr-h1* phosphoserine residue 694 is dephosphorylated and consequently showed significantly higher activity (Kim et al., 2021). In the cotton bollworm (*Helicoverpa armigera*), JH induced the threonine-phosphorylation of Met at Threonine residue 393 (Thr-393) was essential for Met binding to the response element inducing *Kr-h1* expression and prevented binding to its cofactor Taiman (Tai) (Li et al., 2021e). In the red flour beetle (*Tribolim castaneum*) epigentic modifications (e.g., acetylation and deacetylation) regulate JH action as histone deacetylase 1 (HDAC1) suppressed *Kr-h1* expression (George et al., 2019). Although CBP is an accepted transcriptional enhancer and CtBP is an accepted transcriptional repressor, the expression pattern of these are the same within each species. This suggests these factors may have different transcriptional partners. In the migratory locust (*Locusta migratoria*), protein kinase C- alpha (PKCα) phosphorylates Kr-h1 to, which, in adults recruits CtBP to inhibit *E93* expression but in adults recruits CBP to enhance vitellogenesis through upregulating *Ribosomal protein L36* (Wu et al., 2021). JH-induced PKC activation, dependent on phospholipase C (PLC) and calcium/calmodulin- dependent protein kinase II (CaMKII) signaling, was reported to be essential for Met transactivation activity through promoting the binding to JH response elements in *A. aegypti* (Liu et al., 2015a; Ojani et al., 2016). In *H. armigera* JH induced PKC

phosphorylation of heat shock protein 90 (Hsp90) thus promoting the interaction between this chaperone protein and Met (Liu et al., 2013). On the other hand, (Liu et al., 2013) indicated that 20-E suppressed Hsp90 phosphorylation and promoted the interaction between the chaperone protein and Ultraspiracle 1 (USP1). PKC and PLC signaling has been reported in *H. armigera* to lead to the phosphorylation of Broad-Complex, an ecdysone response gene, in the presence of JH thus inhibiting the transcription of other 20-E genes (Cai et al., 2014). MicroRNAs (miRNAs) also may play a role in post-transcriptional regulation. *Kr-h1* transcripts were reported to be scavenged by MiR-2 in the German cockroach (*Blatella germanica*) and downregulated by let-7 and miR-278 in the migratory locust (*Locusta migratoria*) (Lozano et al., 2015; Song et al., 2018). Modulation of the genes and transcription factors within the MF/JH and ecdysone pathway provides a basis and insight to understanding the endocrine-transcriptional regulation (Geens et al., 2024).

In vitro assays showed that YOs responded to compounds acting through the MF signaling. In the present study, intermolt (IM) YOs harvested from *C. maenas* and *G. lateralis* treated with any concentration of MF (0.1 μM, 1.0 μM and 10.0 μM) (*in vitro*) had no effect on ecdysteroid secretion even after 48-hours. These results differ from the findings of Tamone and Chang (1993) that revealed the stimulation of ecdysteroidogenesis in the Dungeness crab (*Metacaricnus magister*) YOs exposed to high concentrations (1.0 μM and 10.0 μM) of MF (*in vitro*) after 24-hours. Even with the use of high concentrations of MF in *C. maenas* and *G. lateralis*, ecdysteroidogensis was not impacted thus proposing the idea of a higher dose to see an elicited response (*in vitro*) and importance of binding proteins (Prestwich et al., 1990, 1996; Li and Borst, 1991; King et al., 1995; Tamone et al., 1997; Takáč et al., 1998; Zhao et al., 2020). However, a high MF-concentration was required to stimulate molting in the whiteleg shrimp

(*Litopenaeus vannamei*) *in vivo* (Alnawafleh et al., 2014). Furthermore, MF stimulated molting and reduced the intervals within the IM and premolt stage in *Travancoriana schirnerae*; however, the optimization of shortening the molt cycle duration was dependent on timing of MF administration and the dose (Raghavan and Ayanath, 2019). Due to the ability to biosynthesize MF, it is likely that the lack of observed effect is due to degradation of MF by endogenous carboxylase activity (Laufer and Albrecht, 1990; King et al., 1995; Homola and Chang, 1997b, 1997a; Takac et al., 1997; Satoh and Hosokawa, 2006; Yu et al., 2009; Kamita and Hammock, 2010; Kamita et al., 2011; Lee et al., 2011; Tao et al., 2017; Xu et al., 2017; Zhu et al., 2018; Zhang et al., 2020; Chen et al., 2021b, 2022a; Li et al., 2021d; Tu et al., 2022).

JH-mimics, also referred to as JH-analogs such as hydroprene, methoprene, fenoxycarb, and pyriproxyfen, are hydrophobic compounds that mimic the action of JH in insects (Dhadialla et al., 1998; Wilson, 2004). JH-mimics are classified as insect growth regulators (IGRs), or insect growth disruptors (IGDs) as they are primarily utilized as insecticides. Specifically, JH-analogs are a third-generation insecticide as they are more ecofriendly and safer to other organisms, compared to first-generation (e.g., inorganic compounds including sulfur arsenic, mercury, and lead) and second-generation insecticides (e.g., organophosphates, carbamates, and DDT also known as dichlorodiphenyltrichloroethane) (Parthasarathy and Palli, 2021). Due to its applicability in the management of vectors of human diseases and agricultural pests, understanding the mode of action of JH-mimics is of high interest as it may contribute to the development to novel and optimal IGRs (Minakuchi and Riddiford, 2006; Noriega and Nouzova, 2020; Apolinário and Feder, 2021; Lai et al., 2021; Devi and Awasthi, 2022; Yokoi, 2024). Some JHAs, such as hydroprene and methoprene, are designed and synthesized to contain one or more ester linkages (similar to naturally occurring JHs) and thereby be metabolized by cytochrome

p450 monoxygenases/carboxylesterases (Mohandass et al., 2006a, 2006b). JHAs are sensitive to several factors including application time, exposure duration, and concentration leading to efficacy variability (Parthasarathy and Palli, 2021). Furthermore, the effectiveness of JHAs is dependent on developmental stage (i.e. stage-specific) and the species tolerance (Parthasarathy and Palli, 2021). For instance, Santos et al. (2017) revealed that the accepted concentration dosage of pyriproxyfen utilized to control *A. aegypti* larvae is lethal to *Daphnia magna* and *Artemia salina*; however, even across crustacean species the effective concentration differs. Additionally, JH-analogs have been shown to work directly through the Met receptor as methoprene and fenoxycarb disturbs Met expression in the Colorado potato beetle (*Leptinotarsa decemlineata*) consequently impacting ecdysteroid concentration (Meng et al., 2018; Jindra and Bittova, 2020).

Pyriproxyfen and its exposure to abdominal integument sternites from pupal mealworms (*Tenebrio molitor*) *in vitro* at 1.0 μM and 10.0 μM inhibited ecdysteroid concentrations (Aribi et al., 2006). Trace amounts of pyriproxyfen in the silkworm larvae (*Bombyx mori*) reduced 20-E hemolymph concentrations, promoted Met phosphorylation thus upregulating *Kr-h1* expression, and inhibited *Br-C* expression (Li et al., 2021a). Wang et al. (2023) additionally showed that pyriproxyfen exposure in *B. mori* larvae lowered 20-E concentrations due to a downregulation of 20-E biosynthetic genes; however, it also upregulated drug metabolism and glycometabolism genes. *Kr-h1* expression in the brain tissue was also downregulated in the worker honey bee when exposed to pyriproxyfen (Litsey and Fine, 2024). Pyriproxyfen had no impact on *C. maenas* YOs at any concentration (0.1 μM, 1.0 μM and 10.0 μM) *in vitro*. Adult copepods that were reported to have a high sensitivity to pyriproxyfen; however, pyriproxyfen has been documented to have several ecotoxicological effects including in daphnids and other crustaceans

(Legrand et al., 2017; Devillers, 2020). In the Chinese mitten crab (*Eriocheir sinensis*), after two- and four-days of insecticide exposure pyriproxyfen had the highest acute toxicity while medium acute toxicity was exhibited in the red swamp crayfish (*Procambarus clarkii*) after two and four-days of exposure (Wang et al., 2022). Pyriproxyfen treatment in the Australian red claw crayfish (*Cherax quadricarinatus*) did not cause significant mortality but delayed spawning (Abdu et al., 2001). Exposure to pyriproxyfen also stimulated premature ovarian development and vitellogenesis were reported in the Christmas Island red crab (*Gecarcoidea natalis*) (Linton et al., 2009). Additionally, pyriproxyfen induced the expression of retinoid X receptor (RXR), a nuclear receptor in the ecdysone signaling pathway in *Gammarus fossarum* (Gouveia et al., 2018).

Fenoxycarb exposure to the Oriental latrine blow fly (*Chrysomya megacephala*) was most effective at 0-hour old larvae in comparison to 24 and 48-hour old last larval instar (Singh and Maddheshiya, 2021). McKenney et al. (2004) showed that 888 μL^{-1} fenoxycarb inhibited embryonic development in grass shrimp (*Palaemonetes pugio*) but had not affect to concentrations less than 502 μL^{-1}. Additionally, *P. pugio* larvae exhibited a higher sensitivity to fenoxycarb than in embryonic stages (McKenney et al., 2004). Fenoxycarb extended the period between zoael development in the American lobster (*Homarus americanus*) (Arnold et al., 2009). Low concentrations (0.1 μM and 1.0 μM) had not significant impact on ecdysteroid production in *C. maenas* IM YOs *in vitro*. However, ecdysteroid secretion in *C. maenas* IM YOs was significantly inhibited after 48-hours post exposure but not at 24-hours when treated with 10.0 μM fenoxycarb *in vitro*. Ecdysteroid secretion was also inhibited in *G. lateralis* IM YOs after 24 and 48-hours post exposure when treated with 10.0 μM fenoxycarb *in vitro*. Even MP *G. lateralis* YOs ecdysteroid production was inhibited after 24-hours. These results show that

although fenoxycarb has a strong inhibitory affect in both *C. maenas* and *G. lateralis* the sensitivity of the YO differs due to the timing of an elicited response. The inhibitory behavior of fenoxycarb in the tested model species is similar strong inhibitory effect in honeybees (Luo et al., 2021).

Methoprene reduced molt frequency in *Daphnia magna* in a dose-dependent manner (Olmstead and Leblanc, 2001). Stueckle et al. (2008) noted that biological sex can impact methoprene sensitivity since male mud fiddler crabs (*Uca pugnax*) had a higher sensitivity to chronic exposure compared to females as post molt (PM) crabs took longer to proceed throughout premolt. *C. maenas* IM YOs exposed at low concentrations (0.1 μM and 1.0 μM) had no effect on ecdysteroid secretion *in vitro* despite its stimulatory effect at 10.0 μM after 24 and 48-hours of exposure. On the contrary, *G. lateralis* IM YOs exposed to any concentration of methopren (0.1 μM, 1.0 μM, and 10. μM) had no effect on ecdysteroid secretion after 24 or 48-hours.

Methoprene also did not impact ecdysteroid secretion after a 24-hour exposure period to MP *G. lateralis* YOs. Hydroprene has been reported to prevent normal development, emergence, and reproduction in insects (Kramer et al., 1990; Mohandass et al., 2006b, 2006a). *C. maenas* IM YOs showed sensitivity to hydroprene at any of the concentrations tested (0.1 μM, 1.0 μM and 10.0 μM) *in vitro* with a similar impact at both 1.0 μM and 10.0 μM. However, by 48-hours there was no significant difference in ecdysteroid production as a stimulatory effect on the *C. maenas* IM YOs was observed by 24-hours thereby suggesting the YO lost sensitivity. Ecdysteroid secretion was inhibited at both 24 and 48 hours in IM *G. lateralis* YOs after 10.0 μM hydropene treament *in vitro*; however, MP *G. lateralis* YOs elicited no response even after 24-hours. These findings suggest that YO sensitivity is time, dose, stage, and species specific. It

is possible that Fenoxycarb has a sublethal effect as there was a strong inhibition between the two brachyuran species. Blackback land crab YOs may have different sensitivity at different phases of the molt cycle considering after 24-hours of hydroprene exposure there was no significant inhibitory effect on MP YOs unlike IM YOs.

Tuberty and Mckenney (2005) reported differences in ecdysteroid responses after the exposure to JH-analogs between daggerblade grass shrimp (*Palaemonetes pugio*) and the Harris mud crab (*Rhithropanopeus harrisii*). These data supports the possibility that the difference of JHA effective in ecdysteroidogenesis is dependent on species as fenoxycarb inhibits ecdysteroid secretion in both brachyuran species tested, S-hydroprene stimulated ecdysteroid synthesis in the *C. maenas* but was inhibited in *G. lateralis*, and methoprene had a stimulatory effect only in *C. maenas*. More specifically, amino acid substitutions in S (red)/T (blue) in the fifth and seventh binding pockets may contribute to differential binding of MF and JH mimics to Met (Miura et al., 2005; Charles et al., 2011; Bernardo and Dubrovsky, 2012; Miyakawa et al., 2013; Zhao et al., 2014; Kolonko et al., 2016; Kakaley et al., 2017; Hirano et al., 2020). Besides an altered affinity to the Met receptor complex some species may require additional binding proteins may be required to reach the targeted tissue (Prestwich et al., 1990, 1996; Li and Borst, 1991; King et al., 1995; Tamone et al., 1997; Takáč et al., 1998; Zhao et al., 2020). The ineffectiveness of the JH-mimics also could be a result of increase in detoxification enzymes, insecticide resistance, cross resistance as observed in some insect species towards some compounds (Wilson, 2004; Mohandass et al., 2006b). Nevertheless, it has been proposed that other interactions between compounds and factors can interfere with the crosstalk between sesquiterpenoid hormones and ecdysteroids, such as methoprene and glyphosate in the amphipod *G. fossarum*; and methoprene, permethrin, and salinity in the crab *U. pugnax* (Stueckle et al., 2009; Gauthier et al., 2023).

Taken together, these data indicates that YO sensitivity to MF and to JH-mimics is dependent on dose and time and the effects varies across species and compound type.

Conclusion

The study constitutes a comprehensive analysis of the MEKRE93 transcriptional network in crustaceans. The determination of the phylogenetic relationships, sequence alignments, and domain and/or motif structure provides insight into the roles that MF plays in development, reproduction, and growth, as well as how pesticides may disrupt these processes. Moreover, the expression these sequences in *G. lateralis*, *C. maenas*, and *Callinectes sapidus* YO transcriptomes and the responses of YOs to JH-mimics support the notion that MF–MEKRE93 signaling regulates YO ecdysteroidogenesis, and that interactions between MEKRE93, ecdysteroid, molt-inhibiting hormone (MIH), mechanistic target of rapamycin complex 1, (mTORC1), and transforming growth factor- Beta (TGFβ) signaling pathways contribute to phenotypic changes in the YO over the molt cycle (Mykles and Chang, 2020; Mykles, 2021, 2024). During intermolt (IM), the YO is kept in the basal state by MIH-mediated inhibition of mTORC1 activity; a drop in MIH activates mTORC1 and the YO transitions to the activated state in early premolt (EP). TGFβ/myostatin signaling meditates the transition of the YO from the activated to committed state in mid premolt (MP). The transition from the committed to repressed stated coincides with the peak in hemolymph 20-E titer in late premolt (LP), suggesting a negative-feedback mechanism mediated by ecdysteroid response genes (Mykles, 2024). The transition of the YO back to the basal state may involve a factor released from the integument upon completion of the synthesis and calcification of the new exoskeleton at the end of post molt (PM) (Mykles, 2024).

It is hypothesized that the activity of the MF MEKRE93 signaling cascade is regulated by the hemolymph 20-E titer, as the YO expresses the EcR/RXR receptor and ecdysteroid response nuclear receptors (Benrabaa et al., 2024; Benrabaa and Mykles, 2025). A model is proposed that incorporates the comediators CBP and CtBP, which have antagonistic effects on *Kr-h1* expression, where CBP acts as a co-activator and CtBP acts as a co-repressor (Figure 2.26). The model assumes that MF is constitutively present, although hemolymph MF titer increases with vitellogenesis and oocyte maturation in females (Borst and Tsukimura, 1991; Homola and Chang, 1997c; Nagaraju, 2007; Liu et al., 2016; Xie et al., 2018; Li et al., 2021c, 2021b). The balance of CBP and CtBP activities is determined by the hemolymph ecdysteroid titer. At low 20-E, such as during intermolt, CtBP is dominant and inhibits *Kr-h1* expression, resulting in increased ecdysteroid synthesis when MIH level falls. At high 20-E, such as in late premolt (LP), CBP is dominant and stimulates *Kr-h1* expression, resulting in reduced ecdysteroid synthesis.

Data availability

The corresponding datasets in this study are available on the Harvard Dataverse online repository (Bentley, Vanessa, 2025, "Methyl farnesoate", https://doi.org/10.7910/DVN/BCG5V4, Harvard Dataverse, V1).

Table 2.1. Taxonomic distribution of identified MEKRE93 transcription factors and transcription modulators. Abbreviations: CBP, CREB-binding protein; CtBP, C-terminal–binding protein; E93, Ecdysone response gene 93; Kr-h1, Krüppel homolog 1; Met, Methoprene-tolerant; and Src, Steroid receptor coactivator.

Taxon						Gene					
						Met	***Src***	***Kr-h1***	***E93***	***CBP***	***CtBP***
Clade Panarthropoda					Phylum Tardigrada	–	–	–	–	2	3
	Phylum Arthropoda				Subphylum Chelicerata	1	–	–	3	2	5
		Clade Pancrustacea			Class Branchiura	–	–	–	1	–	–
			Clade Allotriocarida		Class Insecta	16	6	21	35	15	21
					Class Branchiopoda	2	3	2	–	1	3
			Clade Multicrustacea		Class Copepoda	–	–	2	–	9	9
					Class Thecostraca	–	–	–	–	–	4
				Class Malacostraca	Order Stomatopoda	–	–	–	–	–	2
					Order Isopoda	3	7	19	–	4	8
					Order Amphipoda	6	–	15	2	–	4
					Order Euphausiacea	–	–	3	1	2	2
					Order Decapoda	36	29	56	12	25	69
					Total Number of Contigs	**64**	**45**	**119**	**54**	**60**	**130**
					Total Number of Species	**64**	**38**	**118**	**54**	**60**	**101**

Table 2.2. MEKRE93 signaling transcripts from the *G. lateralis* Y-organ transcriptome (Pérez-Moreno et al., 2023). Abbreviations: aa, amino acids; bp, base pairs; bHLH-PAS, basic helix-loop-helix–Per-Arnt-Sim; C2H2 Znf, Cys2-His2 zinc finger; HTH-Psq, helix-turn-helix, pipsqueak; ID, identification; ORF, open reading frame; and UTR, untranslated region. Asterisk indicates partial sequence (incomplete ORF).

Gene	Class	Contig ID	Length (bp)	ORF (aa)	UTR (bp)	GenBank Accession
Gl-Met	bHLH-PAS	Y EVm001315t1	3511	1001	**5':** 177 **3':** 327	PQ306373
Gl-Src	bHLH-PAS	Y EVm002648t2	3179	707*	**5':** 1056 **3':** –	PQ308086
Gl-Kr-h1	C2H2-Znf	Y EVm003411t1	2476	616	**5':** 345 **3':** 279	PQ306361
Gl-E93	HTH-Psq	Y EVm001885t1	3114	854*	**5':** – **3':** 548	PQ306469
Gl-CBP	Transcriptional Coactivator	Y EVm000165t1	7188	2197	**5':** 54 **3'**: 540	PQ306374
Gl-CtBP	Transcriptional Corepressor	Y EVm005788t1	1905	454	**5':** 427 **3':** 113	PQ306376

Table 2.3. MEKRE93 signaling transcripts from the *C. maenas* Y-organ (Y) and central nervous system (CNS) transcriptomes (Pérez-Moreno et al., 2023). Abbreviations: aa, amino acids; bp, base pairs; bHLH-PAS, basic helix-loop-helix–Per-Arnt-Sim; C2H2 Znf, Cys2-His2 zinc finger; HTH-Psq, helix-turn-helix, pipsqueak; ID, identification; ORF, open reading frame; and UTR, untranslated region. Asterisk indicates partial sequence (incomplete ORF).

Gene	Class	Contig ID	Length (bp)	ORF (aa)	UTR (bp)	GenBank Accession
Cm-Met	bHLH-PAS	Y EVm001443t1	3677	998*	**5':** 682 **3':** –	PQ306465
		CNS EVm002019t1	2986	921*	**5':** 223 **3':** –	PQ321205
Cm-Src	bHLH-PAS	Y EVm000958t2	4878	1185*	**5':** 1323 **3':** –	PQ327774
		CNS EVm001140t3	5299	1174*	**5':** 1777 **3':** –	PQ327775
Cm-Kr-h1	C2H2-Znf	Y EVm004068t1	3842	603	**5':** 1425 **3':** 603	PQ306239
		CNS EVm004576t1	3418	603	**5':** 1020 **3':** 586	PQ317097
Cm-E93	HTH-Psq	Y EVm001380t1	4185	1016	**5':** 158 **3':** 975	PQ306467
		CNS EVm001710t1	3880	989	**5':** 35 **3':** 875	PQ317110
Cm-CBP	Transcriptional Coactivator	Y EVm000144t1	7455	2321*	**5':** 490 **3':** –	PQ306466
		CNS EVm000162t1	7435	2321*	**5':** 470 **3':** –	PQ327773
Cm-CtBP	Transcriptional Corepressor	Y EVm011142t2	1100	278*	**5':** – **3':** 198	PQ327771
		CNS EVm011952t2	1008	326*	**5':** 28 **3':** –	PQ327772

Table 2.4. Consensus sequences of the crustacean C-terminal domain (CTD) motifs in the C-terminal-binding protein (CtBP) transcriptional corepressor. Bolded in red are aromatic residues implicated as amino acid substitutions. Species silhouettes were obtained from PhyloPic (http://phylopic.org).

	Taxon	Motif Consensus Sequences			
		Motif #1	Motif #2	Motif #3	Motif #4
	Brachyura	CVNKEY	G**V**NG–YY	VHSTT	
	Anomura	CVNKEY	G**V**NG–YY or G**V**NG–Y**F**	VHSTT	
	Achelata	CVNKEY	G**V**NG–YY	VHSTT	
	Astacidea	CVNKEY	G**V**NG–YY	VHSTT	
	Dendrobranchiata	CVNKEY	G**V**NG–YY	VHSTT	
	Caridea	CVNKEY	G**V**NG–YY or **SV**NG–YY	VHSTT	
	Amphipoda	CVNKEY	G**V**NG–Y**F**	VHSTT/VHST**A**	
	Isopoda	CVNKEY	G**V**NG–YY	VHSTT	
	Copepoda	CVNKEY or C**I**NKEY	G**M**NG–YY or GLNG–YY/G**P**N**S**–YY	**A**HSTT	
	Euphausiacea	CVNKEY	G**V**NG–YY	VHSTT	
	Cladocera	CVNKEY	GLNG–YY	**A**HS**SA**	
	Stomatopoda	CVNKEY	G**V**NG–YY	VHSTT	
	Notostraca	CVNKEY	GLNG–YY	**A**H**NSA**	
	Thecostraca	CVNKEY	GLNG–YY	**A**HST**S**	S**DI**H

Table 2.5. Summary of the comparative effects of 10.0 µM methyl farnesoate or JH mimics on ecdysteroid secretion in Y-organs from *C. maenas* and *G. lateralis* after a) 24 hours and b) 48 hours *in vitro*. Species silhouettes were obtained from PhyloPic (http://phylopic.org).

a)

24 hours	**Molt stage**	Fenoxycarb 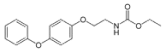	Hydroprene 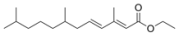	Methoprene 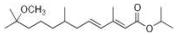	Methyl farnesoate 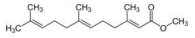
C. maenas 	Intermolt	- (p = 0.060)	**Stimulate** (p = 0.033)	**Stimulate** (p = <0.001)	- (p = 0.310)
G. lateralis 	Intermolt	**Inhibit** (p = 0.005)	**Inhibit** (p = < 0.001)	- (p = 0.712)	- (p = 0.221)
	Mid-premolt	**Inhibit** (p = 0.009)	- (p = 0.489)	- (p = 0.107)	No data

b)

48 hours	**Molt stage**	Fenoxycarb 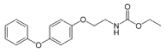	Hydroprene 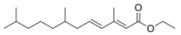	Methoprene 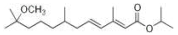	Methyl farnesoate 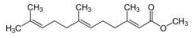
C. maenas 	Intermolt	**Inhibit** (p = 0.039)	- (p= 0.313)	**Stimulate** (p= 0.019)	- (p = 0.986)
G. lateralis 	Intermolt	**Inhibit** (p = 0.001)	**Inhibit** (p = <0.001)	- (p = 0.816)	- (p = 0.750)

Figure 2.1

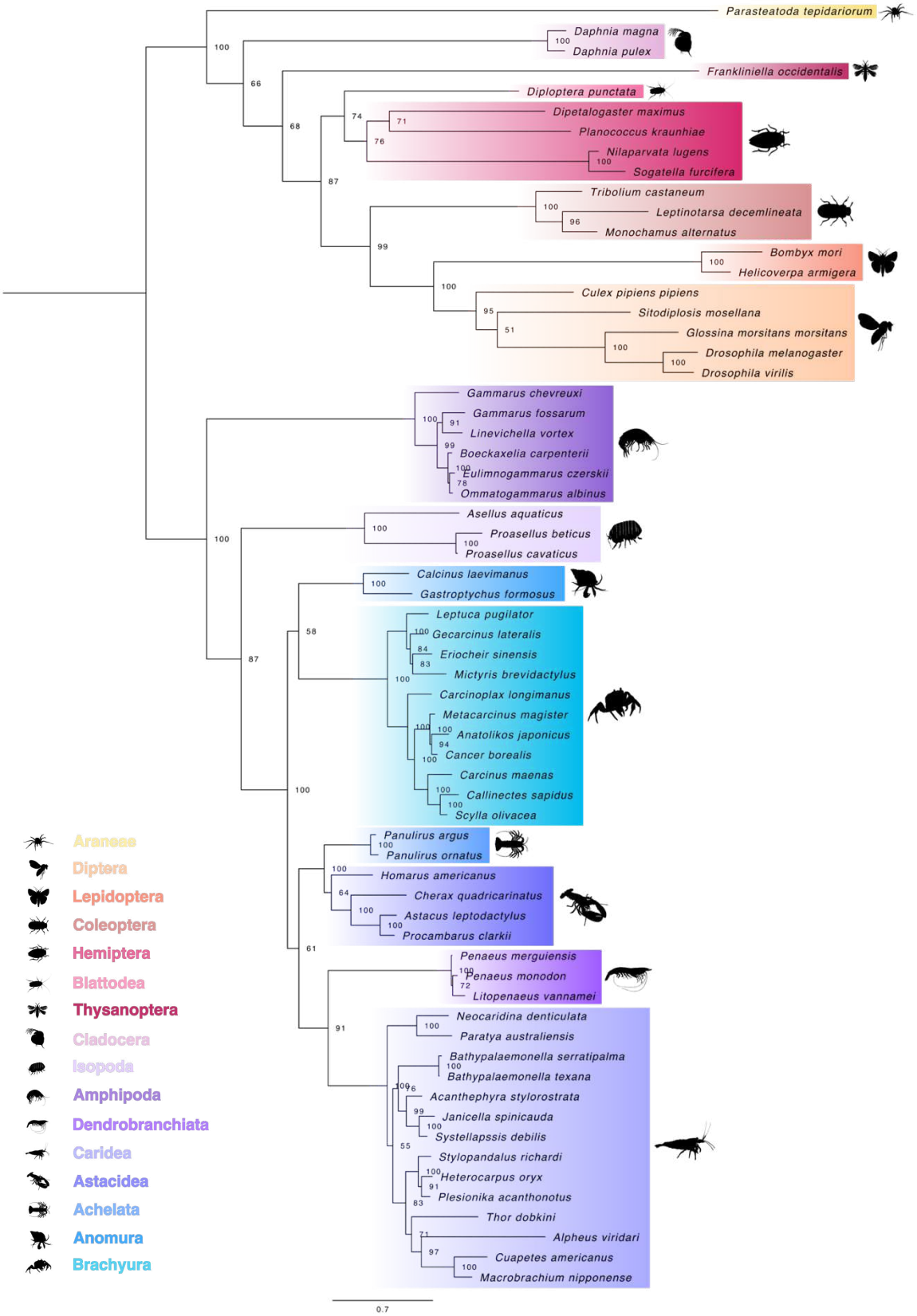
Parasteatoda tepidariorum
Daphnia magna
Daphnia pulex
Frankliniella occidentalis
Diploptera punctata
Dipetalogaster maximus
Planococcus kraunhiae
Nilaparvata lugens
Sogatella furcifera
Tribolium castaneum
Leptinotarsa decemlineata
Monochamus alternatus
Bombyx mori
Helicoverpa armigera
Culex pipiens pipiens
Sitodiplosis mosellana
Glossina morsitans morsitans
Drosophila melanogaster
Drosophila virilis
Gammarus chevreuxi
Gammarus fossarum
Linevichella vortex
Boeckaxelia carpenterii
Eulimnogammarus czerskii
Ommatogammarus albinus
Asellus aquaticus
Proasellus beticus
Proasellus cavaticus
Calcinus laevimanus
Gastroptychus formosus
Leptuca pugilator
Gecarcinus lateralis
Eriocheir sinensis
Mictyris brevidactylus
Carcinoplax longimanus
Metacarcinus magister
Anatolikos japonicus
Cancer borealis
Carcinus maenas
Callinectes sapidus
Scylla olivacea
Panulirus argus
Panulirus ornatus
Homarus americanus
Cherax quadricarinatus
Astacus leptodactylus
Procambarus clarkii
Penaeus merguiensis
Penaeus monodon
Litopenaeus vannamei
Neocaridina denticulata
Paratya australiensis
Bathypalaemonella serratipalma
Bathypalaemonella texana
Acanthephyra stylorostrata
Janicella spinicauda
Systellapssis debilis
Stylopandalus richardi
Heterocarpus oryx
Plesionika acanthonotus
Thor dobkini
Alpheus viridari
Cuapetes americanus
Macrobrachium nipponense
0.7
Araneae
Diptera
Lepidoptera
Coleoptera
Hemiptera
Blattodea
Thysanoptera
Cladocera
Isopoda
Amphipoda
Dendrobranchiata
Caridea
Astacidea
Achelata
Anomura
Brachyura

Figure 2.1. Phylogeny of arthropod Methoprene-tolerant (Met) proteins. The trimmed maximum likelihood phylogenetic tree was constructed with IQ-TREE using the Bayesian information criterion (BIC) best-fit model JTT+F+R5. The relationship confidence values at each branch point were determined with ultrafast bootstrap analysis (UFBoot = 1000). The scale bar for the branch lengths represents the estimated average of substitutions per site as visualized in FigTree. Sequences and databases used in the analysis can be found in the supplementary data spreadsheet on the online repository. Species silhouettes were obtained from PhyloPic (http://phylopic.org).

Figure 2.2. Domain organization of decapod Methoprene-tolerant (Met) proteins. Domains were identified with the NCBI CD search tool and visualized with IBS 2.0 (see Materials and Methods). Dashed configurations indicated partial sequences. The N-terminal region contained the basic helix-loop-helix (bHLH) DNA-binding domain, followed by the PAS-A and PAS-B domains. Information for the sequences is provided in the supplementary data spreadsheet on the online repository. Species silhouettes were obtained from PhyloPic (http://phylopic.org).

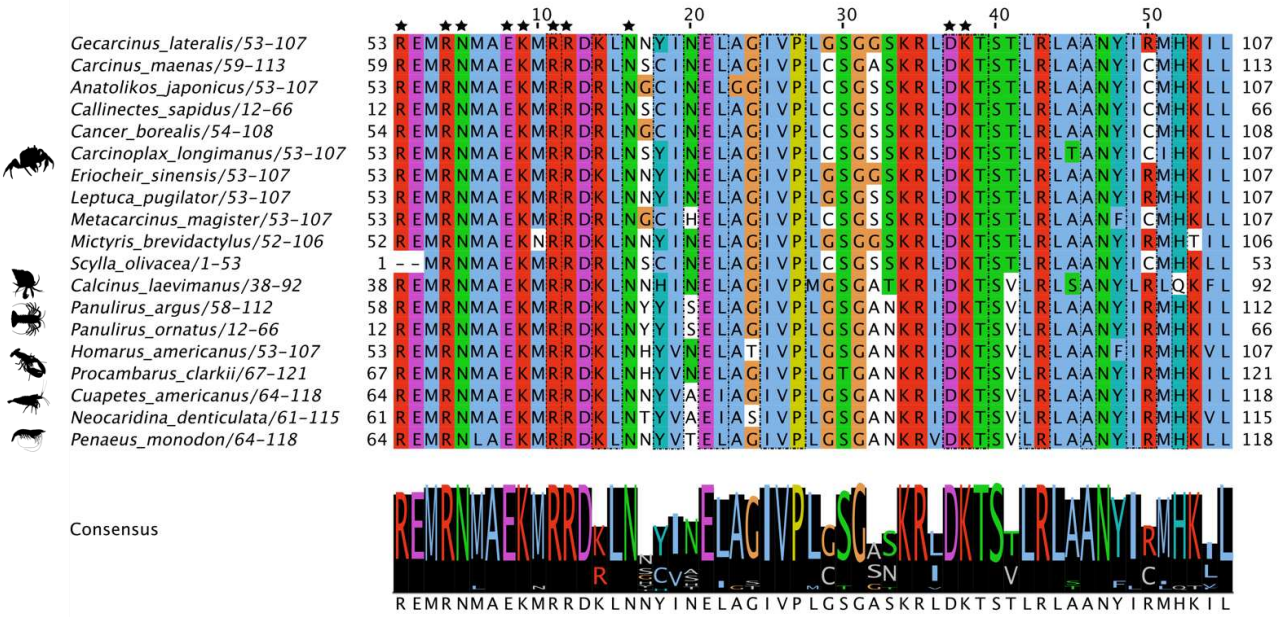

Figure 2.3. Multiple sequence alignment of the decapod Met basic helix-loop-helix (bHLH) domain. The sequences were aligned using the Mafft EINSI parameters, trimmed with ClipKIT, and visualized through Jalview following default Clustal coloring (see Materials and Methods). The consensus sequence is illustrated as a logo schematic. Conserved amino acids involved with DNA binding and dimer interfaces are indicated by black stars and by dashed lines, respectively. Sequences and databases used in the analysis are in the supplementary data spreadsheet on the online repository. Species silhouettes were obtained from PhyloPic (http://phylopic.org).

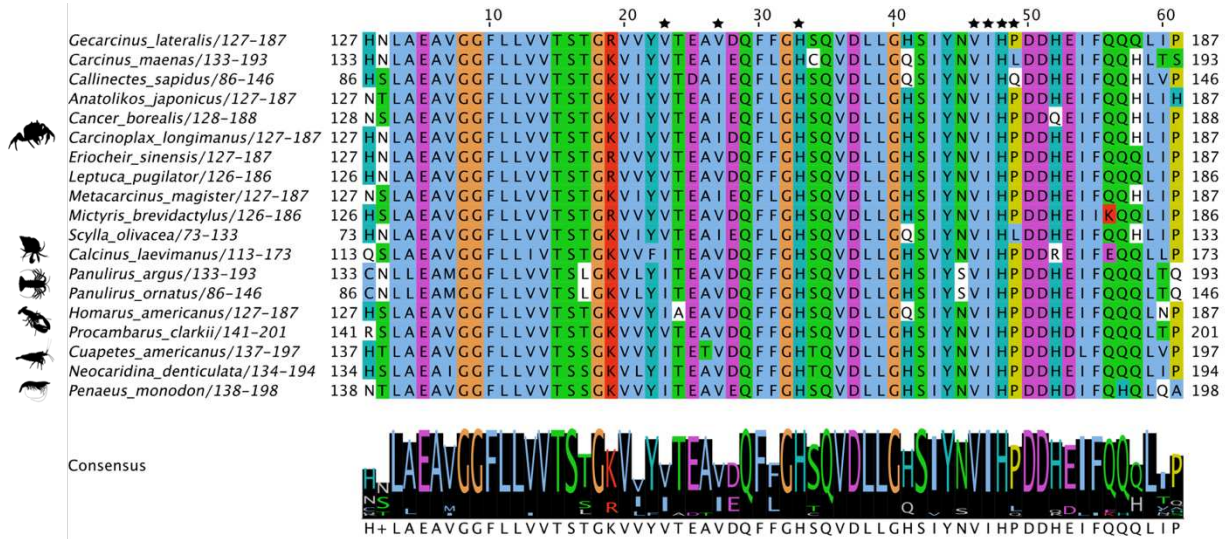

Figure 2.4. Multiple sequence alignment of the decapod Met PAS-A domain. The sequences were aligned using the Mafft EINSI parameters, trimmed with ClipKIT, and visualized through Jalview following default Clustal coloring (see Materials and Methods). The consensus sequence is illustrated as a logo schematic. Conserved amino acids as active sites are indicated by black stars. Sequences and databases used in the analysis are in the supplementary data spreadsheet on the online repository. Species silhouettes were obtained from PhyloPic (http://phylopic.org).

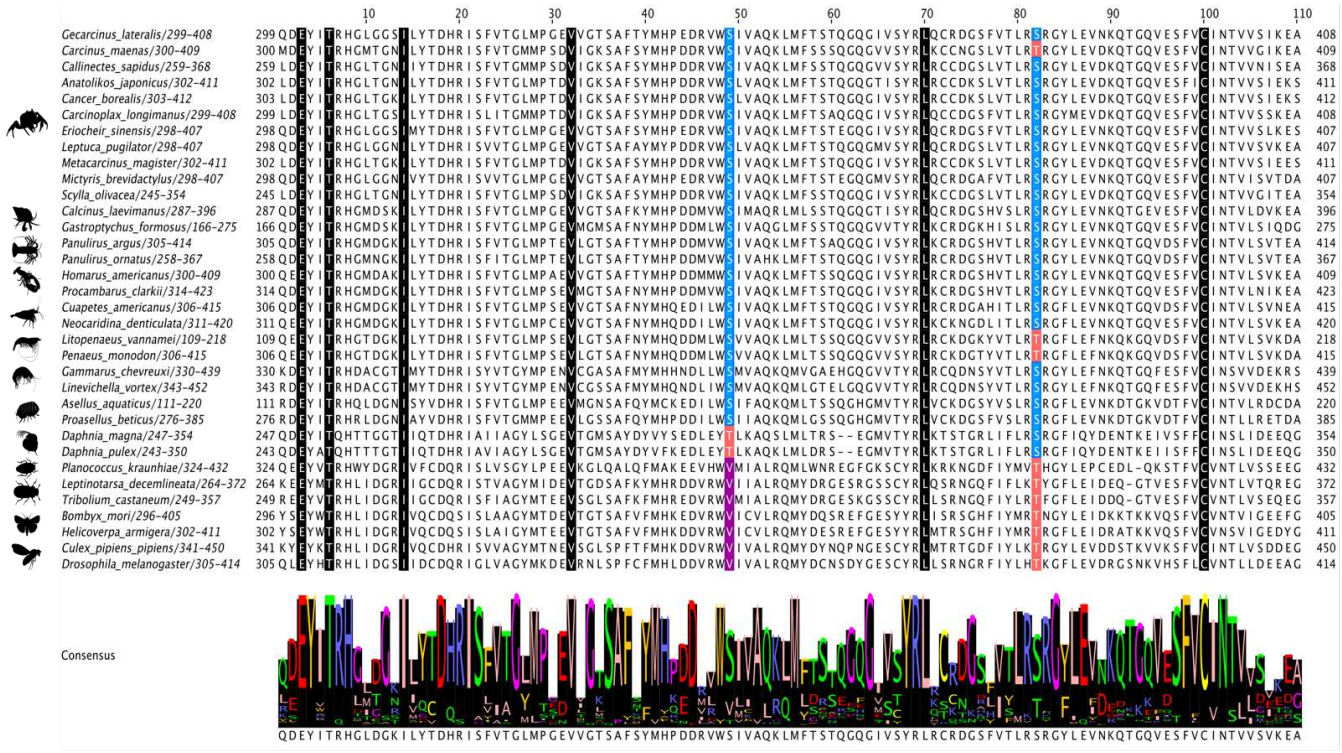

Figure 2.5. Multiple sequence alignment of the Met PAS-B domain in pancrustacean species. The sequences were aligned using the Mafft EINSI parameters, trimmed with ClipKIT, and visualized through Jalview following default Clustal coloring (see Materials and Methods). The consensus sequence is illustrated as a logo schematic.The positions of eight amino acids involved in JH binding in insects are highlighted: invariant amino acids at reference positions #3, #6, #32, #70, and #100 across all taxa are indicated by black shading; substitutions at reference positions #49 and #82 are indicated by either blue for Serine (S), peach for Threonine (T), or purple for Valine (V). Sequences and databases used in the analysis are in supplementary data spreadsheet on the online repository. Species silhouettes were obtained from PhyloPic (http://phylopic.org).

Figure 2.6

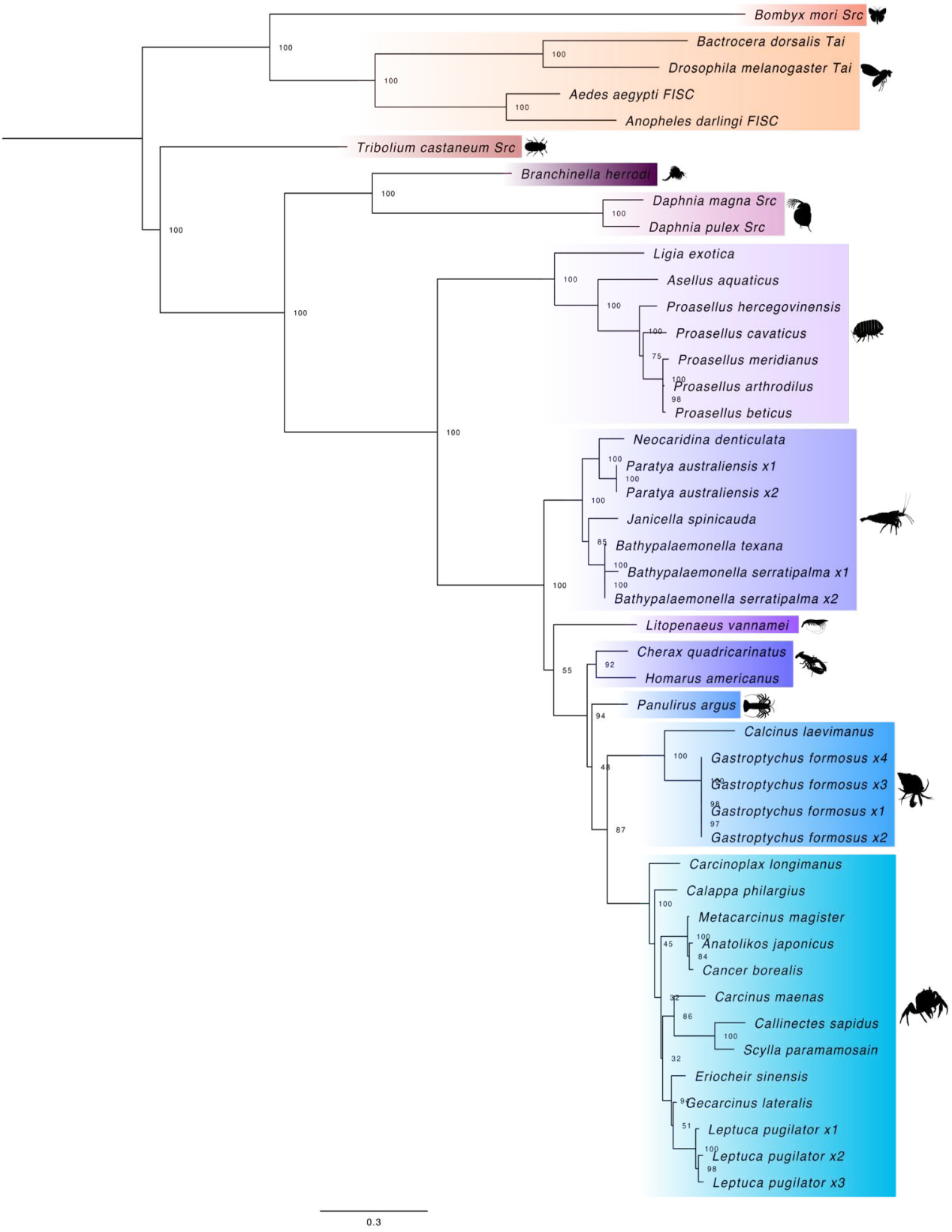
Bombyx mori Src
Bactrocera dorsalis Tai
Drosophila melanogaster Tai
Aedes aegypti FISC
Anopheles darlingi FISC
Tribolium castaneum Src
Branchinella herrodi
Daphnia magna Src
Daphnia pulex Src
Ligia exotica
Asellus aquaticus
Proasellus hercegovinensis
Proasellus cavaticus
Proasellus meridianus
Proasellus arthrodilus
Proasellus beticus
Neocaridina denticulata
Paratya australiensis x1
Paratya australiensis x2
Janicella spinicauda
Bathypalaemonella texana
Bathypalaemonella serratipalma x1
Bathypalaemonella serratipalma x2
Litopenaeus vannamei
Cherax quadricarinatus
Homarus americanus
Panulirus argus
Calcinus laevimanus
Gastroptychus formosus x4
Gastroptychus formosus x3
Gastroptychus formosus x1
Gastroptychus formosus x2
Carcinoplax longimanus
Calappa philargius
Metacarcinus magister
Anatolikos japonicus
Cancer borealis
Carcinus maenas
Callinectes sapidus
Scylla paramamosain
Eriocheir sinensis
Gecarcinus lateralis
Leptuca pugilator x1
Leptuca pugilator x2
Leptuca pugilator x3
0.3

Figure 2.6. Phylogeny of pancrustacean Steroid receptor coactivator (Src) proteins. The trimmed maximum likelihood phylogenetic tree was constructed with IQ-TREE using the Bayesian information criterion (BIC) best-fit model JTT+F+I+G4. The relationship confidence values at each branch point were determined with ultrafast bootstrap analysis (UFBoot = 1000). The scale bar for the branch lengths represents the estimated average of substitutions per site as visualized in FigTree. Sequences and databases used in the analysis are in the supplementary data spreadsheet on the online repository. Species silhouettes were obtained from PhyloPic (http://phylopic.org).

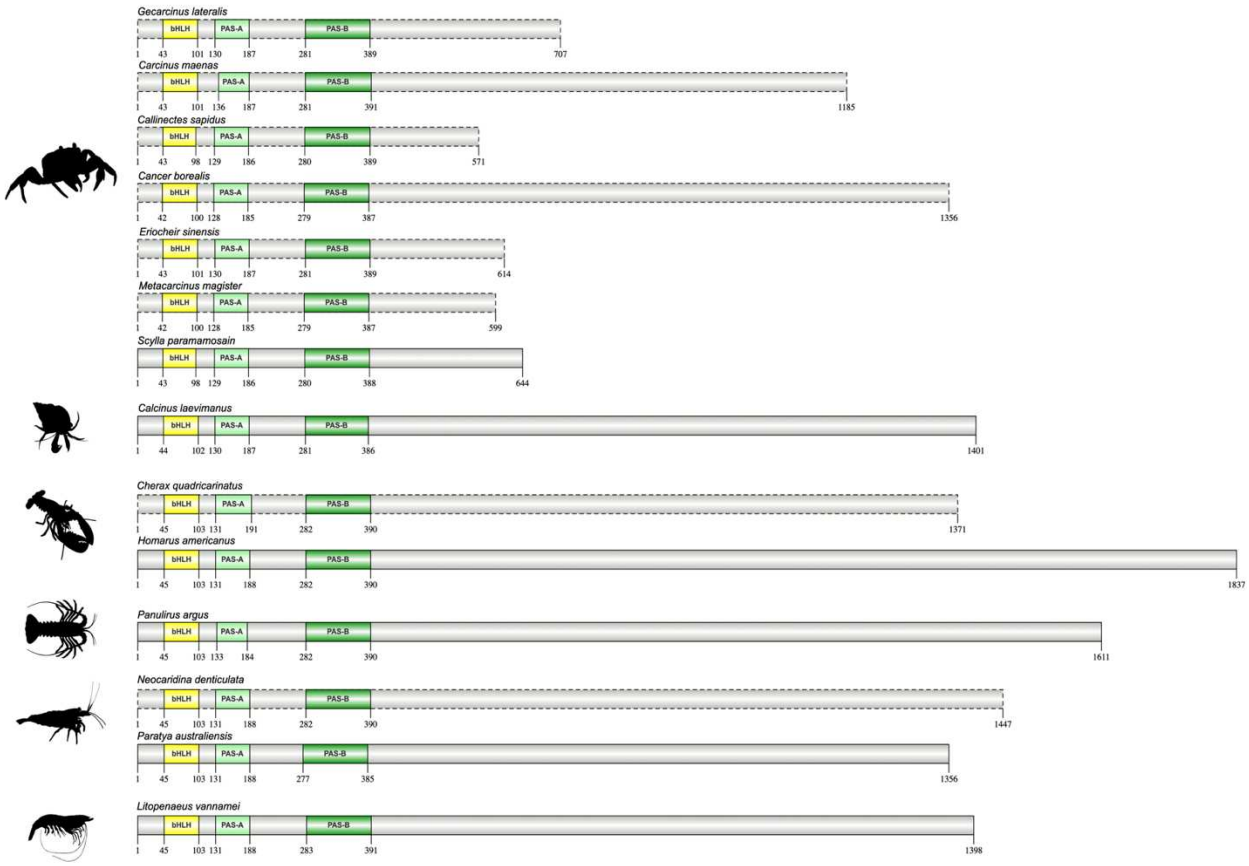

Figure 2.7. Domain organization of decapod Steroid receptor coactivator (Src) proteins. Domains were identified with the NCBI CD search tool and visualized with IBS 2.0 (see Materials and Methods). Dashed configurations indicated partial sequences. The N-terminal region contained the basic helix-loop-helix (bHLH) DNA-binding domain, followed by the PAS-A and PAS-B domains. Information for the sequences is provided in the supplementary data spreadsheet on the online repository. Species silhouettes were obtained from PhyloPic (http://phylopic.org).

Figure 2.8

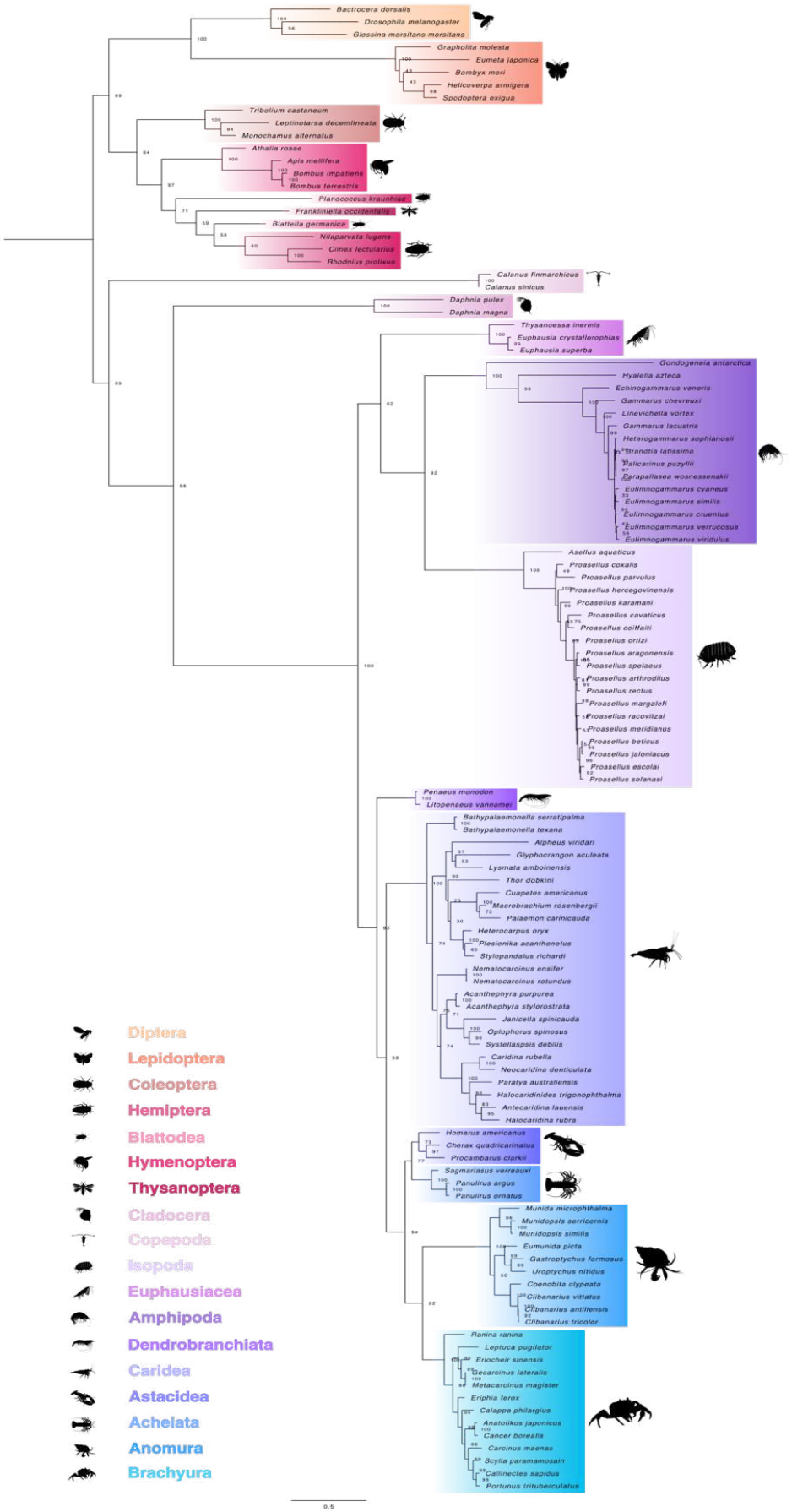
Bactrocera dorsalis
Drosophila melanogaster
Glossina morsitans morsitans
Grapholita molesta
Eumeta japonica
Bombyx mori
Helicoverpa armigera
Spodoptera exigua
Tribolium castaneum
Leptinotarsa decemlineata
Monochamus alternatus
Athalia rosae
Apis mellifera
Bombus impatiens
Bombus terrestris
Planococcus kraunhiae
Frankliniella occidentalis
Blattella germanica
Nilaparvata lugens
Cimex lectularius
Rhodnius prolixus
Calanus finmarchicus
Calanus sinicus
Daphnia pulex
Daphnia magna
Thysanoessa inermis
Euphausia crystallorophias
Euphausia superba
Gondogeneia antarctica
Hyalella azteca
Echinogammarus veneris
Gammarus chevreuxi
Linevichella vortex
Gammarus lacustris
Heterogammarus sophianosii
Brandtia latissima
Palicarinus puzyllii
Carapallasea wosnessenskii
Eulimnogammarus cyaneus
Eulimnogammarus similis
Eulimnogammarus cruentus
Eulimnogammarus verrucosus
Eulimnogammarus viridulus
Asellus aquaticus
Proasellus coxalis
Proasellus parvulus
Proasellus hercegovinensis
Proasellus karamani
Proasellus cavaticus
Proasellus coiffaiti
Proasellus ortizi
Proasellus aragonensis
Proasellus spelaeus
Proasellus arthrodilus
Proasellus rectus
Proasellus margalefi
Proasellus racovitzai
Proasellus meridianus
Proasellus beticus
Proasellus jaloniacus
Proasellus escolai
Proasellus solanasi
Penaeus monodon
Litopenaeus vannamei
Bathypalaemonella serratipalma
Bathypalaemonella texana
Alpheus viridari
Glyphocrangon aculeata
Lysmata amboinensis
Thor dobkini
Cuapetes americanus
Macrobrachium rosenbergii
Palaemon carinicauda
Heterocarpus oryx
Plesionika acanthonotus
Stylopandalus richardi
Nematocarcinus ensifer
Nematocarcinus rotundus
Acanthephyra purpurea
Acanthephyra stylorostrata
Janicella spinicauda
Oplophorus spinosus
Systellaspsis debilis
Caridina rubella
Neocaridina denticulata
Paratya australiensis
Halocaridinides trigonophthalma
Antecaridina lauensis
Halocaridina rubra
Homarus americanus
Cherax quadricarinatus
Procambarus clarkii
Sagmariasus verreauxi
Panulirus argus
Panulirus ornatus
Munida microphthalma
Munidopsis serricornis
Munidopsis similis
Eumunida picta
Gastroptychus formosus
Uroptychus nitidus
Coenobita clypeata
Clibanarius vittatus
Clibanarius antillensis
Clibanarius tricolor
Ranina ranina
Leptuca pugilator
Eriocheir sinensis
Decarcinus lateralis
Metacarcinus magister
Eriphia ferox
Calappa philargius
Anatolikos japonicus
Cancer borealis
Carcinus maenas
Scylla paramamosain
Callinectes sapidus
Portunus trituberculatus
0.5
Diptera
Lepidoptera
Coleoptera
Hemiptera
Blattodea
Hymenoptera
Thysanoptera
Cladocera
Copepoda
Isopoda
Euphausiacea
Amphipoda
Dendrobranchiata
Caridea
Astacidea
Achelata
Anomura
Brachyura

Figure 2.8. Phylogeny of pancrustacean Krüppel homolog 1 (Kr-h1) proteins. The trimmed maximum likelihood phylogenetic tree was constructed with IQ-TREE using the Bayesian information criterion (BIC) best-fit model JTT+I+I+R5. The relationship confidence values at each branch point were determined with ultrafast bootstrap analysis (UFBoot = 1000). The scale bar for the branch lengths represents the estimated average of substitutions per site as visualized in FigTree. Sequences and databases used in the analysis are presented in the supplementary data spreadsheet on the online repository. Species silhouettes were obtained from PhyloPic (http://phylopic.org).

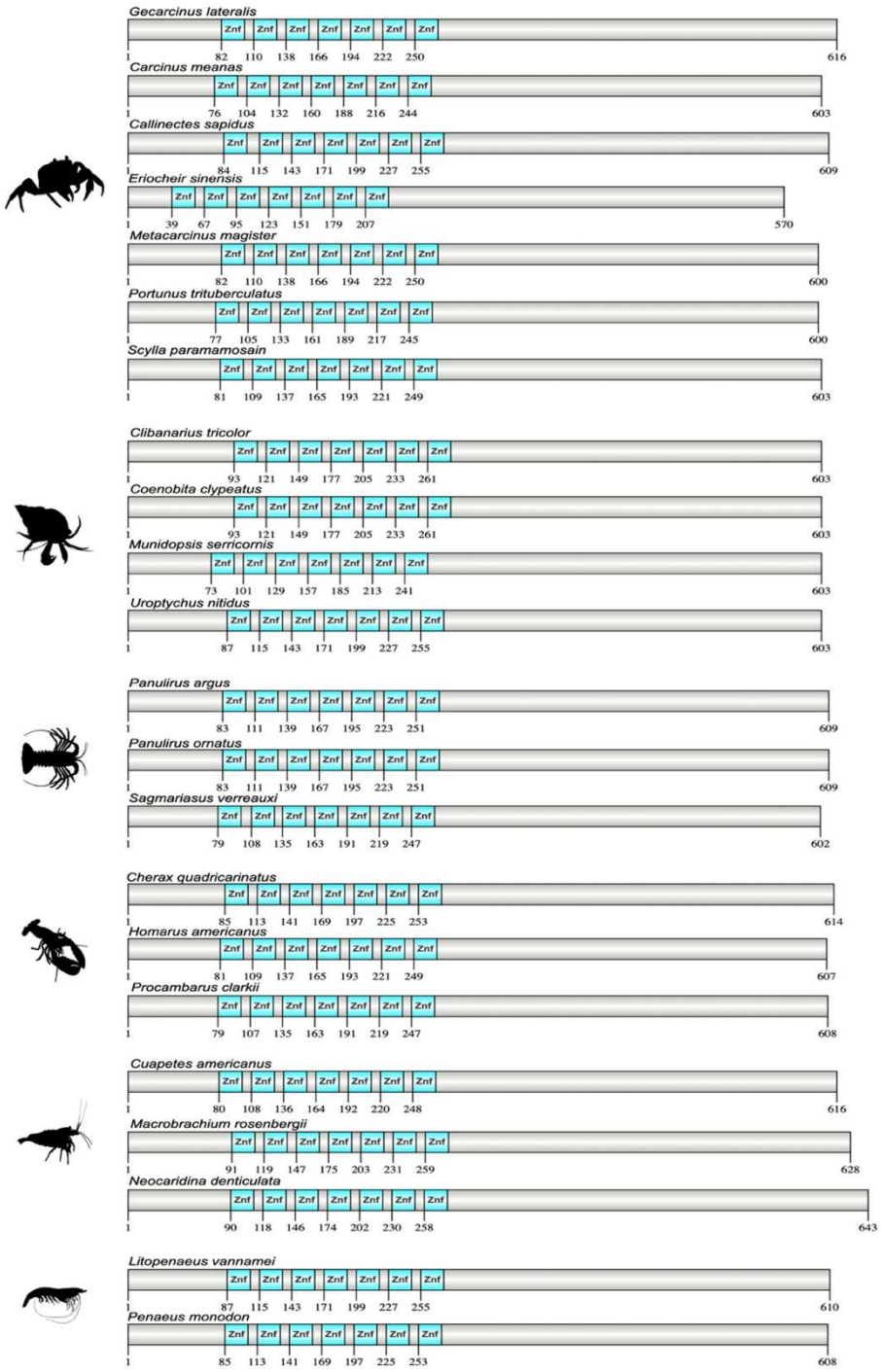

Figure 2.9. Domain organization of decapod Krüppel homolog 1 (Kr-h1) proteins. Domains were identified with the NCBI CD search tool and visualized with IBS 2.0 (see Materials and Methods). Dashed configurations indicated partial sequences. The N-terminal region contained seven zinc finger (Znf) repeats in the DNA-binding domain. Information for the sequences is presented in the supplementary data spreadsheet on the online repository. Species silhouettes were obtained from PhyloPic (http://phylopic.org).

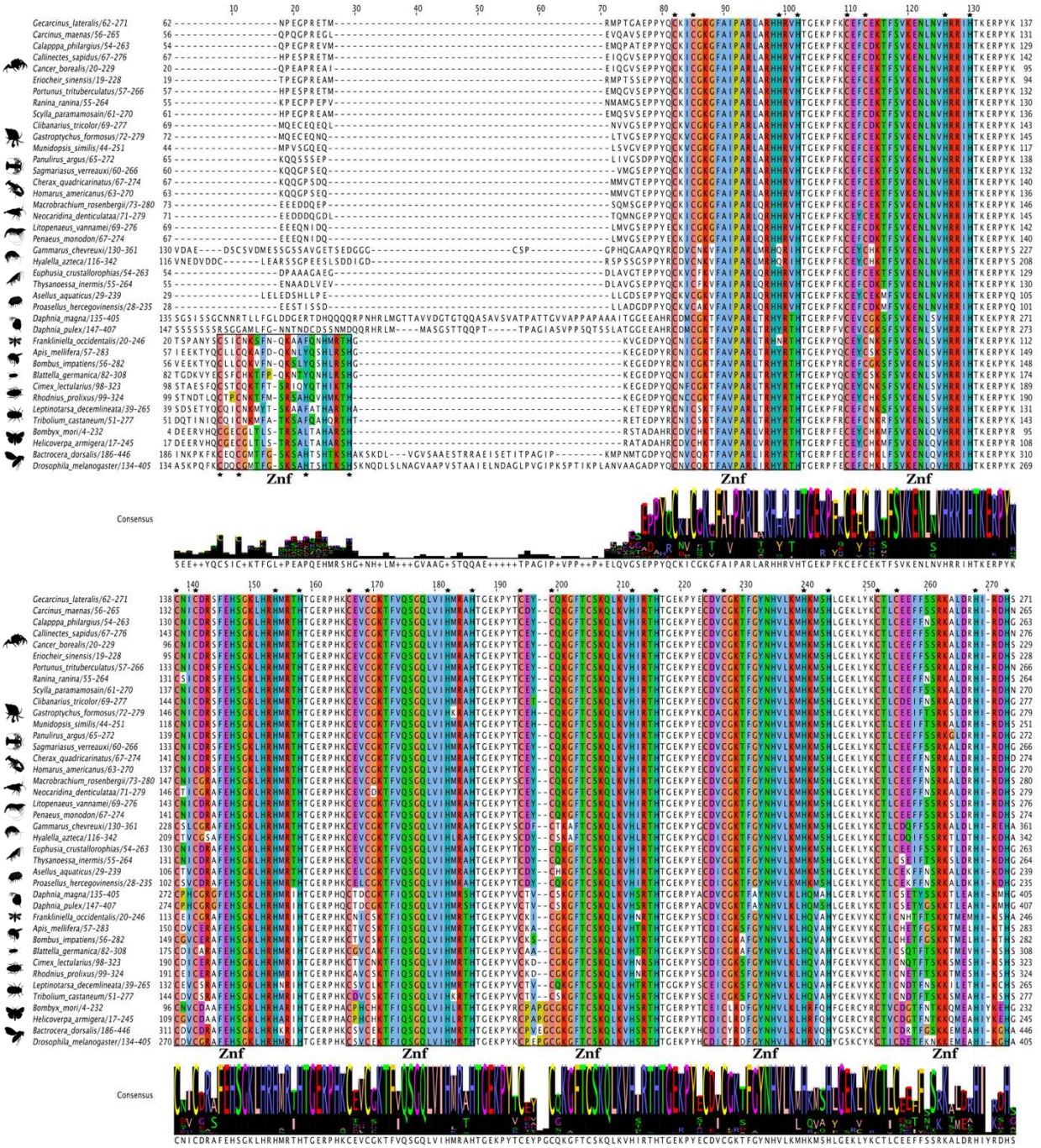

Figure 2.10. Multiple sequence alignment of Krüppel homolog 1 (Kr-h1) proteins in pancrustacean species. The sequences were aligned using the Mafft EINSI parameters, trimmed with ClipKIT, and visualized through Jalview (see Materials and Methods). The consensus sequence is illustrated as a logo schematic. The C2H2 zinc fingers are annotated following default Clustal coloring with the two Cys and His residues indicated by black stars. Sequences and databases used in the analysis are presented in the supplementary data spreadsheet on the online repository. Species silhouettes were obtained from PhyloPic (http://phylopic.org).

Figure 2.11

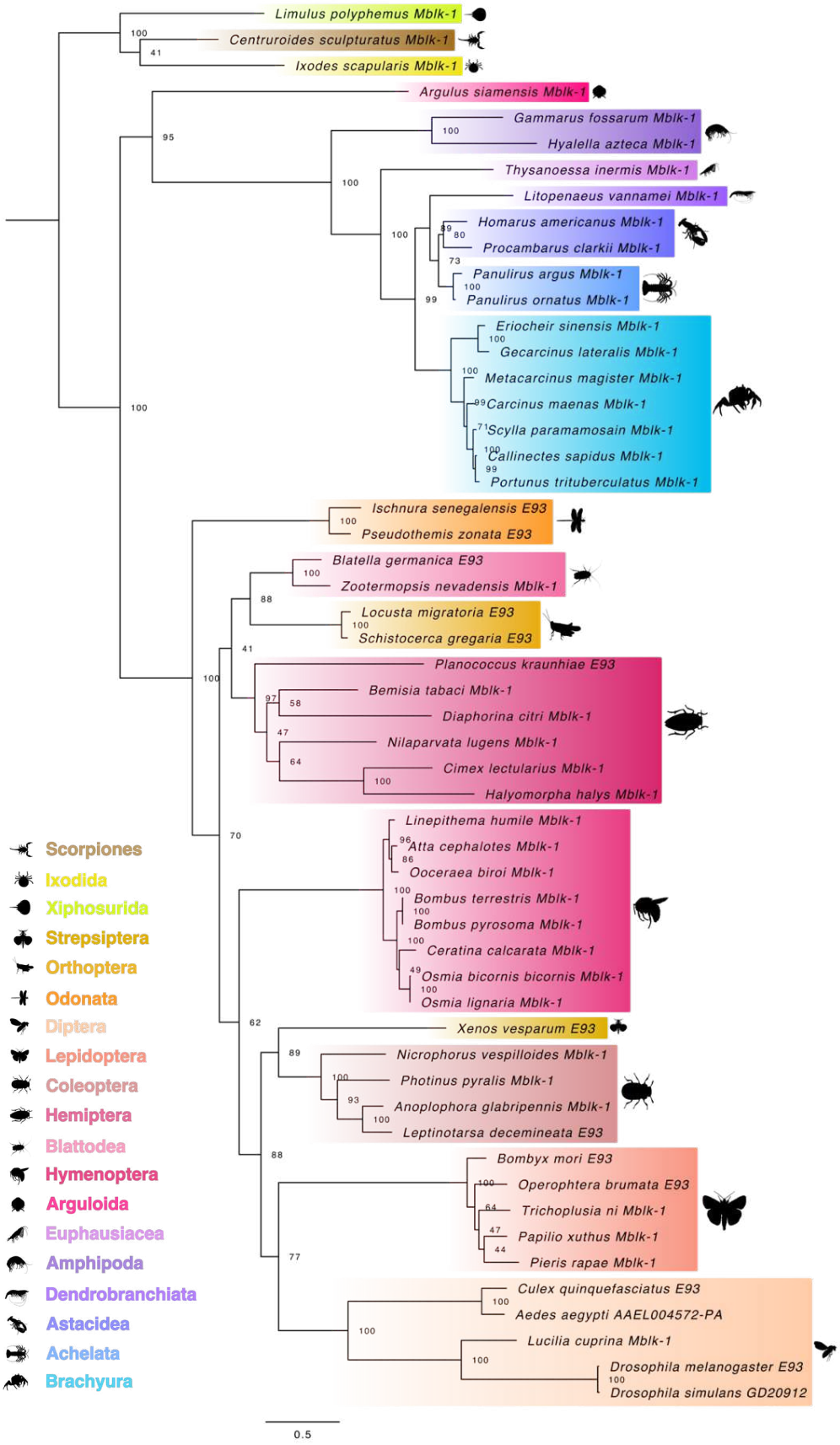
Limulus polyphemus Mblk-1
Centruroides sculpturatus Mblk-1
Ixodes scapularis Mblk-1
Argulus siamensis Mblk-1
Gammarus fossarum Mblk-1
Hyalella azteca Mblk-1
Thysanoessa inermis Mblk-1
Litopenaeus vannamei Mblk-1
Homarus americanus Mblk-1
Procambarus clarkii Mblk-1
Panulirus argus Mblk-1
Panulirus ornatus Mblk-1
Eriocheir sinensis Mblk-1
Gecarcinus lateralis Mblk-1
Metacarcinus magister Mblk-1
Carcinus maenas Mblk-1
Scylla paramamosain Mblk-1
Callinectes sapidus Mblk-1
Portunus trituberculatus Mblk-1
Ischnura senegalensis E93
Pseudothemis zonata E93
Blatella germanica E93
Zootermopsis nevadensis Mblk-1
Locusta migratoria E93
Schistocerca gregaria E93
Planococcus kraunhiae E93
Bemisia tabaci Mblk-1
Diaphorina citri Mblk-1
Nilaparvata lugens Mblk-1
Cimex lectularius Mblk-1
Halyomorpha halys Mblk-1
Linepithema humile Mblk-1
Atta cephalotes Mblk-1
Ooceraea biroi Mblk-1
Bombus terrestris Mblk-1
Bombus pyrosoma Mblk-1
Ceratina calcarata Mblk-1
Osmia bicornis bicornis Mblk-1
Osmia lignaria Mblk-1
Xenos vesparum E93
Nicrophorus vespilloides Mblk-1
Photinus pyralis Mblk-1
Anoplophora glabripennis Mblk-1
Leptinotarsa decemineata E93
Bombyx mori E93
Operophtera brumata E93
Trichoplusia ni Mblk-1
Papilio xuthus Mblk-1
Pieris rapae Mblk-1
Culex quinquefasciatus E93
Aedes aegypti AAEL004572-PA
Lucilia cuprina Mblk-1
Drosophila melanogaster E93
Drosophila simulans GD20912
0.5
Scorpiones
Ixodida
Xiphosurida
Strepsiptera
Orthoptera
Odonata
Diptera
Lepidoptera
Coleoptera
Hemiptera
Blattodea
Hymenoptera
Arguloida
Euphausiacea
Amphipoda
Dendrobranchiata
Astacidea
Achelata
Brachyura

Figure 2.11. Phylogeny of arthropod E93 and Mushroom body large-type Kenyon cell-protein 1 (Mblk-1) proteins. The trimmed maximum likelihood phylogenetic tree was constructed with IQ-TREE using the Bayesian information criterion (BIC) best-fit model JTT+F+I+I+R4. The relationship confidence values at each branch point were determined with ultrafast bootstrap analysis (UFBoot = 1000). The scale bar for the branch lengths represents the estimated average of substitutions per site as visualized in FigTree. Sequences and databases used in the analysis are presented in the supplementary data spreadsheet on the online repository. Species silhouettes were obtained from PhyloPic (http://phylopic.org).

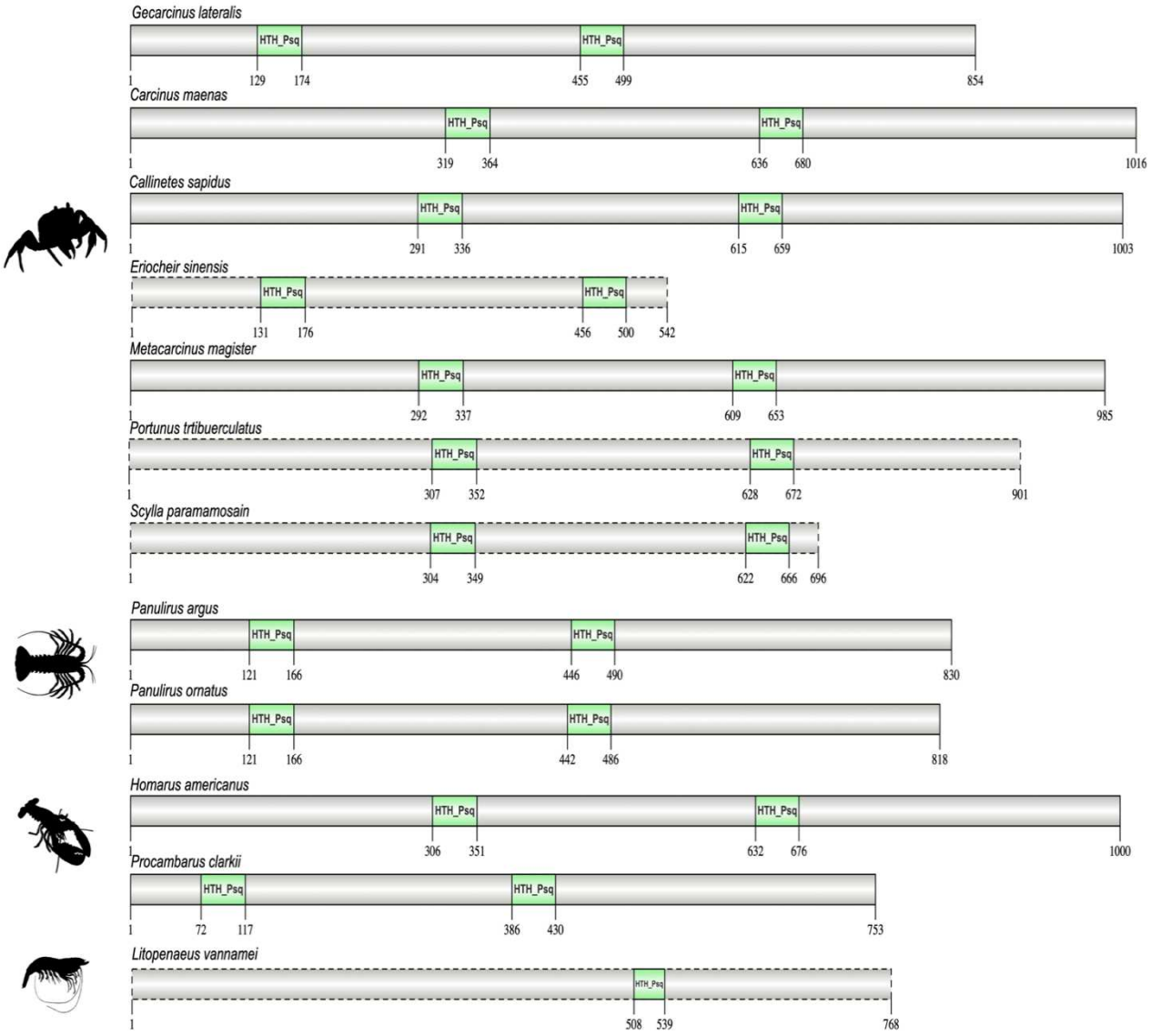

Figure 2.12. Domain organization of decapod E93 proteins. Domains were identified with the NCBI CD search tool and visualized with IBS 2.0 (see Materials and Methods). Dashed configurations indicated partial sequences. Proteins, except Lv-E93, contained two helix-turn-helix Pipsqueak (HTH_Psq) DNA-binding domains. Information for the sequences is provided in the supplementary data spreadsheet on the online repository. Species silhouettes were obtained from PhyloPic (http://phylopic.org).

Figure 2.13

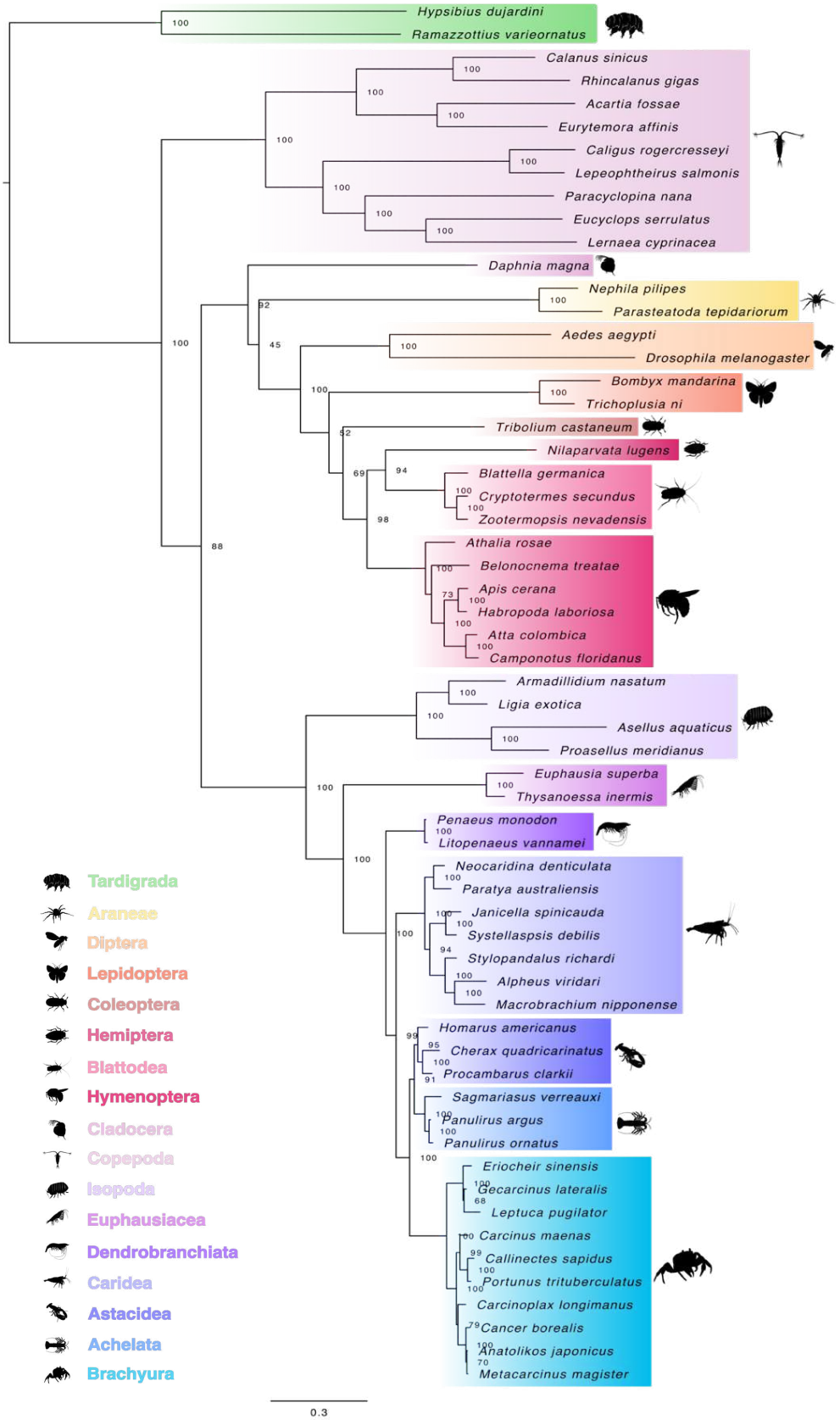
Hypsibius dujardini
Ramazzottius varieornatus
Calanus sinicus
Rhincalanus gigas
Acartia fossae
Eurytemora affinis
Caligus rogercresseyi
Lepeophtheirus salmonis
Paracyclopina nana
Eucyclops serrulatus
Lernaea cyprinacea
Daphnia magna
Nephila pilipes
Parasteatoda tepidariorum
Aedes aegypti
Drosophila melanogaster
Bombyx mandarina
Trichoplusia ni
Tribolium castaneum
Nilaparvata lugens
Blattella germanica
Cryptotermes secundus
Zootermopsis nevadensis
Athalia rosae
Belonocnema treatae
Apis cerana
Habropoda laboriosa
Atta colombica
Camponotus floridanus
Armadillidium nasatum
Ligia exotica
Asellus aquaticus
Proasellus meridianus
Euphausia superba
Thysanoessa inermis
Penaeus monodon
Litopenaeus vannamei
Neocaridina denticulata
Paratya australiensis
Janicella spinicauda
Systellaspsis debilis
Stylopandalus richardi
Alpheus viridari
Macrobrachium nipponense
Homarus americanus
Cherax quadricarinatus
Procambarus clarkii
Sagmariasus verreauxi
Panulirus argus
Panulirus ornatus
Eriocheir sinensis
Gecarcinus lateralis
Leptuca pugilator
Carcinus maenas
Callinectes sapidus
Portunus trituberculatus
Carcinoplax longimanus
Cancer borealis
Anatolikos japonicus
Metacarcinus magister
Tardigrada
Araneae
Diptera
Lepidoptera
Coleoptera
Hemiptera
Blattodea
Hymenoptera
Cladocera
Copepoda
Isopoda
Euphausiacea
Dendrobranchiata
Caridea
Astacidea
Achelata
Brachyura
0.3

Figure 2.13. Phylogeny of panarthropoda CREB-binding proteins (CBPs). The trimmed maximum likelihood phylogenetic tree was constructed with IQ-TREE using the Bayesian information criterion (BIC) best-fit model JTT+F+I+I+R5. The relationship confidence values at each branch point were determined with ultrafast bootstrap analysis (UFBoot = 1000). The scale bar for the branch lengths represents the estimated average of substitutions per site as visualized in FigTree. Sequences and databases used in the analysis are presented in the supplementary data spreadsheet on the online repository. Species silhouettes were obtained from PhyloPic (http://phylopic.org).

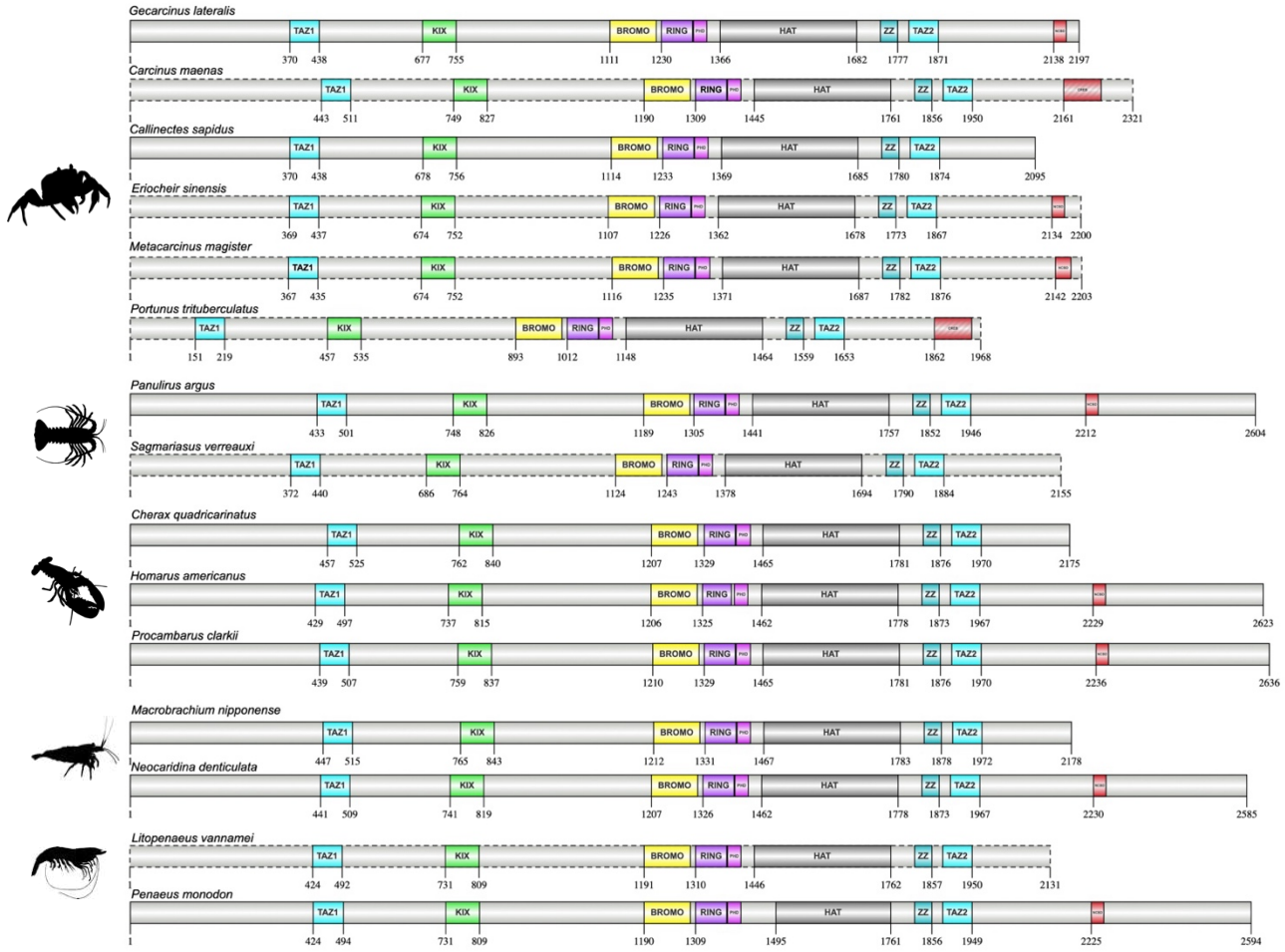

Figure 2.14. Domain organization of decapod CBPs. Domains were identified with the NCBI CD search tool and visualized with IBS 2.0 (see Materials and Methods). Dashed configurations indicated partial sequences. CBP proteins contained the Transcription Adaptor Zinc Finger (TAZ1), Kinase-inducible domain (KID) interacting domain (KIX), Bromodomain (BROMO), Really Interesting New Gene (RING), Plant Homeodomain (PHD), Histone acetyltransferase (HAT), ZZ zinc finger (ZZ), and TAZ2 domains. Coactivator binding sites were contained in the nuclear receptor coactivator binding domain (NCBD) within the CREB binding regions (CREB). Information for the sequences is provided in the supplementary data spreadsheet on the online repository. Species silhouettes were obtained from PhyloPic (http://phylopic.org).

Figure 2.15

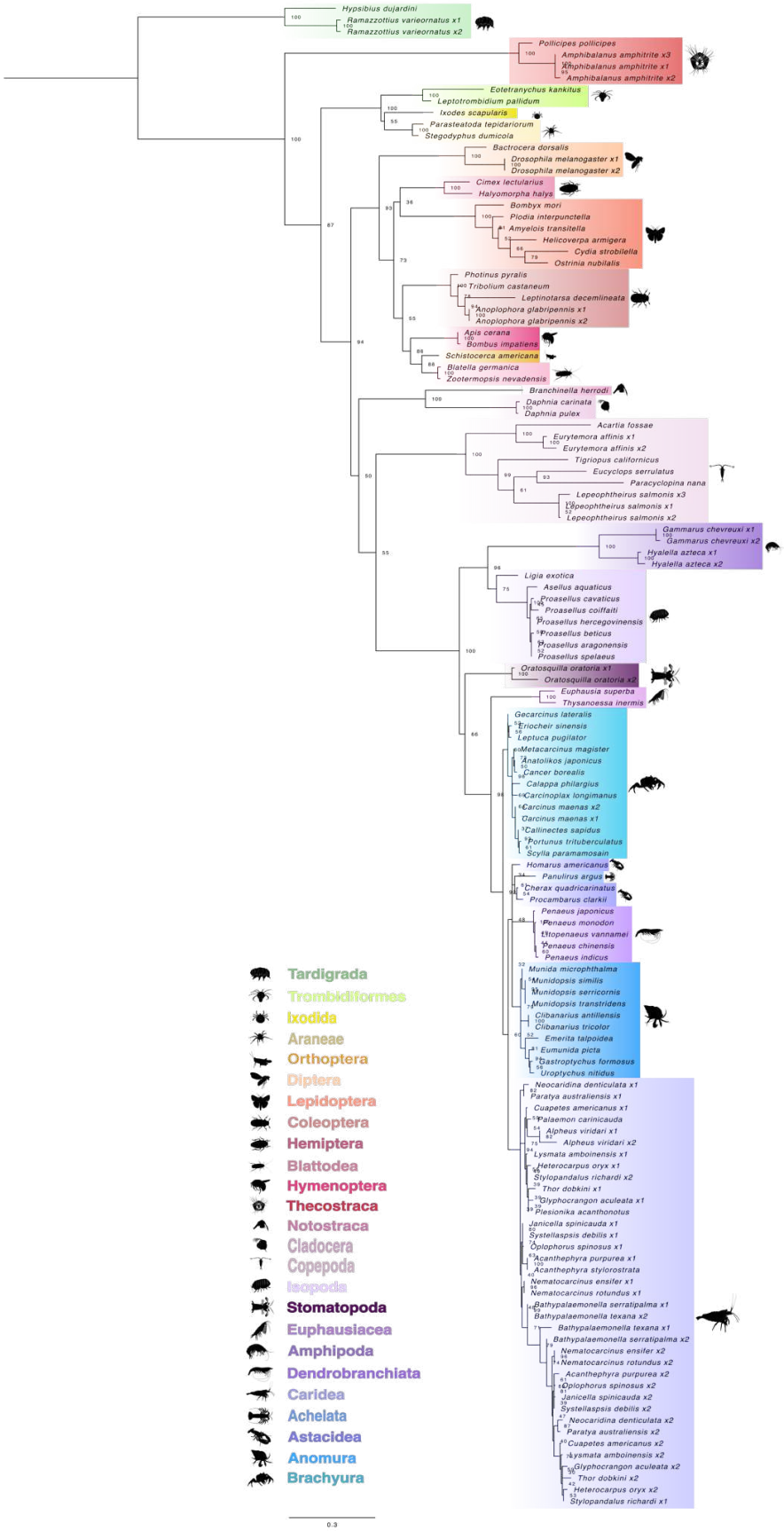
Hypsibius dujardini
Ramazzottius varieornatus x1
Ramazzottius varieornatus x2
Pollicipes pollicipes
Amphibalanus amphitrite x3
Amphibalanus amphitrite x1
Amphibalanus amphitrite x2
Eutetranychus kankitus
Leptotrombidium pallidum
Ixodes scapularis
Parasteatoda tepidariorum
Stegodyphus dumicola
Bactrocera dorsalis
Drosophila melanogaster x1
Drosophila melanogaster x2
Cimex lectularius
Halyomorpha halys
Bombyx mori
Plodia interpunctella
Amyelois transitella
Helicoverpa armigera
Cydia strobilella
Ostrinia nubilalis
Photinus pyralis
Tribolium castaneum
Leptinotarsa decemlineata
Anoplophora glabripennis x1
Anoplophora glabripennis x2
Apis cerana
Bombus impatiens
Schistocerca americana
Blatella germanica
Zootermopsis nevadensis
Branchinella herrodi
Daphnia carinata
Daphnia pulex
Acartia fossae
Eurytemora affinis x1
Eurytemora affinis x2
Tigriopus californicus
Eucyclops serrulatus
Paracyclopina nana
Lepeophtheirus salmonis x3
Lepeophtheirus salmonis x1
Lepeophtheirus salmonis x2
Gammarus chevreuxi x1
Gammarus chevreuxi x2
Hyalella azteca x1
Hyalella azteca x2
Ligia exotica
Asellus aquaticus
Proasellus cavaticus
Proasellus coiffaiti
Proasellus hercegovinensis
Proasellus beticus
Proasellus aragonensis
Proasellus spelaeus
Oratosquilla oratoria x1
Oratosquilla oratoria x2
Euphausia superba
Thysanoessa inermis
Gecarcinus lateralis
Eriocheir sinensis
Leptuca pugilator
Metacarcinus magister
Anatolikos japonicus
Cancer borealis
Calappa philargius
Carcinoplax longimanus
Carcinus maenas x2
Carcinus maenas x1
Callinectes sapidus
Portunus trituberculatus
Scylla paramamosain
Homarus americanus
Panulirus argus
Cherax quadricarinatus
Procambarus clarkii
Penaeus japonicus
Penaeus monodon
Litopenaeus vannamei
Penaeus chinensis
Penaeus indicus
Munida microphthalma
Munidopsis similis
Munidopsis serricornis
Munidopsis transtridens
Clibanarius antillensis
Clibanarius tricolor
Emerita talpoidea
Eumunida picta
Gastroptychus formosus
Uroptychus nitidus
Neocaridina denticulata x1
Paratya australiensis x1
Cuapetes americanus x1
Palaemon carinicauda
Alpheus viridari x1
Alpheus viridari x2
Lysmata amboinensis x1
Heterocarpus oryx x1
Stylopandalus richardi x2
Thor dobkini x1
Glyphocrangon aculeata x1
Plesionika acanthonotus
Janicella spinicauda x1
Systellaspsis debilis x1
Oplophorus spinosus x1
Acanthephyra purpurea x1
Acanthephyra stylorostrata
Nematocarcinus ensifer x1
Nematocarcinus rotundus x1
Bathypalaemonella serratipalma x1
Bathypalaemonella texana x2
Bathypalaemonella texana x1
Bathypalaemonella serratipalma x2
Nematocarcinus ensifer x2
Nematocarcinus rotundus x2
Acanthephyra purpurea x2
Oplophorus spinosus x2
Janicella spinicauda x2
Systellaspsis debilis x2
Neocaridina denticulata x2
Paratya australiensis x2
Cuapetes americanus x2
Lysmata amboinensis x2
Glyphocrangon aculeata x2
Thor dobkini x2
Heterocarpus oryx x2
Stylopandalus richardi x1
Tardigrada
Trombidiformes
Ixodida
Araneae
Orthoptera
Diptera
Lepidoptera
Coleoptera
Hemiptera
Blattodea
Hymenoptera
Thecostraca
Notostraca
Cladocera
Copepoda
Isopoda
Stomatopoda
Euphausiacea
Amphipoda
Dendrobranchiata
Caridea
Achelata
Astacidea
Anomura
Brachyura
0.3

Figure 2.15. Phylogeny of panarthropoda C-terminus-binding proteins (CtBPs). The trimmed maximum likelihood phylogenetic tree was constructed with IQ-TREE using the Bayesian information criterion (BIC) best-fit model Dayhoff+I+R4. The relationship confidence values at each branch point were determined with ultrafast bootstrap analysis (UFBoot = 1000). The scale bar for the branch lengths represents the estimated average of substitutions per site as visualized in FigTree. Sequences and databases used in the analysis are in the supplementary data spreadsheet on the online repository. Species silhouettes were obtained from PhyloPic (http://phylopic.org).

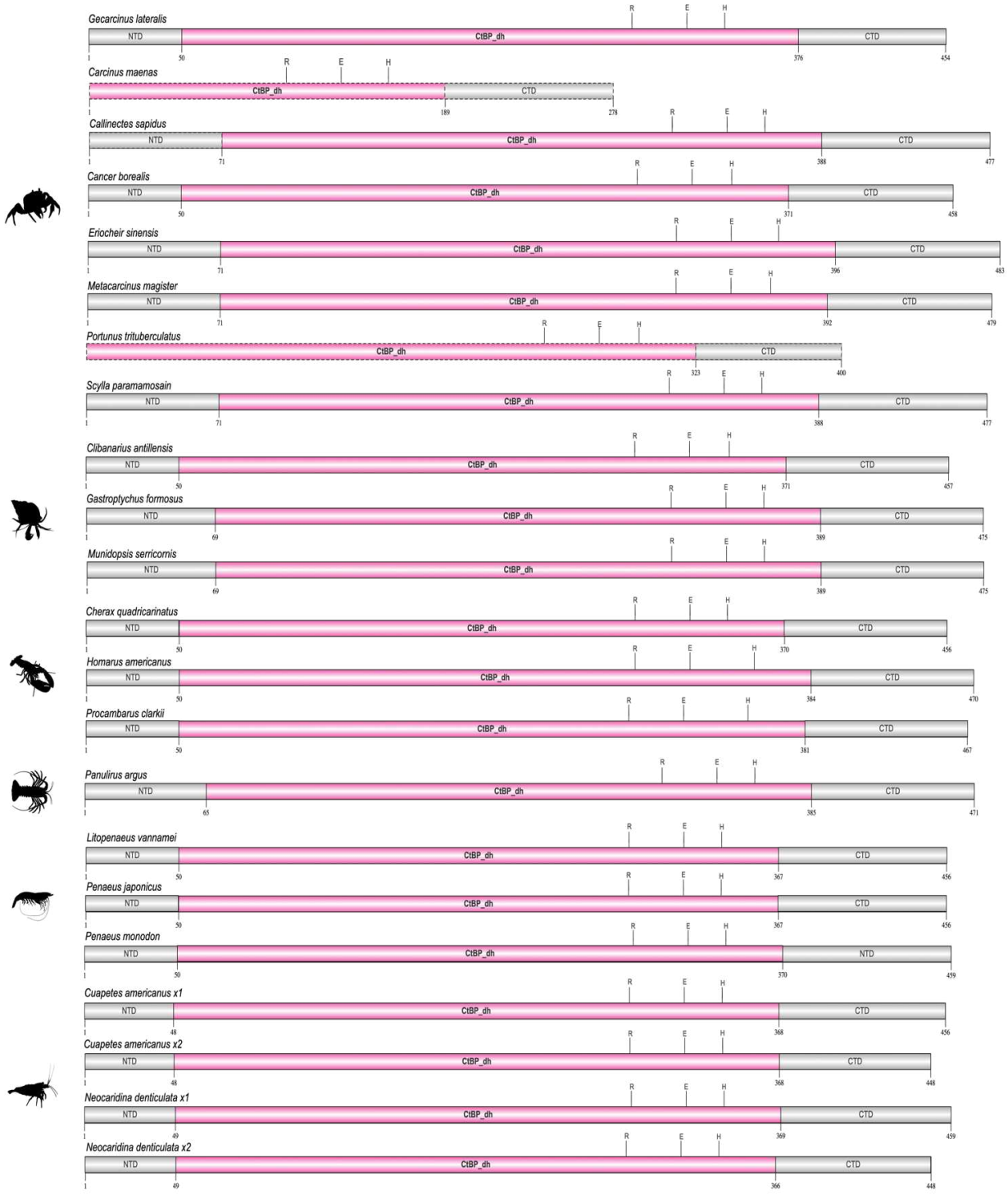

Figure 2.16. Domain organization of decapod CtBPs. Domains were identified with the NCBI CD search tool and visualized with IBS 2.0 (see Materials and Methods). Dashed configurations indicated partial sequences. The CtBP_dh, containing the R-E-H catalytic residue sites, is flanked by the N-terminal domain (NTD) and the C-terminal domain (CTD). Information for the sequences is provided in the supplementary data spreadsheet on the online repository. Species silhouettes were obtained from PhyloPic (http://phylopic.org).

Figure 2.17

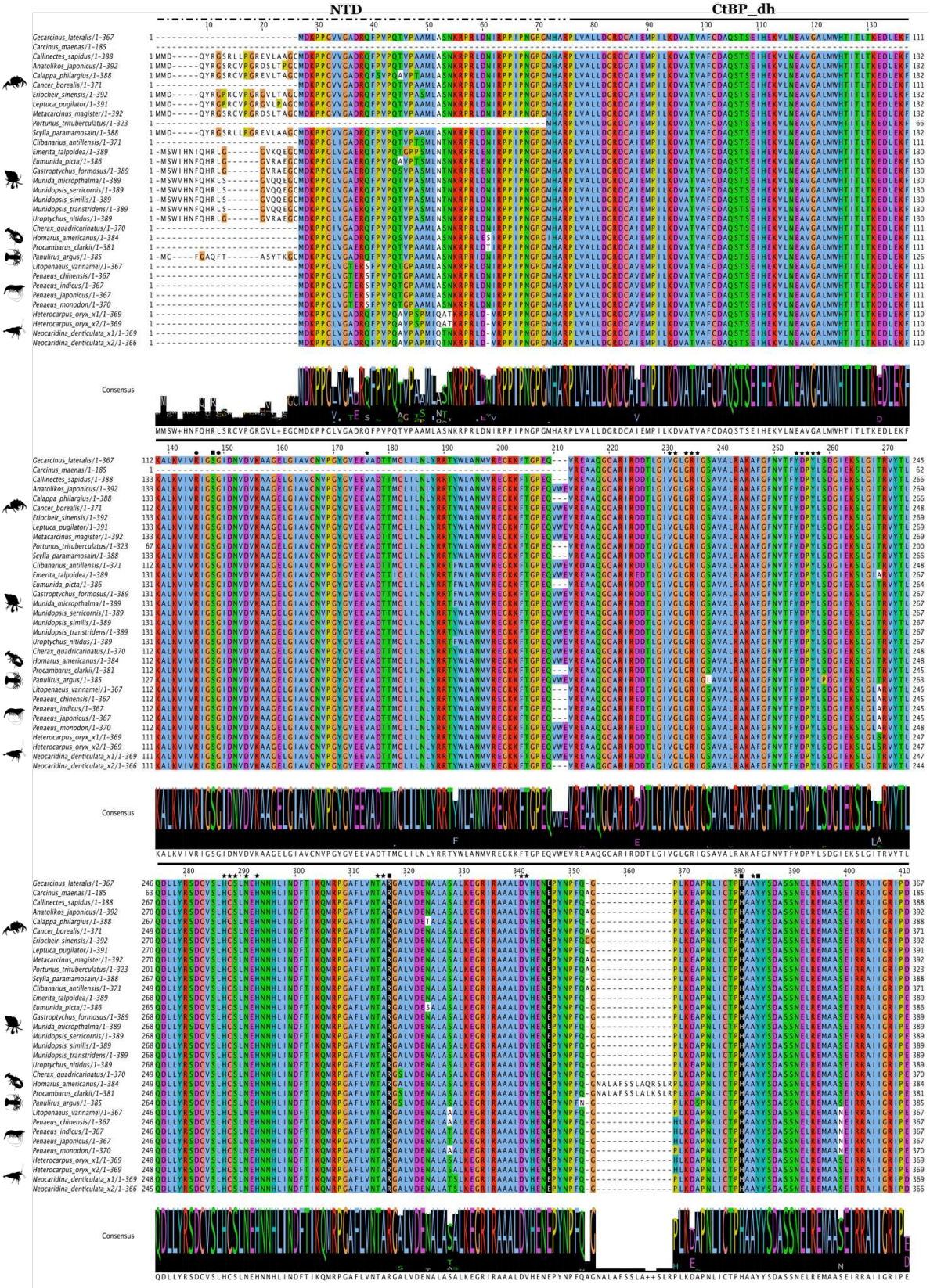

Figure 2.17. Multiple sequence alignment of decapod crustacean CtBP N-terminal region. Within this region is the N-terminal domain (NTD), indicated by the overhead dashed line, that precedes and flanks the dehydrogenase domain (CtBP_dh), shown by the overhead solid line. The sequences were aligned using the Mafft EINSI parameters, trimmed with ClipKIT, and visualized through Jalview following default Clustal coloring (see Materials and Methods). The consensus sequence is illustrated as a logo schematic. Within the CtBP_dh is the Rossmann fold along with the diagnostic catalytic triad of Arginine (R), Glutamic Acid (E), and Histidine (H) (highlighted in black). Black stars indicate conserved amino acids involved in NAD-binding while black circles indicate ligand-binding and black rectangles show NAD/ligand-binding (gray). Sequences and databases used in the analysis are in the supplementary data spreadsheet on the online repository. Species silhouettes were obtained from PhyloPic (http://phylopic.org).

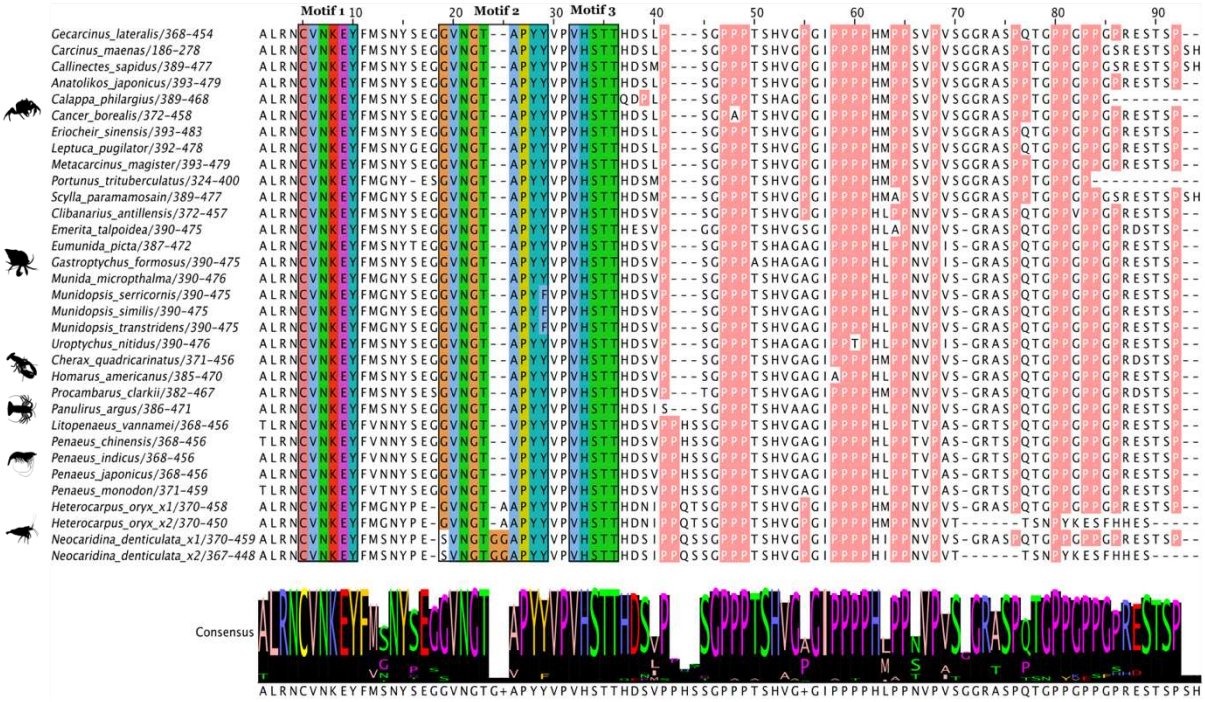

Figure 2.18. Multiple sequence alignment of the disordered C-terminal domain (CTD) of decapod crustacean CtBPs. The sequences were aligned using the Mafft EINSI parameters, trimmed with ClipKIT, and visualized through Jalview (see Materials and Methods). The consensus sequence is illustrated as a logo schematic. The CTD begins with the CVNKEY motif followed by the central block motif (GVNGTAPYY in brachyurans) and later the VHSTT motif visualized following default Clustal coloring. Subsequently following these motifs is a proline (P) rich region shown in peach. Sequences and databases used in the analysis are in the supplementary data spreadsheet on the online repository. Species silhouettes were obtained from PhyloPic (http://phylopic.org).

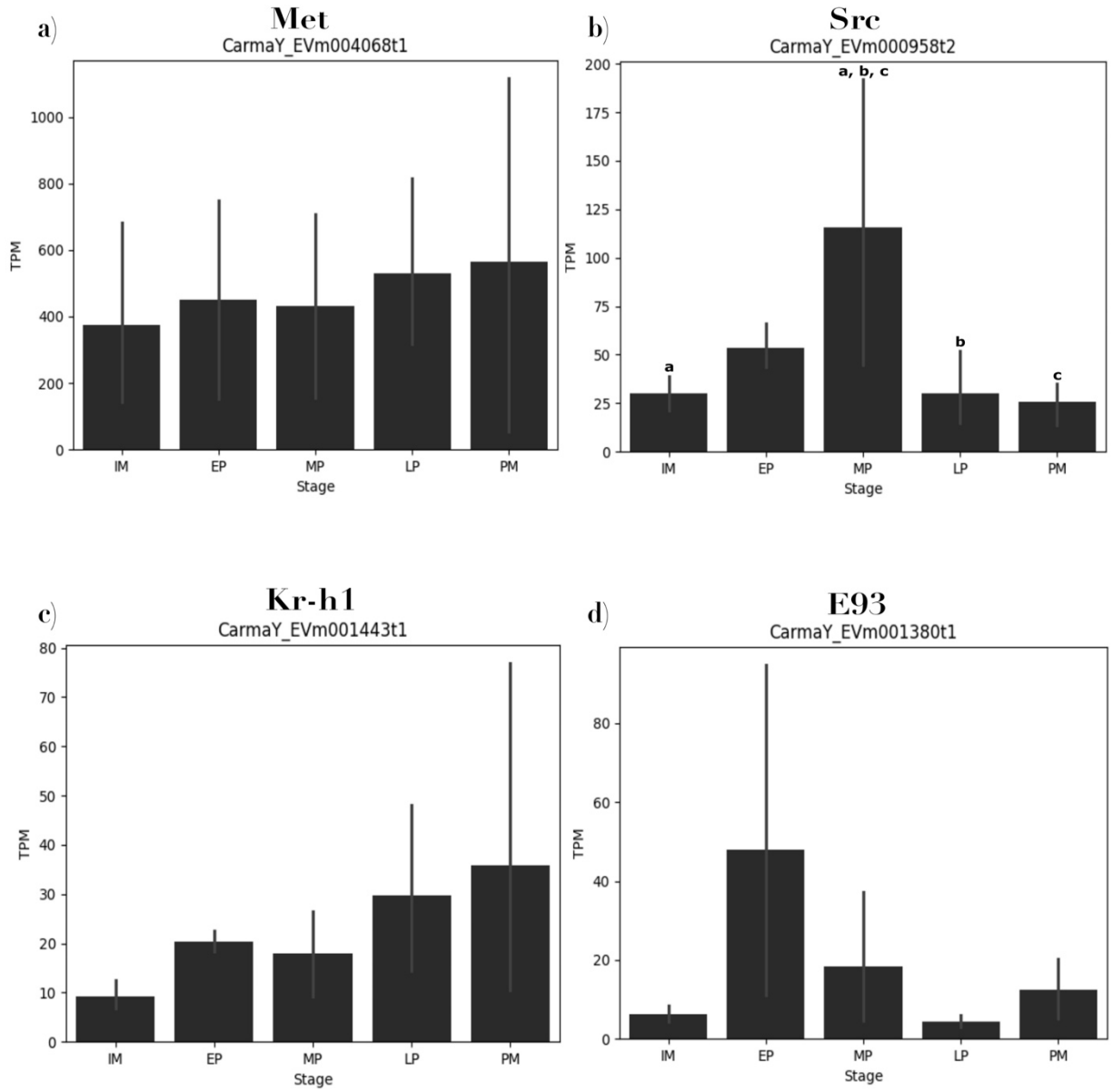

Figure 2.19. Relative gene expression of methyl farnesoate (MF) signaling genes a) *Methoprene tolerant* (*Met*), b) *Steroid receptor coactivator* (*Src*), c) *Krüppel homolog 1* (*Kr-h1*), and d) *Ecdysone response gene 93* (*E93*) in *Carcinus maenas* Y-organs (YO) across the different stages of the molt cycle (abbreviations: IM–intermolt, EP– early premolt, MP– mid premolt, LP– late premolt, and PM– postmolt). Transcript levels are expressed as mean transcripts per million reads (TPM) ± standard error of the mean (SEM); statistical differences were analyzed with Analysis of Variance (ANOVA) and post-hoc Tukey's HSD test ($p < 0.05$) with letters indicating significance. *Cm-Src* expression (b) was significantly higher in MP and significantly lower in intermolt IM, LP, and PM; IM–MP: $p = 0.0471$; LP–MP: $p = 0.047$; MP–PM: $p = 0.0346$. RNA-seq data was obtained from Oliphant et al. (2018) (n = 5 biological replicates of paired YOs) and was quantified with Salmon (v.1.7.0) using the *C. maenas* YO transcriptome assembly included in CrusTome (v.0.1.0) (Pérez-Moreno et al., 2023).

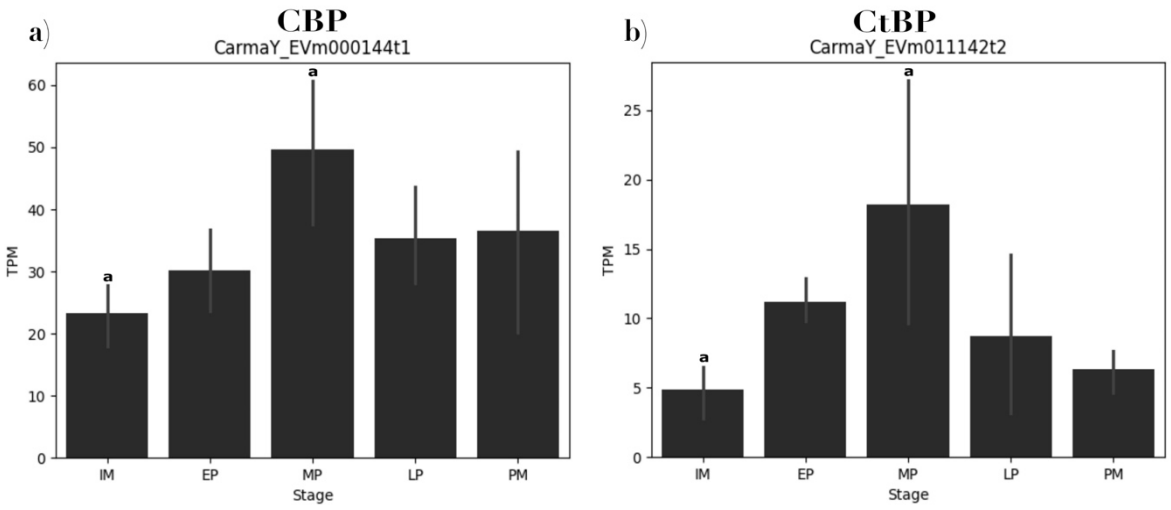

Figure 2.20. Relative gene expression of transcriptional comediators a) *CREB-binding protein* (*CBP*) and b) *C-terminal–binding protein* (*CtBP*) in *Carcinus maenas* Y-organs (YO) across the different stages of the molt cycle (abbreviations: IM–intermolt, EP– early premolt, MP– mid premolt, LP– late premolt, and PM– postmolt). Transcript levels are expressed as mean transcripts per million reads (TPM) ± standard error of the mean (SEM); statistical differences were analyzed with Analysis of Variance (ANOVA) and post-hoc Tukey's HSD test ($p < 0.05$) with letters indicating significance. The mean expression of *Cm-CBP* and *Cm-CtBP* at MP was significantly higher than that at IM; a) *Cm–CBP* IM–MP: $p = 0.022$; b) *Cm–CtBP* IM–MP: $p = 0.035$. RNA-seq data was obtained from Oliphant et al. (2018) (n = 5 biological replicates of paired YOs) and was quantified with Salmon (v.1.7.0) using the *C. maenas* YO transcriptome assembly included in CrusTome (v.0.1.0) (Pérez-Moreno et al., 2023).

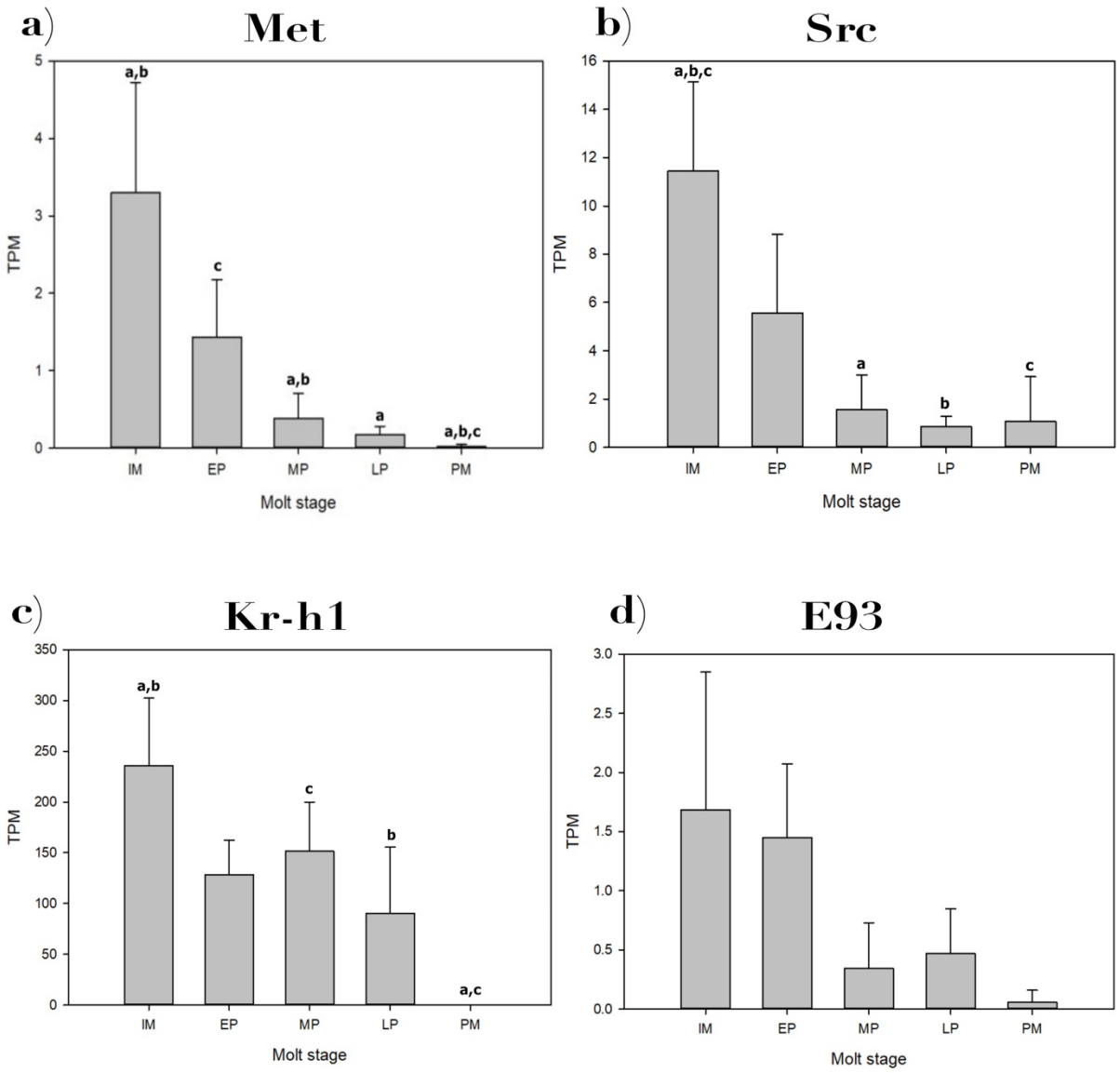

Figure 2.21. Relative gene expression of methyl farnesoate (MF) signaling genes a) *Methoprene tolerant* (*Met*), b) *Steroid receptor coactivator* (*Src*), c) *Krüppel homolog 1* (*Kr-h1*), and d) *E93* in *Gecarcinus lateralis* Y-organs (YO) across the different stages of the molt cycle (abbreviations: IM–intermolt, EP– early premolt, MP– mid premolt, LP– late premolt, and PM–postmolt). Transcript levels are expressed as mean transcripts per million reads (TPM) ± standard error of the mean (SEM); statistical differences were analyzed with Analysis of Variance (ANOVA) and post-hoc Tukey's HSD test ($p < 0.05$) with letters indicating significance. RNA-seq data was obtained from (Das et al., 2018) ($n = 3$ pooled replicates of 3 animals) and was quantified with Salmon (v.1.7.0).

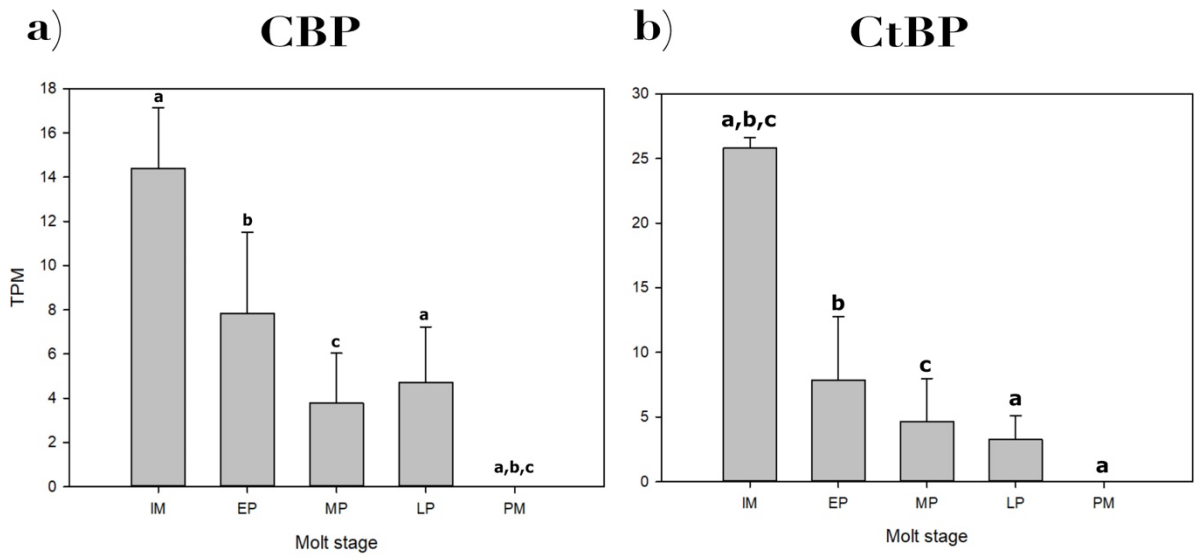

Figure 2.22. Relative gene expression of transcriptional comediators a) *CREB-binding protein* (*CBP*) and b) *C-terminal–binding protein* (*CtBP*) in *Gecarcinus lateralis* Y-organs (YO) across the different stages of the molt cycle (abbreviations: IM–intermolt, EP– early premolt, MP– mid premolt, LP– late premolt, and PM– postmolt). Transcript levels are expressed as mean transcripts per million reads (TPM) ± standard error of the mean (SEM); statistical differences were analyzed with Analysis of Variance (ANOVA) and post-hoc Tukey's HSD test ($p < 0.05$) with letters indicating significance. RNA-seq data was obtained from Das et al. (2018) (n = 3 pooled replicates of 3 animals) and was quantified with Salmon (v.1.7.0).

Figure 2.23

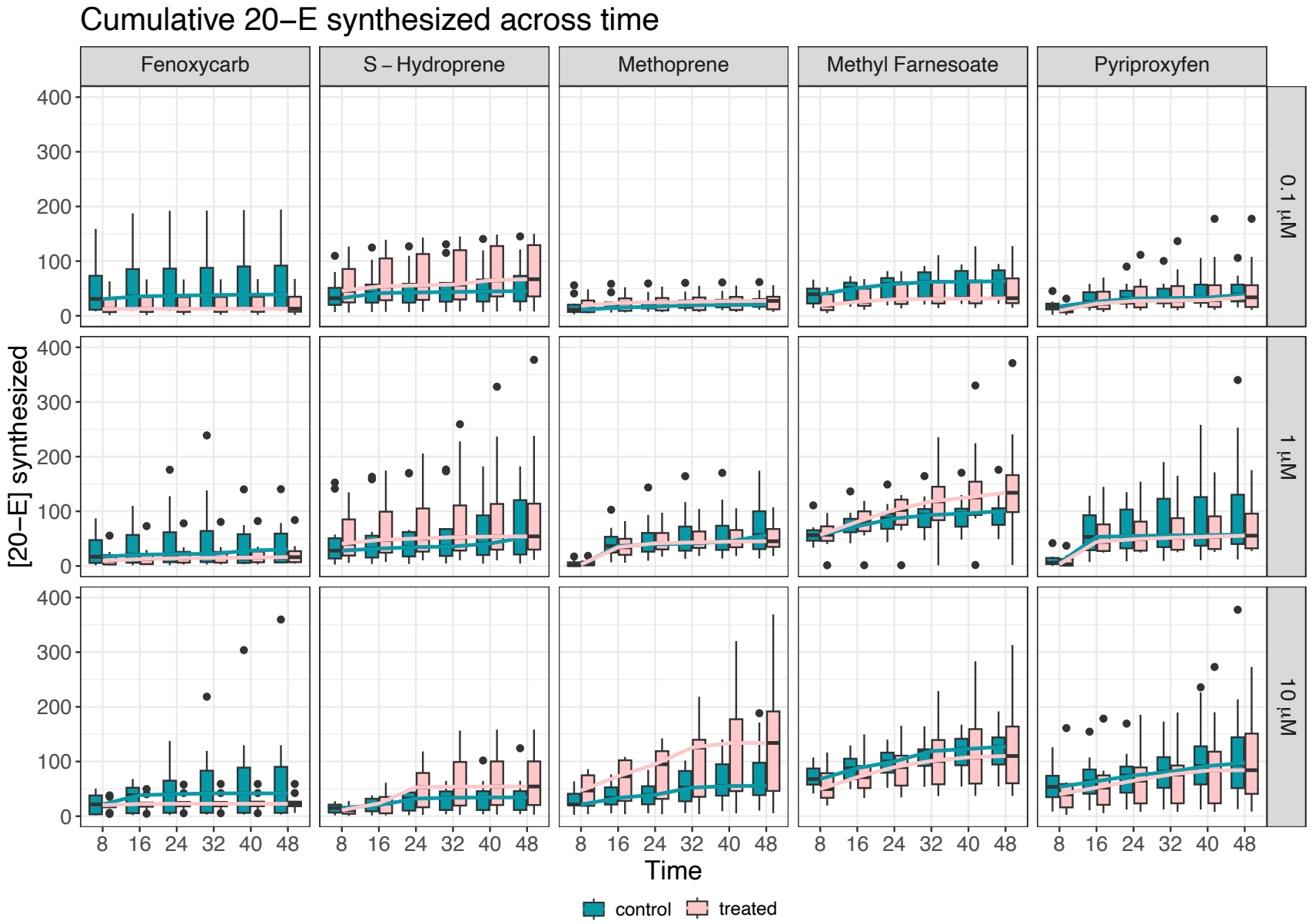
Cumulative 20–E synthesized across time
Fenoxycarb
S – Hydroprene
Methoprene
Methyl Farnesoate
Pyriproxyfen
0.1 µM
1 µM
10 µM
[20–E] synthesized
0
100
200
300
400
8
16
24
32
40
48
Time
control
treated

Figure 2.23. Cumulative 20-E titers (pg/μL) secreted by intermolt (IM) green crab (*C. maenas*) Y-organs (YOs) by treatment group (fenoxycarb, S-hydropene, methoprene, MF, and pyriproxyfen) at various concentration levels (0.1 μM, 1.0 μM, and 10.0 μM) (n = 10 crabs per tested compound at each concentration). The data is displayed as the control-treatment status (control and treated) with the Line for each group represents the median value for that concentration and time. Differences between treated and control groups are largest at higher concentrations and later times. S-Hydroprene and methoprene show larger magnitudes of differences at 10.0 μM and after 24-hours of exposure.

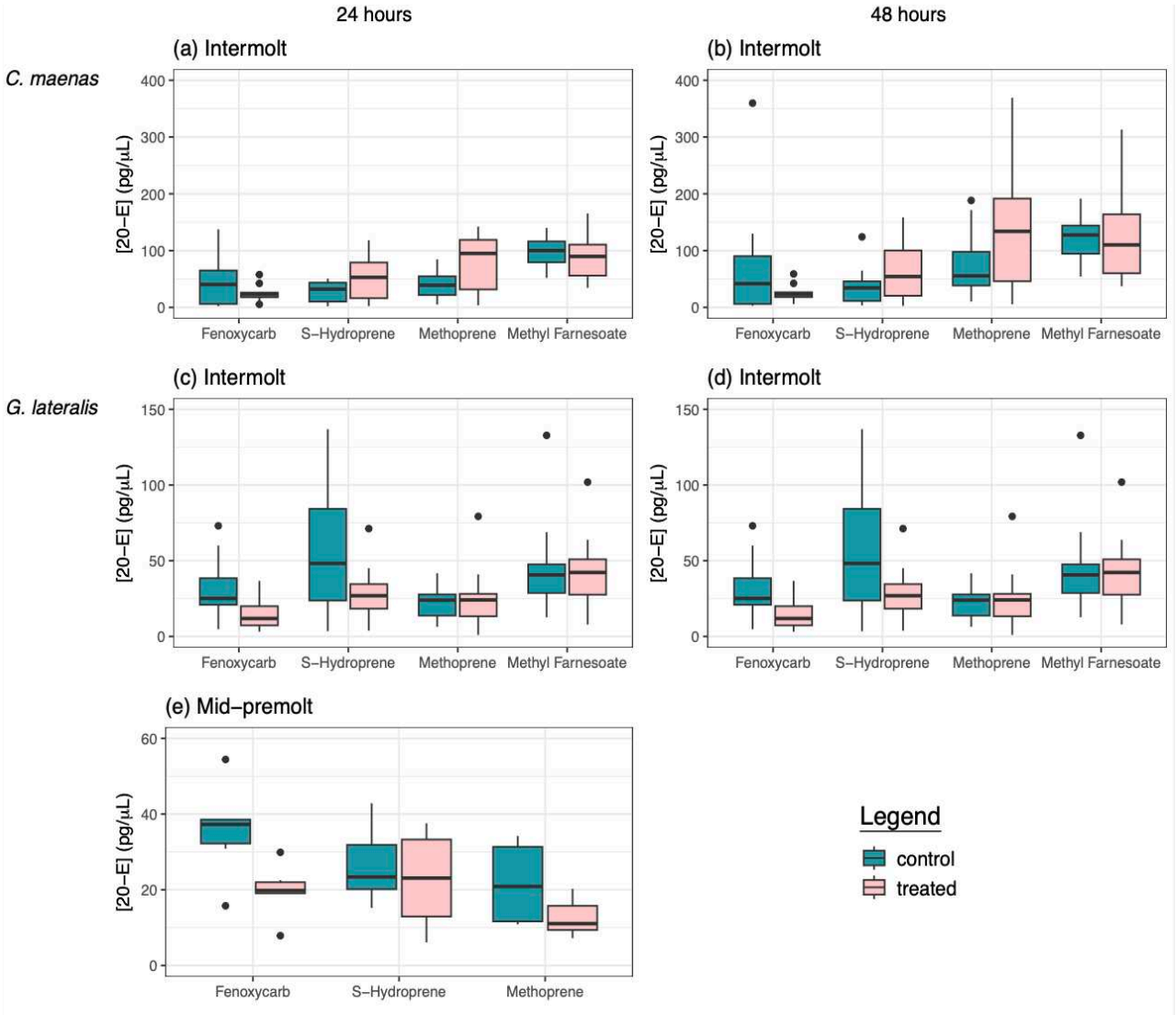

Figure 2.24. Cumulative 20-E concentration (pg/μL) synthesized by the Y-organs (YO) at 24 and 48-hours after exposure to 10.0 μM of MF or a JH-mimic (fenoxycarb, hydroprene, and methoprene; pyriproxyfen data not shown) and their counterpart control YO for green crabs (*C. maenas*) in intermolt (IM) (n = 10 crabs per tested compound) compared to the IM and mid-premolt (MP) blackback land crabs (*G. lateralis*) (n = 10 IM crabs per tested compound and n = 6 MP crabs per tested compound).

Figure 2.25

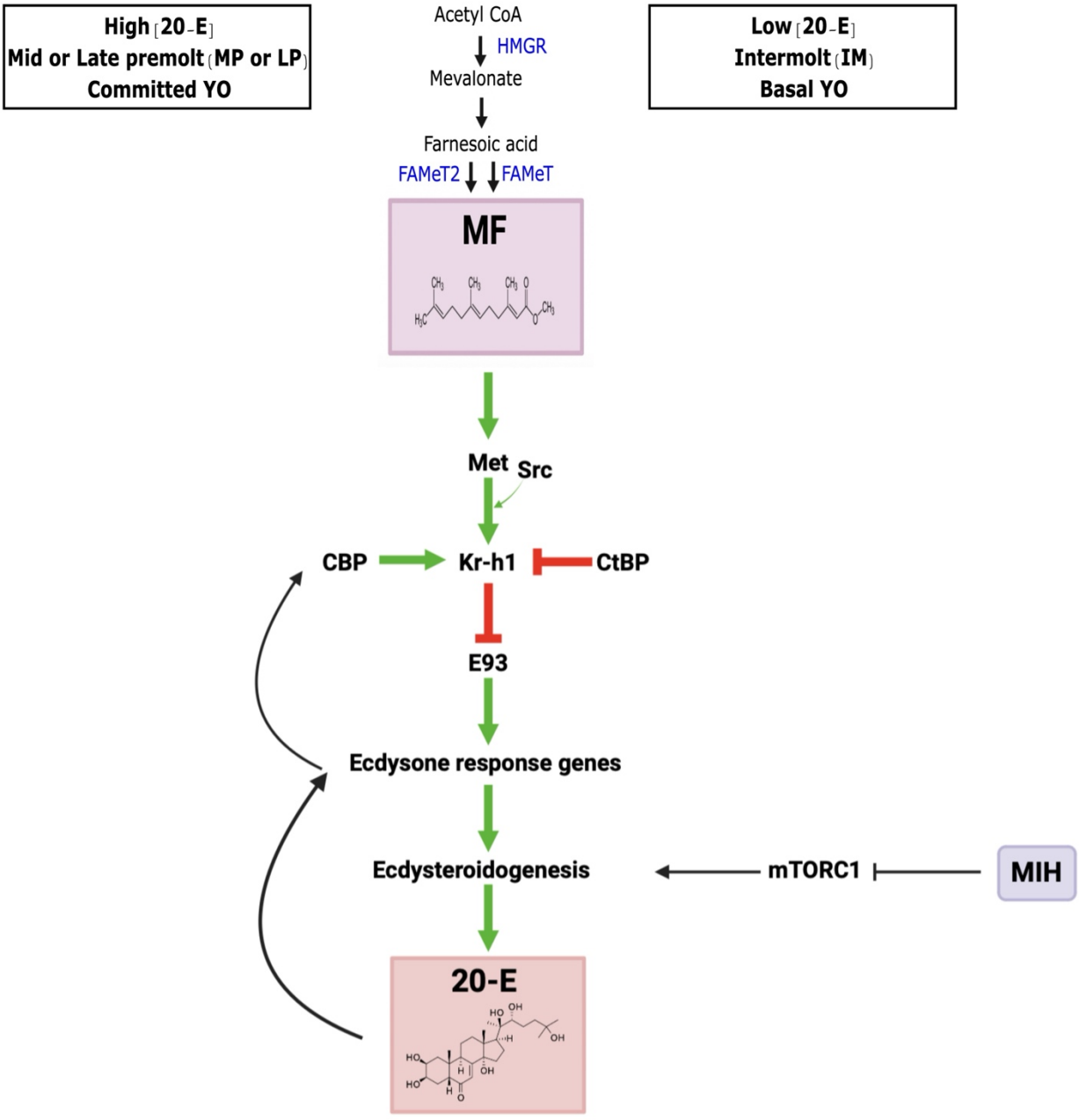
High [20-E]
Mid or Late premolt (MP or LP)
Committed YO
Low [20-E]
Intermolt (IM)
Basal YO
Acetyl CoA
HMGR
Mevalonate
Farnesoic acid
FAMeT2
FAMeT
MF
Met
Src
CBP
Kr-h1
CtBP
E93
Ecdysone response genes
Ecdysteroidogenesis
mTORC1
MIH
20-E

Figure 2.25. Mediation of ecdysteroidogenesis through the methyl farnesoate (MF) transcriptional cascade of Methoprene tolerant (Met) – Krüppel homolog 1 (Kr-h1) – Ecdysone response gene 93 (E93) in the Y-organ (YO). MF is proposed to act as an autocrine factor to regulate the endocrine cross talk with 20-E as the genes encoding for the synthetic enzymes were identified including *3-hydroxy-3-methylglutaryl-CoA reductase* (*HMGR*) and *farnesoic acid O-methyltransferase* (*FAMeT*). High hemolymph titers of 20-E, such as in mid and/or late premolt (MP and/or LP) inhibit 20-E synthesis thus leading to the transition from a committed to repressed state. By contrast, low 20-E titers in the hemolymph, such as in intermolt (IM) when the YO is in a basal or repressed state, stimulate the YO ecdysteroid production. Although molt-inhibiting hormone (MIH) inhibits ecdysteroid synthesis through the mechanistic target of rapamycin complex 1 (mTORC1), MF is proposed to act as an autocrine factor to regulate the endocrine cross talk with 20-E.

REFERENCES

Abdu, U., Barki, A., Karplus, I., Barel, S., Takac, P., Yehezkel, G., Laufer, H., and Sagi, A. (2001). Physiological effects of methyl farnesoate and pyriproxyfen on wintering female crayfish *Cherax quadricarinatus*. *Aquaculture*. **202**, 163–175.

Abdu, U., Takac, P., Laufer, H., and Sagi, A. (1998). Effect of Methyl Farnesoate on Late Larval Development and Metamorphosis in the Prawn *Macrobrachium rosenbergii* (Decapoda, Palaemonidae): A Juvenoid-like Effect? *Reference: Biol. Bull.* **195**, 112–119.

Abuhagr, A. M., Blindert, J. L., Nimitkul, S., Zander, I. A., LaBere, S. M., Chang, S. A., MacLea, K. S., Chang, E. S. (2014). Molt regulation in green and red color morphs of the crab *Carcinus maenas*: gene expression of molt-inhibiting hormone signaling components. *Journal of Experimental Biology.* **217** (5), 796–808.

Adhitama, N., Kato, Y., Matsuura, T., and Watanabe, H. (2020). Roles of and cross-talk between ecdysteroid and sesquiterpenoid pathways in embryogenesis of branchiopod crustacean *Daphnia magna*. *PLoS One*. **15** (10), e0239893.

Alnawafleh, T., Kim, B. K., Kang, H. E., Yoon, T. H., and Kim, H. W. (2014). Stimulation of Molting and Ovarian Maturation by Methyl Farnesoate in the Pacific White Shrimp *Litopenaeus vannamei* (Boone, 1931). *Fish. Aquat. Sci*. **17** (1), 115–121.

Apolinário, R. and Feder, D. (2021). Existing potentials in Insect Growth Regulators (IGR) for crop pest control. *Research, Society and Development*. **10**, e35910111726.

Aribi, N., Smagghe, G., Lakbar, S., Soltani-Mazouni, N., and Soltani, N. (2006). Effects of pyriproxyfen, a juvenile hormone analog, on development of the mealworm, *Tenebrio molitor*. *Pestic Biochem Physiol.* **84** (1), 55–62.

Arnold, K. E., Wells, C., and Spicer, J. I. (2009). Effect of an insect juvenile hormone analogue, Fenoxycarb® on development and oxygen uptake by larval lobsters *Homarus gammarus* (L.). *Comp. Biochem. Physiol. C: Toxicology and Pharmacology.* **149** (3), 393–396.

Baehrecke, E. H. and Thummel, C. S. (1995). The *Drosophila* E93 gene from the 93F early puff displays stage- and tissue-specific regulation by 20-hydroxyecdysone. *Dev Biol.* **171** (1), 85–97.

Belles, X. (2019). The innovation of the final moult and the origin of insect metamorphosis. *Phil. Trans. R. Soc. B.* **374**, 20180415.

Belles, X. and Santos, C. G. (2014). The MEKRE93 (Methoprene tolerant-Krüppel homolog 1-E93) pathway in the regulation of insect metamorphosis, and the homology of the pupal stage. *Insect Biochemistry and Molecular Biology.* **52**, 60–68.

Benrabaa, S. A. M., Chang, S. A., Chang, E. S., and Mykles, D. L. (2024). Effects of molting on the expression of ecdysteroid responsive genes in the crustacean molting gland (Y-organ). *General and Comparative Endocrinology.* **355**, 114548.

Benrabaa, S. A. M. and Mykles, D. L. (2025). Effect of blocking transforming growth factor-β/Activin-Myostatin signaling on the expression of ecdysteroid metabolism and responsive genes in the crustacean molting gland (Y-organ). *General and Comparative Endocrinology.* **362**, 114675.

Bernardo, T. J. and Dubrovsky, E. B. (2012). Molecular Mechanisms of Transcription Activation by Juvenile Hormone: A Critical Role for bHLH-PAS and Nuclear Receptor Proteins. *Insects* **3**, 324–338.

Bliss, D. E. (1968). Transition from Water to Land in Decapod Crustaceans. *Am. Zool.* **8** (3), 355–392.

Bliss, D. E. and Boyer, J. R. (1964). Environmental Regulation of Growth in the Decapod Crustacean *Gecarcinus lateralis*. *General and Comparative Endocrinology.* **4** (1), 15–41.

Bliss, D. E., Wang, S. M. E., and Martinez, E. A. (1966a). Water balance in the land crab, *Gecarcinus lateralis*, during the intermolt cycle. *Am. Zool.* **6** (2), 197–212.

Borst, D. W. and Tsukimura, B. (1991). Quantification of methyl farnesoate levels in hemolymph by high-performance liquid chromatography. *Journal of Chromatography.* **545**, 71–78.

Borst, D. W., Laufer, H., Landau, M., Chang, E. S., Hertz, W. A., Baker, F. C., and Schooley, D. A. (1987). Methyl farnesoate and its role in crustacean reproduction and development. *Insect Biochemistry.* **17** (7) 1123–1127.

Cai, M. J., Liu, W., Pei, X. Y., Li, X. R., He, H. J., Wang, J. X., and Zhao, Z. F. (2014). Juvenile hormone prevents 20-hydroxyecdysone-induced metamorphosis by regulating the phosphorylation of a newly identified broad protein. *J. Biol. Chem.* **289** (38), 26630–26641.

Chafino, S., Ureña, E., Casanova, J., Casacuberta, E., Franch-Marro, X., and Martín, D. (2019). Upregulation of E93 Gene Expression Acts as the Trigger for Metamorphosis Independently of the Threshold Size in the Beetle *Tribolium castaneum*. *Cell Rep.* **27** (4), 1039-1049.e2.

Chang, E. S. (1985). Hormonal Control of Molting in Decapod Crustacea. *Amer. Zool.* **25** (1), 179–185.

Chang, E. S. (1993). Comparative Endocrinology of Molting and Reproduction: Insects and Crustaceans. *Annu. Rev. Entomol.* **38**, 161–180.

Chang, E. S. (1995). Physiological and biochemical changes during the molt cycle in decapod crustaceans: an overview. *Journal of Experimental Marine Biology and Ecology.* **193**, 1–14.

Chang, E. S., Bruce, M. J., and Tamone, S. L. (1993). Regulation of Crustacean Molting: A Multi-Hormonal System. *American Zoologist*. **33** (3), 324–329.

Chang, E. S. (1995). Physiological and biochemical changes during the molt cycle in decapod crustaceans: an overview. *Journal of Experimental Marine Biology and Ecology.* **193**, 1–14.

Charles, J. P., Iwema, T., Epa, V. C., Takaki, K., Rynes, J., and Jindra, M. (2011). Ligand-binding properties of a juvenile hormone receptor, Methoprene-tolerant. *Proc. Natl. Acad. Sci. U. S. A.* **108** (52), 21128–21133.

Chen, T., Diao, Y., Xu, R., Sheng, N., Liu, F., Xie, Q., Su, S., Ma, K., and Li, X. (2022a). Cloning and expression analysis of juvenile hormone epoxide hydrolase-like (*EsJHEH-like*) from *Eriocheir sinensis*, and its potential roles in methyl farnesoate metabolism. *Invertebrate Reproduction & Development*. **66** (1), 23–32.

Chen, X., Gao, Q., Cheng, H., Peng, F., Wang, C., and Xu, B. (2021b). Molecular cloning and expression pattern of the juvenile hormone epoxide hydrolase gene from the giant freshwater prawn *Macrobrachium rosenbergii* during larval development and the moult cycle. *Aquac. Res.* **52**, 3890–3899.

Clamp, M., Cuff, J., Searle, S. M., and Barton, G. J. (2004). The Jalview Java alignment editor. *Bioinformatics.* **20** (3), 426–427.

Covi, J. A., Bader, B. D., Chang, E. S., and Mykles, D. L. (2010). Molt cycle regulation of protein synthesis in skeletal muscle of the blackback land crab, *Gecarcinus lateralis*, and the differential expression of a myostatin-like factor during atrophy induced by molting or unweighting. *J. Exp. Biol.* **213** (1), 172–183.

Covi, J. A., Chang, E. S., and Mykles, D. L. (2009). Conserved role of cyclic nucleotides in the regulation of ecdysteroidogenesis by the crustacean molting gland. *Comp. Biochem. Physiol. A Mol. Integr. Physiol.* **152** (4), 470–477.

Das, S., Vraspir, L., Zhou, W., Durica, D. S., and Mykles, D. L. (2018). Transcriptomic analysis of differentially expressed genes in the molting gland (Y-organ) of the blackback land crab, *Gecarcinus lateralis*, during molt-cycle stage transitions. *Comp. Biochem. Physiol. Part D Genomics Proteomics* **28**, 37–53.

Devi, S., Raghavan, A., and Ayanath, A. (2018). Effect of Methyl Farnesoate Administration on Ovarian Growth and Maturation in the Freshwater Crab *Travancoriana schirnerae*. *Egypt J. Aquat. Biol. Fish.* **22** (5), 257–271.

Devi, V. and Awasthi, P. (2022). Juvenile hormone mimics with phenyl ether and amide functionality to be insect growth regulators (IGRs): synthesis, characterization, computational and biological study. *J. Biomol. Struct. Dyn.* **40** (23), 13246–13264.

Dhadialla, T. S., Carlson, G. R., and Le, D. P. (1998). New insecticides with ecdysteroidal and juvenile hormone activity. *Annu. Rev. Entomol.* **43**, 545–69.

Fernandez-Nicolas, A., Machaj, G., Ventos-Alfonso, A., Pagone, V., Minemura, T., Ohde, T., Ylla, G. and Belles, X. (2023). Reduction of embryonic E93 expression as a hypothetical driver of the evolution of insect metamorphosis. *Proc. Natl. Acad. Sci. U. S. A.* 120 (7), e2216640120.

Fingerman, M. (1997). Crustacean endocrinology: a retrospective, prospective, and introspective analysis. *Physiol. Zool.* **70** (3), 257–269.

Gauthier, M., Defrance, J., Jumarie, C., Vulliet, E., Garric, J., Boily, M., and Geffard, O. (2023). Disruption of oogenesis and molting by methoprene and glyphosate in *Gammarus fossarum*: involvement of retinoic acid? *Environ. Sci. Pollut. Res. Int.* **30** (36), 86060–86071.

Ge, F., Yu, Q., Zhang, J., Han, Y., Zhu, D., and Xie, X. (2024). E93 gene in the swimming crab, *Portunus trituberculatus*: Responsiveness to 20-hydroxyecdysone and methyl farnesoate and role on regulating ecdysteroid synthesis. *Comp. Biochem. Physiol. B Biochem. Mol. Biol.* **270**, 110910.

Geens, B., Goossens, S., Li, J., Van de Peer, Y., and Vanden Broeck, J. (2024). Untangling the gordian knot: The intertwining interactions between developmental hormone signaling and epigenetic mechanisms in insects. *Molecular and Cellular Endocrinology.* **585**, 112178.

George, S., Gaddelapati, S. C., and Palli, S. R. (2019). Histone deacetylase 1 suppresses Krüppel homolog 1 gene expression and influences juvenile hormone action in *Tribolium castaneum*. *Proc. Natl. Acad. Sci. U. S. A.* **116** (36), 17759–17764.

Gianazza, E., Eberini, I., Palazzolo, L., and Miller, I. (2021). Hemolymph proteins: An overview across marine arthropods and molluscs. *Journal of Proteomics.* **245**, 104294.

Gilbert, L. I., Rybczynski, R., and Warren, J. T. (2001). Control and biochemical nature of the ecdysteroidogenic pathway. *Annu. Rev. Entomol.* **47**, 883–916.

Giribet, G. and Edgecombe, G. D. (2019). The Phylogeny and Evolutionary History of Arthropods. *Current Biology.* **29** (12), R592–R602.

Gouveia, D., Bonneton, F., Almunia, C., Armengaud, J., Quéau, H., Degli-Esposti, D., Geffard, O., and Chaumot, A. (2018). Identification, expression, and endocrine-disruption of three ecdysone-responsive genes in the sentinel species *Gammarus fossarum*. *Sci. Rep.* **8**, 3793.

Guindon, S. (2018). Accounting for Calibration Uncertainty: Bayesian Molecular Dating as a "Doubly Intractable" Problem. *Syst. Biol.* **67** (4), 651–661.

He, Q. and Zhang, Y. (2022). Kr-h1, a Cornerstone Gene in Insect Life History. *Front. Physiol.* **13**, 905441.

He, Q., Wen, D., Jia, Q., Cui, C., Wang, J., Pallii, S. R., and Li, S. (2014). Heat shock protein 83 (Hsp83) facilitates methoprene-tolerant (Met) nuclear import to modulate juvenile hormone signaling. *Journal of Biological Chemistry.* **289** (40), 27874–27885.

He, Q., Zhang, Y., Zhang, X., Xu, D. D., Dong, W., Li, S., and Wu, R. (2017b). Nucleoporin Nup358 facilitates nuclear import of Methoprene-tolerant (Met) in an importin β- and Hsp83-dependent manner. *Insect Biochem. Mol. Biol.* **81**, 10–18.

Hirano, M., Toyota, K., Ishibashi, H., Tominaga, N., Sato, T., Tatarazako, N., and Iguchi, T. (2020). Molecular Insights into Structural and Ligand Binding Features of Methoprene-Tolerant in Daphnids. *Chem. Res. Toxicol.* **33** (11), 2785–2792.

Hoang, D. T., Chernomor, O., von Haeseler, A., Minh, B. Q., and Vinh, L. S. (2017). UFBoot2: Improving the Ultrafast Bootstrap Approximation. *Mol. Biol. Evol.* **35** (2), 518–522.

Homola, E. and Chang, E. S. (1997a). Assay Methods for Methyl Farnesoate Esterases in Crustaceans. *Arch. Insect Biochem. Physiol.* **36** (2), 115–128.

Homola, E. and Chang, E. S. (1997b). Distribution and Regulation of Esterases That Hydrolyze Methyl Farnesoate in *Homarus americanus* and Other Crustaceans. *General and Comparative Endocrinoology.* **106**, (1) 62–72.

Homola, E. and Chang, E. S. (1997c). Methyl Farnesoate: Crustacean Juvenile Hormone in Search of Functions. *Comparative Biochemistry and Physiology Part B: Biochemistry and Molecular Biology.* **117** (3), 347–356.

Hopkins, P. M. (1982). Growth and Regeneration Patterns in the Fiddler Crab, *Uca pugilator*. *Biol. Bull.* **163** (2), 301–319.

Hyde, C. J., Elizur, A., and Ventura, T. (2019a). The crustacean ecdysone cassette: A gatekeeper for molt and metamorphosis. *Journal of Steroid Biochemistry and Molecular Biology.* **185**, 172–183.

Hyde, C. J., Fitzgibbon, Q. P., Elizur, A., Smith, G. G., and Ventura, T. (2020). CrustyBase: an interactive online database for crustacean transcriptomes. *BMC Genomics.* **21**, 637.

Hyde, C. J. and Ventura, T. (2024). CrustyBase v.2.0: new features and enhanced utilities to support open science. *BMC Genomics.* **25**, 121.

Jindra, M. and Bittova, L. (2020). The juvenile hormone receptor as a target of juvenoid "insect growth regulators." *Arch. Insect Biochem. Physiol.* **103** (3), e21615.

Jindra, M., Palli, S. R., and Riddiford, L. M. (2013). The juvenile hormone signaling pathway in insect development. *Annu. Rev. Entomol.* **58**, 181–204.

Kakaley, E. K. M., Wang, H. Y., and LeBlanc, G. A. (2017). Agonist-mediated assembly of the crustacean methyl farnesoate receptor. *Sci. Rep.* **7**, 45071.

Kalavathy, Y., Mamatha, P., and Reddy, P. S. (1999). Methyl farnesoate stimulates testicular growth in the freshwater crab *Oziotelphusa senex sene*x fabricius. *Naturwissenschaften.* **86**, 394–395.

Kalyaanamoorthy, S., Minh, B. Q., Wong, T. K. F., Von Haeseler, A., and Jermiin, L. S. (2017). ModelFinder: Fast model selection for accurate phylogenetic estimates. *Nat. Methods.* **14**, 587–589.

Kamita, S. G. and Hammock, B. D. (2010). Juvenile hormone esterase: biochemistry and structure. *J. Pestic. Sci.* **35** (3), 265–274.

Kamita, S. G., Hintona, A. C., Wheelock, C. E., Wogulis, M. D., Wilson, D. K., Wolf, N. M., Stok, J. E., Hock, B., and Hammock, B. D. (2003). Juvenile hormone (JH) esterase: Why are you so JH specific? *Insect Biochem. Mol. Biol.* **33** (12), 1261–1273.

Kamita, S. G., Samra, A. I., Liu, J. Y., Cornel, A. J., and Hammock, B. D. (2011). Juvenile hormone (JH) esterase of the mosquito *Culex quinquefasciatus* is not a target of the JH analog insecticide methoprene. *PLoS One.* **6**. (12), e28392.

Kamsoi, O. and Belles, X. (2020). E93-depleted adult insects preserve the prothoracic gland and molt again. *Development.* **147** (22), dev190066.

Katoh, K. and Toh, H. (2008). Recent developments in the MAFFT multiple sequence alignment program. *Brief. Bioinform.* **9** (4), 286–298.

Kayukawa, T., Jouraku, A., Ito, Y., and Shinoda, T. (2017). Molecular mechanism underlying juvenile hormone-mediated repression of precocious larval-adult metamorphosis. *Proc. Natl. Acad. Sci. U. S. A.* **114** (5), 1057–1062.

Kayukawa, T., Minakuchi, C., Namiki, T., Togawa, T., Yoshiyama, M., Kamimura, M., Mita, K., Imanishi, S., Kiuchi, M., Ishikawa, Y., and Shinoda, T. (2012). Transcriptional regulation of juvenile hormone-mediated induction of Krüppel homolog 1, a repressor of insect metamorphosis. *Proc. Natl. Acad. Sci. U. S. A.* **109** (29), 11729–11734.

Kim, K., Albishi, N. M., and Palli, S. R. (2021). Identification of juvenile hormone-induced posttranslational modifications in the yellow fever mosquito, *Aedes aegypti*. *J. Proteomics.* **242**, 104257.

King, L. E., Ding, Q., Prestwtch, G. D., and Tobe, S. S. (1995). The Characterization of a Haemolymph Methyl Farnesoate Binding Protein and the Assessment of Methyl Farnesoate Metabolism by the Haemolymph and Other Tissues from *Procambrus clarkii*. *Insect Biochem. Mol. Biol.* **25** (4), 495–501.

Kingan, T. G. (1989). A Competitive Enzyme-Linked Immunosorbent Assay: Applications in the assay of peptides, steroids, and cyclic nucleotides. *Analytical Biochemistry.* **183** (2), 283–289.

Kolonko, M., Ozga, K., Hołubowicz, R., Taube, M., Kozak, M., Ozyhar, A., and Greb-Markieqicz, B. (2016). Intrinsic Disorder of the C-terminal Domain of *Drosophila* Methoprene-Tolerant Protein. *PLoS One.* **11** (9), e0162950.

Kramer, R. D., Koehler, P. G., and Patterson, R. S. (1990). Effects of hydroprene exposure on the physiology and insecticide susceptibility of German cockroaches (Orthoptera: Blattellidae). *J. Econ. Entomol.* **83** (6), 2310–2316.

Lachaise, F., Le Roux, A., Hubert, M., and Lafont, R. (1993). The Molting Gland of Crustaceans: Localization, Activity, and Endocrine Control (A Review). *Journal of Crustacean Biology.* **13** (2), 198–234.

Lai, R., Bai, J., Gu, G., Zhou, T., Mi, Y., Zhang, B., Han, M., and Bai, J. (2021). Juvenoids on aphids to prolong optimal stages. *Entomol. Res.* **51** (3), 133–142.

Lam, G., Nam, H. J., Velentzas, P. D., Baehrecke, E. H., and Thummel, C. S. (2022). *Drosophila* E93 promotes adult development and suppresses larval responses to ecdysone during metamorphosis. *Dev. Biol.* **481**, 104–115.

Laufer, H., Ahl, J., Rotllant, G., and Baclaski, B. (2002). Evidence that ecdysteroids and methyl farnesoate control allometric growth and differentiation in a crustacean. *Insect Biochem. Mol. Biol.* **32** (2), 205–210.

Laufer, H. and Albrecht, K. H. (1990). Metabolism of Methyl Farnesoate In Vitro by Peripheral Tissues of the Spider Crab, *Libinia emarginata* (Decapoda). *Advances in Invertebrate Reproduction*. **5**, 217–222.

Laufer, H. and Biggers, W. J. (2001). Unifying Concepts Learned from Methyl Farnesoate for Invertebrate Reproduction and Post-Embryonic Development. *Amer. Zool.* **41** (3), 4–8.

Laufer, H., Borst, D., Baker, F. C., Reuter, C. C., Tsai, L. W., Schooley, D. A., Carrasco, C., and Sinkus, M. (1987a). Identification of a Juvenile Hormone-Like Compound in a Crustacean. *Science.* **235** (4785), 202–205.

Laufer, H., Demir, N., Pan, X., Stuart, J. D., and Ahl, J. S. B. (2005). Methyl farnesoate controls adult male morphogenesis in the crayfish, *Procambarus clarkii*. *Journal of Insect Physiology*. **51** (4), 379–384.

Laufer, H., Landau, M., Homola, E., and Borst, D. W. (1987b). Methyl Farnesoate: Its site of synthesis and regulation of secretion in a juvenile crustacean. *Insect Biochem.* **17** (7), 1129–1131.

Lee, S. O., Jeon, J. M., Oh, C. W., Kim, Y. M., Kang, C. K., Lee, D. S., Mykles, D. L., and Kim, H. W. (2011). Two juvenile hormone esterase-like carboxylesterase cDNAs from a Pandalus shrimp (*Pandalopsis japonica*): Cloning, tissue expression, and effects of eyestalk ablation. *Comparative Biochemistry and Physiology - B Biochemistry and Molecular Biology.* **159** (3), 148–156.

Li, K., Jia, Q. Q., and Li, S. (2018a). Juvenile hormone signaling – a mini review. *Insect Sci*. **26** (4), 600–606.

Li, K. L., Yuan, S. Y., Nanda, S., Wang, W. X., Lai, F. X., Fu, Q., and Wan, P. J. (2018b). The Roles of E93 and Kr-h1 in Metamorphosis of *Nilaparvata lugens*. *Front. Physiol.* **9**, 1677.

Li, G., Lan, H., Lu, Q., He, C., Wei, Y., Mo, D., Qu, D., and Xu, K. (2021a). The JH-Met2-Kr-h1 pathway is involved in pyriproxyfen-induced defects of metamorphosis and silk protein synthesis in silkworms, *Bombyx mori*. *Pestic. Biochem. Physiol.* **179**, 104980.

Li, H. and Borst, D. W. (1991). Characterization of a Methyl Farnesoate Binding Protein in Hemolymph from *Libinia emarginata*. *Gen. Comp. Endocrinol.* **81** (3), 335–342.

Li, X., Chen, T., Han, Y., Huang, M., Jiang, H., Huang, J., Tao, M., Xu, R., Xie, Q., and Su, S. (2021b). Potential role of Methoprene-tolerant (Met) in methyl farnesoate-mediated vitellogenesis in the Chinese mitten crab (*Eriocheir sinensis*). *Comp. Biochem. Physiol. B Biochem. Mol. Biol.* **252**, 110524.

Li, X., Chen, T., Jiang, H., Huang, J., Huang, M., Xu, R., Xie., Q., Zhu, H., and Su, S. (2021c). Effects of methyl farnesoate on Krüppel homolog 1 (Kr-h1) during vitellogenesis in the Chinese mitten crab (*Eriocheir sinensis*). *Anim. Reprod. Sci.* **224**, 106653.

Li, X., Chen, T., Xu, R., Huang, M., Huang, J., Xie, Q., Liu, F., Su, S., and Ma, K. (2021d). Identification, characterization and mRNA transcript abundance profiles of the carboxylesterase (CXE5) gene in *Eriocheir sinensis* suggest that it may play a role in methyl farnesoate degradation. *Comp. Biochem. Physiol. B Biochem. Mol. Biol.* **256**, 110630.

Li, Y. X., Wang, D., Zhao, W. L., Zhang, J. Y., Kang, X. L., Li, Y. L., and Zhao X. F. (2021e). Juvenile hormone induces methoprene-tolerant 1 phosphorylation to increase interaction with Taiman in *Helicoverpa armigera*. *Insect Biochem. Mol. Biol.* **130**, 103519.

Linton, S., Barrow, L., Davies, C., and Harman, L. (2009). Potential endocrine disruption of ovary synthesis in the Christmas Island red crab *Gecarcoidea natalis* by the insecticide pyriproxyfen. *Comparative Biochemistry and Physiology - A Molecular and Integrative Physiology.* **154**, 289–297.

Litsey, E. M. and Fine, J. D. (2024). Developmental exposure to hormone-mimicking insect growth disruptors alters expression of endocrine-related genes in worker honey bee (Hymenoptera: Apidae) brains and hypopharyngeal glands. *J. Econ. Entomol.* **117**, 377–387.

Liu, M., Xie, X., Tao, T., Jiang, Q., Shao, J., and Zhu, D. (2016). Molecular characterization of methoprene-tolerant gene (Met) in the swimming crab *Portunus trituberculatus*: Its putative role in methyl farnesoate-mediated vitellogenin transcriptional activation. *Anim. Reprod. Sci.* **174**, 132–142.

Liu, P., Peng, H. J., and Zhu, J. (2015a). Juvenile hormone-activated phospholipase C pathway enhances transcriptional activation by the methoprene-tolerant protein. *Proc. Natl. Acad. Sci. U. S. A.* **112**, E1871–E1879.

Liu, S., Li, K., Gao, Y., Liu, X., Chen, W., Ge, W., Feng, Q., Palli, S. R., and Sheng, L. (2018). Antagonistic actions of juvenile hormone and 20-hydroxyecdysone within the ring gland determine developmental transitions in *Drosophila*. *Proc. Natl. Acad. Sci. U. S. A.* **115** (1), 139–144.

Liu, W., Zhang, F. X., Cai, M. J., Zhao, W. L., Li, X. R., Wang, J. X., and Zhao, X.F. (2013). The hormone-dependent function of Hsp90 in the crosstalk between 20-hydroxyecdysone and juvenile hormone signaling pathways in insects is determined by differential phosphorylation and protein interactions. *Biochim. Biophy. Acta. Gen. Subj.* **1830** (11), 5184–5192.

Liu, X., Dai, F., Guo, E., Li, K., Ma, L., Tian, L., Cao, Yang, Zhang, G., Palli, S. R., and Li, S. (2015b). 20-Hydroxyecdysone (20E) Primary Response Gene E93 Modulates 20E Signaling to Promote *Bombyx* Larval-Pupal Metamorphosis. *Journal of Biological Chemistry* **290** (45), 27370–27383.

Lozano, J. and Belles, X. (2011). Conserved repressive function of Krüppel homolog 1 on insect metamorphosis in hemimetabolous and holometabolous species. *Sci. Rep.* **1**, 163.

Lozano, J., Montañez, R., and Bellesa, X. (2015). MiR-2 family regulates insect metamorphosis by controlling the juvenile hormone signaling pathway. *Proc. Natl. Acad. Sci. U. S. A* **112** (12), 3740–3745.

Luo, J., Liu, S., Hou, J., Chen, L., Li, H., Liao, S., Tan, Q., Yang, T., Yi, G., Zhang, F., and Li, X. (2021). The comparison of juvenile hormone and transcriptional changes between three different juvenile hormone analogs insecticides on honey bee worker larval's development. *Agronomy.* **11** (12), 2497.

Martín, D., Chafino, S., and Franch-Marro, X. (2021). How stage identity is established in insects: the role of the Metamorphic Gene Network. *Curr. Opin. Insect Sci.* **43**, 29–38.

Mazina, M. Y. and Vorobyeva, N. E. (2019). Mechanisms of transcriptional regulation of ecdysone response. *Vavilovskii Zhurnal Genet Selektsii.* **23** (2), 212–218.

McKenney, C. L., Cripe, G. M., Foss, S. S., Tuberty, S. R., and Hoglund, M. (2004). Comparative embryonic and larval developmental responses of estuarine shrimp (*Palaemonetes pugio*) to the juvenile hormone agonist fenoxycarb. *Arch. Environ. Contam. Toxicol.* **47**, 463–470.

Meng, Q. W., Xu, Q. Y., Deng, P., Fu, K. Y., Guo, W. C., and Li, G. Q. (2018). Transcriptional response of Methoprene-tolerant (Met) gene to three insect growth disruptors in *Leptinotarsa decemlineata* (Say). *J. Asia Pac. Entomol.* **21**, 466–473.

Minakuchi, C., Zhao, X., and Riddiford, L. M. (2008). Krüppel homolog 1 (Kr-h1) mediates juvenile hormone action during metamorphosis of *Drosophila melanogaster*. *Mech. Dev.* **125**, 91–105.

Minh, B. Q., Schmidt, H. A., Chernomor, O., Schrempf, D., Woodhams, M. D., Von Haeseler, A., and Lanfear, R. (2020). IQ-TREE 2: New Models and Efficient Methods for Phylogenetic Inference in the Genomic Era. *Mol. Biol. Evol.* **37** (8), 1530–1534.

Miura, K., Oda, M., Makita, S., and Chinzei, Y. (2005). Characterization of the *Drosophila* Methoprene-tolerant gene product: Juvenile hormone binding and ligand-dependent gene regulation. *FEBS Journal.* **272**, 1169–1178.

Miyakawa, H., Toyota, K., Hirakawa, I., Ogino, Y., Miyagawa, S., Oda, S., Tatarazako, N. Miura, T. Colbourne, J, K., and Iguchi, T. (2013). A mutation in the receptor Methoprene-tolerant alters juvenile hormone response in insects and crustaceans. *Nat. Commun.* **4**, 1856.

Mohandass, S., Arthur, F. H., Zhu, K. Y., and Throne, J. E. (2006a). Hydroprene Prolongs Developmental Time and Increases Mortality of Indian meal Moth (Lepidoptera: Pyralidae) Eggs. *Journal of Economic Entomology.* **99** (3), 1007–1016.

Mohandass, S. M., Arthur, F. H., Zhu, K. Y., and Throne, J. E. (2006b). Hydroprene: Mode of action, current status in stored-product pest management, insect resistance, and future prospects. *Crop Protection.* **25**, 902–909.

Mou, X., Duncan, D. M., Baehrecke, E. H., and Duncan, I. (2012). Control of target gene specificity during metamorphosis by the steroid response gene E93. *Proc. Natl. Acad. Sci. U. S. A.* **109**, 2949–2954.

Mu, X. and LeBlanc, G. A. (2004). Cross communication between signaling pathways: Juvenoid hormones modulate ecdysteroid activity in a crustacean. *J. Exp. Zool. A Comp. Exp. Biol.* **301**, 793–801.

Muhd-Farouk, H., Nurul, H. A., Abol-Munafi, A. B., Mardhiyyah, M. P., Hasyima-Ismail, N., Manan, H., Fatihah, S. N., Amin-Safwan, A., and Ikhwanuddin, M. (2019). Development of ovarian maturations in orange mud crab, *Scylla olivacea* (Herbst, 1796) through induction of eyestalk ablation and methyl farnesoate. *Arab J. Basic Appl. Sci.* **26** (1), 171–181.

Mykles, D. L. (2021). Signaling Pathways That Regulate the Crustacean Molting Gland. *Front Endocrinol.* **12**.

Mykles, D. L. (2024). "Molting Physiology," in *Frontiers in Invertebrate Physiology A Collection of Review*, eds. S. Saleuddin, S. P. Leys, R. D. Roer, and I. C. Wilkie (Apple Academic Press). **229**.

Mykles, D. L. and Chang, E. S. (2020). Hormonal control of the crustacean molting gland: Insights from transcriptomics and proteomics. *Gen. Comp. Endocrinol.* **294**.

Nagaraju, G. P. C. (2007). Is methyl farnesoate a crustacean hormone? *Aquaculture.* **272**, 39–54.

Nong, W., Chai, Z. Y. H., Jiang, X., Qin, J., Ma, K. Y., Chan, K. M., Chan, T. F., Chow, B. K. C., Kwan, H. S., Wong, C. K. C., Qiu, J. W., Hui, J. H. L., and Chu, K. H. (2020). A crustacean annotated transcriptome (CAT) database. *BMC Genomics.* **21**, 32.

Noriega, F. G. and Nouzova, M. (2020). Approaches and tools to study the roles of juvenile hormones in controlling insect biology. *Insects.* **11**, 1–9.

Ojani, R., Liu, P., Fu, X., and Zhu, J. (2016). Protein kinase C modulates transcriptional activation by the juvenile hormone receptor methoprene-tolerant. *Insect Biochem. Mol. Biol.* **70**, 44–52.

Oliphant, A., Alexander, J. L., Swain, M. T., Webster, S. G., and Wilcockson, D. C. (2018). Transcriptomic analysis of crustacean neuropeptide signaling during the moult cycle in the green shore crab, *Carcinus maenas*. *BMC Genomics.* **19**, 711.

Olmstead, A. W. and Leblanc, G. L. (2001). Low Exposure Concentration Effects of Methoprene on Endocrine-Regulated Processes in the Crustacean *Daphnia magna*. *Toxicological Sciences.* **62**, 268–273.

Orchard, I. and Lange, A. B. (2024a). The neuroendocrine and endocrine systems in insect – Historical perspective and overview. *Mol. Cell Endocrinol.* **580**.

Pecasse, F., Beck, Y., Ruiz, C., and Richards, G. (2000b). Krüppel-homolog, a Stage-Specific Modulator of the Prepupal Ecdysone Response, Is Essential for *Drosophila* Metamorphosis. *Dev. Biol.* **221**, 53–67.

Parthasarathy, R. and Palli, S. R. (2021). Stage-specific action of juvenile hormone analogs. *J Pestic. Sci.* **46**, 16–22.

Paran, B. C., Fierro, I. J., and Tsukimura, B. (2010). Stimulation of ovarian growth by methyl farnesoate and eyestalk ablation in penaeoidean model shrimp, *Sicyonia ingentis* Burkenroad, 1938. *Aquac. Res.* **41**, 1887–1897.

Pérez-Moreno, J. L., Kozma, M. T., DeLeo, D. M., Bracken-Grissom, H. D., Durica, D. S., and Mykles, D. L. (2023). CrusTome: a transcriptome database resource for large-scale analyses across Crustacea. *G3: Genes, Genomes, Genetics.* **13**.

Prestwich, G. D., Bruce, M. J., Ujvary, I., and Chang, E. S. (1990). Binding Proteins for Methyl Farnesoate in Lobster Tissues: Detection by Photoaffinity Labeling. *Gen Comp Endocrinol* **80**, 232–237.

Prestwich, G. D., Wojtasek, H., Lentz, A. J., and Rabinovich, J. M. (1996). Biochemistry of Proteins That Bind and Metabolize Juvenile Hormones. *Arch. Insect Biochem. Physiol.* **32**, 407–419.

Qin, J., Hu, Y., Ma, K. Y., Jiang, X., Ho, C. H., Tsang, L. M., Yi, L., Leung, R. W. T., and Chu, K. H. (2017). CrusTF: A comprehensive resource of transcriptomes for evolutionary and functional studies of crustacean transcription factors. *BMC Genomics.* **18**, 908.

Raghavan, S. D. A. and Ayanath, A. (2019). Effect of 20-OH ecdysone and methyl farnesoate on moulting in the freshwater crab *Travancoriana schirnerae*. *Invertebr. Reprod. Dev.* **63**, 309–318.

Rambaut, A. (2010). FigTree v1.4.4.

Reddy, P. S. and Ramamurthi, R. (1998). Methyl farnesoate stimulates ovarian maturation in the freshwater crab *Oziotelphusa senex senex* Fabricius. *Current Science.* **74**, 68–70.

Reddy, P. R., Purna, G., Nagaraju, C., and Reddy, P. S. (2004). Involvement of Methyl Farnesoate in the Regulation of Molting and Reproduction in the Freshwater Crab *Oziotelphusa senex senex*. *Journal of Crustacean Biology.* **24**, 511–515.

Riley, L. G. and Tsukimura, B. (1998). Yolk Protein Synthesis in the Riceland Tadpole Shrimp, *Triops longicaudatus*, Measured by In Vitro Incorporation of 3H-Leucine. *J. Exp. Zool.* **281**, 238–247.

Rotllant, G., Takac, P., Liu, L., Scott, G. L., Laufer, H., and Laufer, H. (2000). Role of ecdysteroids and methyl farnesoate in morphogenesis and terminal moult in polymorphic males of the spider crab *Libinia emarginata*. *Aquaculture.* **190**, 103–118.

Rozewicki, J., Li, S., Amada, K. M., Standley, D. M., and Katoh, K. (2019). MAFFT-DASH: Integrated protein sequence and structural alignment. *Nucleic Acids Res.* **47**, W5–W10.

Santos, V. S. V., Caixeta, E. S., Campos Júnior, E. O. de, and Pereira, B. B. (2017). Ecotoxicological effects of larvicide used in the control of *Aedes aegypti* on nontarget organisms: Redefining the use of pyriproxyfen. *Journal of Toxicology and Environmental Health - Part A: Current Issues.* **80** (3), 155–160.

Satoh, T. and Hosokawa, M. (2006). Structure, function and regulation of carboxylesterases. *Chem. Biol. Interact.* **162**, 195–211.

Siegmund, T. and Lehmann, M. (2002). The *Drosophila* Pipsqueak protein defines a new family of helix-turn-helix DNA-binding proteins. *Dev. Genes Evol.* **212**, 152–157.

Singh, K. P. and Maddheshiya, R. (2021). Effect of Juvenile Hormone Analogue, Fenoxycarb on Post Embryonic Development of Blow Fly, *Chrysomya megacephala*. *J. Exp. Zool. India.* **24**, 405–413.

Skinner, D. M. (1962). The Structure and Metabolism of a Crustacean Integumentary Tissue During a Molt Cycle. *Biol. Bull.* **123** (3), 635–647.

Skinner, D. M. (1985a). Interacting Factors in the Control of the Crustacean Molt Cycle. *American Zool.* **25**, 275–284.

Skinner, D. M. (1985b). "Molting and Regeneration," in *Biology of Crustacea*, (Academic Press), 550.

Skinner, D. M. and Graham, D. E. (1972). Loss of Limbs as a Stimulus to Ecdysis in Brachyura (True Crabs). *Biol. Bull.* **143**, 222–233.

Smith, P. A., Clare, A. S., Rees, H. H., Prescott, M. C., Wainwright, G., and Thorndyke, M. C. (2000). Identification of methyl farnesoate in the cypris larva of the barnacle, *Balanus amphitrite*, and its role as a juvenile hormone. *Insect Biochem. Mol. Biol.* **30**, 885–890.

Song, J., Li, W., Zhao, H., Gao, L., Fan, Y., and Zhou, S. (2018). The microRNAs let 7 and mir 278 regulate insect metamorphosis and oogenesis by targeting the juvenile hormone early response gene Krüppel homolog. *Development.* **145** (24), dev170670.

Spindler, K. D., Hönl, C., Tremmel, C., Braun, S., Ruff, H., and Spindler-Barth, M. (2009). Ecdysteroid hormone action. *Cellular and Molecular Life Sciences.* **66**, 3837–3850.

Steenwyk, J. L., Buida, T. J., Li, Y., Shen, X. X., and Rokas, A. (2020). ClipKIT: A multiple sequence alignment trimming software for accurate phylogenomic inference. *PLoS Biol.* **18**.

Stueckle, T. A., Likens, J., and Foran, C. M. (2008). Limb regeneration and molting processes under chronic methoprene exposure in the mud fiddler crab, *Uca pugnax*. *Comparative Biochemistry and Physiology - C Toxicology and Pharmacology.* **147,** 366–377.

Stueckle, T. A., Shock, B., and Foran, C. M. (2009). Multiple Stressor Effects of Methoprene, Permethrin, and Salinity on Limb Regeneration and Molting in the Mud Fiddler Crab (*Uca pugnax*). *Environ. Toxicol. Chem.* **28**, 2348–2359.

Suzuki, Y., Shiotsuki, T., Jouraku, A., Miura, K., and Minakuchi, C. (2021). Characterization of E93 in neometabolous thrips *Frankliniella occidentalis* and *Haplothrips brevitubus*. *PLoS One.* **16**.

Takac, P., Ahl, J. S. B., and Laufer, H. (1997). Seasonal differences in methyl farnesoate esterase activity in tissues of the spider crab *Libinia emarginata*. *Invertebr. Reprod. Dev.* **31**, 211–216.

Takác, **P.**, Ahl, J. S. B., and Laufer, H. (1998). Methyl farnesoate binding proteins in tissues of the spider crab, *Libinia emarginata*. *Comparative Biochemistry and Physiology Part B.* **120**, 769–775.

Tamone, S. L. and Chang, E. S. (1993). Methyl farnesoate stimulates Ecdysteroid Secretion from Crab Y-organs *in Vitro*. *General and Comparative Endocrinology.* **89** (3), 425–432.

Tamone, S. L., Prestwich, G. D., and Chang, E. S. (1997). Identification and Characterization of Methyl Farnesoate Binding Proteins from the Crab, *Cancer magister*. *Gen. Comp. Endocrinol.* **105**, 168–175.

Tao, T., Xie, X., Liu, M., Jiang, Q., and Zhu, D. (2017). Cloning of two carboxylesterase cDNAs from the swimming crab *Portunus trituberculatus*: Molecular evidences for their putative roles in methyl farnesoate degradation. *Comp. Biochem. Physiol. B Biochem. Mol. Biol.* **203**, 100–107.

Tobe, S. S., Young, D. A., and Khoo, H. W. (1989a). Production of Methyl Farnesoate by the Mandibular Organs of the Mud Crab, *Scylla serrata*: Validation of a Radiochemical Assay. *General and Comparative Endocrinology.* **73**, 342–353.

Toyota, K., Yamane, F., and Ohira, T. (2020b). Impacts of Methyl Farnesoate and 20-Hydroxyecdysone on Larval Mortality and Metamorphosis in the Kuruma Prawn *Marsupenaeus japonicus*. *Front. Endocrinol.* **11**.

Tu, S., Tuo, P., Xu, D., Wang, Z., Wang, M., Xie, X., and Zhu, D. (2022). Molecular Characterization of the Cytochrome P450 Epoxidase (CYP15) in the Swimming Crab *Portunus trituberculatus* and Its Putative Roles in Methyl Farnesoate Metabolism. *Biological Bulletin.* **242**, 75–86.

Ureña, E., Chafino, S., Manjón, C., Franch-Marro, X., and Martín, D. (2016). The Occurrence of the Holometabolous Pupal Stage Requires the Interaction between E93, Krüppel-Homolog 1 and Broad-Complex. *PLoS Genet.* **12** (5), e1006020.

Ureña, E., Manjón, C., Franch-Marro, X., and Martín, D. (2014). Transcription factor E93 specifies adult metamorphosis in hemimetabolous and holometabolous insects. *Proc. Natl. Acad. Sci. U. S. A.* **111** (19), 7024–7029.

Wang, D., Lv, W., Yuan, Y., Zhang, T., Teng, H., Losey, J. E., and Chang, X. (2022). Effects of insecticides on malacostraca when managing diamondback moth (*Plutella xylostella*) in combination planting-rearing fields. *Ecotoxicol. Environ. Saf.* **229**, 113090.

Wang, P., Cui, Q., Wang, X., Liu, Y., Zhang, Y., Huang, X., Jian, S., Jiang, M., Bi, L., Li, B., Wei, W., and Pan, Z. (2023). The inhibition of ecdysone signal pathway was the key of pyriproxyfen poisoning for silkworm, *Bombyx mori. Pestic. Biochem. Physiol.* **189**, 105307.

Waterhouse, A. M., Procter, J. B., Martin, D. M. A., Clamp, M., and Barton, G. J. (2009). Jalview Version 2- A multiple sequence alignment editor and analysis workbench. *Bioinformatics.* **25** (9), 1189–1191.

Wu, Z., Yang, L., Li, H., and Zhou, S. (2021). Krüppel-homolog 1 exerts anti-metamorphic and vitellogenic functions in insects via phosphorylation-mediated recruitment of specific cofactors. *BMC Biol.* **19**, 222.

Xie, X., Liu, M., Jiang, Q., Zheng, H., Zheng, L., and Zhu, D. (2018). Role of Kruppel homolog 1 (Kr-h1) in methyl farnesoate-mediated vitellogenesis in the swimming crab *Portunus trituberculatus*. *Gene.* **679**, 260–265.

Xie, Y., Li, H., Luo, X., Li, H., Gao, Q., Zhang, L., Teng, Y., Zhao, Q., Zuo, Z., and Ren, R. (2022). IBS 2.0: an upgraded illustrator for the visualization of biological sequences. *Nucleic Acids Res.* **50** (W1), W420–W426.

Xu, Y., Zhao, M., Deng, Y., Yang, Y., Li, X., Lu, Q., Ge, J., Pan, J., and Xu, Z. (2017). Molecular cloning, characterization and expression analysis of two juvenile hormone esterase-like carboxylesterase cDNAs in Chinese mitten crab, *Eriocheir sinensis*. *Comp. Biochem. Physiol. B Biochem. Mol. Biol.* **205**, 46–53.

Yamada, K. D., Tomii, K., and Katoh, K. (2016). Application of the MAFFT sequence alignment program to large data - Reexamination of the usefulness of chained guide trees. *Bioinformatics.* **32** (21), 3246–3251.

Yamamoto, H., Okino, T., Yoshimura, E., Tachibana, A., Shimizu, K., and Fusetani, N. (1997). Methyl farnesoate induces larval metamorphosis of the barnacle, *Balanus amphitrite* via protein kinase C activation. *Journal of Experimental Zoology.* **278** (6), 349–355.

Yokoi, T. (2024). Design, synthesis, and biological evaluation of insect hormone agonists. *J. Pestic. Sci.* **49** (4), 303–310.

Yu, Q. Y., Lu, C., Li, W. Le, Xiang, Z. H., and Zhang, Z. (2009). Annotation and expression of carboxylesterases in the silkworm, *Bombyx mori*. *BMC Genomics.* **10**, 553.

Yu, X., Chang, E. S., and Mykles, D. L. (2002). Characterization of Limb Autotomy Factor-Proecdysis (LAF_{pro}), Isolated From Limb Regenerates, That Suspends Molting in the Land Crab *Gecarcinus lateralis*. *Bio. Bull.* **202** (3), 204–212.

Zhang, J., Liu, X., Liu, Y., An, Y., Fang, H., Michaud, J. P., Zhang, H., Li, Y., Zhang, Q., and Li, Z. (2019a). Molecular Characterization of Primary Juvenile Hormone Responders Methoprene-Tolerant (Met) and Krüppel Homolog 1 (Kr-h1) in *Grapholita molesta* (Lepidoptera: Tortricidae) with Clarification of Their Roles in Metamorphosis and Reproduction. *J. Econ. Entomol.* **112** (5), 2369–2380.

Zhang, X., Yuan, J., Sun, Y., Li, S., Gao, Y., Yu, Y., Liu, C., Wang, Q., Lv, X., Zhang, X., Ma, K. Y., Wang, X., Lin, W., Wang, L., Zhu, X., Zhang, C., Zhang, J., Jin, S., Yu, K., Kong, J., Xu, P., Chen, J., Zhang, H., Sorgeloos, P. Sagi, A., Alcivar–Warren, Liu, Z., Wang, L., Ruan, J., Chu, K. H., Liu, B., Li, F., and Xiang, J. (2019b). Penaeid shrimp genome provides insights into benthic adaptation and frequent molting. *Nat. Commun.* **10**, 356.

Zhang, Z., Xu, J., Sheng, Z., Sui, Y., and Palli, S. R. (2011). Steroid receptor co-activator is required for juvenile hormone signal transduction through a bHLH-PAS transcription factor, methoprene tolerant. *Journal of Biological Chemistry.* **286** (10), 8437–8447.

Zhang, X., Yuan, J., Zhang, X., Xiang, J., and Li, F. (2020). Genomic Characterization and Expression of Juvenile Hormone Esterase-Like Carboxylesterase Genes in Pacific White Shrimp, *Litopenaeus vannamei*. *Int. J. Mol. Sci.* **21** (15), 5444.

Zhao, M., Wang, W., Ma, C., Zhang, F., and Ma, L. (2020). Characterization and expression analysis of seven putative JHBPs in the mud crab *Scylla paramamosain*: Putative relationship with methyl farnesoate. *Comp. Biochem. Physiol. B Biochem. Mol. Biol.* **241**, 110390.

Zhao, W. L., Liu, C. Y., Liu, W., Wang, D., Wang, J. X., and Zhao, X. F. (2014). Methoprene-tolerant 1 regulates gene transcription to maintain insect larval status. *J. Mol. Endocrinol.* **53** (1), 93–104.

Zhu, X. J., Xiong, Y., He, W., Jin, Y., Qian, Y. Q., Liu, J., and Dai, Z. M. (2018). Molecular cloning and expression analysis of a prawn (*Macrobrachium rosenbergii*) juvenile hormone esterase-like carboxylesterase following immune challenge. *Fish Shellfish Immunol.* **80**, 10–14.

CHAPTER 3

METHYL FARNESOATE SYNTHETIC GENE ANNOTATION AND RNA-SEQ ANALYSIS IN BRACHYURAN Y-ORGANS

Abstract

Methyl farnesoate (MF) is an acyclic sesquiterpenoid hormone produced by the crustacean mandibular organ (MO) that has roles in morphogenesis, metamorphosis, reproduction, and molting. However, the underlying mechanism of how MF mediates the molting gland (Y-organ or YO) production of ecdysteroids is unknown. MF is synthesized through the mevalonate and farnesyl diphosphate/isopentenoid pathway in which farnesoic acid *O*-methyltransferase (FAMeT) converts farneosic acid (FA) into MF in crustaceans. Crustacean FAMeT contains two methyltransferase domains and is a S-adenosyl-L-methionine (SAM) independent methyltransferase contrary to juvenile hormone acid methyl transferase (JHAMT), a SAM-dependent transferase involved in insect (and potentially crustacean) biosynthesis of JH and/or sesquiterpenoid hormones.

MF synthetic genes *3-hydroxy-3-methylglutaryl-CoA reductase* (*HMGR*), *FAMeT* (*a/b*), and *FAMeT2* were identified in the European green shore crab (*Carcinus maenas*) and the blackback land crab (*Gecarcinus lateralis*) YO transcriptome along with other related species. Phylogenetic analysis and sequence analysis indicated that HMGR is highly conserved while FAMeT and FAMeT2 are distinct transferases. Analysis of the *C. maenas* YO RNA-seq data showed *HMGR*, *FAMeT* (*a/b*), and *FAMeT2* were expressed at all stages of the molt cycle. *FAMeTa* nonetheless was largely more expressed in comparison to the other synthetic genes.

Analysis of *C. maenas* YO RNA-seq data showed that *Met, Src, Kr-h1, E93, CBP, CtBP* were expressed at all the molt stages. Analysis of *G. lateralis* YO RNA-seq data showed that *HMGR, FAMeT, FAMeT2* were expressed at the different molt stages besides in post molt (PM). However, *Gl-FAMeT* was expressed at higher levels compared to the other synthetic genes and was upregulated in mid premolt (MP).

These data indicate that the YO has the machinery to biosynthesize MF and/or a MF-like hormone. Moreso, FAMeT and FAMeT2 may serve different functionalities. Besides ecdysteroids, it is proposed that the YO may produce other hormones that impact ecdysteroidogenesis.

Introduction

Methyl farnesoate (MF) is a hydrophobic, acyclic sesquiterpenoid hormone, discovered by Laufer et al. (1987) in the spider crab, *Libinia emarginata*. MF is synthesized the mandibular organs (MO), a pair of highly vascularized endocrine glands, that were first described by Le Roux (1968) (Laufer et al., 1987a). The MO, analogous to the insect corpus allatum (CA) with ultrastructural similarities to the crustacean Y-organ (YO), is located at the base of the mandibular tendon (Table 3.1) (Laufer et al., 1987b; Tobe et al., 1989a; Nagaraju et al., 2004). The MO contains an unfolded and folded region to which the unfolded region contains C-type cells, large cells with numerous mitochondria and large vacuoles (Borst et al., 1994). On the other hand, fan-fold region contains A and B cells of which A cells are undifferentiated while the B cells contained numerous vacuoles and thus B cells are likely the site of MF synthesis (Borst et al., 1994). The MOs from the giant mud crab (*Scylla serrata*) have been shown to secrete (*in vitro*) both FA and MF with the FA secretion rate 10-fold higher than of MF; however,

hemolymph analyses detected the presence of only MF and not FA (Tobe et al., 1989b; Borst and Tsukimura, 1991; Tiu et al., 2012). As suggested by these results, although FA may potentially serve a biological importance itself, FA is likely to be quickly metabolized, sequestered, and/or taken up by other target tissues (Tobe et al., 1989b; Tiu et al., 2012). The MO is repressed by mandibular inhibiting hormone (MOIH), a neuropeptide produced by the X-organ, sinus gland complex (XO) within the eyestalk ganglia, through the action of second messenger cyclic guanosine monophosphate (cGMP) (Laufer et al., 1987b; Tsukimura and Borst, 1992; Wainwright et al., 1998; Borst et al., 2001). Neurotransmitters, such as serotonin, may indirectly stimulate MF synthesis by inhibiting MOIH secretion from the sinus gland (Girish et al., 2017; Farhadi et al., 2020).

MF is often referred by its nickname 'the crustacean juvenile hormone (JH)' as it is the unepoxidated form of the insect JH III and is implicated in several physiological processes (Borst et al., 1987b; Tsukimura et al., 1993; Homola and Chang, 1997c; Laufer and Biggers, 2001; Nagaraju, 2007). MF was shown to control morphogenesis in adult male red swamp crayfish (*Procambarus clarkii*) and spider crabs (Rotllant et al., 2000; Laufer et al., 2002, 2005). Additionally, MF stimulates gonad maturation and vitellogenesis in the freshwater crabs *Oziotelphusa senex senex* and *Travancoriana schirnerae*, the orange mud crab (*Scylla olivaecea*), the whiteleg shrimp (*Litopenaeus vannamei*), and the ridgeback shrimp (*Sicyonia ingentis*), but no effect on the Australian freshwater crayfish (*Cherax quadricarinatus*) (Reddy and Ramamurthi, 1998; Kalavathy et al., 1999; Abdu et al., 2001; Reddy et al., 2004; Paran et al., 2010; Alnawafleh et al., 2014; Devi et al., 2018; Muhd-Farouk et al., 2019). Crustacean development and metamorphosis is also affected by MF in the barnacle *Balanus amphitrite* cypris larva, karuma prawn larval (*Marsupenaeus japonicus*), and the giant freshwater prawn

(*Macrobrachium rosenbergii*) (Yamamoto et al., 1997; Abdu et al., 1998; Smith et al., 2000; Toyota et al., 2020a). Tamone and Chang (1993) showed that Dungeness crab YOs exposed to MF stimulated ecdysteroidogenesis (*in vitro*). MF and its stimulatory role in ecdysteroid production and molting has been further supported by other studies in *L. vannamei, O. senex senex, C. quadricarinatus,* and *T. schirnerae* (Abdu et al., 2001; Reddy et al., 2004; Alnawafleh et al., 2014; Raghavan and Ayanath, 2019).

MF biosynthesis is split into two phases: 1) the mevalonate (MVA) pathway and 2) the farnesyl diphosphate/isopentenoid pathway as summarized in Figure 3.1. In the first phase, acetyl coenzyme A (acetyl-CoA) is converted to hydroxymethylglutharyl-CoA (HMG-CoA) and then undergoes a rate-limiting reduction by 3-hydroxy-3-methylglutaryl coenzyme A (HMG-CoA reductase or HMGR) thus resulting in the production of mevalonate (Goldstein and Brown, 1990; Bellés et al., 2005). HMGR is a membrane-bound enzyme with a variable number of transmembrane domains that is highly conserved across living organisms (Bellés et al., 2005). Mevalonate undergoes a series of enzymatic events resulting in the conversion to farnesyl pyrophosphate (FPP), an important intermediate in the synthesis of cholesterol and other bioactive terpenoids, by the specific action of farnesyl diphosphate synthase (FPPS) (Bellés et al., 2005). Independent studies have demonstrated that RNA interference (RNAi) mediated knockdown of *HMGR* and *FPPS* have consequences on MF regulated physiological processes, including vitellogenesis in the Chinese mitten crab (*Eriocheir sinensis*) and vitellogenesis and metabolic gene responses in the red cherry shrimp (*Neocaridina denticulta sinensis*) (Chen et al., 2022b; Liu et al., 2022a).

Transitioning into the second phase, pyrophosphatase activity converts FPP to farnesol and subsequently into farnesoic acid (FA) by dehydrogenase activity (Bellés et al., 2005).

Farnesoic *O*-methyltransferase (FAMeT) converts FA into MF; however, depending on the type of JH and in which insect taxonomic order, FA can undergo two enzymatic steps resulting in the JH production (Noriega, 2014; Qu et al., 2015). Either FA is epoxidized by CYP15C1 into JH acid (JHA) and then is esterified by juvenile hormone methyl transferase (JHAMT), or it is esterified by JHAMT first and later epoxidized by CYP15A1 (Shinoda and Itoyama, 2003; Defelipe et al., 2011; Qu et al., 2018). JHAMT and FAMeT are distinct, critical enzymes for the biosynthesis of MF, JH, and/or additional potential terpenoids. However, these biosynthetic enzymes are often confused for one another due to inadequate information at the time of identification leading to poor annotations. The increase in data availability and power of bioinformatic tools provides the opportunity for a more thorough identification and/or reclassification of these biosynthetic enzymes. In terpenoid biosynthesis, it is understood that JHAMT is an insect innovation, while crustaceans utilize FAMeT; however, JHAMT has also been identified in crustaceans (Hui et al., 2010; Noriega, 2014; Cheong et al., 2015; Qu et al., 2015; Sin et al., 2015b; Miyakawa et al., 2018; Nouzova et al., 2021).

The *JHAMT* gene was first characterized in the domestic silk moth (*Bombyx mori*) and demonstrated to possess methyl transferase activity in the presence of both juvenile JHA and FA as substrates (Shinoda and Itoyama, 2003; Cheng et al., 2014). JHAMT and JHAMT-like enzymes encompass a variable number of methyltransf_12 domains (Cheng et al., 2014). JHAMT enzymes are S-adenosyl-L-methionine (SAM)-dependent methyltransferases, consisting of a substrate binding and Rossman-fold cofactor binding region (Shinoda and Itoyama, 2003; Guo et al., 2021). The SAM molecule is an essential cofactor that provides the methyl group to a substrate and generates the corresponding product S-adenosyl-L-homocysteine (SAH) (Shinoda and Itoyama, 2003; Guo et al., 2021). JHAMT has been identified in crustaceans the water flea

(*Daphnia pulex),* the giant tiger prawn (*Penaeus monodon*), and the gazami crab (*Portunus trituberculatus*) (Toyota et al., 2015; Xie et al., 2016a; Semchuchot et al., 2023). Although MF is understood to be synthesized by the MO, *FAMeT* transcripts have been identified in a variety of different tissues in various crustaceans (Table 3.2). FAMeT is a SAM-independent methyltransferase that contains two methyltransferase domains and many putative phosphorylation sites (Liu et al., 2022b).

To enhance the understanding of the role of MF on ecdysteroidogenesis, MF synthetic genes were investigated in adult, male brachyuran YO transcriptomes. In the current study, *HMGR*, *FAMeT* (*a/b*), and *FAMeT2* orthologs were identified and characterized in the European green shore crab (*Carcinus maenas*) and the blackback land crab (*Gecarcinus lateralis*) YO. The expression levels for each identified mRNA transcript were profiled throughout the progression of the molt cycle. These results are anticipated to help clarify if the YO synthesizes an innate source of MF and utilizing it as an autocrine regulatory factor.

Materials and methods

Animals

Adult male blackback land crabs (*Gecarcinus lateralis*) were collected from the Dominican Republic and shipped by air cargo to Colorado State University (CSU) (Fort Collins, Colorado). The land crabs were subsequently kept in an environmental chamber at a temperature of 27 °C with 75-80% humidity under a 12-hour light:12-hour dark cycle (Bliss and Boyer, 1964; Bliss, 1968). The animals were housed in large, plastic communal enclosures lined with Tekland Envigo Aspen Bedding Laboratory Grade #7093 shavings saturated with 5 parts per thousand (ppt) Instant Ocean® deionized water. The crabs were fed twice a week on a diet of

lettuce, carrots, and raisins coated with calcium powder. Before any experimental testing or tissue harvesting was conducted, the animals were acclimated to laboratory conditions for one month, while the third right leg was autotomized to monitor for any potential spontaneous molting (Covi et al., 2009). Molting was induced by removing five to eight walking legs, also referred to as multiple leg autotomy (MLA) (Skinner, 1962, 1985a, 1985b; Hopkins, 1982; Chang, 1995; Yu et al., 2002). Premolt progression was monitored by measuring the limb regenerate growth as determined by the regeneration index (R-index = [mm limb regenerate length x 100]/mm carapace width) (Bliss et al., 1966a; Hopkins, 1982). In addition to the R-index, molt stage was further confirmed by the hemolymph 20-hydroxyecdysone (20-E) titer; presence of the membranous layer, the innermost layer of the exoskeleton; and the presence of gastroliths (Skinner, 1962, 1985a, 1985b; Hopkins, 1982; Chang, 1995; Yu et al., 2002).

On the day of tissue harvesting, 100 μL of hemolymph was drawn using 22-gauge sterile, hypodermic needles from the randomly sampled individuals. The hemolymph sample was combined with 300 μL of 100% methanol (MeOH) in O-ring microcentrifuge tubes, quickly vortexed to prevent coagulation, and then stored at -20°C (Gianazza et al., 2021). 20-Hydroxyecdysone (20-E) titers were quantified with a competitive enzyme-linked immunosorbent assay (ELISA) using the AffiniPure™ Goat Anti-Rabbit IgG, Fc fragment specific secondary antibody (Jackson ImmunoResearch Inc. 111-005-008) and the SeraCare TMB Peroxidase Kit as described and modified by Kingan (1989) and Abuhagr et al. (2014), respectively (Yu et al., 2002).

In silico identification and feature recognition: phylogenetic, sequence, and domain characterization

Previously identified and/or annotated protein sequences of MF synthetic enzymes were used as queries in the National Center for Biotechnology Information Basic Local Alignment Search Tool (NCBI BLAST) program to search for candidate genes. Upon searching CrusTome and GenBank databases, additional sequences were collected; identities were verified through a reciprocal BLAST search (Pérez-Moreno et al., 2023). The reference sequence and the BLAST hit queries for each gene were aligned using the Multiple Alignment using Fast Fourier Transform (MAFFT) (v.7.490) with the *dash* parameter to refine the multiple sequence alignment (MSA) from the Database of Aligned Structural Homologs (DASH) (Katoh and Toh, 2008; Yamada et al., 2016; Rozewicki et al., 2019). Multiple sequence alignments (MSAs) were trimmed with ClipKIT with the smart-gap parameter to remove gaps, while preserving informative sites (Steenwyk et al., 2020). Additionally, phylogenetic analyses were performed on maximum likelihood phylogenetic trees using protein sequences constructed with IQ-Tree and the suitable model, as determined by ModelFinder, following the Baeysian Information Criteria (BIC) with branch support evaluated with 1,000 ultrafast bootstrap iterations (UFBoot = 1,000) (Hoang et al., 2017; Kalyaanamoorthy et al., 2017; Guindon, 2018; Minh et al., 2020). The phylogenetic trees were then rooted and visualized in FigTree (v1.4.4) and Inkscape (Rambaut, 2010). Sequences were further analyzed with the NCBI Conserved Domain Database (CDD) platform to predict conserved domains and residues. The contig architecture was visualized and annotated with Illustrator for Biological Sequences 2.0 (IBS 2.0) (Xie et al., 2022). NetPhos 3.1 web server (https://services.healthtech.dtu.dk/services/NetPhos-3.1/) was utilized to identify putative serine, threonine, and tyrosine phosphorylation sites (Blom et al., 1999, 2004). Species

taxonomic ranks were annotated according to the classifications defined by Giribet and Edgecombe (2019).

Differential gene expression (DGE)

C. maenas relative gene expression was acquired from the YO RNA-seq data generated by Oliphant et al. (2018) and assembled in the CrusTome database (v.0.1.0) (n = 5 biological replicates of paired YOs per molt stage) (Pérez-Moreno et al., 2023). Relative gene expression in the YOs was determined for *G. lateralis* using RNA-seq data from animals induced to molt by multiple leg autotomy (MLA) (n = pooled replicates of 3 animals each) (Das et al., 2018). Gene expression, measured as transcripts per million reads (TPM), was quantified using Salmon (v.1.7.0) with the "*--seqBias --gcBias –validateMappings*" parameters for quantitative accuracy and mitigation of possible biases. Transcript expression was graphed as mean TPM ± standard error of the mean (SEM). Statistical differences were analyzed with Analysis of Variance (ANOVA) and post-hoc Tukey's HSD test ($p < 0.05$).

Results

Identification and characterization of MF synthetic genes

To investigate crustacean MF synthetic genes, BLAST inquiry analyses of the CrusTome transcriptome database were performed using candidate genes, as indicated by the asterisk on the corresponding spreadsheet found on the online repository supplementary data. The *3-hydroxy-3-methyl-glutaryl-coenzyme reductase* (*HMGR*) gene was identified across different taxa within Clade Panarthropoda (Table 3.3). Genes encoding for the rate limiting biosynthetic enzymes were identified brachyuran YO transcriptomes accessed from the CrusTome database.

In *G. lateralis*, complete sequences of *Gl-HMGR, Gl-FAMeTa, Gl-FAMeTb,* and *Gl-FAMeT2* were identified in the YO transcriptome (Table 3.4). In *C. maenas*, complete *Cm-HMGR, Cm-FAMeTa,* and *Cm-FAMeT2* contigs and a partial *Cm-FAMeTb,* were identified in the YO transcriptome (Table 3.5). Each contig identity was verified through reciprocal BLAST searches as presented within the corresponding spreadsheet found in the supplementary data on the online repository.

3-Hydroxy-3-methyl-glutaryl-coenzyme reductase (HMGR)

Phylogenetic analysis of the HMGR maximum likelihood tree, constructed using protein sequences, revealed the partition into pancrustacean, chelicerate, and tardigrade clades (Figure 3.2). Further analysis of Clade Pancrustacea showed that related species were generally clustered according to lower hierarchal taxonomic ranks (e.g., class, order, and infraorder), except for copepods and *Daphnia*. Although copepods are members of Clade Multicrustacea, they were positioned at the split for Clade Allotriocarida, which includes insects and *Daphnia*. *Daphnia* was positioned between the clade division of Allotriocarida and Multicrustacea. Class Malacostraca were subdivided into their respective orders, with amphipods grouping closer to isopods than to the decapods. Moreover, decapod crustaceans were partitioned between the crab infraorders (Infraorders Anomura and Brachyura) and the lobsters and shrimp infraorders. However, penaeid shrimp orthologs were more similar to lobsters than to caridean shrimp orthologs.

While pancrustacean HMGR ortholog lengths vary across taxa, the length was overall similar across orders with the HMGR domain spanning most of the protein (Figure 3.3; Figures B1 and B2). Anomuran HMGR orthologs were relatively longer (<1000 amino acids in length)

than the other decapod infraorders, but were more similar in length to other crustaceans (e.g. amphipods and some copepods) and tardigrades (Figure 3.3 and Figure B1). Except for *C. maenas*, brachyuran HMGR proteins were ~920 – 970 amino acids in length, which was similar to the lobster and shrimp orthologs. However, HMGR in *C. maeans* (860 amino acids) and *Litopenaeus vannamei* (876 amino acids) were shorter in length compared to other species. Full-length HMGR contig sequences were extracted from *G. lateralis* and *C. maenas* YO transcriptome assemblies. A *Gl-HMGR* contig encoded a 961-amino acid protein (Table 3.4; Figure B3). A *Cm-HMGR* contig encoded an 860-amino acid protein (Table 3.5; Figure B4).

Farnesoic acid O-methyltransferase (FAMeT and FAMeT2)

Phylogenetic analysis of FAMeT proteins showed a clear division between insect and crustacean sequences (Figures 3.5 and 3.6). The crustacean sequences were further divided into FAMeT and FAMeT2 subclades with more FAMeT transcripts and isoforms identified compared to FAMeT2 (Figures 3.5 and 3.6). FAMeT transcripts were identified in euphausids, amphipods, isopods, and all representative decapod infraorders (Figures 3.5 and 3.6). Malacostracan crustacean FAMeT orthologs were divided into their respective orders with krill (euphausids) further separated from Orders Isopoda, Amphipoda, and Decapoda. Moreover, isopods and amphipods clustered closer together than to the decapod crustaceans. Most decapod infraorders followed taxonomic rank, except for the anomurans in which the hermit crabs and squat lobsters were segregated (Figures 3.5 and 3.6). FAMeT2 transcripts were identified in euphausids, amphipods, isopods, and all representative decapod infraorders, except for Infraorder Astacidea (Figures 3.5 and 3.6). Further analysis of malacostracan FAMeT2 showed that related species were clustered together at the order level with the euphausids set apart from the other represented

orders (Figures 3.5 and 3.6). The decapod crustaceans were divided between the crab infraorders (Infraorders Anomura and Brachyura) and the lobsters and shrimp infraorders; however, caridean shrimp orthologs were shown to be more similar to the crabs than to penaeid shrimp and spiny lobsters.

Crustacean FAMeT orthologs ranged between 274 and 302 amino acids in length and encompassed two methyltransferase (Methyltransf_FA) domains. Spiny lobster (Infraorder Achelata) orthologs were longer in length compared to the rest of the crustaceans (Figures 3.6 and B5). Decapod species exhibited various FAMeT isoforms that varied in length (e.g., long and short) (Figures 3.6 and B5). Two FAMeT isoforms (FAMeTa and FAMeTb) were identified in the blue crab (*Callinectes sapidus*), *C. maenas* (*Cm-FAMeTa/b*), and *G. lateralis* (*Gl-FAMeTa/b*) YO. *Cm-FAMeTa* and *Gl-FAMeTa* orthologs encoded a 280-amino acid protein, while *Cm-FAMeTa* and *Gl-FAMeTb* encoded shorter proteins (206 and 275 amino acids, respectively) (Tables 3.4 and 3.5). All the *FAMeT* transcripts identified in *G. lateralis* (Figures B6 and B7) and *C. maenas* (Figures B8 and B9) contained numerous putative phosphorylation sites (e.g., serine, threonine, and/or tyrosine). Crustacean FAMeT2 orthologs consisted of 324 to 355 amino acids (Figure 3.7). FAMeT2 differed from FAMeT as it contained one Methyltransf_FA domain that was followed by the domain of unknown function 3421 (DUF3421) (Figures 3.7 and B10).

Gene expression analysis

The relative gene expression of *HMGR*, *FAMeT2*, and *FAMeTa*, and *FAMeTb* was determined in the *C. maenas* YO across the different molt stages. All four genes were constitutively expressed, with *Cm-FAMeT* expressed at higher levels than the other three genes (Figure 3.15). There was no significant effect of molt stage on the relative expression of the four

genes. In *G. lateralis*, the relative gene expression of *Gl-HMGR*, *Gl-FAMeT2*, and *Gl-FAMeTa/b* (*a* and *b* combined), was determined in the YO across the different molt stages. *Gl-FAMeT* was expressed at significantly higher levels than the other two genes and was upregulated in mid-premolt (MP). All three genes; however, were downregulated and/or not expressed in postmolt (PM) (Figure 3.16).

Discussion

MF is a sesquiterpenoid hormone that regulates several physiological processes is conventionally understood to be produced by the crustacean MO(Homola and Chang, 1997c; Nagaraju, 2007). MF is biosynthesized through transferase activity of FA through FAMeT; however, there is difference between the enzyme(s) (FAMeT and JHAMT) that are responsible for MF synthesis. It was reported that *in vitro* FAMeT catalyzes FA into MF in the greasyback shrimp (*Metapenaeus ensis*), but not in the brown crab (*Cancer pagarus*) or the American lobster (*Homarus americanus*) (Gunawardene et al., 2002; Ruddell et al., 2003; Holford et al., 2004). Additionally, *Macrobrachium rosenbergii* FAMeT activity was affected by JHAMT and *Daphnia* JHAMT catalyzed FA into MF (Toyota et al., 2015; Qian and Liu, 2019). JHAMT has been identified in *P. trituberculatus* and *Neocaridina denticulata* (Sin et al., 2015b; Xie et al., 2016a). RNAi of *FAMeT* did not affect molting in postmolt *Neocaridina sinensis* individuals, unlike in *Litopenaeus vannemi* individuals where molting was inhibited and led to higher mortality (Hui et al., 2008; Liu et al., 2022b). With consideration to these data and the presence of FAMeT in various crustacean tissues, it is possible that FAMeT activity for the conversion of FA to MF may be subjected to the presence of binding proteins (Table 3.2).

Using GenBank and the CrusTome database, the MF biosynthetic rate limiting enzymes in HMGR and FAMeT were identified in pancrustacean taxa. The extracted contig sequences obtained from *G. lateralis* and *C. maenas* and *G. lateralis* YO transcriptomes were identified and characterized (Tables 3.4 and 3.5). Phylogenetic and bioinformatic analysis revealed high conservation of the domain organization, which will aid in the proper identification and annotation of new sequences as transcriptomes and genomes are added to GenBank and other repositories. HMGR sequences were identified in many crustacean species; however, HMGR was also identified in other arthropods (e.g. chelicerates) and even in an arthropod ancestor– the tardigrade (panarthropoda). The structure of HMGR was highly conserved across all taxa thus supporting that hypothesis that the mevalonate pathway is an ancestral signaling pathway involved in the isoprenoid biosynthesis (Lombard and Moreira, 2011).

Crustacean FAMeT is conventionally to have two methyltransferase domains (Methyltrans_FA) while insect FAMeT orthologs contain a Methyltrans_FA domain and a number of DM9 repeats. Phylogenetic analysis confirmed the divergence of the pancrustacean FAMeTs as crustacean FAMeT sequences formed a distinct group divergent from insect FAMeT orthologs. A FAMeT containing a DM9 repeat has been identified in the current study and in the mud crab *S. paramamosain*; however, its role in MF synthesis and in turn physiological roles, more specifically the differing effects in comparison to FAMeT is unknown (Zhao et al., 2018). Although, a DM9-containing protein was identified in the Chinese mitten crab (*Eriocheir sinensis*) and was reported to have roles in immunity, the relationship of FAMeT2 and DM9 containing proteins are not well understood (Li et al., 2024). This data supports the idea that the crustacean FAMeT is not orthologous to the insect FAMeT. FAMeT2 sequences were segregated from the FAMeT sequences, to, which, encompassed the conventional two Methyltrans_FA

domains. 21 genes with 37 isoforms implicated in MF biosynthesis were identified in the green mud crab (*Scylla paramamosain*) in the variety of tissues; the YO was not specifically investigated (Zhao et al., 2022). Out of the mutual genes of interest between the current study, Zhao et al. (2015), and Zhao et al. (2022), *FAMeT* and *FAMeT2* were not identified but only *HMGR* across the three brachyurans: two in *S. paramamosain,* one in *C. maenas,* and one in *G. lateralis*. In a previous study, *FAMeT2* was identified in also in *S. paramosain* (*Sp–FAMeT2*) (Zhao et al., 2018). During larval development there was a significant difference in the expression of *Sp-FAMeT2* and exhibited a similar expression that to *Sp–HMGR* (Zhao et al., 2015, 2018).

The MF biosynthetic genes were expressed in the *G. lateralis* and *C. maen*as YO at all molt stages. However, expression patterns were not consistent between species for each gene. The present study has profiled the expression of *C. maenas* MF synthetic genes *Cm-FAMeT a, Cm-FAMeTb, Cm-FAMeT2* and *Cm-HMGR* orthologs; however, these particular MF synthetic genes displayed no statistical difference between the stages. Although *Cm-FAMeTa* was expressed at higher levels in comparison to *Cm-FAMeTb*. *Cm-FAMeTb* was expressed at its highest point during while *Cm-FAMeTa* was downregulated in MP and subsequently LP. This data suggests that the two *Cm-FAMeT* variants have differing effects in the YO during the molt cycle. In the *G. lateralis* YO, *Gl-FAMeT* was highly expressed in MP in comparison to *Gl-FAMeT2* and *Gl-HMGR*. Gl-*FAMeT2* and *Gl-HMGR* was upregulated in IM but downregulated throughout the substages of premolt and post molt stages.

Conclusion

MF and sesquiterpenoid hormones are critical physiological endocrine regulators. The two rate-limiting enzymes involved in MF biosynthesis were characterized in the present study, including determining the phylogenetic relationships and the domain organization. The identification and characterization of these contiguous sequences in brachyuran YO suggests that the YO utilizes an innate MF version as an autocrine factor to regulate ecdysteroid synthesis. The interaction of FA with these various biosynthetic enzymes may result in different types of MF hormones and/or prohormones that serve different purposes. These results call for improvement in the annotations of pancrustacean FAMeT and like FAMeT-like enzymes as well as functional studies of each enzyme and the biproducts.

Data availability

The corresponding datasets in this study are available on the Harvard Dataverse online repository (Bentley, Vanessa, 2025, "Methyl farnesoate", https://doi.org/10.7910/DVN/BCG5V4, Harvard Dataverse, V1).

Table 3.1. Comparison of the histology and ultrastructure of the crustacean mandibular organ (MO) and the Y-organ (YO).

	Mandibular organ (MO)	Both MO and YO	Y-organ (YO)
Characteristics	▪ Large cell size, with centered nuclei containing ample cytoplasm, generally arranged in clusters ▪ Site of MF production ▪ Identified by Le Roux (1968)	▪ Vascularized endocrine glands ▪ Contains an extensive smooth endoplasmic reticulum and abundant in mitochondria ▪ Located in the cephalothorax ▪ Experiences ultrastructural changes (e.g. hypertrophy) throughout the molt cycle and/or reproductive cycles	▪ Relatively small cell size, with peripherally located nuclei, tightly packed together ▪ Site of ecdysteroid production ▪ Identified by Gabe (1953)
Species & References	▪ *Barytelphusa cunicularis* (Gopal et al., 2018) ▪ *Callinectes sapidus* (Yudin et al., 1980) ▪ *Libinia emargnata* (Hinsch, 1977) ▪ *Homarus americanus* (Byard et al., 1975) (Borst et al., 1994) ▪ *Penaeus japonicus* (Taketomi and Kawano, 1985)	▪ *Carcinus maenas* (Buchholz and Adelung, 1980) ▪ *Hemigrapsus nudus* (Buchholz and Adelung, 1980) ▪ *Procambarus clarkii* (Taketomi and Nakano, 2007) ▪ *Palaemon paucidens* (Aoto et al., 1974)	▪ *Scylla olivacea* (Achdiat et al., 2024) ▪ *Portunus trituberculatus* (Taketomi and Hyodo, 1986) ▪ *Cancer antennarius* (Hinsch et al., 1980) ▪ *Travancoriana schirnerae* (Ayanath and Raghavan, 2021) (Smija and Sudha Devi, 2016) ▪ *Libinia emargnata* (Hinsch and Hajj, 1975)

Table 3.2. Tissue distribution of farnesoic acid *O*-methyl transferase (FAMeT) transcripts identified in decapod crustaceans. Abbreviations: Br, brain; CNS, central nervous system; Ep, epidermis; EG, eyestalk ganglia; Gi, gill; Hc, hemocytes; Hp, hepatopancreas; Ht, heart; In, intestine; MO, mandibular organ; Mu, muscle; NC, nerve cord; Ov, ovary; St, stomach; Te, testis; TG, thoracic ganglion, and YO, Y-organ.[2]

Species	Gene #	Br	CNS	Ep	EG	Gi	Hc	Hp	Ht	In	MO	Mu	NC	Ov	St	Te	TG	YO
Brachyura																		
Cancer pagurus[a]	1			X	X	X		X	X	X	X	X		X				
Eriocheir sinensis[b]	1					X		X	X	X				X	X			
Portunus pelagicus[c]	3	X		X	X						X	X						X
Portunus trituberculatus[d]	1					X		X	X		X	X		X		X	X	X
Scylla olivacea[e]	1										X							
Scylla paramamosain[f]	3	X			X	X		X	X		X	X		X	X		X	
	1*	X		X		X	X	X	X		X	X		X			X	
Astacidea																		
Homarus americanus[g]	1										X	X						
Procambarus clarkii[h]	1				X				X		X	X	X					
Dendrobranchiata																		
Litopenaeus vannameii[i]	2				X			X	X			X	X					
Metapenaeus ensis[h, j]	1			X	X			X	X		X	X	X	X		X		
Penaeus chinensis[k]	1				X	X	X	X	X			X		X		X		
Penaeus indicus[l]	1		X		X			X	X	X		X		X				
Penaeus monodon[m]	2													X				
Caridea																		
Exopalaemon carinicauda[n]	1				X	X	X	X		X		X		X	X			
Macrobrachium rosenbergii[o]	1			X	X	X	X	X	X	X		X			X	X		
Neocaridina denticulata[p]	1				X	X		X	X	X		X		X		X		

[2]Asterisk (*) indicated the FAMeT containing one methyltransferase domain and one DM9-repeat containing domain of unknown function (DUF) unlike the conventional two methyltransferase domains. The presence of the FAMeT transcript in which gonadal tissue in *P. chinensis* was not specified and thereby both Ov and Te are denotated. References: [a]Ruddell et al., 2003; [b]Chen et al., 2021; [c]Kuballa et al., 2007; [d]Xie et al., 2013, 2015; [e]Sunarti et al., 2016; Tahya et al., 2016; [f]Yang et al., 2012; Zhao et al., 2018; [g]Holford et al., 2004; [h]Gunawardene et al., 2003; [i]Hui et al., 2008; [j]Gunawardene et al., 2001, 2002; [k]Li et al., 2013; [l]Saikrithi et al., 2019; [m]Buaklin et al., 2015; [n]Duan et al., 2014; [o]Qian and Liu, 2019; [p]Liu et al., 2022.

Table 3.3. Taxonomic distribution of identified 3-hydroxy-3-methyl-glutaryl-coenzyme reductase (HMGR).

Taxon						Gene *HMGR*
Clade Panarthropoda					Phylum Tardigrada	3
	Phylum Arthropoda				Subphylum Chelicerata	3
		Clade Pancrustacea	Clade Allotriocarida		Class Insecta	33
					Class Branchiopoda	1
			Clade Multicrustacea		Class Copepoda	7
				Class Malacostraca	Order Isopoda	7
					Order Amphipoda	18
					Order Decapoda	32
					Total Number of Contigs	**104**
					Total Number of Species	**96**

Table 3.4. Methyl farnesoate (MF) synthetic genes from the *G. lateralis* Y-organ (YO) transcriptome (Pérez-Moreno et al., 2023). Abbreviations: aa, amino acids; bp, base pairs; ID, identification; ORF, open reading frame; and UTR, untranslated region. Asterisk indicates partial sequence (incomplete ORF).

Gene	Class	Contig ID	Length (bp)	ORF (aa)	UTR (bp)	GenBank Accession
Gl-HMGR	Reductase	Y EVm001453t1	5289	961	**5':** 25 **3':** 2378	PQ346928
Gl-FAMeTa	Transferase	Y EVm010627t1	1403	280	**5':** 124 **3':** 435	PV020720
Gl-FAMeTb	Transferase	Y EVm010627t2	1388	275	**5':** 124 **3':** 435	PV020721
Gl-FAMeT2	Transferase	Y EVm014805t1	814	206*	**5':** 157 **3':** 36	PV019009

Table 3.5. Methyl farnesoate (MF) synthetic genes from the *C. maenas* Y-organ (YO) transcriptome (Pérez-Moreno et al., 2023). Abbreviations: aa, amino acids; bp, base pairs; ID, identification; ORF, open reading frame; and UTR, untranslated region. Asterisk indicates partial sequence (incomplete ORF).

Gene	Class	Contig ID	Length (bp)	ORF (aa)	UTR (bp)	GenBank Accession
Cm-HMGR	Reductase	Y EVm002033t1	2659	860	**5':** 36 **3':** 40	PV019008
Cm-FAMeTa	Transferase	Y EVm013262t1	1405	280	**5':** 133 **3':** 429	PV020722
Cm-FAMeTb	Transferase	Y EVm013262t2	1051	206*	**5':** – **3':** 429	PV020723
Cm-FAMeT2	Transferase	Y EVm010974t1	1264	330	**5':** 251 **3':** 18	PV018988

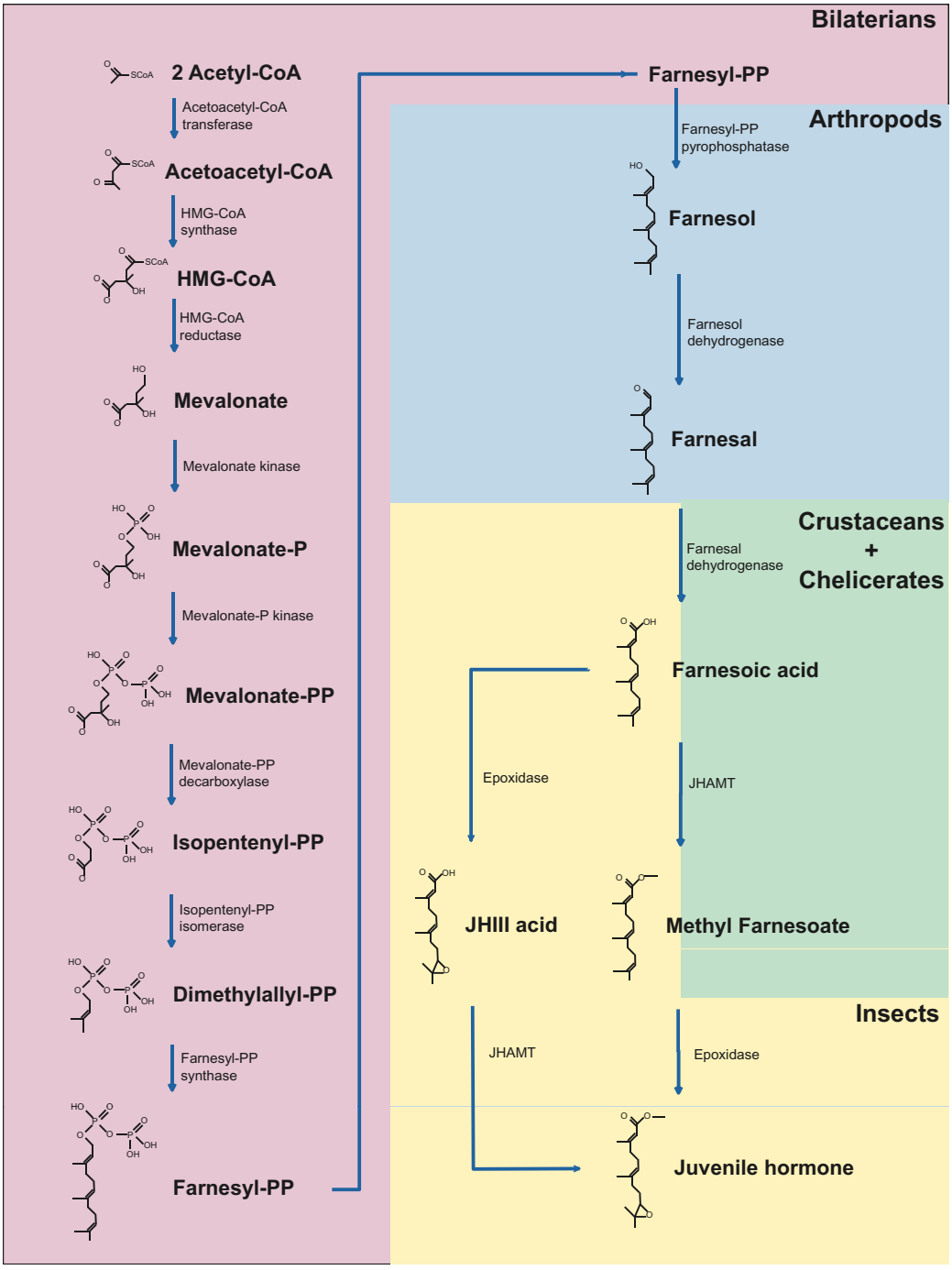

Figure 3.1. An overlook at the methyl farnesoate (MF) and juvenile hormone (JH) biosynthetic pathway. Figure adapted and modified from Cheong et al. (2015).

Figure 3.2

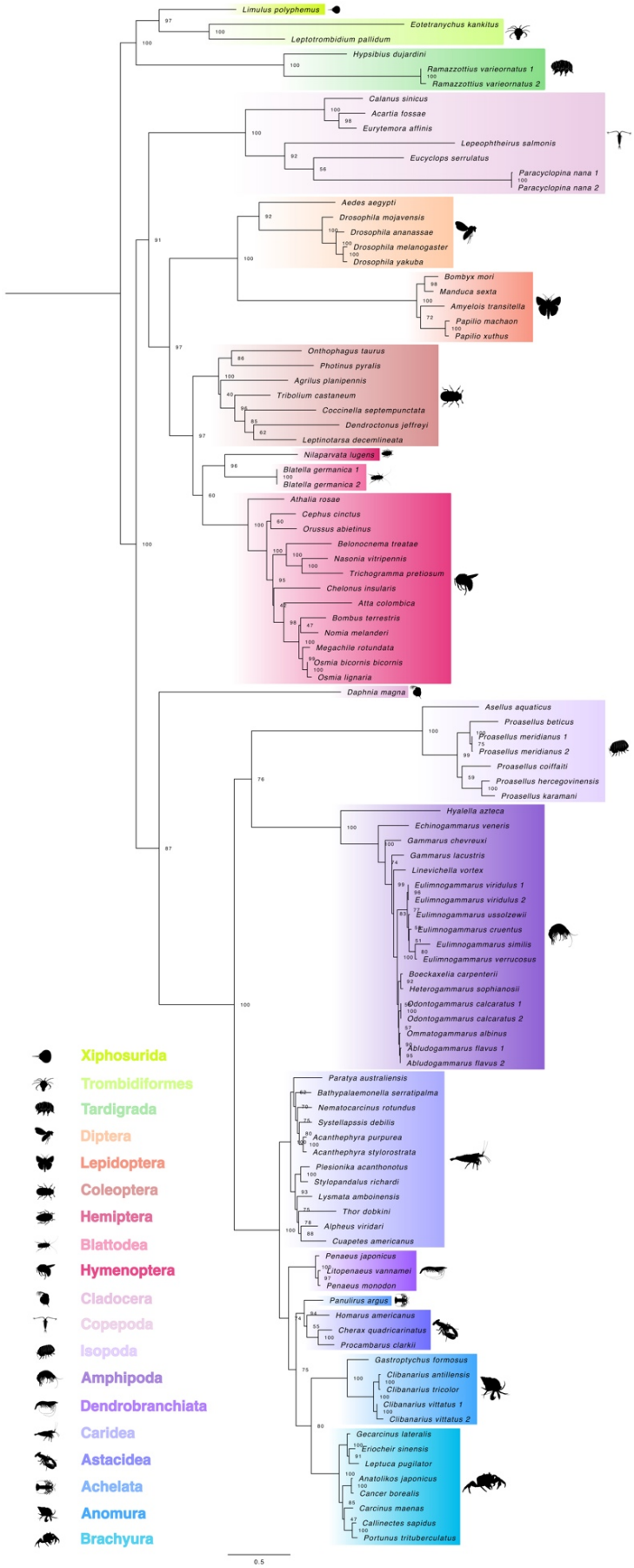
Limulus polyphemus
Eotetranychus kankitus
Leptotrombidium pallidum
Hypsibius dujardini
Ramazzottius varieornatus 1
Ramazzottius varieornatus 2
Calanus sinicus
Acartia fossae
Eurytemora affinis
Lepeophtheirus salmonis
Eucyclops serrulatus
Paracyclopina nana 1
Paracyclopina nana 2
Aedes aegypti
Drosophila mojavensis
Drosophila ananassae
Drosophila melanogaster
Drosophila yakuba
Bombyx mori
Manduca sexta
Amyelois transitella
Papilio machaon
Papilio xuthus
Onthophagus taurus
Photinus pyralis
Agrilus planipennis
Tribolium castaneum
Coccinella septempunctata
Dendroctonus jeffreyi
Leptinotarsa decemlineata
Nilaparvata lugens
Blatella germanica 1
Blatella germanica 2
Athalia rosae
Cephus cinctus
Orussus abietinus
Belonocnema treatae
Nasonia vitripennis
Trichogramma pretiosum
Chelonus insularis
Atta colombica
Bombus terrestris
Nomia melanderi
Megachile rotundata
Osmia bicornis bicornis
Osmia lignaria
Daphnia magna
Asellus aquaticus
Proasellus beticus
Proasellus meridianus 1
Proasellus meridianus 2
Proasellus coiffaiti
Proasellus hercegovinensis
Proasellus karamani
Hyalella azteca
Echinogammarus veneris
Gammarus chevreuxi
Gammarus lacustris
Linevichella vortex
Eulimnogammarus viridulus 1
Eulimnogammarus viridulus 2
Eulimnogammarus ussolzewii
Eulimnogammarus cruentus
Eulimnogammarus similis
Eulimnogammarus verrucosus
Boeckaxelia carpenterii
Heterogammarus sophianosii
Odontogammarus calcaratus 1
Odontogammarus calcaratus 2
Ommatogammarus albinus
Abludogammarus flavus 1
Abludogammarus flavus 2
Paratya australiensis
Bathypalaemonella serratipalma
Nematocarcinus rotundus
Systellapsis debilis
Acanthephyra purpurea
Acanthephyra stylorostrata
Plesionika acanthonotus
Stylopandalus richardi
Lysmata amboinensis
Thor dobkini
Alpheus viridari
Cuapetes americanus
Penaeus japonicus
Litopenaeus vannamei
Penaeus monodon
Panulirus argus
Homarus americanus
Cherax quadricarinatus
Procambarus clarkii
Gastroptychus formosus
Clibanarius antillensis
Clibanarius tricolor
Clibanarius vittatus 1
Clibanarius vittatus 2
Gecarcinus lateralis
Eriocheir sinensis
Leptuca pugilator
Anatolikos japonicus
Cancer borealis
Carcinus maenas
Callinectes sapidus
Portunus trituberculatus
0.5
Xiphosurida
Trombidiformes
Tardigrada
Diptera
Lepidoptera
Coleoptera
Hemiptera
Blattodea
Hymenoptera
Cladocera
Copepoda
Isopoda
Amphipoda
Dendrobranchiata
Caridea
Astacidea
Achelata
Anomura
Brachyura

Figure 3.2. Phylogeny of panarthropod HMGR proteins. The trimmed maximum likelihood phylogenetic tree was constructed with IQ-TREE using the Bayesian information criterion (BIC) best-fit model JTT+I+I+R6. The relationship confidence values at each branch point were determined with ultrafast bootstrap analysis (UFBoot = 1000). The scale bar for the branch lengths represents the estimated average of substitutions per site as visualized in FigTree. Sequences and databases used in the analysis are in the supplementary data spreadsheet found on the online repository. Species silhouettes were obtained from PhyloPic (http://phylopic.org).

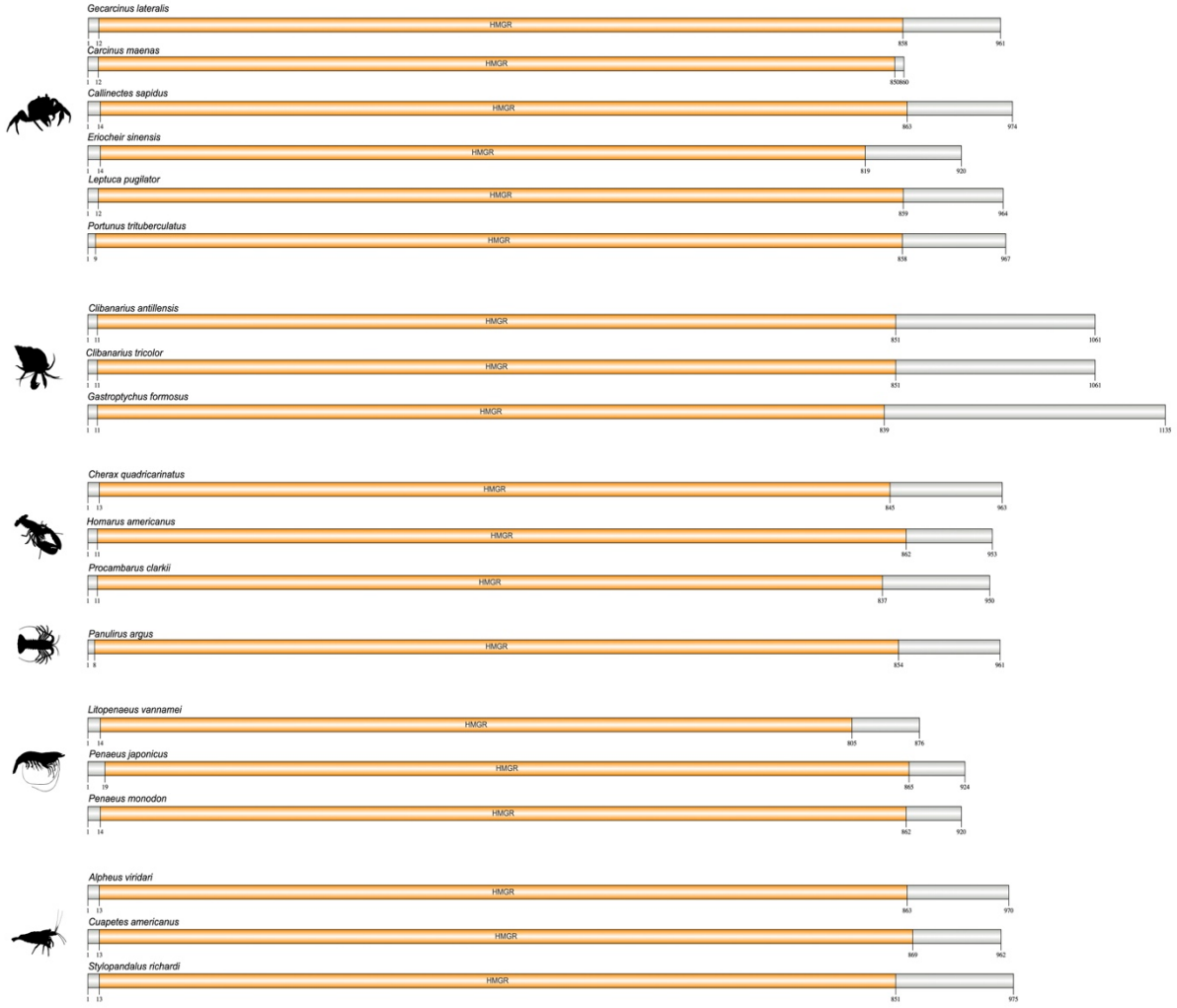

Figure 3.3. Domain organization of decapod crustaceans 3-hydroxy-3-methyl-glutaryl-coenzyme reductase (HMGR) proteins. Domains were identified with the NCBI CD search tool and visualized with IBS 2.0 (see Materials and Methods). Information for the sequences is provided in the supplementary data spreadsheet on the online repository. Species silhouettes were obtained from PhyloPic (http://phylopic.org).

Figure 3.4

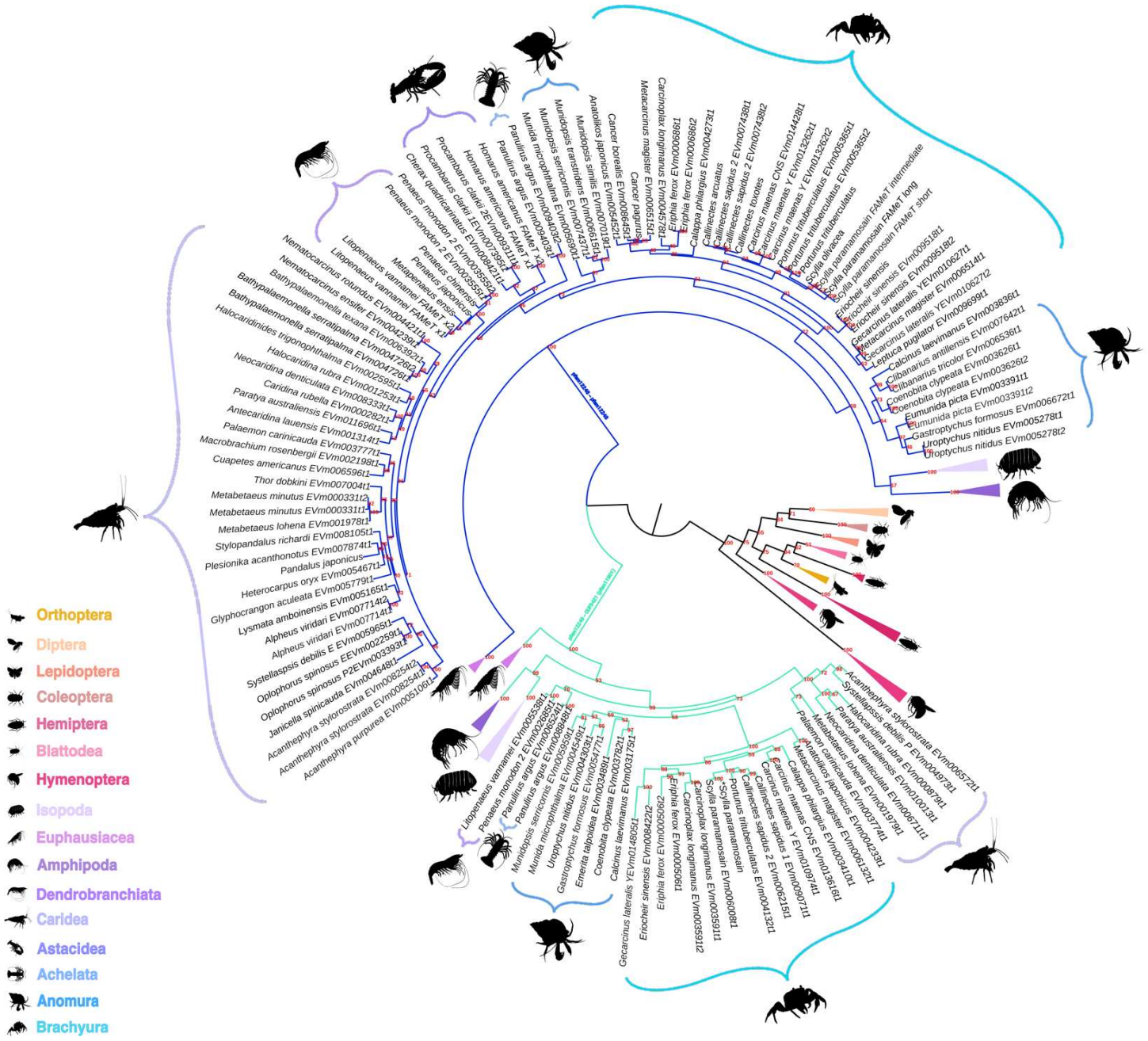
Orthoptera
Diptera
Lepidoptera
Coleoptera
Hemiptera
Blattodea
Hymenoptera
Isopoda
Euphausiacea
Amphipoda
Dendrobranchiata
Caridea
Astacidea
Achelata
Anomura
Brachyura

Figure 3.4. Phylogenetic tree of pancrustacean farnesoic acid *O*-methyltransferase (FAMeT) trimmed maximum likelihood phylogenetic tree constructed with IQ-TREE using the Bayesian information criterion (BIC) best-fit model Q.pfam+R6 visualized with TreeViewer. The relationship confidence levels are denoted with ultrafast bootstrap analysis (UFBoot = 1000) and the scale bar representing the estimated average of substitutions per site. Two FAMeT transcripts exist with differing domain architectures. FAMeT2 encompassed a methyl transferase (pfam12248) and a domain of unknown function (DUF3421; pfam11901) as indicated in green branches. FAMeT, depicted in blue branches, consisted of two sequential methyl transferase domains (Methyltransf_FA; pfam12248). Refer to Figure 8 for different phylogenetic representation including insect relatives. Sequences and databases used in the analysis are in the supplementary data spreadsheet on the online repository. Species silhouettes were obtained from PhyloPic (http://phylopic.org).

Figure 3.5

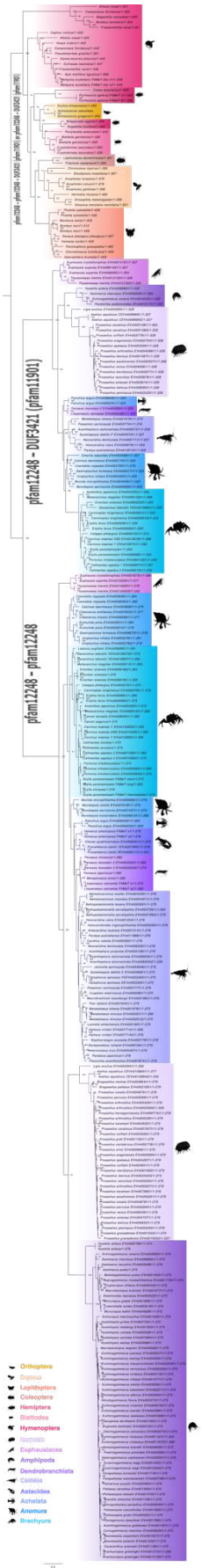
pfam12248 – DUF3421 (pfam11901)
pfam12248 – pfam12248
Orthoptera
Blattoa
Lepidoptera
Coleoptera
Hemiptera
Blattodea
Hymenoptera
Isopoda
Euphausiacea
Amphipoda
Dendrobranchiata
Caridea
Astacidea
Achelata
Anomura
Brachyura

Figure 3.5 (continued)

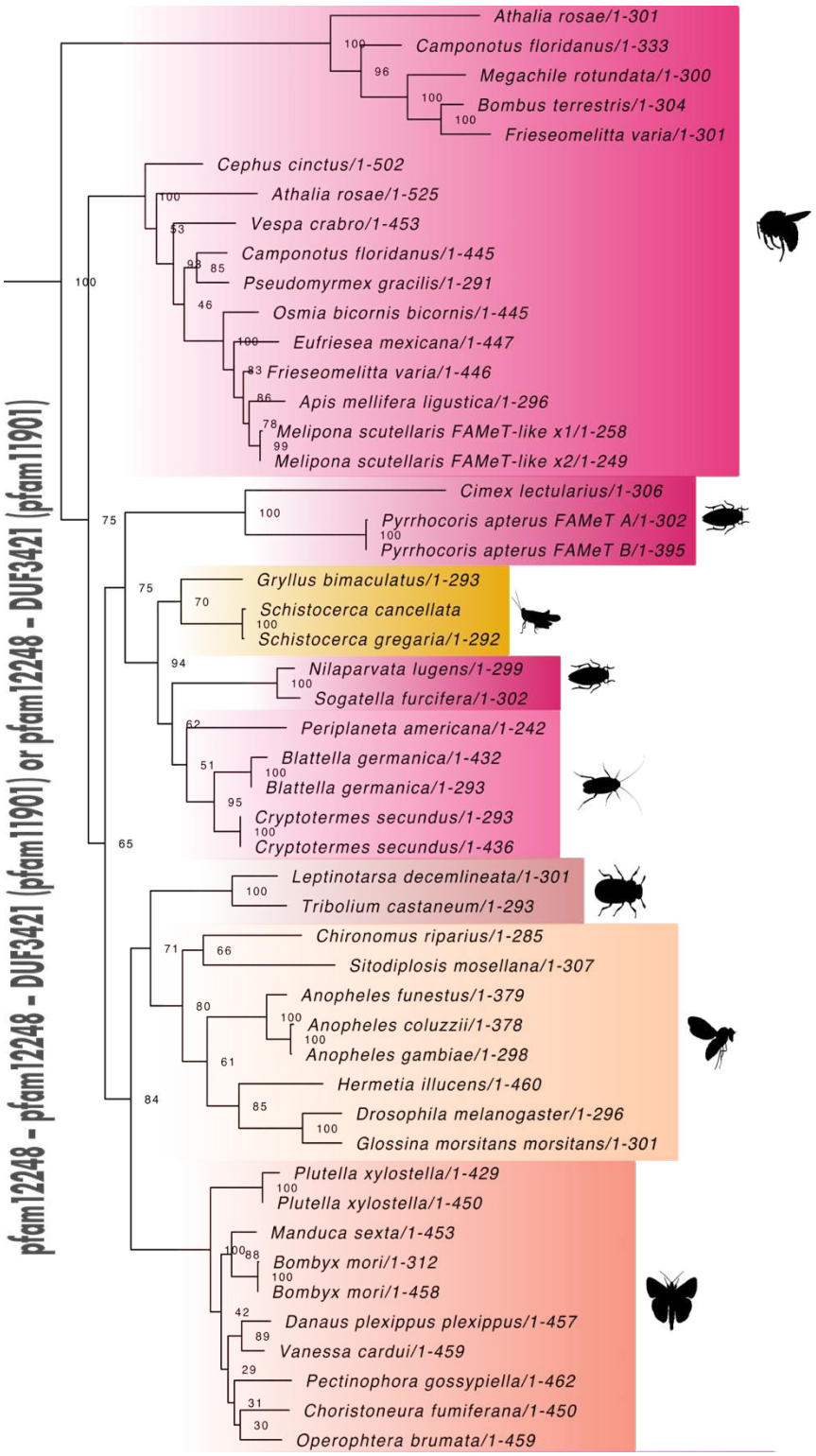

Figure 3.5 (continued)

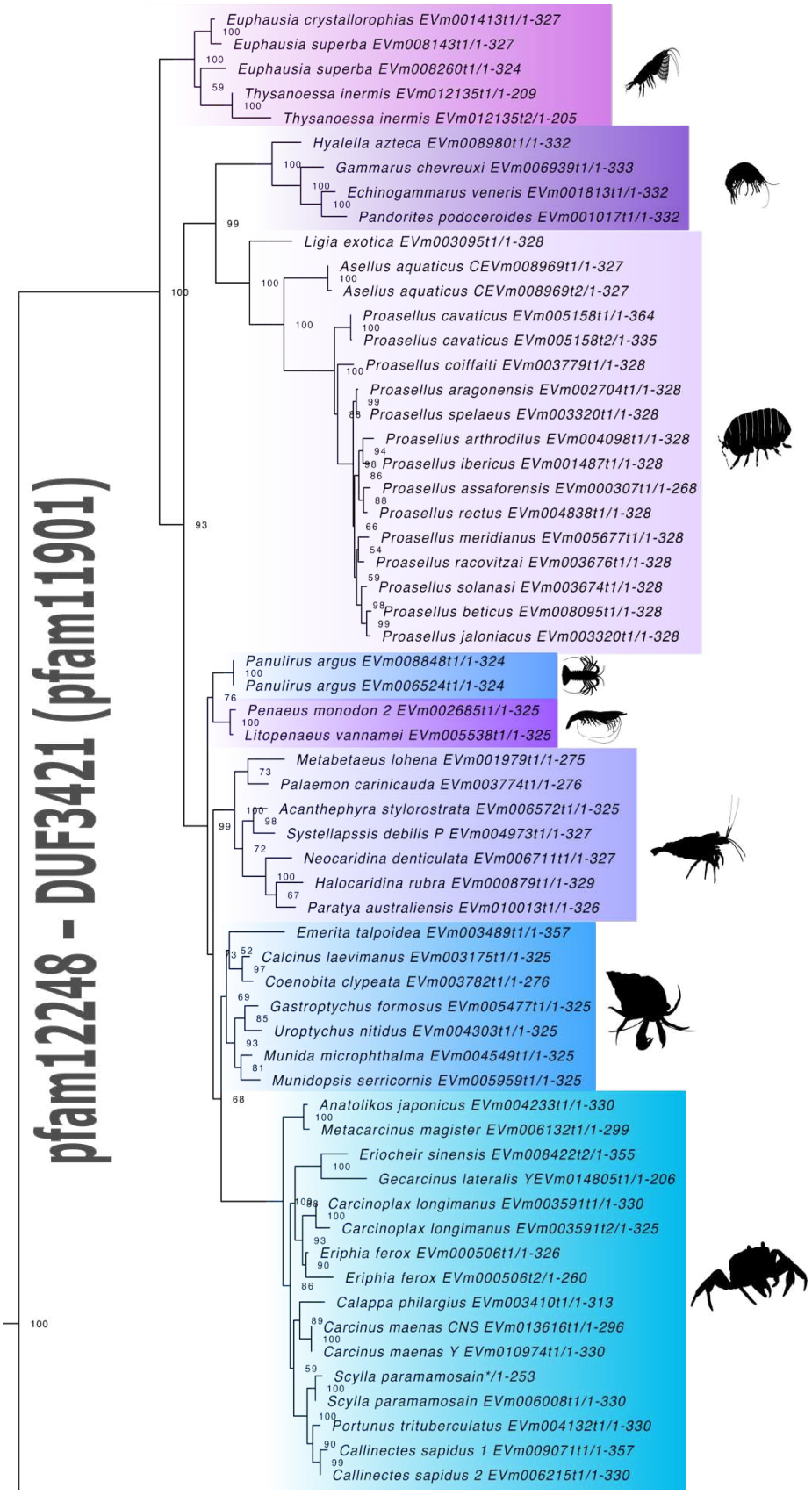

Figure 3.5 (continued)

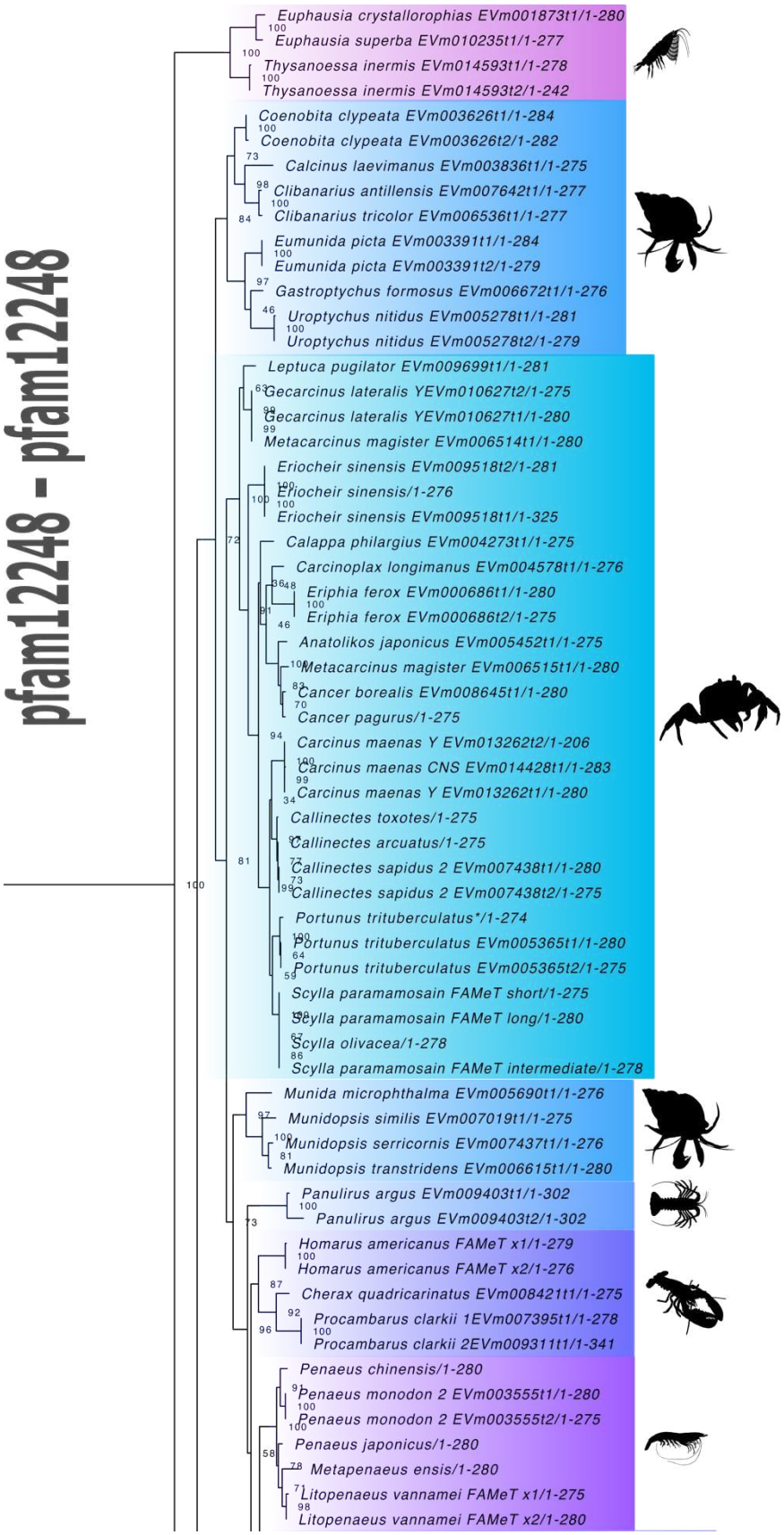

Figure 3.5 (continued)

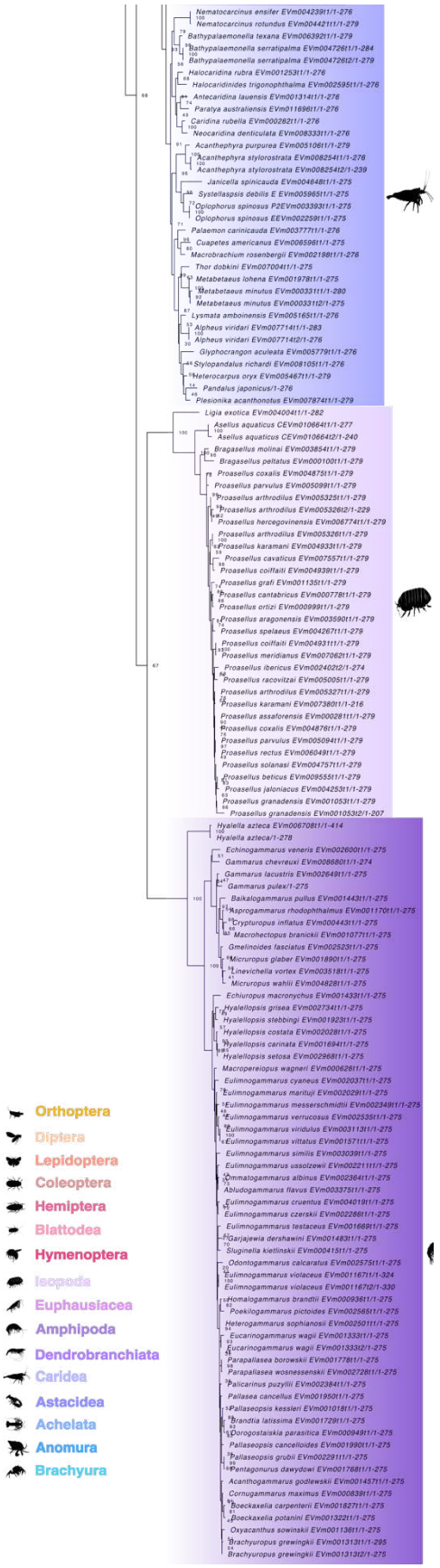

Figure 3.5. Phylogenetic tree of pancrustacean farnesoic acid *O*-methyltransferase (FAMeT) trimmed maximum likelihood phylogenetic tree constructed with IQ-TREE using the Bayesian information criterion (BIC) best-fit model Q.pfam+R6 visualized with TreeViewer. The relationship confidence levels are denoted with ultrafast bootstrap analysis (UFBoot = 1000) and the scale bar representing the estimated average of substitutions per site. Two FAMeT transcripts exist with differing domain architectures. FAMeT2 encompassed a methyl transferase (pfam12248) and a domain of unknown function (DUF3421;pfam11901) while FAMeT consisted of two sequential Methyltransf_FA (pfam12248) domains. Sequences and databases used in the analysis are in the supplementary data spreadsheet found on the online repository. Species silhouettes were obtained from PhyloPic (http://phylopic.org).

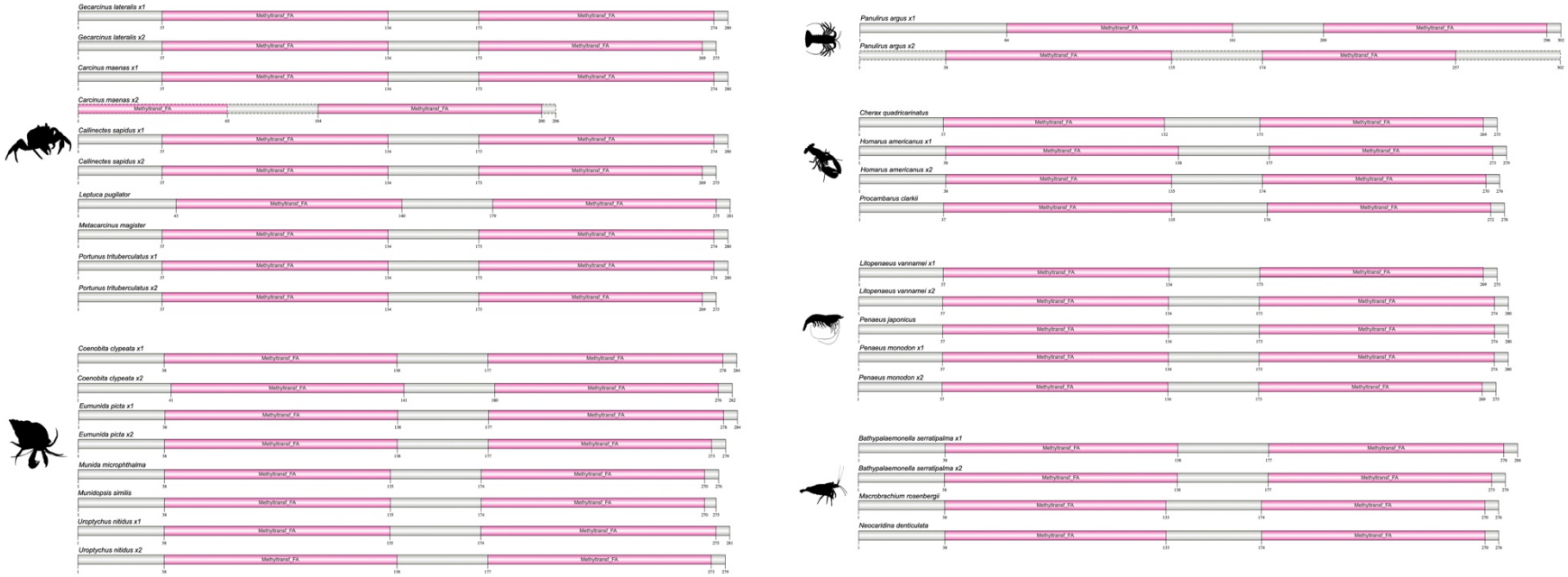

Figure 3.6. Domain organization of crustacean farnesoic acid *O*-methyl transferase (FAMeT) proteins. Two Methyltransf_FA domains were identified in the transcripts regardless of variant length. Domains were the NCBI CD search tool and visualized with IBS 2.0 (see Materials and Methods). Information for the sequences is provided in the supplementary data spreadsheet found on the online repository. Species silhouettes were obtained from PhyloPic (http://phylopic.org).

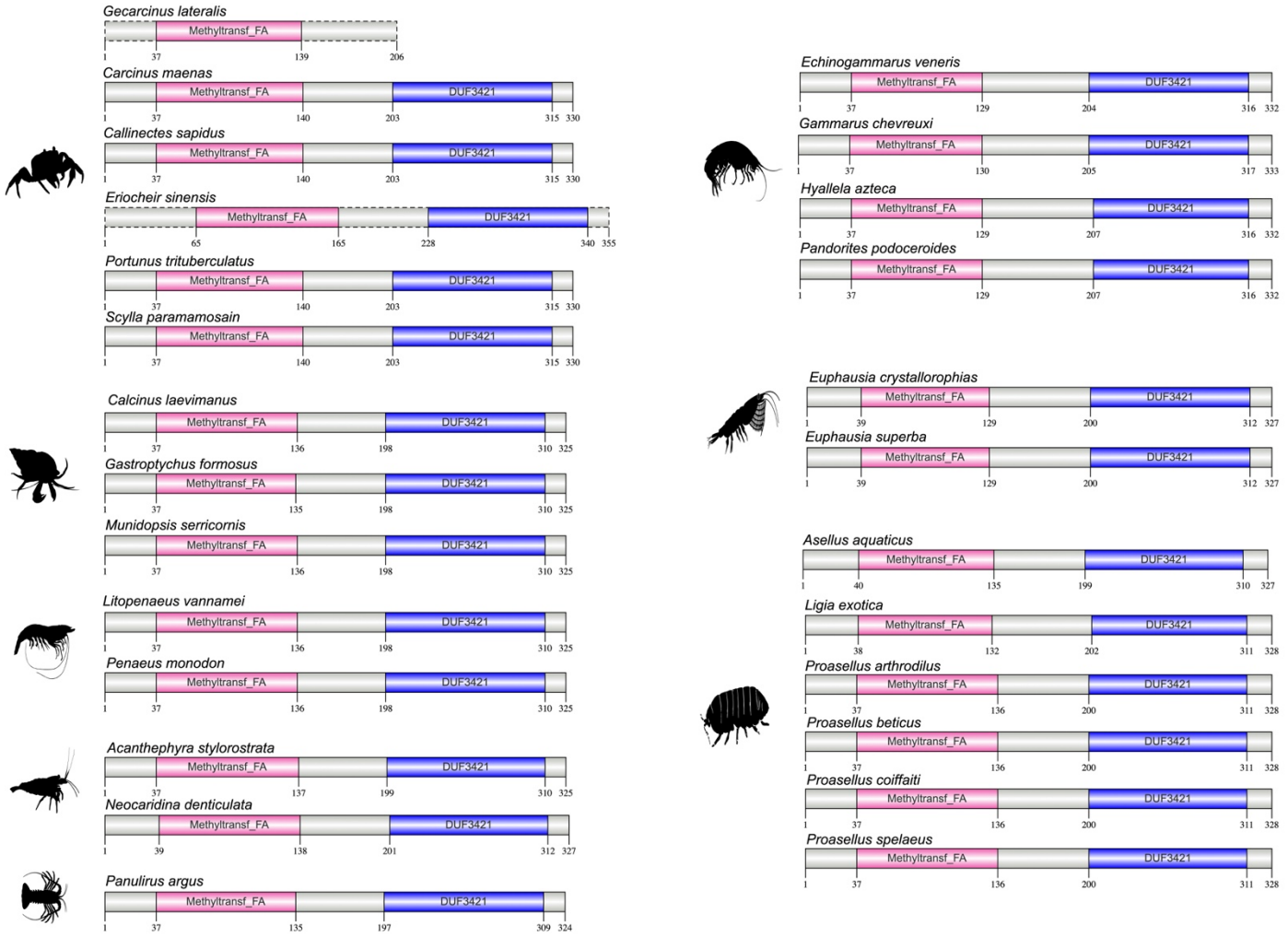

Figure 3.7. Domain organization of malacostracan crustacean farnesoic acid *O*-methyl transferase 2 (FAMeT2) proteins. Domains were identified with the NCBI CD search tool and visualized with IBS 2.0 (see Materials and Methods). The N-terminal region contained the Methyltransf_FA domain followed by the protein of unknown function domain, or DUF3421 (pfam11901). Information for the sequences is provided in the supplementary data spreadsheet found on the online repository. Species silhouettes were obtained from PhyloPic (http://phylopic.org).

Figure 3.8

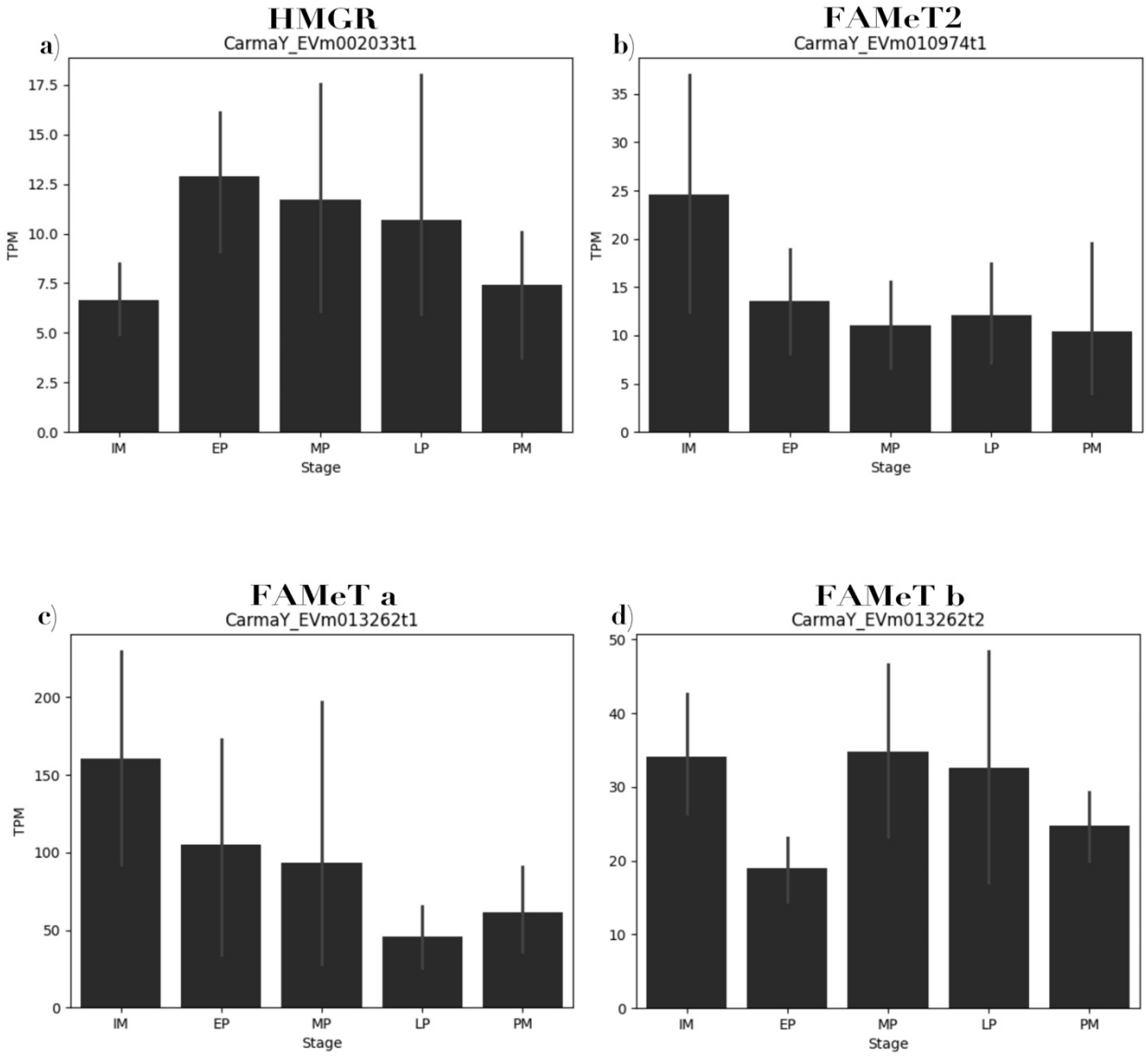
HMGR
a)
CarmaY_EVm002033t1
TPM
Stage
IM
EP
MP
LP
PM
FAMeT2
b)
CarmaY_EVm010974t1
FAMeT a
c)
CarmaY_EVm013262t1
FAMeT b
d)
CarmaY_EVm013262t2

Figure 3.8. Relative gene expression of methyl farnesoate (MF) synthetic genes a) *HMGR*, b) *FAMeT2*, c) *FAMeTa*, and d) *FAMeTb* in *Carcinus maenas* Y-organs (YO) across the different stages of the molt cycle (abbreviations: IM–intermolt, EP– early premolt, MP– mid premolt, LP– late premolt, and PM– postmolt). Transcript levels are expressed as mean transcripts per million reads (TPM) ± standard error of the mean (SEM); statistical differences were analyzed with Analysis of Variance (ANOVA) and post-hoc Tukey's HSD test ($p < 0.05$) with letters indicating significance. RNA-seq data was obtained from Oliphant et al. (2018) (n = 5 biological replicates of paired YOs) and quantified with Salmon (v.1.7.0) using the *C. maenas* YO transcriptome assembly included in CrusTome (v.0.1.0) (Pérez-Moreno et al., 2023).

Figure 3.9

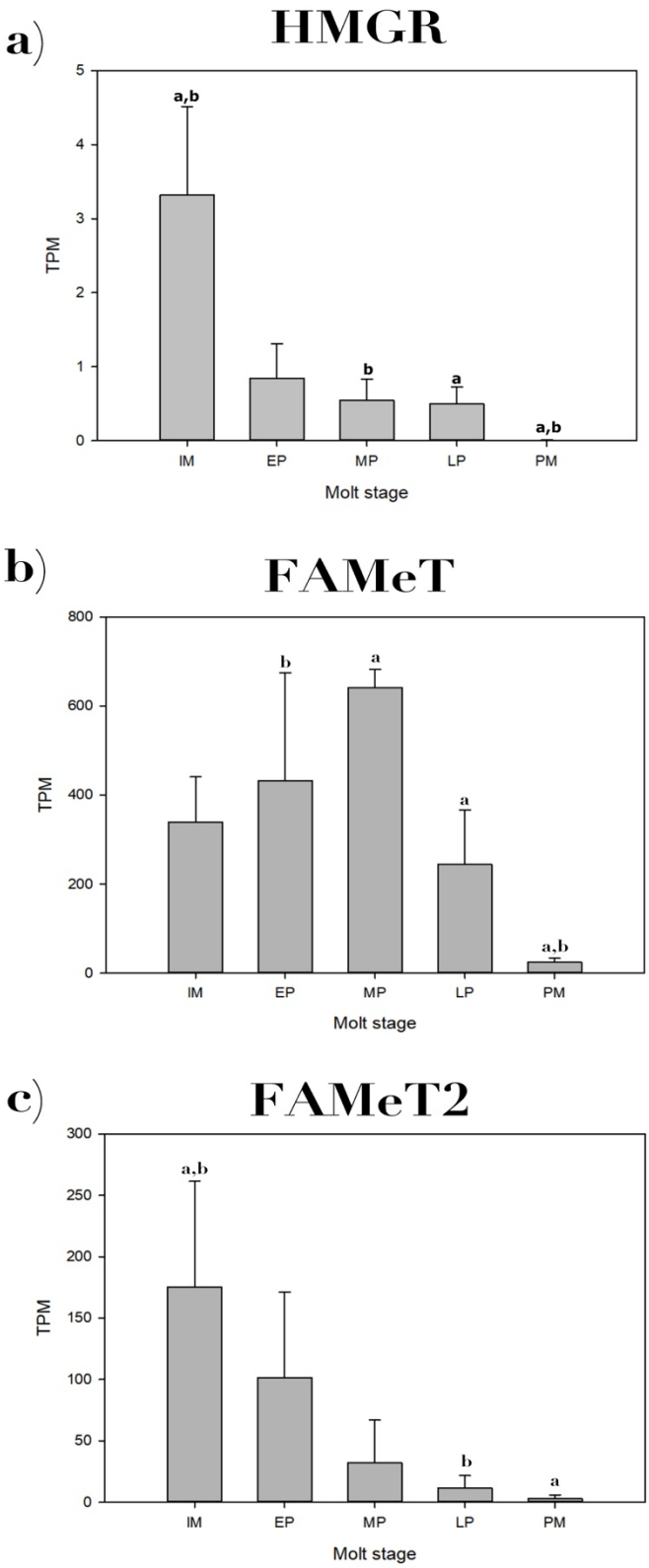
a)
HMGR
TPM
Molt stage
IM
EP
MP
LP
PM
a,b
b
a
a,b
b)
FAMeT
TPM
Molt stage
b
a
a
a,b
c)
FAMeT2
TPM
Molt stage
a,b
b
a

Figure 3.9. Relative gene expression of methyl farnesoate (MF) synthetic genes a) *HMGR*, b) *FAMeT* (a and b combined), and c) *FAMeT2* in *Gecarcinus lateralis* Y-organs (YO) across the different stages of the molt cycle (abbreviations: IM–intermolt, EP– early premolt, MP– mid premolt, LP– late premolt, and PM– postmolt). Transcript levels are expressed as mean transcripts per million reads (TPM) ± standard error of the mean (SEM); statistical differences were analyzed with Analysis of Variance (ANOVA) and post-hoc Tukey's HSD test (n = pooled replicates of 3 animals each) with letters indicating significance ($p < 0.05$). RNA-seq data was obtained from Das et al. (2018).

REFERENCES

Abdu, U., Barki, A., Karplus, I., Barel, S., Takac, P., Yehezkel, G., Laufer, H., and Sagi, A. (2001). Physiological effects of methyl farnesoate and pyriproxyfen on wintering female crayfish *Cherax quadricarinatus*. *Aquaculture*. **202**, 163–175.

Abdu, U., Takac, P., Laufer, H., and Sagi, A. (1998). Effect of Methyl Farnesoate on Late Larval Development and Metamorphosis in the Prawn *Macrobrachium rosenbergii* (Decapoda, Palaemonidae): A Juvenoid-like Effect? *Reference: Biol. Bull.* **195**, 112–119.

Abuhagr, A. M., Blindert, J. L., Nimitkul, S., Zander, I. A., LaBere, S. M., Chang, S. A., MacLea, K. S., Chang, E. S. (2014). Molt regulation in green and red color morphs of the crab *Carcinus maenas*: gene expression of molt-inhibiting hormone signaling components. *Journal of Experimental Biology.* **217** (5), 796–808.

Achdiat, M., Fujaya, Y., Fazhan, H., Rozaimi, R., Chung, J. S., Wang, Y., Tan, K., Shu-Chien, A. C., Maulidiani, M., and Waiho, K. (2024). Identification and Characterization of the Y-Organ of Orange Mud Crab *Scylla Olivacea*. *Microscopy Research and Technique*. **0**, 1–12.

Alnawafleh, T., Kim, B. K., Kang, H. E., Yoon, T. H., and Kim, H. W. (2014). Stimulation of Molting and Ovarian Maturation by Methyl Farnesoate in the Pacific White Shrimp *Litopenaeus vannamei* (Boone, 1931). *Fish. Aquat. Sci*. **17** (1), 115–121.

Aoto, T., Kamiguchi, Y., and Hisano, S. (1974). Histological and Ultrastructural Studies on the Y Organ and the Mandibular Organ of the Freshwater Prawn, *Palaemon paucidens*, with Special Reference to Their Relation with the Molting Cycle. *Jour. Fac. Sci. Hokkaido Univ. Ser. VI, Zool.* **19** (2).

Ayanath, A. and Raghavan, S. D. A. (2021). Effect of 20-OH ecdysone and methyl farnesoate on histomorphology of the Y-organ during late intermoult and postmoult stages in the freshwater crab *Travancoriana schirnerae* Bott, 1969 (Crustacea: Gecarcinucidae). *Nauplius.* **29**, e2021037.

Bellés, X., Martín, D., and Piulachs, M. D. (2005). The Mevalonate Pathway and the Synthesis of Juvenile Hormone in Insects. *Annu. Rev. Entomol.* **50**, 181–199.

Bliss, D. E. (1968). Transition from Water to Land in Decapod Crustaceans. *Am. Zool.* **8** (3), 355–392.

Bliss, D. E. and Boyer, J. R. (1964). Environmental Regulation of Growth in the Decapod Crustacean *Gecarcinus lateralis*. *General and Comparative Endocrinology.* **4** (1), 15–41.

Bliss, D. E., Wang, S. M. E., and Martinez, E. A. (1966a). Water balance in the land crab, *Gecarcinus lateralis*, during the intermolt cycle. *Am. Zool.* **6** (2), 197–212.

Blom, N., Gammeltoft, S., and Brunak, S. (1999). Sequence and Structure-based Prediction of Eukaryotic Protein Phosphorylation Sites. *J. Mol. Biol.* **294**, 1351–1362.

Blom, N., Sicheritz-Potén, T., Gupta, R., Gammeltoft, S., and Brunak, S. (2004). Prediction of post-translational glycosylation and phosphorylation of proteins from the amino acid sequence. *Proteomics.* **4**, 1633–1649.

Borst, D. W. and Tsukimura, B. (1991). Quantification of methyl farnesoate levels in hemolymph by high-performance liquid chromatography. *Journal of Chromatography.* **545**, 71–78.

Borst, D. W., Laufer, H., Landau, M., Chang, E. S., Hertz, W. A., Baker, F. C., and Schooley, D. A. (1987). Methyl farnesoate and its role in crustacean reproduction and development. *Insect Biochemistry.* **17** (7) 1123–1127.

Borst, D. W., Ogan, J., Tsukimura, B., Claerhout, T., and Holford, K. C. (2001). Regulation of the Crustacean Mandibular Organ. *Amer. Zool.* **41** (3), 430–441.

Borst, D. W., Tsukimura, B., Laufer, H., and Couch, E. F. (1994). Regional Differences in Methyl Farnesoate Production by the Lobster Mandibular Organ. *Biol. Bull.* **186** (1), 9–16.

Buaklin, A., Jantee, N., Sittikankaew, K., Chumtong, P., Janpoom, S., Menasveta, P., Klinbunga, S., and Khamnamtong, B. (2015). Expression and polymorphism of farnesoic acid *O*-methyltransferase (FAMeT) and association between its SNPs and reproduction-related parameters of the giant tiger shrimp *Penaeus monodon*. *Aquaculture.* 441, 106–117.

Buchholz, C. and Adelung, D. (1980). The ultrastructural basis of steroid production in the Y-organ and the mandibular organ of the crabs Hemigrapsus nudus (Dana) and *Carcinus maenas* L. *Cell and Tissue Res*. **206** (1), 83–94.

Byard, E. H., Shivers, R. R., and Aiken, D. E. (1975). The mandibular organ of the lobster, *Homarus americanus*. *Cell and Tissue Res*. **162** (1), 13–22.

Chang, E. S. (1995). Physiological and biochemical changes during the molt cycle in decapod crustaceans: an overview. *Journal of Experimental Marine Biology and Ecology.* **193**, 1–14.

Chen, T., Xu, R., Sheng, N., Che, S., Zhu, L., Liu, F., Su, S., Ding, S., and Li, X. (2022b). RNAi silencing of the 3-hydroxy-3-methylglutaryl coenzyme A reductase (*HMGR*) gene inhibits vitellogenesis in Chinese mitten crab *Eriocheir sinensis*. *Comp. Biochem. Physiol. A Mol. Integr. Physiol.* **263**, 111078.

Chen, T., Xu, R., Sheng, N., Che, S., Zhu, L., Liu, F., Su, S., Ding, S., and Li, X. (2021a). Molecular evidence for farnesoic acid O-methyltransferase (FAMeT) involved in the biosynthesis of vitellogenin in the Chinese mitten crab *Eriocheir sinensis*. *Animal Reproduction Science.* **234**, 106868.

Cheng, D., Meng, M., Peng, J., Qian, W., Kang, L., and Xia, Q. (2014). Genome-wide comparison of genes involved in the biosynthesis, metabolism, and signaling of juvenile hormone between silkworm and other insects. *Genetics and Molecular Biology*. **37** (2), 444–459.

Cheong, S. P. S., Huang, J., Bendena, W. G., Tobe, S. S., and Hui, J. H. L. (2015). Evolution of Ecdysis and Metamorphosis in Arthropods: The Rise of Regulation of Juvenile Hormone. *Integr. Comp. Biol*. **55** (5), 878–890.

Covi, J. A., Chang, E. S., and Mykles, D. L. (2009). Conserved role of cyclic nucleotides in the regulation of ecdysteroidogenesis by the crustacean molting gland. *Comp. Biochem. Physiol. A Mol. Integr. Physiol.* **152** (4), 470–477.

Das, S., Vraspir, L., Zhou, W., Durica, D. S., and Mykles, D. L. (2018). Transcriptomic analysis of differentially expressed genes in the molting gland (Y-organ) of the blackback land crab, *Gecarcinus lateralis*, during molt-cycle stage transitions. *Comp. Biochem. Physiol. Part D Genomics Proteomics* **28**, 37–53.

Defelipe, L. A., Dolghih, E., Roitberg, A. E., Nouzova, M., Mayoral, J. G., Noriega, F. G., and Turjanski, A. G. (2011). Juvenile hormone synthesis: "esterify then epoxidize" or " epoxidize then esterify" ? Insights from the structural characterization of juvenile hormone acid methyltransferase. *Insect Biochem. Mol. Biol.* **41** (4), 228–235.

Devi, S., Raghavan, A., and Ayanath, A. (2018). Effect of Methyl Farnesoate Administration on Ovarian Growth and Maturation in the Freshwater Crab *Travancoriana schirnerae*. *Egypt J. Aquat. Biol. Fish.* **22** (5), 257–271.

Duan, Y., Liu, P., Li, J., Wang, Y., Li, J., and Chen, P. (2014). A farnesoic acid O-methyltransferase (FAMeT) from *Exopalaemon carinicauda* is responsive to Vibrio anguillarum and WSSV challenge. *Cell Stress Chaperones.* **19** (3), 367–377.

Farhadi, A., Harlioğu, M. M., and Yilmaz, Ö. (2020). Effect of serotonin injection on the reproductive parameters and haemolymph methyl farnesoate level in the narrow-clawed crayfish *Pontastacus leptodactylus* (Eschscholtz, 1823). *Aquaculture Research*. **51**, 155–163.

Gabe, M. (1953). Sur l'existence, chez quelques crustacés Malacostraces, d'un organe comparable a la glande de la mue des Insects. *Comptes Rendus Hebdomadaires de l'Academie des Sciences.* **327**, 1111–1113.

Gianazza, E., Eberini, I., Palazzolo, L., and Miller, I. (2021). Hemolymph proteins: An overview across marine arthropods and molluscs. *Journal of Proteomics.* **245**, 104294.

Giribet, G. and Edgecombe, G. D. (2019). The Phylogeny and Evolutionary History of Arthropods. *Current Biology.* **29** (12), R592–R602.

Girish, B. P., Swetha, C. H., and Reddy, P. S. (2017). Serotonin induces ecdysteroidogenesis and methyl farnesoate synthesis in the mud crab, *Scylla serrata*. *Biochemical and Biophysical Researach Communications.* **490** (4), 1340–1345.

Goldstein, J. L. and Brown, M. S. (1990). Regulation of the mevalonate pathway. *Nature.* **343** (6257), 425–430.

Gopal, N. and Devi, A. R. S. (2018). Morphology and Histology of Mandibular Organ in Relation to Growth and Reproduction in the Freshwater Crab *Barytelphusa cunicularis*. *International Journal of Oceans and Oceanography.* **12** (2), 93–109.

Guindon, S. (2018). Accounting for Calibration Uncertainty: Bayesian Molecular Dating as a "Doubly Intractable" Problem. *Syst. Biol.* **67** (4), 651–661.

Guo, P., Zhang, Y., Zhang, L., Xu, H., Zhang, H., Wang, Z., Jiang, Y., Molloy, D., Zhao, P., and Xia, Q. (2021). Structural basis for juvenile hormone biosynthesis by the juvenile hormone acid methyltransferase. *J. Biol. Chem.* **297** (5), 101234.

Gunawardene, S. Y. I. N., Chow, B. K. C., He, J. G., and Chan, S. M. (2001). The shrimp FAMeT cDNA is encoded for a putative enzyme involved in the methylfarnesoate (MF) biosynthetic pathway and is temporally expressed in the eyestalk of different sexes. *Insect Biochem. Mol. Biol.* **31** (11), 1115–1124.

Gunawardene, S. Y. I. N., Tobe, S. S., Bendena, W. G., Chow, B. K. C., Yagi, K. J., and Chan, S. M. (2002). Function and cellular localization of farnesoic acid O-methyltransferase (FAMeT) in the shrimp, *Metapenaeus ensis*. *Eur. J. Biochem.* **269** (14), 3587–3595.

Gunawardene, Y. I. N. S., Bendena, W. G., Tobe, S. S., and Chan, S. M. (2003). Comparative immunohistochemistry and cellular distribution of farnesoic acid O-methyltransferase in the shrimp and the crayfish. *Peptides*. **24** (10), 1591–1597.

Hinsch, G. W. (1977). Fine structural changes in the mandibular gland of the male spider crab, *Libinia emarginata* (L). Following eyestalk ablation. *J. Morphol.* **154** (2), 307–315.

Hinsch, G. W. and Hajj, H. Al (1975). The ecdysial gland of the spider crab, *Libinia emarginata* (L). Ultrastructure of the gland in the male. *J. Morphol.* **145** (2), 179–187.

Hinsch, G. W., Spaziani, E., and Vensel, W. H. (1980). Ultrastructure of the y-organs *of Cancer antennarius* in normal and de-eyestalked crabs. *J. Morphol.* **163** (2), 167–174.

Hoang, D. T., Chernomor, O., von Haeseler, A., Minh, B. Q., and Vinh, L. S. (2017). UFBoot2: Improving the Ultrafast Bootstrap Approximation. *Mol. Biol. Evol.* **35** (2), 518–522.

Holford, K. C., Edwards, K. A., Bendena, W. G., Tobe, S. S., Wang, Z., and Borst, D. W. (2004). Purification and characterization of a mandibular organ protein from the American lobster, *Homarus americanus*: A putative farnesoic acid O-methyltransferase. *Insect Biochem. Mol. Biol.* **34** (8), 785–798.

Homola, E. and Chang, E. S. (1997c). Methyl Farnesoate: Crustacean Juvenile Hormone in Search of Functions. *Comparative Biochemistry and Physiology Part B: Biochemistry and Molecular Biology.* **117** (3), 347–356.

Hopkins, P. M. (1982). Growth and Regeneration Patterns in the Fiddler Crab, *Uca pugilator*. *Biol. Bull.* **163** (2), 301–319.

Hui, J. H. L., Tobe, S. S., and Chan, S. M. (2008). Characterization of the putative farnesoic acid O-methyltransferase (LvFAMeT) cDNA from white shrimp, *Litopenaeus vannamei*: Evidence for its role in molting. *Peptides.* **29** (2), 252–260.

Hui, J. H. L., Hayward, A., Bendena, W. G., Takahashi, T., and Tobe, S. S. (2010). Evolution and functional divergence of enzymes involved in sesquiterpenoid hormone biosynthesis in crustaceans and insects. *Peptides.* **31** (3), 451–455.

Kalavathy, Y., Mamatha, P., and Reddy, P. S. (1999). Methyl farnesoate stimulates testicular growth in the freshwater crab *Oziotelphusa senex sene*x fabricius. *Naturwissenschaften.* **86**, 394–395.

Kalyaanamoorthy, S., Minh, B. Q., Wong, T. K. F., Von Haeseler, A., and Jermiin, L. S. (2017). ModelFinder: Fast model selection for accurate phylogenetic estimates. *Nat. Methods.* **14**, 587–589.

Katoh, K. and Toh, H. (2008). Recent developments in the MAFFT multiple sequence alignment program. *Brief. Bioinform.* **9** (4), 286–298.

Kingan, T. G. (1989). A Competitive Enzyme-Linked Immunosorbent Assay: Applications in the assay of peptides, steroids, and cyclic nucleotides. *Analytical Biochemistry.* **183** (2), 283–289.

Kuballa, A. V., Guyatt, K., Dixon, B., Thaggard, H., Ashton, A. R., Paterson, B., Merritt, D. J., and Elizur, A. (2007). Isolation and expression analysis of multiple isoforms of putative farnesoic acid *O*-methyltransferase in several crustacean species. *Gen. Comp. Endocrinol.* **150** (1), 48–58.

Laufer, H., Ahl, J., Rotllant, G., and Baclaski, B. (2002). Evidence that ecdysteroids and methyl farnesoate control allometric growth and differentiation in a crustacean. *Insect Biochem. Mol. Biol.* **32** (2), 205–210.

Laufer, H. and Biggers, W. J. (2001). Unifying Concepts Learned from Methyl Farnesoate for Invertebrate Reproduction and Post-Embryonic Development. *Amer. Zool.* **41** (3), 4–8.

Laufer, H., Borst, D., Baker, F. C., Reuter, C. C., Tsai, L. W., Schooley, D. A., Carrasco, C., and Sinkus, M. (1987a). Identification of a Juvenile Hormone-Like Compound in a Crustacean. *Science.* **235** (4785), 202–205.

Laufer, H., Demir, N., Pan, X., Stuart, J. D., and Ahl, J. S. B. (2005). Methyl farnesoate controls adult male morphogenesis in the crayfish, *Procambarus clarkii*. *Journal of Insect Physiology*. **51** (4), 379–384.

Laufer, H., Landau, M., Homola, E., and Borst, D. W. (1987b). Methyl Farnesoate: Its site of synthesis and regulation of secretion in a juvenile crustacean. *Insect Biochem.* **17** (7), 1129–1131.

Le Roux, A. (1968). Description d'organes mandibulaires nouveaux chez les crustaces decapods. *CR Acad. Sci. Paris.* **266**, 1414–14717.

Li, Y., Yang, W., Sun, J., Lian, X., Li, X., Zhao, X., Liu, Y., Wang, L., and Song, L. (2024). A DM9-containing protein from crab *Eriocheir sinensis* functions as a novel multipotent pattern recognition receptor. *Fish Shellfish Immunol.* **145**, 109356.

Li, Z., Xu, X., Wang, J., and Wang, C. (2013). Possible Roles of Farnesoic Acid O-Methyltransferase in Regulation of Molting in the Shrimp, *Penaeus Chinensis*. *J. World Aquac. Soc.* **44** (6), 826–834.

Liu, M., Wu, Z., Yan, C., Liu, Y., Xing, K., Zhang, J., and Sun, Y. (2022a). Ovarian transcriptome and metabolic responses of RNAi-mediated farnesyl pyrophosphate synthase knockdown in *Neocaridina denticulata sinensis*. *Genomics.* **114** (6), 110484.

Liu, M., Yan, C., Liu, Y., Wu, Z., Zhang, J., and Sun, Y. (2022b). Cloning, expression analysis and RNAi of farnesoic acid *O*-methylransferase gene from *Neocaridina denticulata sinensis*. *Comp. Biochem. Physiol. B Biochem. Mol. Biol.* **259**, 110719.

Lombard, J. and Moreira, D. (2011). Origins and Early Evolution of the Mevalonate Pathway of Isoprenoid Biosynthesis in the Three Domains of Life. *Mol. Biol. Evol.* **28** (1), 87–99.

Ming, Z., Zhang, F., Wang, W., Liu, Z., Ma, C., Fu, Y., Chen, W., and Ma, L. (2022). Two Transcripts of HMG-CoA Reductase Related with Developmental Regulation from *Scylla paramamosain*: Evidences from cDNA Cloning and Expression Analysis. **23**, 9451.

Minh, B. Q., Schmidt, H. A., Chernomor, O., Schrempf, D., Woodhams, M. D., Von Haeseler, A., and Lanfear, R. (2020). IQ-TREE 2: New Models and Efficient Methods for Phylogenetic Inference in the Genomic Era. *Mol. Biol. Evol.* **37** (8), 1530–1534.

Miyakawa, H., Sato, T., Song, Y., Tollesfen, K. E., and Iguchi, T. (2018). Ecdysteroid and juvenile hormone biosynthesis, receptors and their signaling in the freshwater microcrustacean *Daphnia*. *Journal of Steroid Biochemistry and Molecular Biology*. **184**, 62–68.

Muhd-Farouk, H., Nurul, H. A., Abol-Munafi, A. B., Mardhiyyah, M. P., Hasyima-Ismail, N., Manan, H., Fatihah, S. N., Amin-Safwan, A., and Ikhwanuddin, M. (2019). Development of ovarian maturations in orange mud crab, *Scylla olivacea* (Herbst, 1796) through induction of eyestalk ablation and methyl farnesoate. *Arab J. Basic Appl. Sci.* **26** (1), 171–181.

Nagaraju, G. P. C. (2007). Is methyl farnesoate a crustacean hormone? *Aquaculture.* **272**, 39–54.

Nagaraju, G. P. C., Reddy, P. R., and Reddy, P. S. (2004). Mandibular organ: it's relation to body weight, sex, molt and reproduction in the crab, *Oziotelphusa senex senex* Fabricius (1791). *Aquaculture*. **232**, 603–612.

Noriega, F. G. (2014). Juvenile Hormone Biosynthesis in Insects: What Is New, What Do We Know, and What Questions Remain? *Int. Sch. Res. Notices*. **2014**, 967361.

Nouzova, M., Edwards, M. J., Michalkova, V., Ramirez, C. E., Ruiz, M., Areiza, M., DeGennaro, M., Fernandez-Lima, F., Feyereisen, R., Jindra, M. and Noriega, F. G. (2021). Epoxidation of juvenile hormone was a key innovation improving insect reproductive fitness. *PNAS.* **118**, 1–9.

Oliphant, A., Alexander, J. L., Swain, M. T., Webster, S. G., and Wilcockson, D. C. (2018). Transcriptomic analysis of crustacean neuropeptide signaling during the moult cycle in the green shore crab, *Carcinus maenas*. *BMC Genomics.* **19**, 711.

Paran, B. C., Fierro, I. J., and Tsukimura, B. (2010). Stimulation of ovarian growth by methyl farnesoate and eyestalk ablation in penaeoidean model shrimp, *Sicyonia ingentis* Burkenroad, 1938. *Aquac. Res.* **41**, 1887–1897.

Pérez-Moreno, J. L., Kozma, M. T., DeLeo, D. M., Bracken-Grissom, H. D., Durica, D. S., and Mykles, D. L. (2023). CrusTome: a transcriptome database resource for large-scale analyses across Crustacea. *G3: Genes, Genomes, Genetics.* **13**.

Qian, Z. and Liu, X. (2019). Elucidation of the role of farnesoic acid *O*-methyltransferase (FAMeT) in the giant freshwater prawn, *Macrobrachium rosenbergii*: Possible functional correlation with ecdysteroid signaling. *Comp. Biochem. Physiol. A Mol. Integr. Physiol.* **232**, 1–12.

Qu, Z., Kenny, N. J., Lam, H. M., Chan, T. F., Chu, K. H., Bendena, W. G., Tobe, S. S., and Hui J. H. L. (2015). How Did Arthropod Sesquiterpenoids and Ecdysteroids Arise? Comparison of Hormonal Pathway Genes in Noninsect Arthropod Genomes. *Genome Biol. Evol.* **7**, 1951–1959.

Qu, Z., Bendena, W. G., Tobe, S. S., and Hui, J. H. L. (2018). Juvenile hormone and sesquiterpenoids in arthropods: Biosynthesis, signaling, and role of MicroRNA. *Journal of Steroid Biochemistry and Molecular Biology.* **184**, 69–76.

Raghavan, S. D. A. and Ayanath, A. (2019). Effect of 20-OH ecdysone and methyl farnesoate on moulting in the freshwater crab *Travancoriana schirnerae*. *Invertebr. Reprod. Dev.* **63**, 309–318.

Rambaut, A. (2010). FigTree v1.4.4.

Reddy, P. S. and Ramamurthi, R. (1998). Methyl farnesoate stimulates ovarian maturation in the freshwater crab *Oziotelphusa senex senex* Fabricius. *Current Science.* **74**, 68–70.

Reddy, P. R., Purna, G., Nagaraju, C., and Reddy, P. S. (2004). Involvement of Methyl Farnesoate in the Regulation of Molting and Reproduction in the Freshwater Crab *Oziotelphusa senex senex*. *Journal of Crustacean Biology.* **24**, 511–515.

Rotllant, G., Takac, P., Liu, L., Scott, G. L., Laufer, H., and Laufer, H. (2000). Role of ecdysteroids and methyl farnesoate in morphogenesis and terminal moult in polymorphic males of the spider crab *Libinia emarginata*. *Aquaculture.* **190**, 103–118.

Rozewicki, J., Li, S., Amada, K. M., Standley, D. M., and Katoh, K. (2019). MAFFT-DASH: Integrated protein sequence and structural alignment. *Nucleic Acids Res.* **47**, W5–W10.

Ruddell, C. J., Wainwright, G., Geffen, A., White, M. R. H., Webster, S. G., and Rees, H. H. (2003). Cloning, Characterization, and Developmental Expression of a Putative Farnesoic Acid *O*-Methyl Transferase in the Female Edible Crab *Cancer pagurus*. *Biol. Bull.* **205** (3), 308–318.

Saikrithi, P., Balasubramanian, C. P., Otta, S. K., and Tomy, S. (2019). Characterization and expression profile of farnesoic acid *O*-methyltransferase gene from Indian white shrimp, *Penaeus indicus*. *Comp. Biochem. Physiol. B Biochem. Mol. Biol.* **232**, 79–86.

Semchuchot, W., Chotwiwatthanakun, C., Santimanawong, W., Krunangjum, T., Thajiongrak, P., Withyachumnarnkul, B., and Vanichviriyakit, R. (2023). Sesquiterpenoid pathway in the mandibular organ of *Penaeus monodon*: Cloning, expression, characterization of *PmJHAMT* and its alteration response to eyestalk ablation. *General and Comparative Endocrinology*. **331**, 114176.

Shinoda, T. and Itoyama, K. (2003). Juvenile hormone acid methyltransferase: A key regulatory enzyme for insect metamorphosis. *PNAS.* **100**, 11986–11991.

Sin, Y. W., Kenny, N. J., Qu, Z., Chan, K. W., Chan, K. W. S., Cheong, S. P. S., Leung, R. W. T., Chan, T. F., Bendena, W. G., Chu, K. H., Tobe, S. S., and Hui., J. H. L. (2015). Identification of putative ecdysteroid and juvenile hormone pathway genes in the shrimp *Neocaridina denticulata*. *Gen. Comp. Endocrinol.* **214**, 167–176.

Skinner, D. M. (1962). The Structure and Metabolism of a Crustacean Integumentary Tissue During a Molt Cycle. *Biol. Bull.* **123** (3), 635–647.

Skinner, D. M. (1985a). Interacting Factors in the Control of the Crustacean Molt Cycle. *American Zool.* **25**, 275–284.

Skinner, D. M. (1985b). "Molting and Regeneration," in *Biology of Crustacea*, (Academic Press), 550.

Skinner, D. M. and Graham, D. E. (1972). Loss of Limbs as a Stimulus to Ecdysis in Brachyura (True Crabs). *Biol. Bull.* **143**, 222–233.

Smija, M. K. and Sudha Devi, A. R. (2016). Histological changes of Y organ in *Travancoriana schirnerae* during moult cycle and in de-eyestalked crabs. *Turk. J. Fish. Aquat. Sci.* **16**, 533–544.

Smith, P. A., Clare, A. S., Rees, H. H., Prescott, M. C., Wainwright, G., and Thorndyke, M. C. (2000). Identification of methyl farnesoate in the cypris larva of the barnacle, *Balanus amphitrite*, and its role as a juvenile hormone. *Insect Biochem. Mol. Biol.* **30**, 885–890.

Steenwyk, J. L., Buida, T. J., Li, Y., Shen, X. X., and Rokas, A. (2020). ClipKIT: A multiple sequence alignment trimming software for accurate phylogenomic inference. *PLoS Biol.* **18**.

Sunarti, Y., Soejoedono, R. D., Mayasari, N. L. P. I., and Tahya, A. M. (2016). RNA expression of farnesoic acid *O*-methyl transferase in mandibular organ of intermolt and premolt mud crabs *Scylla olivacea*. *AACL Bioflux.* **9** (2), 270–275.

Tahya, A. M., Zairin Junior, M., Boediono, A., Artika, I. M., and Suprayudi, M. A. (2016a). Expression of RNA encode FAMeT in mandibular organ of mud crabs *Scylla olivacea*. *Int. J. Pharmtech Res.* **9**, 219–223.

Taketomi, Y. and Hyodo, M. (1986). The Y Organ of the Crab, *Portunus trituberculatus*: Effects of Ecdysterone on the Ultrastructure. *Cell Biol. Int. Rep.* **70**, 367–374.

Taketomi, Y. and Kawano, Y. (1985). Ultrastructure of the mandibular organ of the shrimp, *Penaeus japonicus*, in untreated and experimentally manipulated individuals. *Cell Biol. Int. Rep.* **9**, 1069–1074.

Taketomi, Y. and Nakano, Y. (2007). Y-organ and mandibular organ of the crayfish *Procambarus clarkii* during the molt cycle. *Crustacean Research* 36, 25–36.

Tamone, S. L. and Chang, E. S. (1993). Methyl farnesoate stimulates Ecdysteroid Secretion from Crab Y-organs *in Vitro*. *General and Comparative Endocrinology.* **89** (3), 425–432.

Tiu, S. H. K., Hult, E. F., Yagi, K. J., and Tobe, S. S. (2012). Farnesoic acid and methyl farnesoate production during lobster reproduction: Possible functional correlation with retinoid X receptor expression. *Gen. Comp. Endocrinol.* **175**, 259–269.

Tobe, S. S., Young, D. A., and Khoo, H. W. (1989a). Production of Methyl Farnesoate by the Mandibular Organs of the Mud Crab, *Scylla serrata*: Validation of a Radiochemical Assay. *General and Comparative Endocrinology.* **73**, 342–353.

Tobe, S. S., Young, D. A., Khoo, H. W., and Baker, F. C. (1989b). Farnesoic acid as a major product of release from crustacean mandibular organs in vitro. *Journal of Experimental Zoology.* **249**, 165–171.

Toyota, K., Miyakawa, H., Hiruta, C., Furuta, K., Ogino, Y., Shinoda, T., Tatarazko, N., Miyagawa, S., Shaw, J. R., and Iguchi, T. (2015). Methyl farnesoate synthesis is necessary for the environmental sex determination in the water flea *Daphnia pulex*. *Journal of Insect Physiology*. **80**, 22–30.

Toyota, K., Yamane, F., and Ohira, T. (2020b). Impacts of Methyl Farnesoate and 20-Hydroxyecdysone on Larval Mortality and Metamorphosis in the Kuruma Prawn *Marsupenaeus japonicus*. *Front. Endocrinol.* **11**.

Tsukimura, B. and Borst, D. W. (1992). Regulation of Methyl Farnesoate in the Hemolymph and Mandibular Organ of the Lobster, *Homarus americanus*. *Gen. Comp. Endocrinol.* **86**, 297–303.

Tsukimura, B., Kamemoto, F. I., and Borst, D. W. (1993). Cyclic nucleotide regulation of methyl farnesoate synthesis by the mandibular organ of the lobster, *Homarus americanus*. *Journal of Experimental Zoology.* **265**, 427–431.

Wainwright, G., Webster, S. G., and Rees, H. H. (1998). Neuropeptide regulation of biosynthesis of the juvenoid, methyl farnesoate, in the edible crab, *Cancer pagurus*. *Biochem. J.* **334**, 651–657.

Xie, X. I., Zhu, D., Li, Y., Qiu, X., Cui, X., and Tang, J. (2015). Hemolymph Levels of Methyl Farnesoate During Ovarian Development of the Swimming Crab *Portunus trituberculatus*, and Its Relation to Transcript Levels of HMG-CoA Reductase and Farnesoic Acid O-Methyltransferase. *Biol. Bull.* **228** (2), 118–124.

Xie, X., Tao, T., Liu, M., Zhou, Y., Liu, Z., and Zhu, D. (2016a). The potential role of juvenile hormone acid methyltransferase in methyl farnesoate (MF) biosynthesis in the swimming crab, *Portunus trituberculatus*. *Anim. Reprod. Sci.* **168**, 40–49.

Xie, X., Zhu, D., Cui, X., Tang, J., and Qiu, X. (2013). Cloning and expression analysis of farnesoic acid O-methyl transferase (FAMeT) during molting in *Portunus trituberculatus*. *Journal of Fisheries of China.* **37**, 994–1001.

Xie, Y., Li, H., Luo, X., Li, H., Gao, Q., Zhang, L., Teng, Y., Zhao, Q., Zuo, Z., and Ren, R. (2022). IBS 2.0: an upgraded illustrator for the visualization of biological sequences. *Nucleic Acids Res.* **50** (W1), W420–W426.

Yamada, K. D., Tomii, K., and Katoh, K. (2016). Application of the MAFFT sequence alignment program to large data - Reexamination of the usefulness of chained guide trees. *Bioinformatics.* **32** (21), 3246–3251.

Yamamoto, H., Okino, T., Yoshimura, E., Tachibana, A., Shimizu, K., and Fusetani, N. (1997). Methyl farnesoate induces larval metamorphosis of the barnacle, *Balanus amphitrite* via protein kinase C activation. *Journal of Experimental Zoology.* **278** (6), 349–355.

Yang, Y., Ye, H., Huang, H., Jin, Z., and Li, S. (2012). Cloning, expression and functional analysis of farnesoic acid *O*-methyltransferase (FAMeT) in the mud crab, *Scylla paramamosain*. *Mar. Freshw. Behav. Physiol.* **45**, 209–222.

Yu, X., Chang, E. S., and Mykles, D. L. (2002). Characterization of Limb Autotomy Factor-Proecdysis (LAF_{pro}), Isolated From Limb Regenerates, That Suspends Molting in the Land Crab *Gecarcinus lateralis*. *Bio. Bull.* **202** (3), 204–212.

Yudin, A. I., Diener, R. A., Clark, W. H., and Chang, E. S. (1980). Mandibular Gland of the Blue Crab *Callinectes sapidus*. *Biol. Bull.* **159** (3), 760–772.

Zhao, M., Zhang, F., Jiang, K., Wang, W., Chen, W., Ma, C., Song, W., and Ma, L. (2018). Cloning, characterization, and expression profile of an insect farnesoic acid O-methyltransferase orthologue from the mud crab *Scylla paramamosain* Estampador, 1950 (Brachyura: Portunidae): Putative relationship with methyl farnesoate. *Journal of Crustacean Biology.* **38** (4), 443–450.

Zhao, M., Jiang, K., Song, W., Ma, C., Wang, J., Meng, Y., Wei, H., Chen, K., Qiao, Z., Zhang, F., and Ma, L. (2015). Two Transcripts of HMG-CoA Reductase Related with Developmental Regulation from *Scylla paramamosain*: Evidences from cDNA Cloning and Expression Analysis. *IUBMB Life*. **67** (12), 954–965.

CHAPTER 4

CONCLUDING REMARKS

Molting is a crucial physiological process that allows arthropod growth, development, and/or regeneration and is initiated by an increase in ecdysteroid levels. In crustaceans, mTORC1 and TGF-β signaling are required for Y-organ (YO) activation and commitment, respectively. It is hypothesized that the peak in ecdysteroid titers in late premolt (PM) triggers the repression of the YO through a negative feedback loop on the ecdysone biosynthetic genes (Halloween genes) to, which, are mediated by the ecdysone response gene transcriptional network. Moreover, ecdysone response gene expression is hypothesized to be suppressed by Krüppel homolog 1 (Kr-h1), acting through the methyl farnesoate (MF)–Methoprene tolerant (Met)–Kr-h1–Ecdysone response gene 93 (E93) transcriptional cascade. The repressive behavior of Kr-h1 may be impacted by the recruitment of transcriptional comediators [e.g., CREB-binding protein (CBP) and C-terminal-binding protein (CtBP)]; however, the transcription factors involved in the MEKRE93 network is subjected to post-transcriptional modifications (Figure 4.1).

From the European green shore crab (*Carcinus maenas*) and the blackback land crab (*Gecarinus lateralis*) YO transcriptomes, the MF signaling genes (*Met, Src, Kr-h1,* and *E93*), transcriptional comediators (*CBP* and *CtBP*), and MF synthetic genes (*HMGR, FAMeTa, FAMeTb, FAMeT2*) were successfully identified and characterized. Each of these components identified exhibited high sequence identities with orthologs from other pancrustaceans, arthropods, and/or panarthropodans. Phylogenetic analysis showed that the contig sequences clustered with the corresponding orthologs in other related species. Taken together, these results indicate that pancrustacean MF signaling pathway orthologs are highly conserved and evolved

from a common lineage, while MF synthetic gene *FAMeT* is not orthologous to the insect *FAMeT.*

RNA-seq analysis of the *C. maenas* and the *G. lateralis* indicate that the YOs express the MF signaling and synthetic gene transcripts. The expression pattern of these transcripts varies between the two species throughout the molt cycle progression thus suggesting the possibility of differing MEKRE93 mechanisms. Furthermore, expression of transcriptional mediators *CBP* and *CtBP* was correlated within each species, suggesting that despite the behavior of these factors enhancing and repressing transcription, they may be working synergistically on different transcription factor targets in different molt stages. The expression of *FAMeT* and/or *FAMeT2* proposes the idea that the YO may synthesize its own innate MF to regulate the YO as an autocrine factor.

An important next step regarding this research would be to differentiating the roles of FAMeT between FAMeT2 in MF biosynthesis, including other potential *FAMeT-like* genes. FA with FAMeT2 may result in a product that is different from that of FA with FAMeT and have different physiological effects. Another future direction would be to investigate the mode of action of each JH-mimic to determine the toxicity due to direct the downregulation of ecdysone response and/or biosynthetic genes. Binding of these insecticides to the Met receptor complex can vary due to mutations; therefore, determining their binding on the intrinsically disorder C-terminus can inform the actions on other transcriptional effectors and/or comediators. Additionally, it would be informative to determine if these species have developed resistance or cross resistances to these compounds. To determine if the lack of effect of MF on the YOs (*in vitro*) was due to metabolism, one could test an esterase inhibitor, such as 3-octylthio-1,1,1-trifluoropropan-2-one (OTFP). Determining the behavior and expression of specific

carboxylesterases and/or other degradation enzymes can provide insight to see if the compounds increase metabolic activity and/or if these compounds are specific. Although so much work has been done already and yet, so much work remains to be done in order to break the MF curse.

Figure 4.1

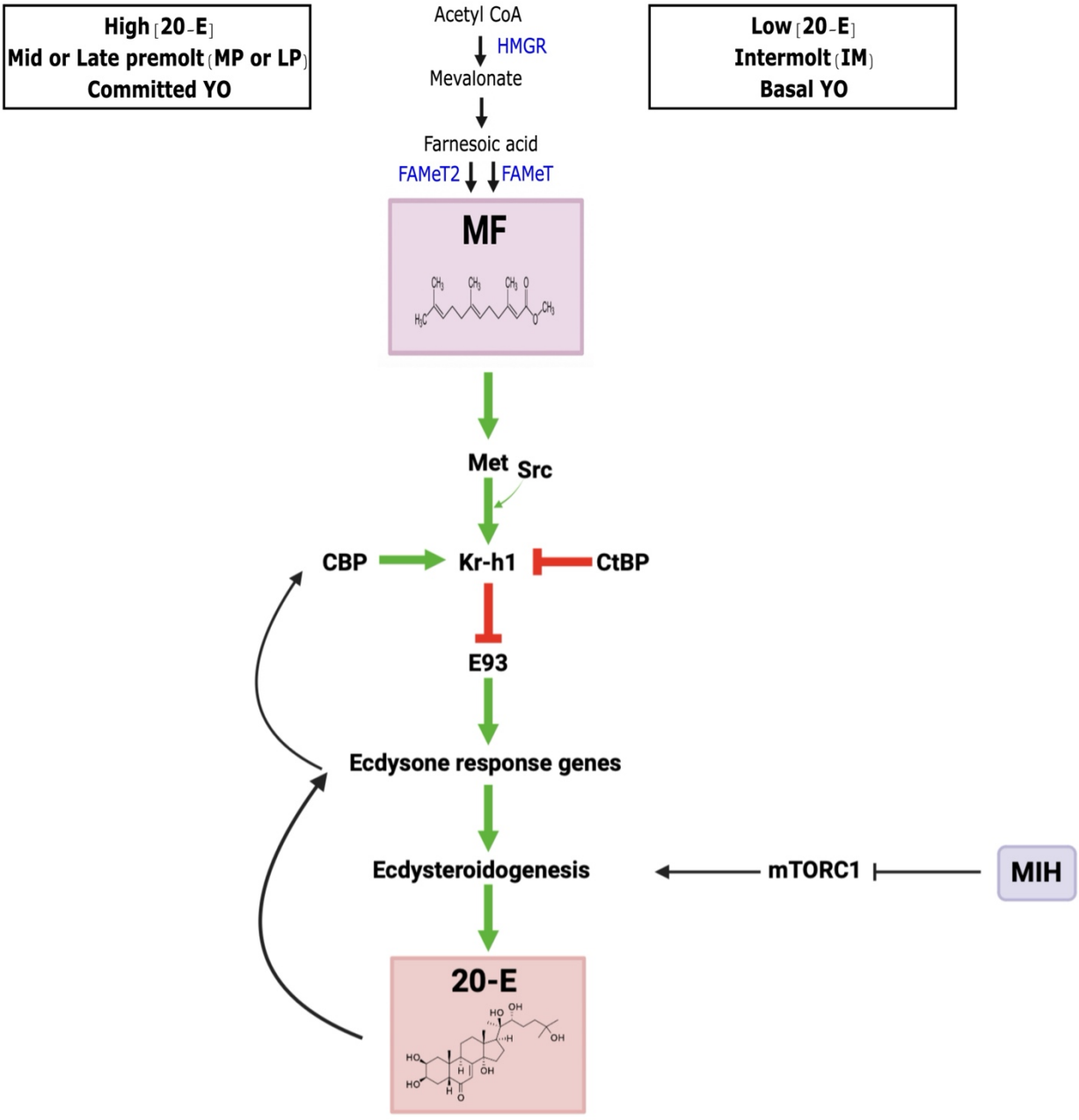
High [20-E]
Mid or Late premolt (MP or LP)
Committed YO
Acetyl CoA
HMGR
Mevalonate
Farnesoic acid
FAMeT2
FAMeT
MF
Low [20-E]
Intermolt (IM)
Basal YO
Met
Src
CBP
Kr-h1
CtBP
E93
Ecdysone response genes
Ecdysteroidogenesis
mTORC1
MIH
20-E

Figure 4.1 Control of ecdysteroidogenesis through the methyl farnesoate (MF) transcriptional cascade of Methoprene tolerant (Met) – Krüppel homolog 1 (Kr-h1) – Ecdysone response gene 93 (E93) in the Y-organ (YO). MF is proposed to act as an autocrine factor to regulate the endocrine cross talk with 20-E as the genes encoding for the synthetic enzymes were identified including *3-hydroxy-3-methylglutaryl-CoA reductase* (*HMGR*) and *farnesoic acid O-methyltransferase* (*FAMeT*). High hemolymph titers of 20-E, such as in mid and/or late premolt (MP and/or LP) inhibit 20-E synthesis thus leading to the transition from a committed to repressed state. By contrast, low 20-E titers in the hemolymph, such as in intermolt (IM) when the YO is in a basal or repressed state, stimulate the YO ecdysteroid production. Although molt-inhibiting hormone (MIH) inhibits ecdysteroid synthesis through the mechanistic target of rapamycin complex 1 (mTORC1), MF is proposed to act as an autocrine factor to regulate the endocrine cross talk with 20-E.

APPENDICES

APPENDIX A

Table A1. Compound information utilized for the *G. lateralis* and *C. maenas* YO *in vitro* cultures.

Compound	Formula	Molecular weight (g/mol)	Company	Product number (Lot)	Expiration
Fenoxycarb 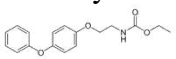	$C_{17}H_{19}NO_4$	301.34	Sigma Aldrich	34343 (BCBT7968)	January 2022
Hydroprene 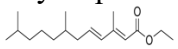	$C_{17}H_{30}O_2$	266.42	Sigma Aldrich	46426 (BCBW5576)	February 2023
Methoprene 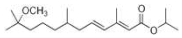	$C_{19}H_{34}O_3$	310.47	Sigma Aldrich	33375 (BCCD7840)	August 2022
Pyriproxyfen 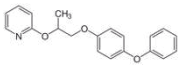	$C_{20}H_{19}NO_3$	321.37	Sigma Aldrich	34174 (BCBZ9221	December 2021
Methyl farnesoate 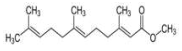	$C_{16}H_{26}O_2$	250.38	Echelon Inc.	S-1053 (E00282-017-05)	May 2021

Table A2. Average paired difference in cumulative 20-E (in pg/μL) synthesized and paired *t*-statistic for each chemical across the concentration levels for intermolt green crabs. The paired difference considered is treated YO minus control YO from the same host animal. In general, we observe larger magnitudes of average paired differences for larger concentrations and after longer periods of times.

	8 hours	16 hours	24 hours	32 hours	40 hours	48 hours
0.1 μM	$\bar{x}_d(t_d)$					
Fenoxycarb	-30.8(-1.8)	-37.8(-1.9)	-38.7(-1.9)	-39.5(-2.0)	-40.6(-2.0)	-40.9(-2.0)
S-Hydroprene	15.1(1.1)	17.4(1.1)	19.2(1.2)	19.7(1.2)	21.4(1.3)	20.1(1.2)
Methoprene	1.9(0.3)	1.1(0.2)	0.6(0.1)	-0.4(-0.1)	-0.7(-0.1)	-1.0(-0.1)
Methyl Farnesoate	-13.7(-1.5)	-12.1(-1.2)	-12.1(-1.1)	-9.0(-0.6)	-6.8(-0.4)	-6.0(-0.4)
Pyriproxyfen	-6.3(-1.4)	-0.6(-0.1)	1.5(0.1)	3.5(0.2)	8.1(0.4)	6.2(0.4)
1.0 μM						
Fenoxycarb	-16.7(-1.6)	-20.2(-1.7)	-28.1(-1.5)	-35.6(-1.5)	-54.8(-1.5)	-62.7(-1.3)
S-Hydroprene	6.5(0.3)	14.1(0.6)	19.5(0.8)	25.9(0.9)	29.0(0.9)	27.6(0.8)
Methoprene	1.2(2.0)	-5.1(-0.4)	-6.3(-0.5)	-11.5(-0.8)	-12.8(-0.8)	-19.9(-1.2)
Methyl Farnesoate	-2.7(-0.3)	0.7(0.1)	5.6(0.4)	25.9(1.4)	43.9(1.8)	52.4(1.9)
Pyriproxyfen	-1.9(-0.3)	-4.9(-0.3)	-7.3(-0.4)	-16.7(-0.6)	-24.4(-0.8)	-38.4(-1.0)
10.0 μM						
Fenoxycarb	-1.9(-0.4)	-9.5(-1.6)	-19.8(-2.0)	-35.0(-2.0)	-45.3(-1.8)	-51.4(-1.7)
S-Hydroprene	-2.9(-1.8)	3.8(1.0)	22.6(2.7)	29.9(2.9)	27.0(3.2)	24.6(3.1)
Methoprene	18.4(1.8)	27.5(2.3)	38.6(2.8)	47.0(2.5)	58.8(2.4)	58.9(2.3)
Methyl Farnesoate	-13.2(-1.8)	-11.9(-1.8)	-10.5(-1.4)	-3.5(-0.2)	-0.2(-0.0)	-0.4(-0.0)
Pyriproxyfen	-11.2(-0.7)	-9.8(-0.6)	-5.4(-0.3)	-5.0(-0.3)	-13.8(-0.6)	-47.7(-1.2)

Figure A1

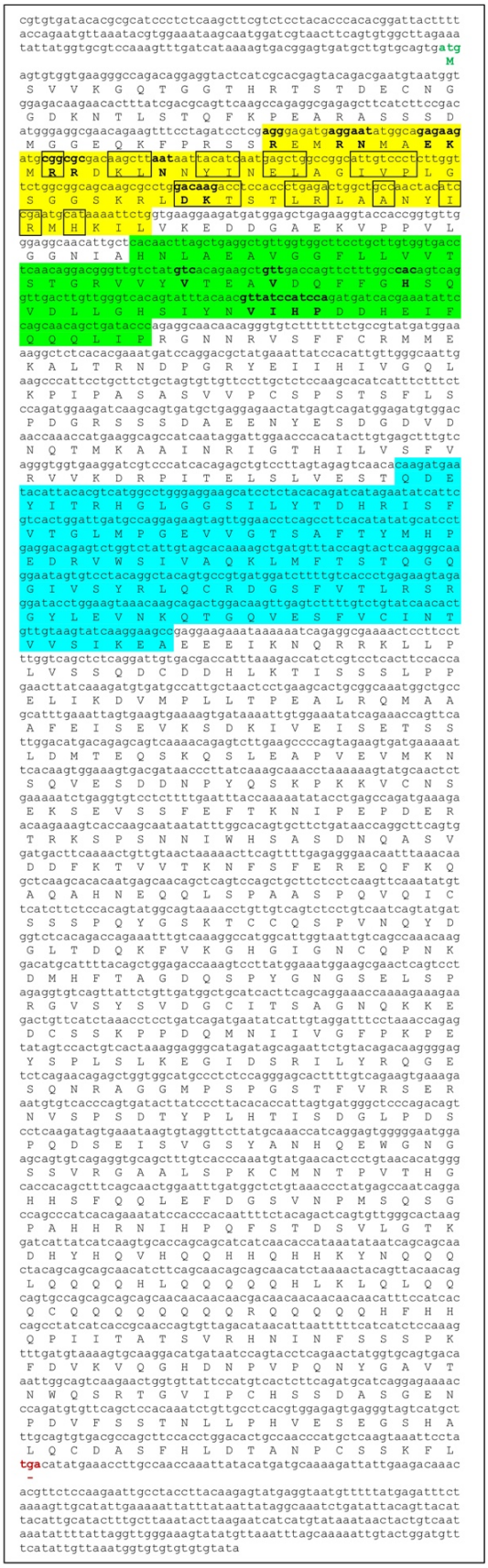

Figure A1. Nucleotide (nt) and deduced amino acid (aa) sequence of the *G. lateralis* Methoprene tolerant (Met) contig (Y EVm001315t1) isolated from the Y-organ (YO) transcriptome. The contig sequence included a 5' and 3' untranslated region (UTR) consisting of 177 and 327 base pairs (bp) respectively; the start codon (atg) is bolded in green and the stop codon (tga) in red. The 1001 aa open reading frame (ORF) includes the basic-helix-loop-helix (bHLH) domain shown in yellow (53-107 aa) which contains putative DNA binding sites (bolded) and dimer interfaces (boxed). Subsequently following the bHLH domain are two Per-ARNT-Sim (PAS) domains. The PAS A domain highlighted in green (127-187 aa) contains putative active sites (bolded). Indicated in blue is the PAS B domain (299-408 aa) that acts as the ligand binding domain (LBD).

Figure A2

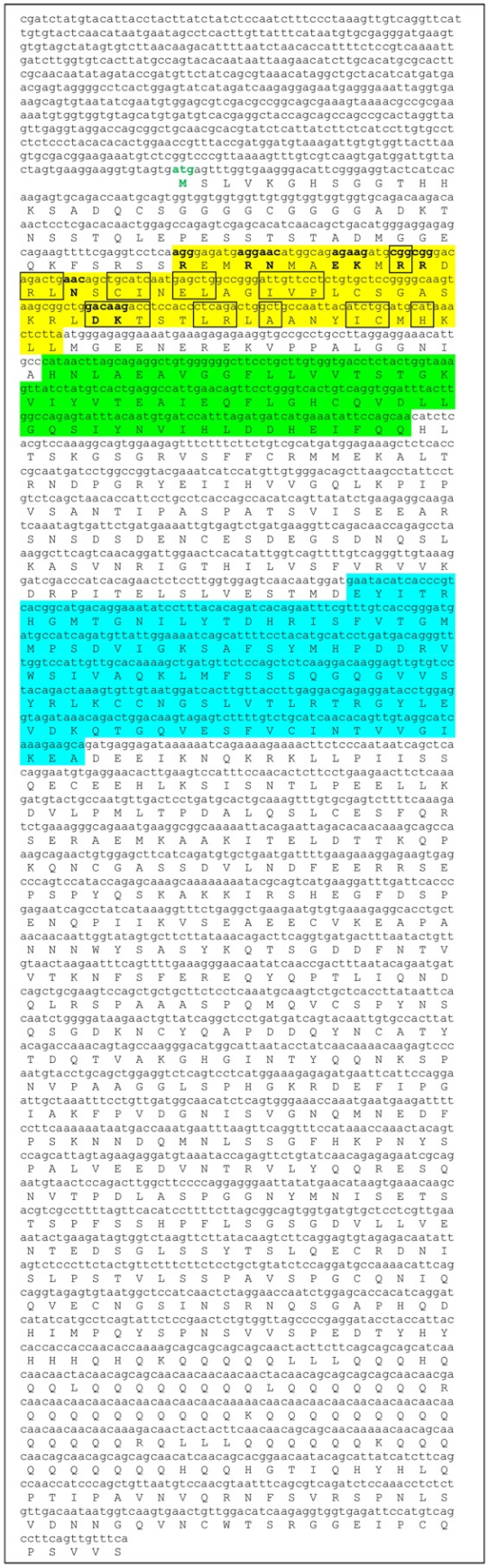

Figure A2. Nucleotide (nt) and deduced amino acid (aa) sequence of the *C. maenas* Methoprene tolerant (Met) contig (Y EVm001443t1) isolated from the Y-organ (YO) transcriptome. The partial contig sequence included a 5' untranslated region (UTR) consisting of 682 base pairs (bp) with the start codon (atg) bolded in green. Within the 998 aa open reading frame (ORF) is the basic-helix-loop-helix (bHLH) domain shown in yellow (61-115 aa) which contains putative DNA binding sites (bolded) and dimer interfaces (boxed). Subsequently followed are two Per-ARNT-Sim (PAS) domains, A (135-191 aa) and B (309-416 aa) highlighted in green and blue respectively.

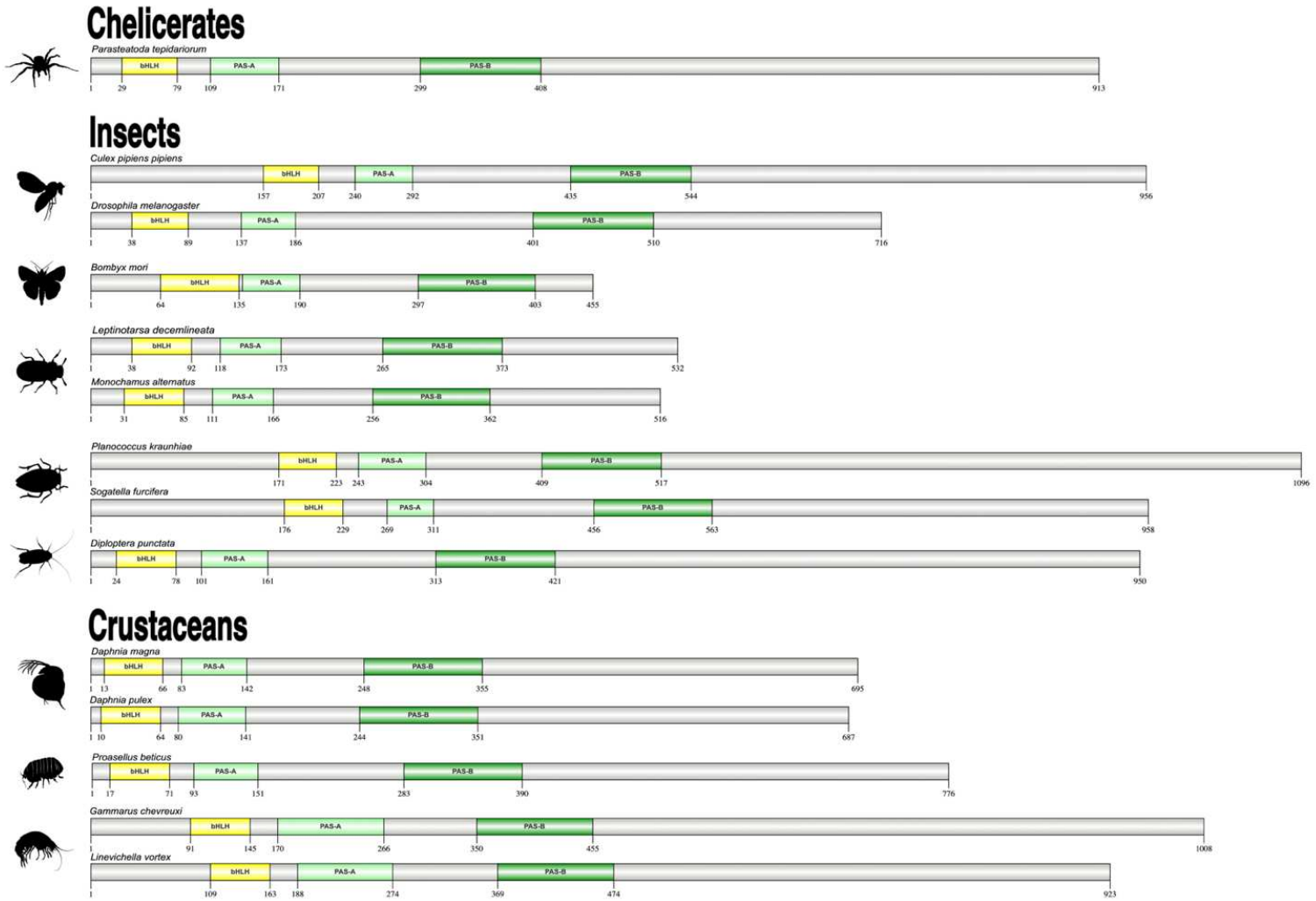

Figure A3. Domain architecture of arthropod Methoprene tolerant (Met) orthologues. Domains were identified with the NCBI CD search tool and visualized with IBS 2.0 (see Materials and Methods). Met contained a structured 5' N-terminus containing the basic, helix-loop-helix (bHLH) DNA binding domain followed by two PAS domains, A and B respectively. Information for the sequences is provided in the supplementary data spreadsheet on the online repository. Species silhouettes were obtained from PhyloPic (http://phylopic.org).

Figure A4

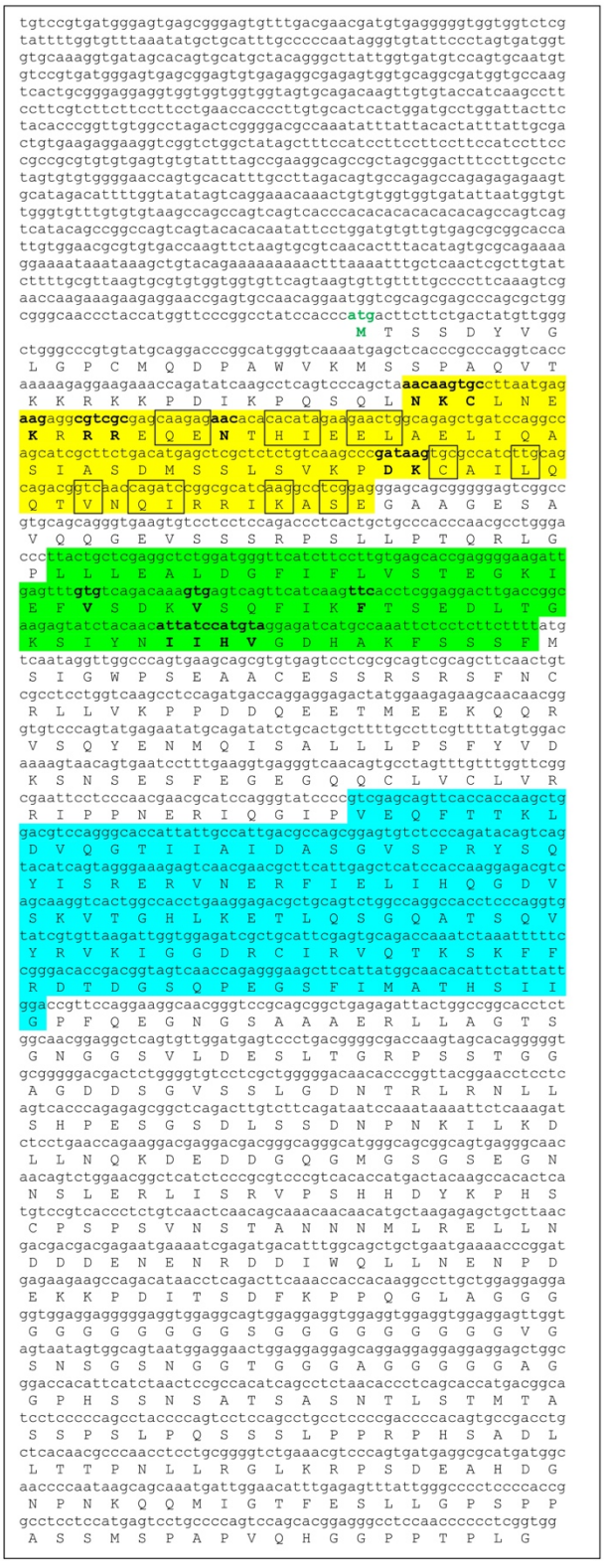

Figure A4. Nucleotide (nt) and deduced amino acid (aa) sequence of the *G. lateralis* Src contig (Y EVm002648t2) isolated from the Y-organ (YO) transcriptome. The contig sequence included a 1056 (bp) 5' untranslated region (UTR) with the start codon (atg) bolded in green. The 707 aa partial open reading frame (ORF) contains the basic-helix-loop-helix (bHLH) domain indicated in yellow (43-101 aa) which contains putative DNA binding sites (bolded) and dimer interfaces (boxed). Subsequently followed are two Per-ARNT-Sim (PAS) domains, A (130-187 aa) and B (281-389 aa) highlighted in green and blue respectively. Putative active sites within the PAS A domain are bolded.

Figure A5

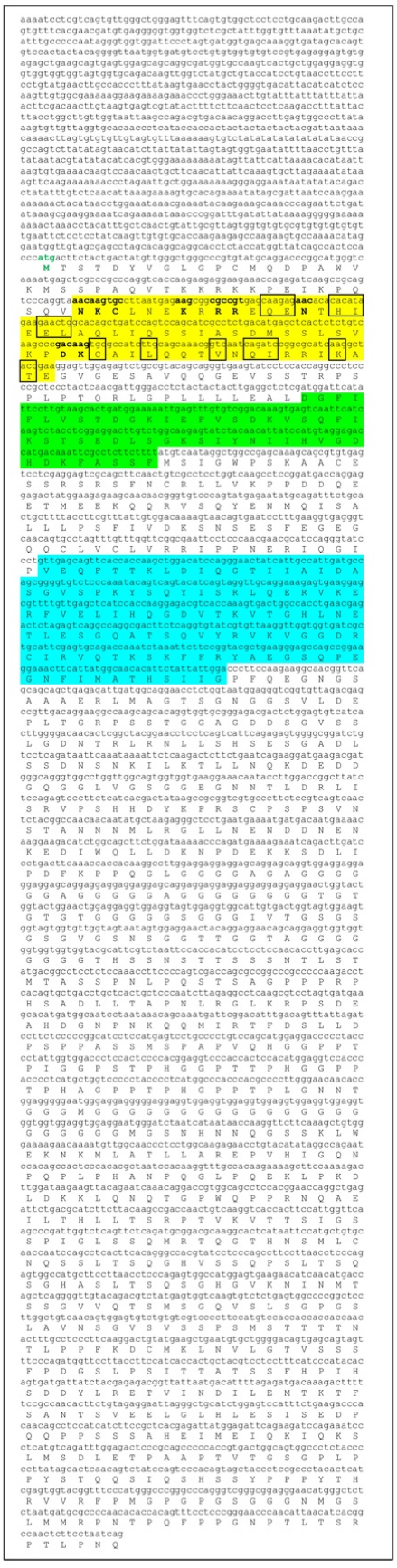

Figure A5. Nucleotide (nt) and deduced amino acid (aa) sequence of the *C. maenas* Src contig (Y EVm000958t2) isolated from the Y-organ (YO) transcriptome. The contig sequence included a 1323 (bp) 5' untranslated region (UTR) with the start codon (atg) bolded in green. Within the 1185 aa partial open reading frame (ORF) is the basic-helix-loop-helix (bHLH) domain shown indicated in yellow (43-101 aa) which contains putative DNA binding sites (bolded) and dimer interfaces (boxed). Subsequently followed are two Per-ARNT-Sim (PAS) domains, A (136-187 aa) and B (281-391 aa) highlighted in green and blue respectively.

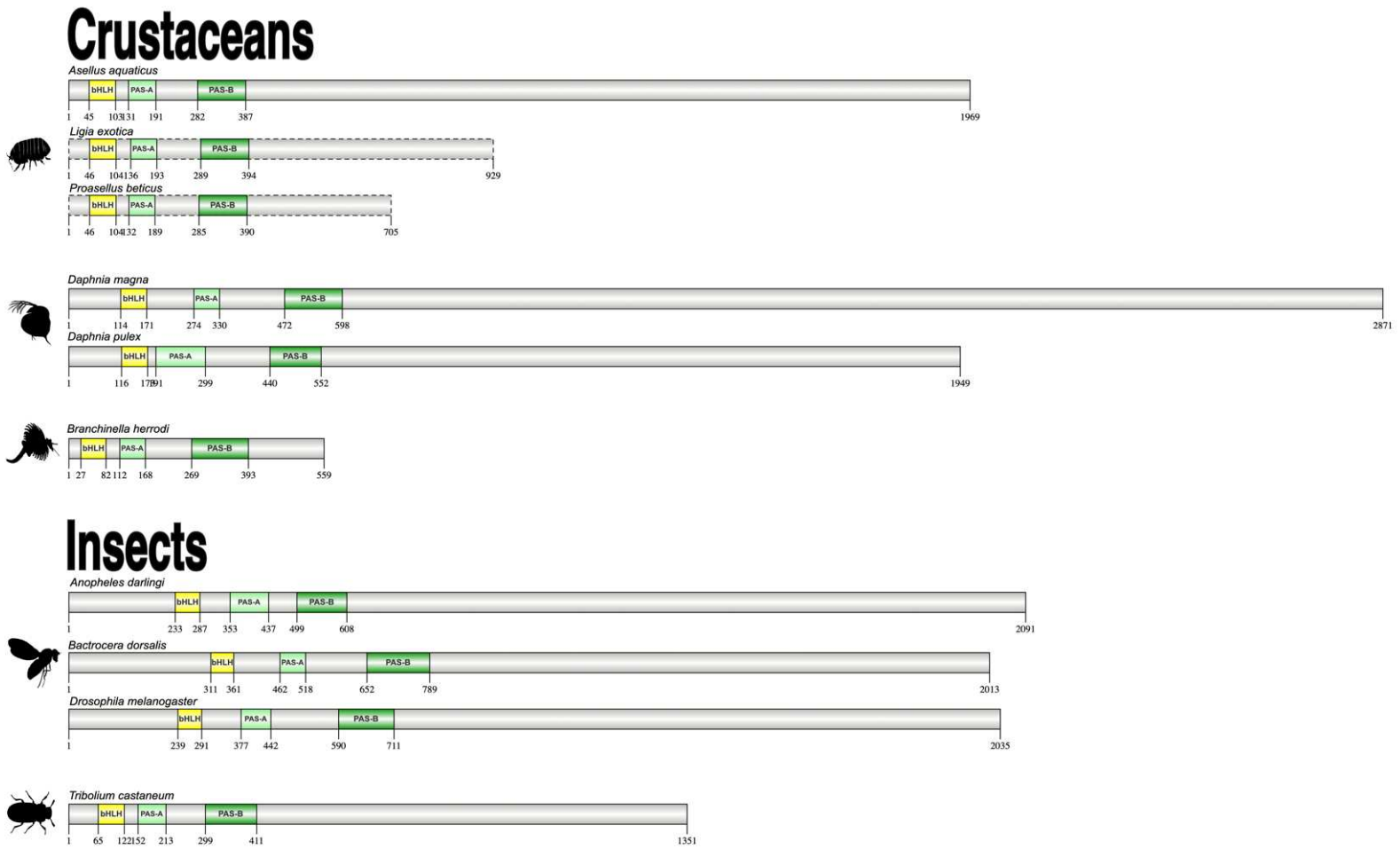

Figure A6. Domain architecture of pancrustacean Steroid receptor co-activator (Src) orthologs. Domains were identified with the NCBI CD search tool and visualized with IBS 2.0 (see Materials and Methods). Dashed configurations indicated a partial sequence. Information for the sequences is provided in the supplementary data spreadsheet on the online repository. Species silhouettes were obtained from PhyloPic (http://phylopic.org).

Figure A7

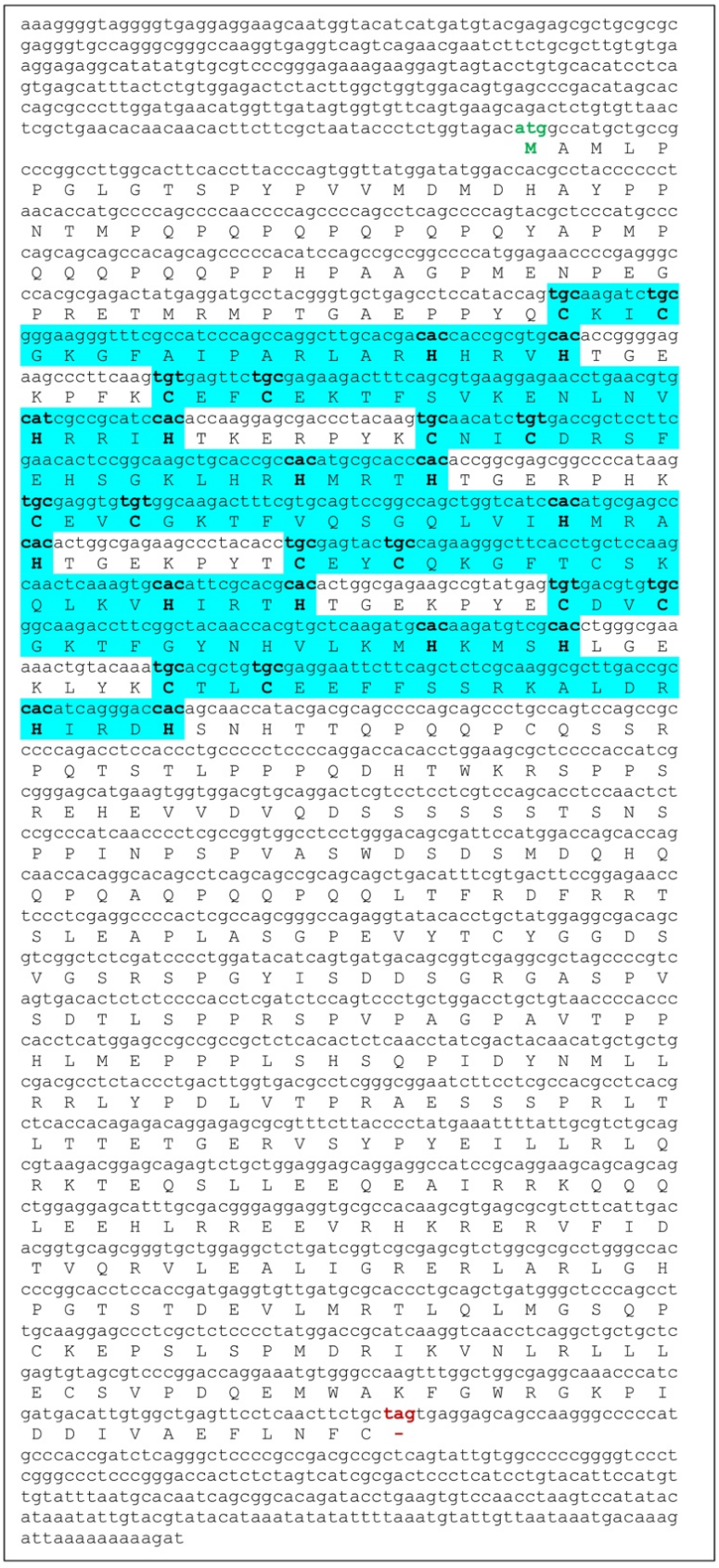
aaaggggtaggggtgaggaggaagcaatggtacatcatgatgtacgagagcgctgcgcgc
gagggtgccagggcgggccaaggtgaggtcagtcagaacgaatcttctgcgcttgtgtga
aggagaggcatatatgtgcgtcccgggagaaagaaggagtagtacctgtgcacatcctca
gtgagcatttactctgtggagactctacttggctggtggacagtgagcccgacatagcac
cagcgcccttggatgaacatggttgatagtggtgttcagtgaagcagactctgtgttaac
tcgctgaacacaacaacacttcttcgctaataccctctggtagacatggccatgctgccg
M A M L P
cccggccttggcacttcaccttacccagtggttatggatatggaccacgcctacccccct
P G L G T S P Y P V V M D M D H A Y P P
aacaccatgccccagccccaaccccagccccagcctcagccccagtacgctcccatgccc
N T M P Q P Q P Q P Q P Q P Q P Q Y A P M P
cagcagcagccacagcagcccccacatccagccgccgccccatggagaaccccgagggc
Q Q Q P Q Q P P H P A A G P M E N P E G
ccacgcgagactatgaggatgcctacgggtgctgagcctccataccagtgcaagatctgc
P R E T M R M P T G A E P P Y Q C K I C
gggaagggtttcgccatcccagccaggcttgcacgacaccaccgcgtgcaccaccggggag
G K G F A I P A R L A R H H R V H T G E
aagcccttcaagtgtgagttctgcgagaagactttcagcgtgaaggagaacctgaacgtg
K P F K C E F C E K T F S V K E N L N V
catcgccgcatccacaccaaggagcgaccctacaagtgcaacatctgtgaccgctccttc
H R R I H T K E R P Y K C N I C D R S F
gaacactccggcaagctgcaccgccacatgcgcacccacaccggcgagcggccccataag
E H S G K L H R H M R T H T G E R P H K
tgcgaggtgtgtggcaagactttcgtgcagtccggccagctggtcatccacatgcgagcc
C E V C G K T F V Q S G Q L V I H M R A
cacactggcgagaagccctacacctgcgagtactgccagaagggcttcacctgctccaag
H T G E K P Y T C E Y C Q K G F T C S K
caactcaaagtgcacattcgcacgcacactggcgagaagccgtatgagtgtgacgtgtgc
Q L K V H I R T H T G E K P Y E C D V C
ggcaagaccttcggctacaaccacgtgctcaagatgcacaagatgtcgcacctgggcgaa
G K T F G Y N H V L K M H K M S H L G E
aaactgtacaaatgcacgctgtgcgaggaattcttcagctctgcgaaggcgcttgaccgc
K L Y K C T L C E E F F S S R K A L D R
cacatcagggaccacagcaaccatacgacgcagccccagcagccctgccagtccagccgc
H I R D H S N H T T Q P Q Q P C Q S S R
ccccagacctccacctgccccctccccaggaccacacctggaagcgctccccaccatcg
P Q T S T L P P P Q D H T W K R S P P S
cgggagcatgaagtggtggacgtgcaggactcgtcctcctcgtccagcacctccaactct
R E H E V V D V Q D S S S S S S T S N S
ccgcccatcaacccctcgccggtggcctcctgggacagcgattccatggaccagcaccag
P P I N P S P V A S W D S D S M D Q H Q
caaccacaggcacagcctcagcagccgcagcagctgacatttcgtgacttccggagaacc
Q P Q A Q P Q Q P Q Q L T F R D F R R T
tccctcgaggcccactcgccagcgggccagaggtatacacctgctatggaggcgacagc
S L E A P L A S G P E V Y T C Y G G D S
gtcggctctcgatcccctggatacatcagtgatgacagcggtcgaggcgctagccccgtc
V G S R S P G Y I S D D S G R G A S P V
agtgacactctctccccacctcgatctccagtccctgctggacctgctgtaaccccaccc
S D T L S P P R S P V P A G P A V T P P
cacctcatggagccgccgccgctctcacactctcaacctatcgactacaacatgctgctg
H L M E P P P L S H S Q P I D Y N M L L
cgacgcctctaccctgacttggtgacgcctcgggcggaatcttcctcgccacgcctcacg
R R L Y P D L V T P R A E S S S P R L T
ctcaccacagagacaggagagcgcgtttcttacccctatgaaattttattgcgtctgcag
L T T E T G E R V S Y P Y E I L L R L Q
cgtaagacggagcagagtctgctggaggagcaggaggccatccgcaggaagcagcagcag
R K T E Q S L L E E Q E A I R R K Q Q Q
ctggaggagcatttgcgacgggaggaggtgcgccacaagcgtgagcgcgtcttcattgac
L E E H L R R E E V R H K R E R V F I D
acggtgcagcgggtgctggaggctctgatcggtcgcgagcgtctggcgcgcctgggccac
T V Q R V L E A L I G R E R L A R L G H
cccggcacctccaccgatgaggtgttgatgcgcaccctgcagctgatgggctcccagcct
P G T S T D E V L M R T L Q L M G S Q P
tgcaaggagccctcgctctcccctatggaccgcatcaaggtcaacctcaggctgctgctc
C K E P S L S P M D R I K V N L R L L L
gagtgtagcgtcccggaccaggaaatgtgggccaagtttggctggcgaggcaaacccatc
E C S V P D Q E M W A K F G W R G K P I
gatgacattgtggctgagttcctcaacttctgctagtgaggagcagccaagggcccccat
D D I V A E F L N F C -
gcccaccgatctcagggctccccgccgacgccgctcagtattgtggccccggggtccct
cgggccctcccgggaccactctctagtcatcgcgactccctcatcctgtacattccatgt
tgtatttaatgcacaatcagcggcacagatacctgaagtgtccaacctaagtccatatac
ataaatattgtacgtatacataaatatatattttaaatgtattgttaataaatgacaaag
attaaaaaaaaaagat

Figure A7. Nucleotide (nt) and deduced amino acid (aa) sequence alignment of the *G. lateralis* Krüppel homolog 1 (Kr-h1) contig (Y EVm003411t1) isolated from the Y-organ (YO) transcriptome. The contig sequence included a 5' and 3' untranslated region (UTR) consisting of 345 and 279 base pairs (bp) respectively; the start codon (atg) is indicated in green and the stop codon (tga) in red. Within the 616 aa open reading frame (ORF) are seven C2H2 zinc finger (Znf) domains (highlighted in aqua) with the zinc binding sites bolded. Each zinc finger consists of 21 aa and are separated by seven amino acids.

Figure A8

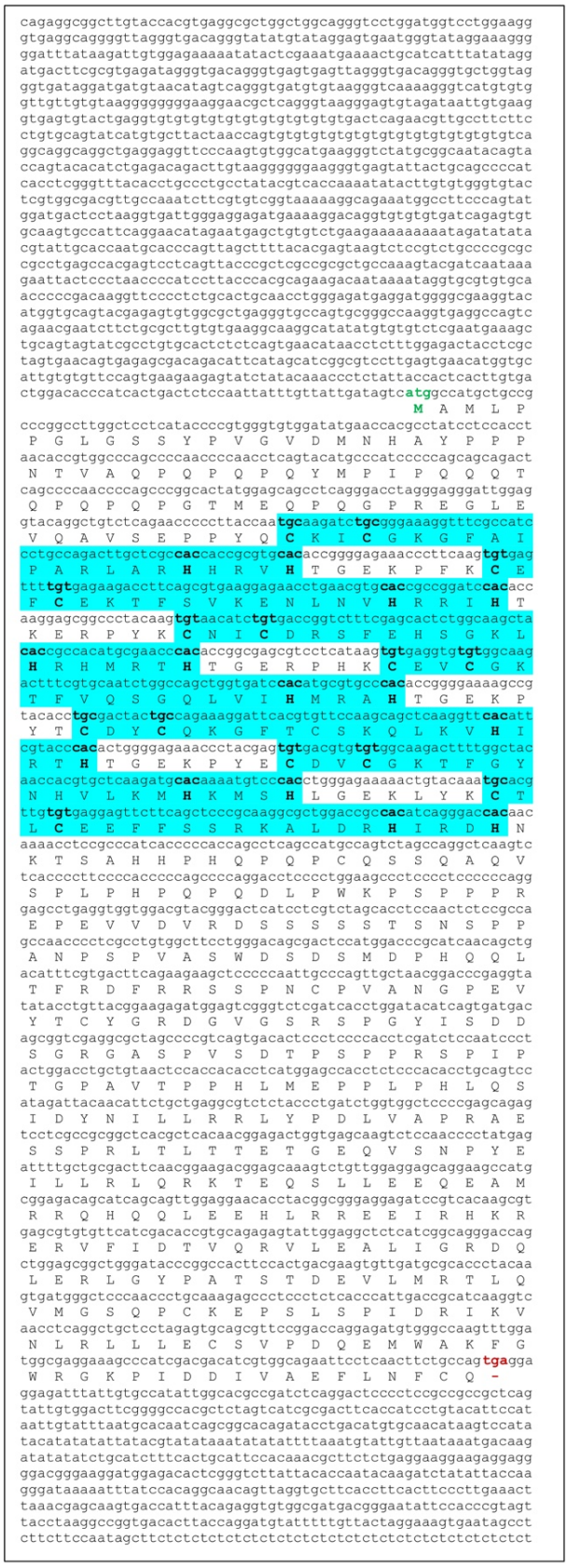

Figure A8. Nucleotide (nt) and deduced amino acid (aa) sequence of the *C. maenas* Krüppel homolog 1 (Kr-h1) contig (Y EVm004068t1) isolated from the Y-organ (YO) transcriptome. The contig sequence included a 5' and 3' untranslated region (UTR) consisting of 1425 and 603 base pairs (bp) respectively; the start codon (atg) is indicated in green and the stop codon (tga) in red. Within the 603 aa open reading frame (ORF) are seven C2H2 zinc finger (Znf) domains, highlighted in multiple colors with zinc binding sites bolded, consisting of 21 aa of which each is separated by seven amino acids.

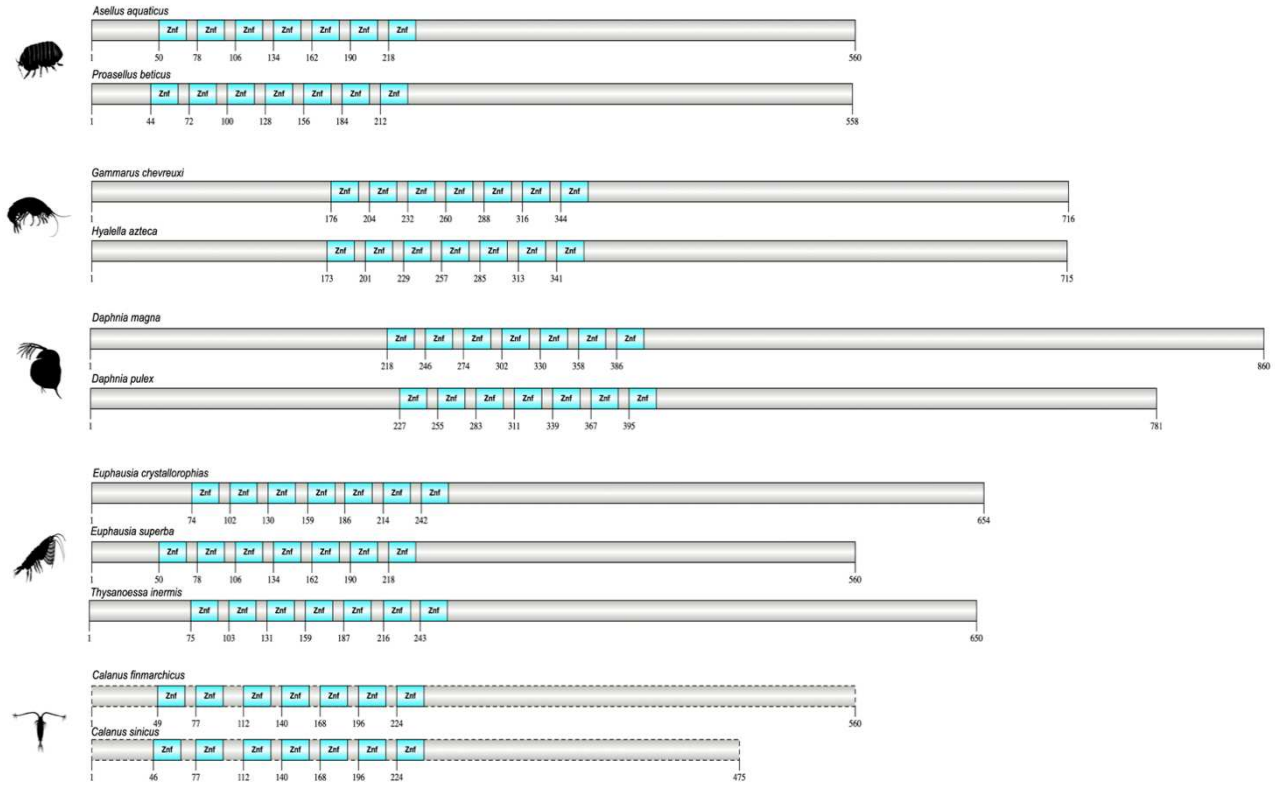

Figure A9. Domain structure of Krüppel homolog 1 (Kr-h1) orthologs in non-decapod crustaceans. Seven zinc finger (Znf) repeats were identified with the NCBI CD search tool and visualized with IBS 2.0 (see Materials and Methods). Dashed configurations indicated a partial sequence. Information for the sequences is provided in the supplementary data spreadsheet on the online repository. Species silhouettes were obtained from PhyloPic (http://phylopic.org).

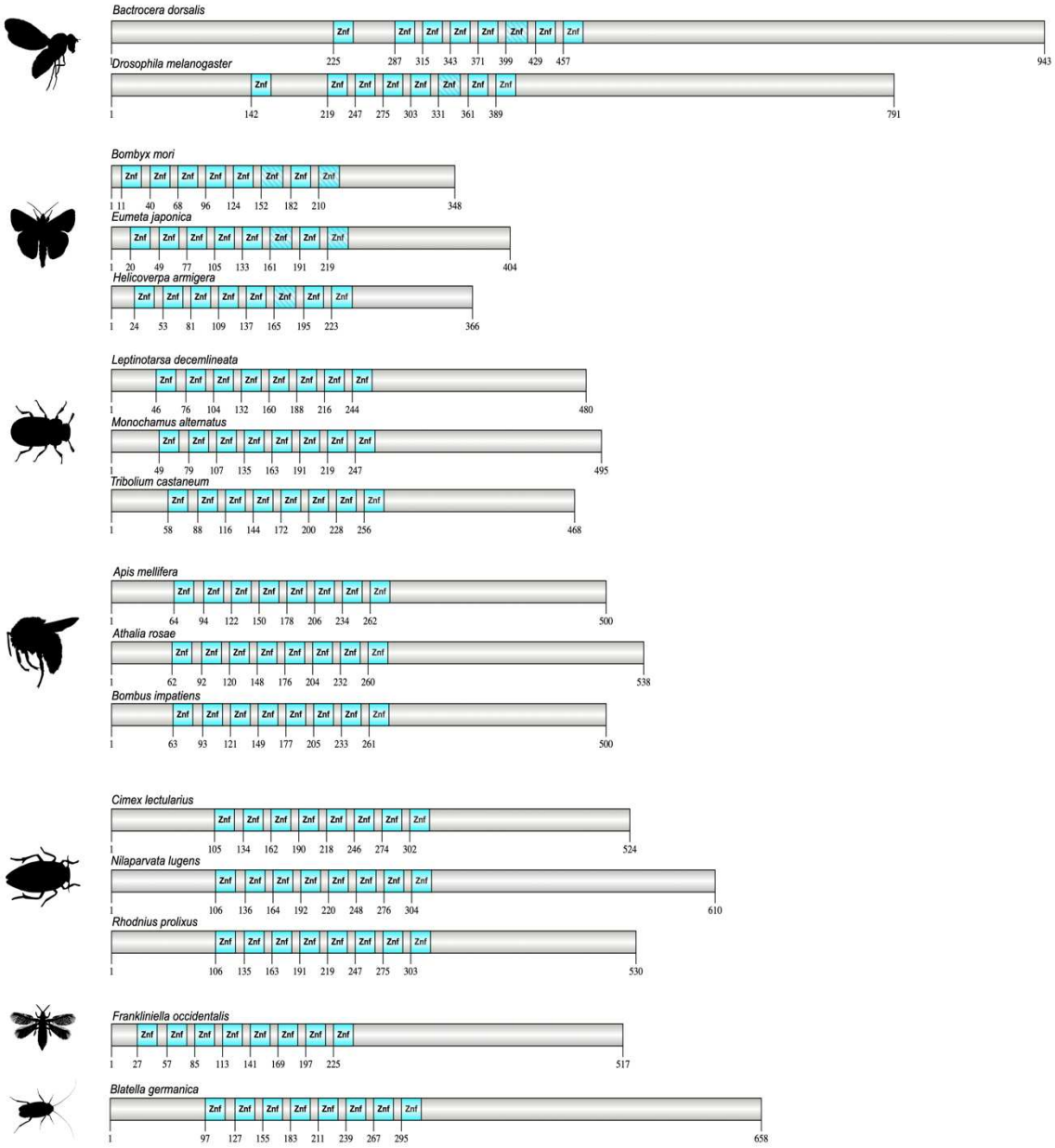

Figure A10. Domain structure of Krüppel homolog 1 (Kr-h1) orthologs in various insect orders. Eight zinc finger (Znf) repeats were identified with the NCBI CD search tool and visualized with IBS 2.0 (see Materials and Methods). Information for the sequences is provided in the supplementary data spreadsheet on the online repository. Species silhouettes were obtained from PhyloPic (http://phylopic.org).

Figure A11

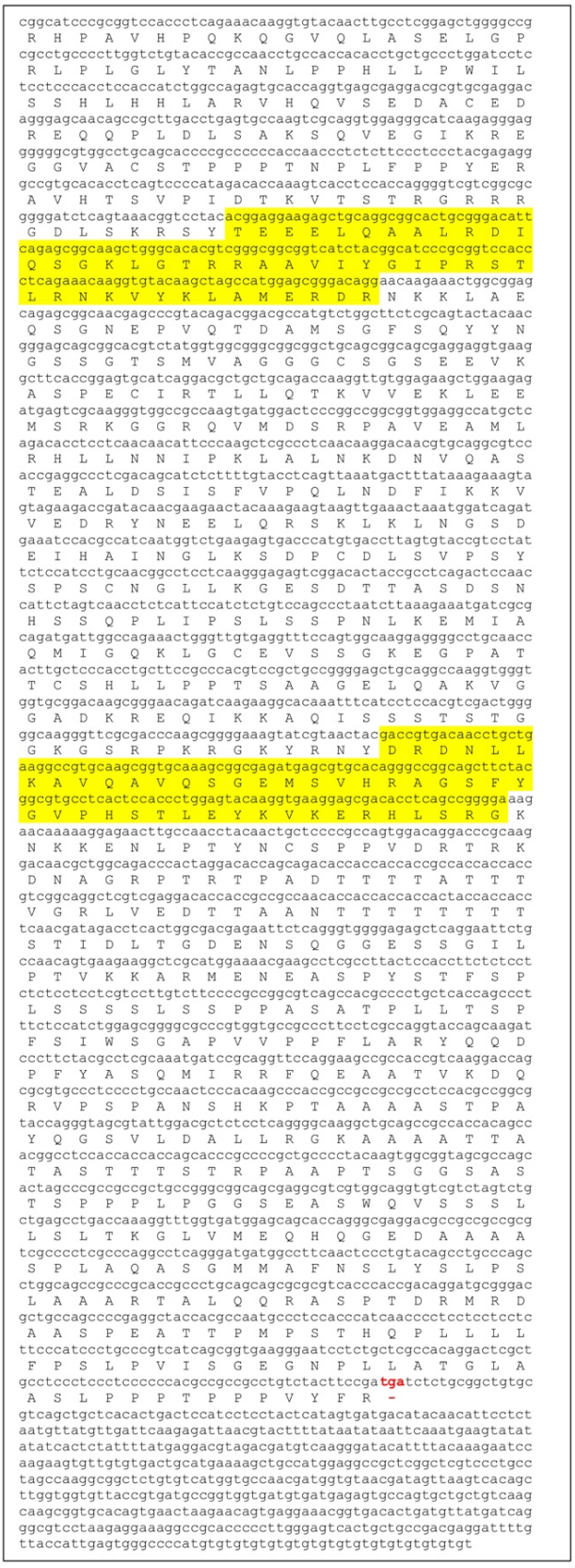
cggcatcccgcggtccacccctcagaaacaaggtgtacaacttgcctcggagctggggccg
R H P A V H P Q K Q G V Q L A S E L G P
cgcctgccccttggtctgtacaccgccaacctgccaccacacctgctgccctggatcctc
R L P L G L Y T A N L P P H L L P W I L
tcctcccacctccaccatctggccagagtgcaccaggtgagcgaggacgcgtgcgaggac
S S H L H H L A R V H Q V S E D A C E D
agggagcaacagccgcttgacctgagtgccaagtcgcaggtggagggcatcaagagggag
R E Q Q P L D L S A K S Q V E G I K R E
gggggcgtggcctgcagcaccccgccccccaccaaccctctcttccctccctacgagagg
G G V A C S T P P P T N P L F P P Y E R
gccgtgcacacctcagtccccatagacaccaaagtcacctccaccaggggtcgtcggcgc
A V H T S V P I D T K V T S T R G R R R
ggggatctcagtaaacggtcctacacggaggaagagctgcaggcggcactgcgggacatt
G D L S K R S Y T E E E L Q A A L R D I
cagagcggcaagctgggcacacgtcgggcggcggtcatctacggcatcccgcggtccacc
Q S G K L G T R R A A V I Y G I P R S T
ctcagaaacaaggtgtacaagctagccatggagcgggacaggaacaagaaactggcggag
L R N K V Y K L A M E R D R N K K L A E
cagagcggcaacgagcccgtacagacggacgccatgtctggcttctcgcagtactacaac
Q S G N E P V Q T D A M S G F S Q Y Y N
gggagcagcggcacgtctatggtggcgggcggcggctgcagcggcagcgaggaggtgaag
G S S G T S M V A G G G C S G S E E V K
gcttcaccggagtgcatcaggacgctgctgcagaccaaggttgtggagaagctggaagag
A S P E C I R T L L Q T K V V E K L E E
atgagtcgcaagggtggccgccaagtgatggactcccggccggcggtggaggccatgctc
M S R K G G R Q V M D S R P A V E A M L
agacacctcctcaacaacattcccaagctcgccctcaacaaggacaacgtgcaggcgtcc
R H L L N N I P K L A L N K D N V Q A S
accgaggccctcgacagcatctcttttgtacctcagttaaatgacttttataaagaaagta
T E A L D S I S F V P Q L N D F I K K V
gtagaagaccgatacaacgaagaactacaaagaagtaagttgaaactaaatggatcagat
V E D R Y N E E L Q R S K L K L N G S D
gaaatccacgccatcaatggtctgaagagtgacccatgtgaccttagtgtaccgtcctat
E I H A I N G L K S D P C D L S V P S Y
tctccatcctgcaacggcctcctcaagggagagtcggacactaccgcctcagactccaac
S P S C N G L L K G E S D T T A S D S N
cattctagtcaacctctcattccatctctgtccagccctaatcttaaagaaatgatcgcg
H S S Q P L I P S L S S P N L K E M I A
cagatgattggccagaaactgggttgtgaggtttccagtggcaaggaggggcctgcaacc
Q M I G Q K L G C E V S S G K E G P A T
acttgctcccacctgcttccgcccacgtccgctgccgggagctgcaggccaaggtgggt
T C S H L L P P T S A A G E L Q A K V G
ggtgcggacaagcgggaacagatcaagaaggcacaaatttcatcctccacgtcgactggg
G A D K R E Q I K K A Q I S S S T S T G
ggcaaggttcgcgacccaagcggggaaagtatcgtaactacgaccgtgacaacctgctg
G K G S R P K R G K Y R N Y D R D N L L
aaggccgtgcaagcggtgcaaagcggcgagatgagcgtgcacagggccggcagcttctac
K A V Q A V Q S G E M S V H R A G S F Y
ggcgtgcctcactccacctggagtacaaggtgaaggagcgacacctcagccgggaaaag
G V P H S T L E Y K V K E R H L S R G K
aacaaaaaggagaacttgccaacctacaactgctccccgccagtggacaggacccgcaag
N K K E N L P T Y N C S P P V D R T R K
gacaacgctggcagacccactaggacaccagcagacaccaccaccaccgccaccaccacc
D N A G R P T R T P A D T T T T A T T T
gtcggcaggctcgtcgaggacaccaccgccgccaacaccaccaccaccactaccaccacc
V G R L V E D T T A A N T T T T T T T T
tcaacgatagacctcactggcgacgagaattctcagggtggggagagctcaggaattctg
S T I D L T G D E N S Q G G E S S G I L
ccaacagtgaagaaggctcgcatggaaaacgaagcctcgccttactccaccttctctcct
P T V K K A R M E N E A S P Y S T F S P
ctctcctcctcgtccttgtcttccccgccggcgtcagccacgccctgctcaccagccct
L S S S S L S S P P A S A T P L L T S P
ttctccatctggagcggggcgcccgtggtgccgcccttcctcgccaggtaccagcaagat
F S I W S G A P V V P P F L A R Y Q Q D
cccttctacgcctcgcaaatgatccgcaggttccaggaagccgccaccgtcaaggaccag
P F Y A S Q M I R R F Q E A A T V K D Q
cgcgtgccctcccctgccaactcccacaagcccaccgccgccgccgcctccacgccggcg
R V P S P A N S H K P T A A A A S T P A
taccagggtagcgtattggacgctctcctcaggggcaaggctgcagccgccaccacagcc
Y Q G S V L D A L L R G K A A A A A T T A
acggcctccaccaccaccagcacccgccccgctgcccctacaagtggcggtagcgccagc
T A S T T T S T R P A A P T S G G S A S
actagcccgccgccgctgccgggcggcagcgaggcgtcgtggcaggtgtcgtctagtctg
T S P P P L P G G S E A S W Q V S S S L
ctgagcctgaccaaaggtttggtgatggagcagcaccagggcgaggacgccgccgccgcg
L S L T K G L V M E Q H Q G E D A A A A
tcgcccctcgcccaggcctcagggatgatggccttcaactccctgtacagcctgcccagc
S P L A Q A S G M M A F N S L Y S L P S
ctggcagccgcccgcaccgccctgcagcagcgcgcgtcacccaccgacaggatgcgggac
L A A A R T A L Q Q R A S P T D R M R D
gctgccagccccgaggctaccacgccaatgccctccacccatcaaccctcctcctcctc
A A S P E A T T P M P S T H Q P L L L L
ttcccatccctgcccgtcatcagcggtgaagggaatcctctgctcgccacaggactcgct
F P S L P V I S G E G N P L L A T G L A
gcctcccctcctccccccacgccgccgcctgtctacttccgatgatctctgcggctgtgc
A S L P P P T P P P V Y F R -
gtcagctgctcacactgactccatcctcctactcatagtgatgacatacaacattcctct
aatgttatgttgattcaagagattaacgtacttttataatataattcaaatgaagtatat
atatcactctatttttatgaggacgtagacgatgtcaagggatacattttacaaagaatcc
aagaagtgttgtgtgactgcatgaaaagctgccatggaggccgctcggctcgtccctgcc
tagccaaggcggctctgtgtcatggtgccaacgatggtgtaacgatagttaagtcacagc
ttggtggtgttaccgtgatgccggtggtgatgtgatgagagtgccagtgctgctgtcaag
caagcggtgcacagtgaactaagaacagtgaggaaacggtgacactgatgttatgatcag
ggcgtcctaagaggaaaggccgcacccccttgggagtcactgctgccgacgaggattttg
ttaccattgagtgggccccatgtgtgtgtgtgtgtgtgtgtgtgtgtgtgtgt

Figure A11. Nucleotide (nt) and deduced amino acid (aa) sequence of the *G. lateralis* Mushroom body large-type Kenyon-cell protein-1 (Mblk-1) contig (Y EVm001885t1) isolated from the Y-organ (YO) transcriptome. The partial open reading frame (ORF) of 854 aa contains two helix-turn-helix, pipsqueak (HTH_psq) domains; the stop codon (tga) bolded in red is followed by a 548 base pair (bp) 3' untranslated region (UTR).

Figure A12

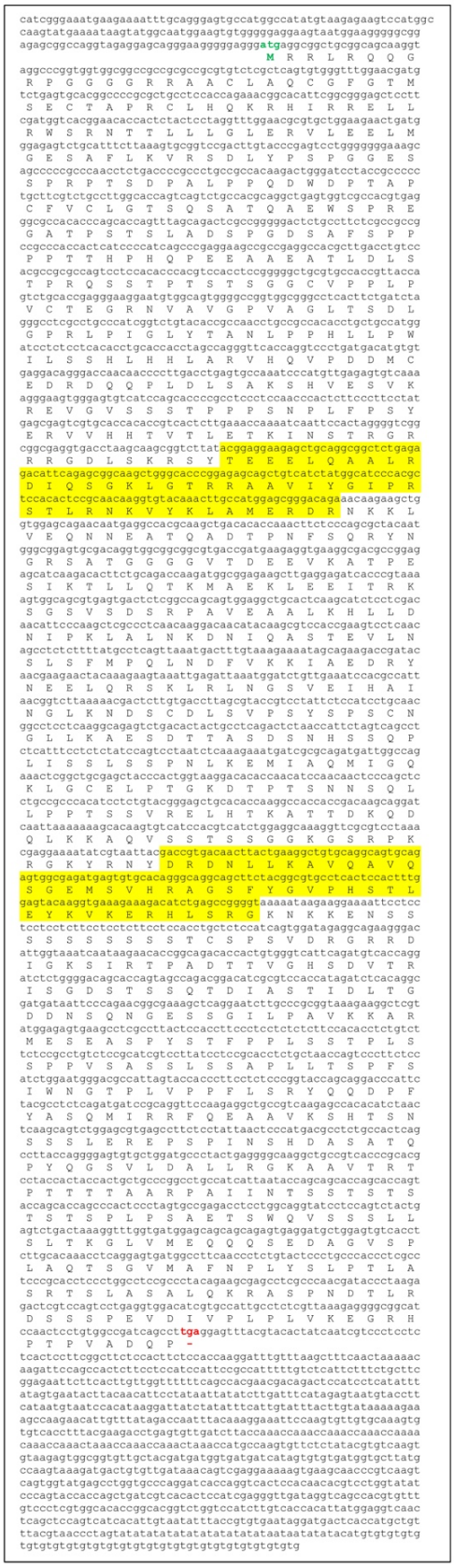

Figure A12. Nucleotide (nt) and deduced amino acid (aa) sequence of the *C. maenas* Mushroom body large-type Kenyon-cell protein-1 (Mblk-1) contig (Y EVm001380t1) isolated from the Y-organ (YO) transcriptome. The 1016 aa open reading frame (ORF) contains two helix-turn-helix, pipsqueak (HTH_psq) domains; bolded are the start (atg) and stop (tga) codons in green and red respectively. The contig contains a 158 base pair (bp) 5' untranslated region (UTR) and 975 bp 3' UTR.

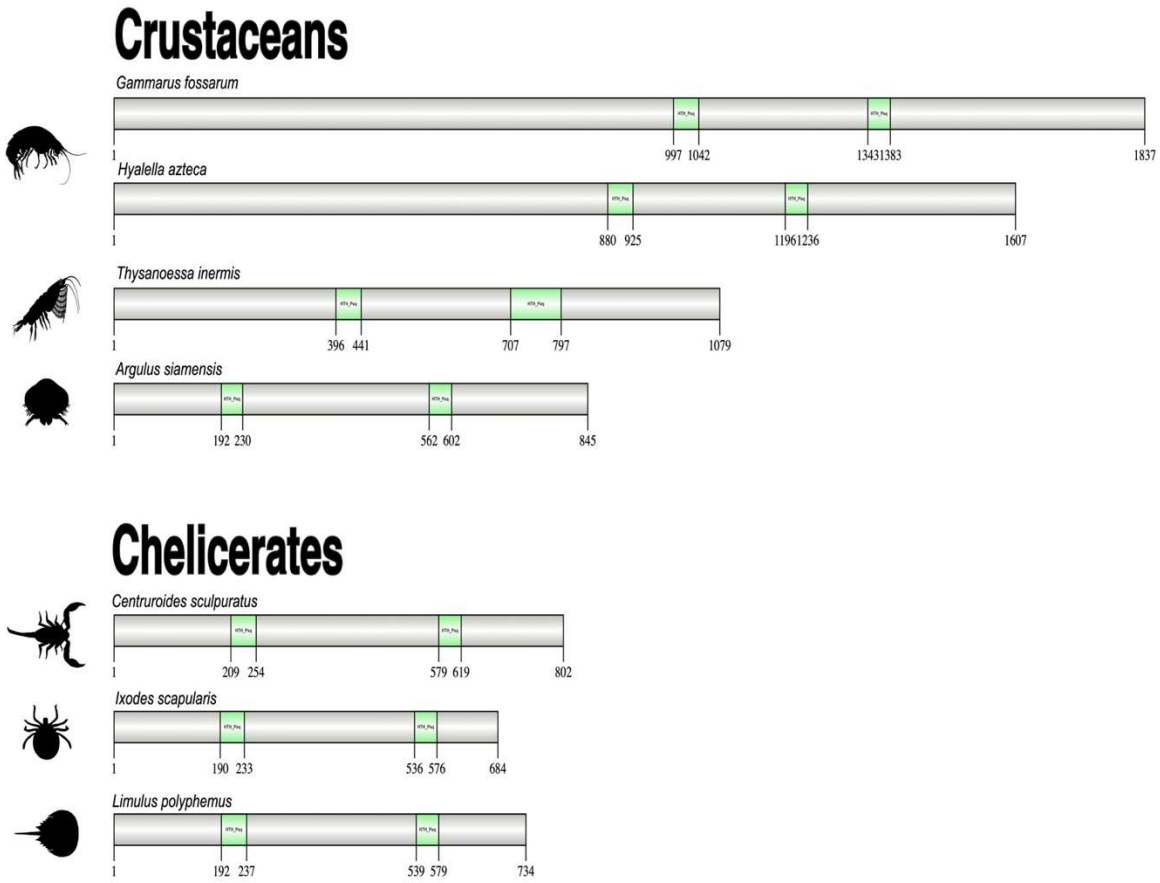

Figure A13. Comparison of E93/Mblk-1 orthologs between non-decapod crustaceans and chelicerates. Two helix-turn-helix, pipsqueak (HTH_Psq) were predicted with the NCBI CD search tool and visualized with IBS 2.0 (see Materials and Methods). Information for the sequences is provided in the supplementary data spreadsheet on the online repository. Species silhouettes were obtained from PhyloPic (http://phylopic.org).

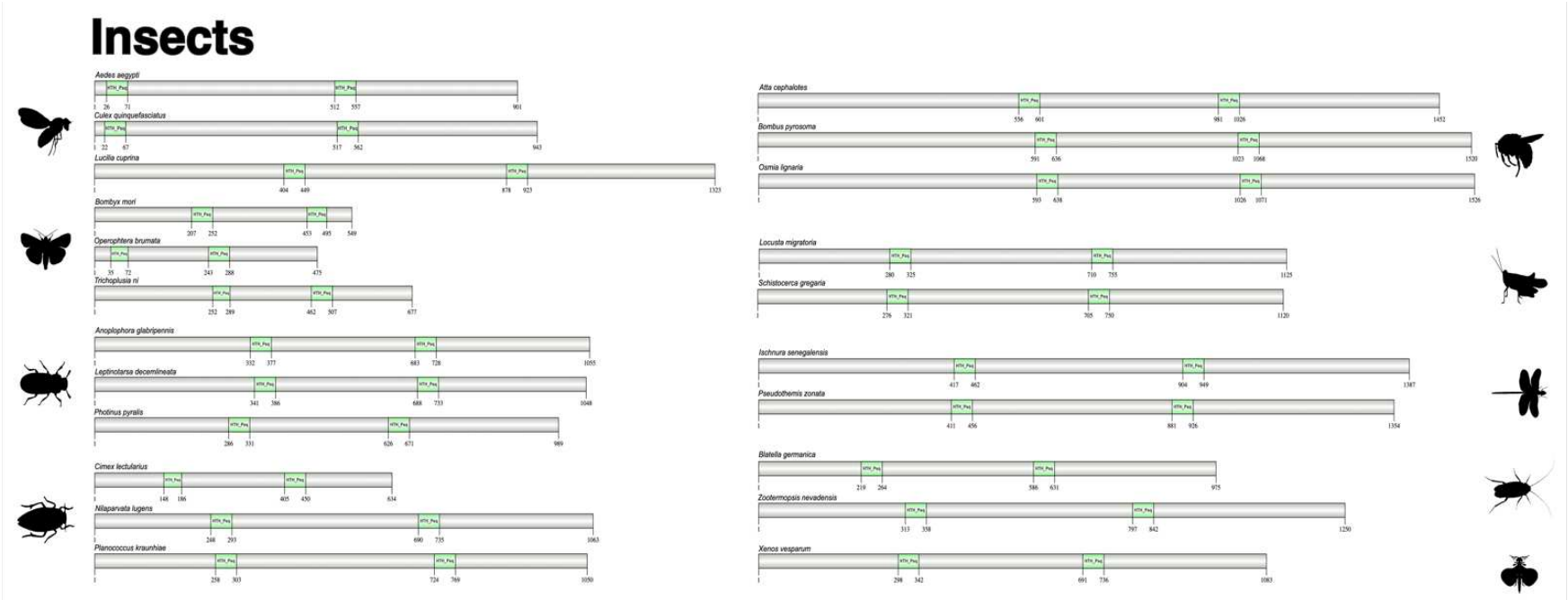

Figure A14. Comparison of E93/Mblk-1 orthologs across various insect orders. Two helix-turn-helix, pipsqueak (HTH_Psq) were predicted with the NCBI CD search tool and visualized with IBS 2.0 (see Materials and Methods). Information for the sequences is provided in the Supplementary Data spreadsheet. Species silhouettes were obtained from PhyloPic (http://phylopic.org).

Figure A15

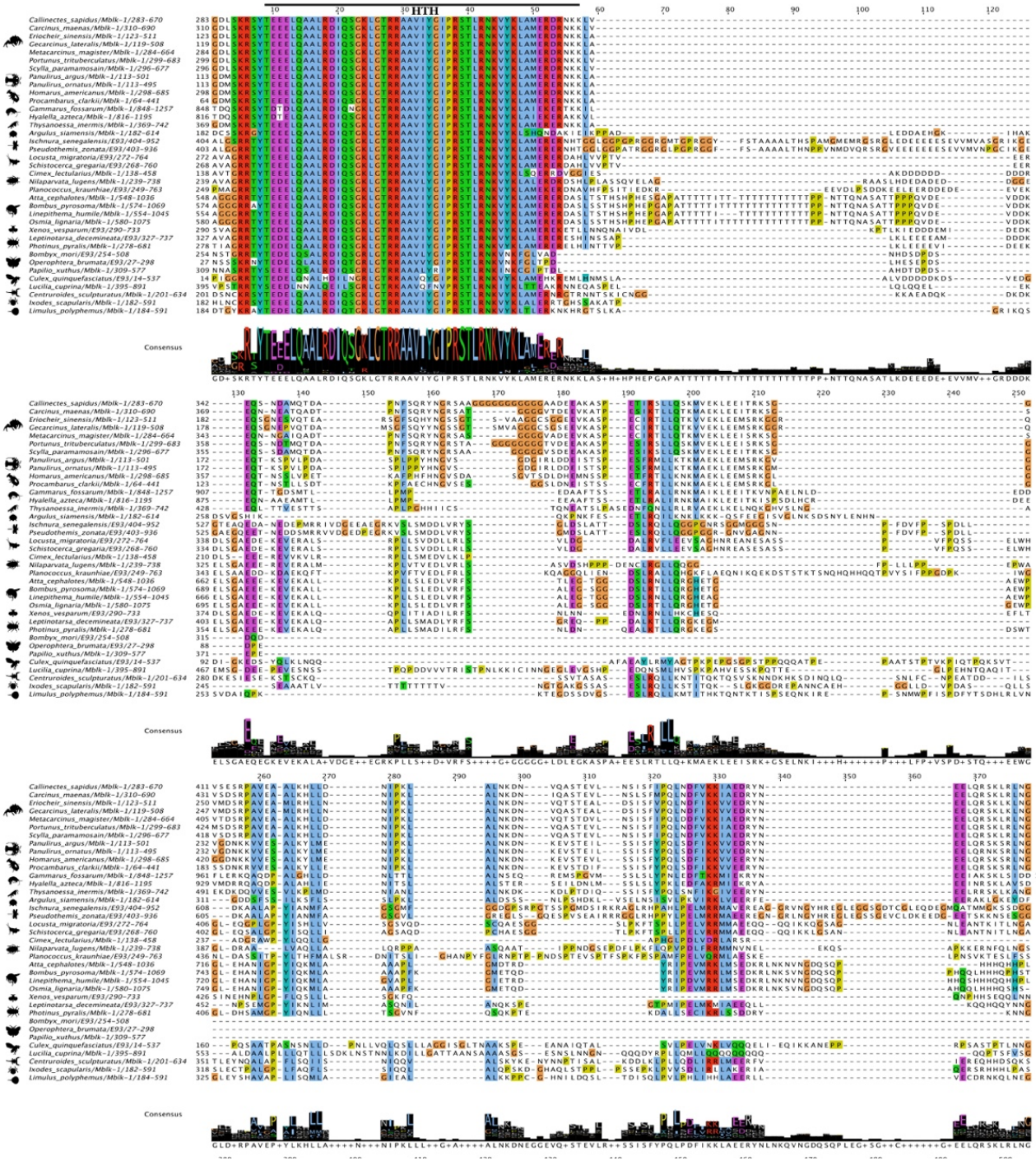

Figure A15 (continued)

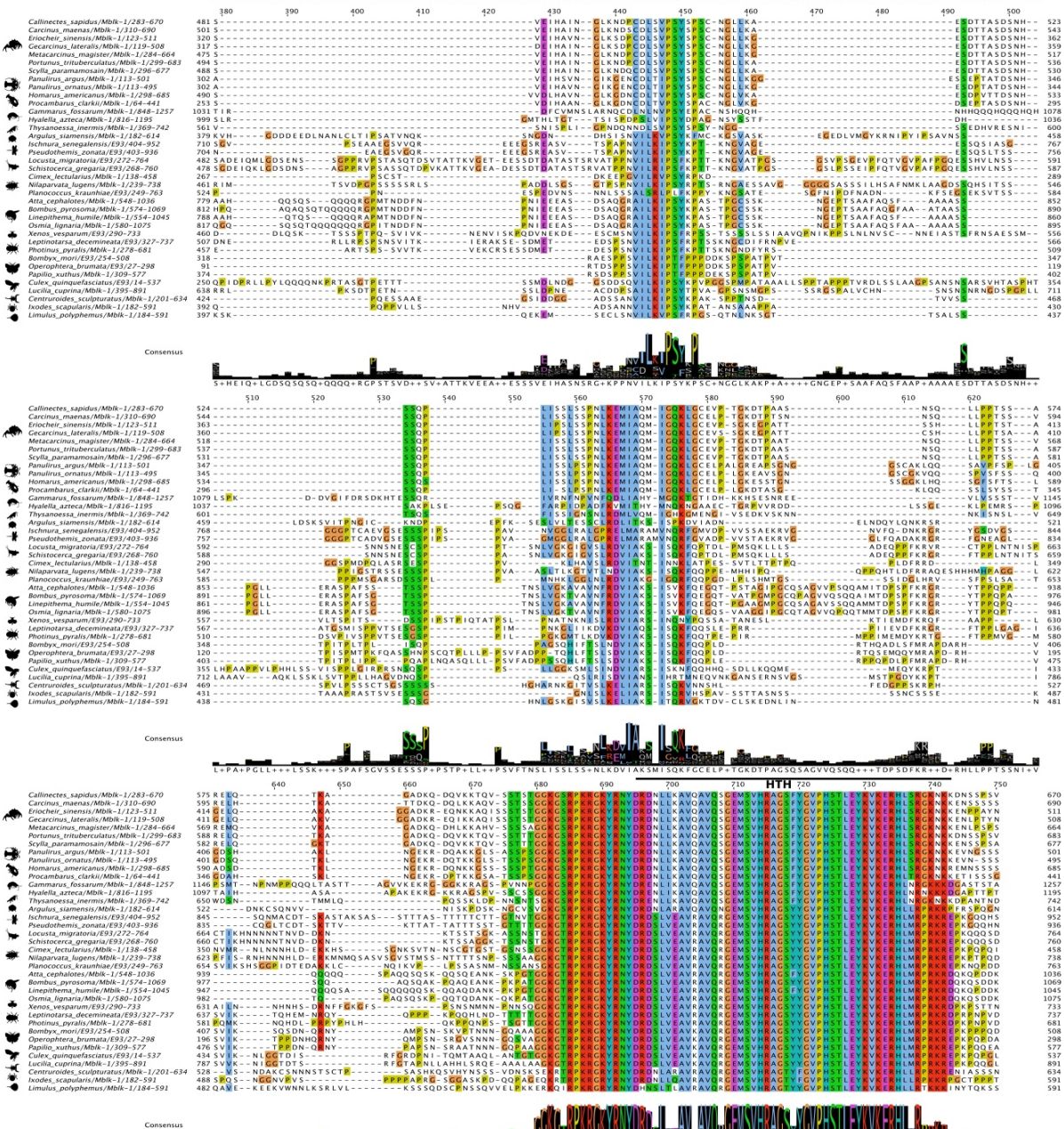

Figure A15. Multiple sequence alignment of the arthropod E93/Mblk-1 sequences. The sequences were aligned using the Mafft EINSI parameters, trimmed with ClipKIT, and visualized through Jalview following default Clustal coloring (see Materials and Methods). The consensus sequence is illustrated as a logo schematic. Two helix-turn-helix (HTH) domains exhibited high sequence identity and are indicated by an overhead solid line. Sequences and databases used in the analysis are in the supplementary data spreadsheet on the online repository. Species silhouettes were obtained from PhyloPic (http://phylopic.org).

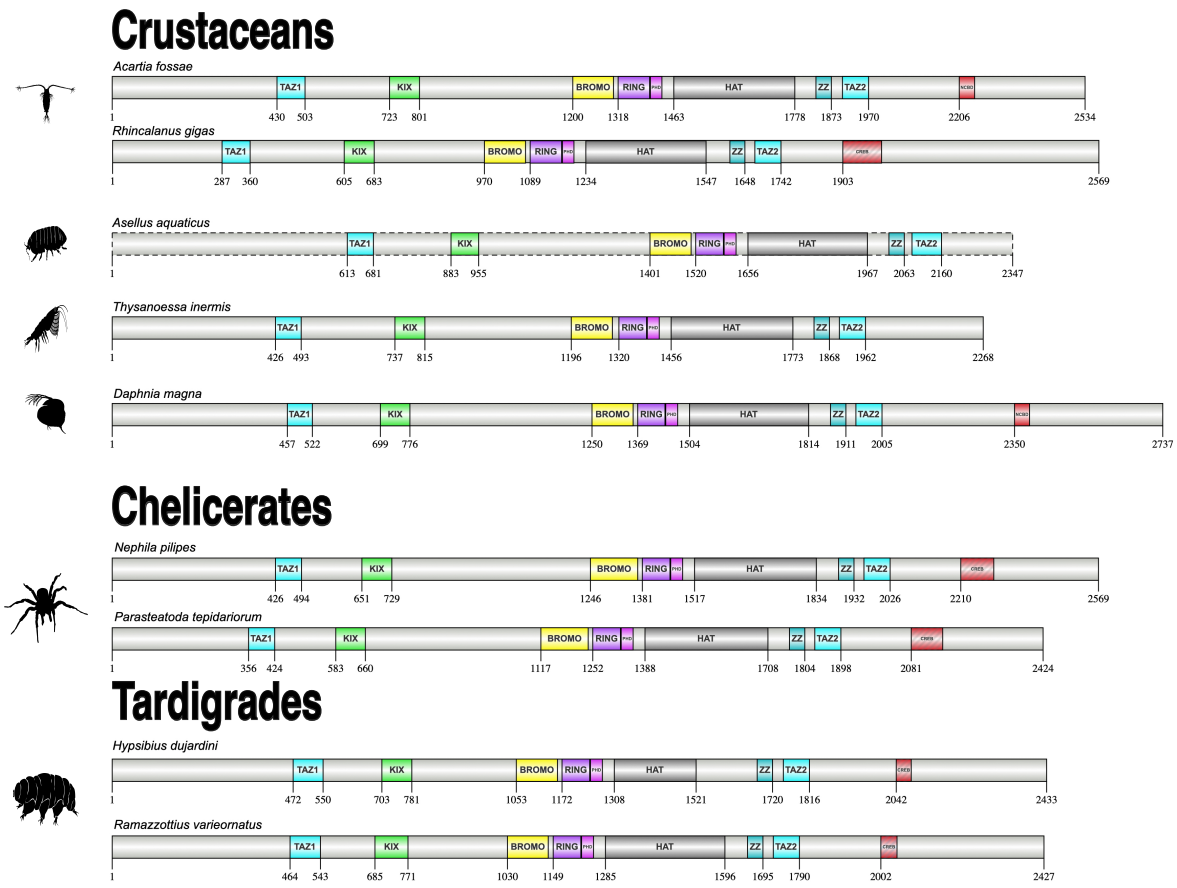

Figure A16. Domain architecture of CREB binding protein (CBP) orthologs in Clade Panarthropoda (non-decapod crustaceans, chelicerates, tardigrades, and various orders of insects) as identified with the NCBI CD search tool and visualized with IBS 2.0; dashed configurations indicate a partial sequence. CBP structure is organized through a series of domains starting with the Transcription Adaptor Zinc Finger (TAZ1) domain, followed by the KIX, Bromodomain (BROMO) with acetyllysine binding sites, the RING with zinc-binding sites and HAT interfaces, the PHD with histone H3 binding sites, HAT, ZZ with zinc-binding sites, and TAZ2 domain. At the 3' C-terminal region is the CREB binding domain which contains coactivator binding sites. Refer to the supplementary data spreadsheet on the online repository. Various species silhouettes were obtained from PhyloPic (http://phylopic.org).

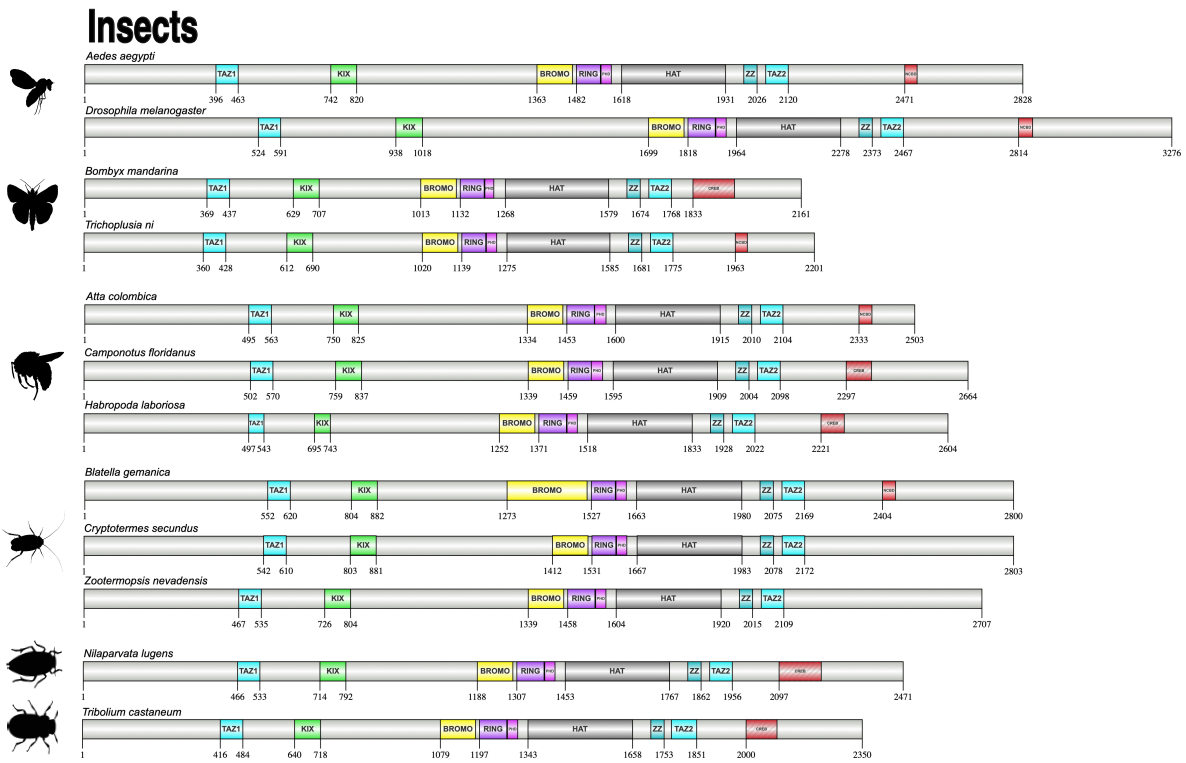

Figure A17. Domain structure of CREB binding protein (CBP) orthologs in various insect orders. Domains were identified with the NCBI CD search tool and visualized with IBS 2.0 (see Materials and Methods). CBP proteins contained the Transcription Adaptor Zinc Finger (TAZ1), Kinase-inducible domain (KID) interacting domain (KIX), Bromodomain (BROMO), Really Interesting New Gene (RING), Plant Homeodomain (PHD), Histone acetyltransferase (HAT), ZZ zinc finger (ZZ), and TAZ2 domains. Coactivator binding sites were contained in the nuclear receptor coactivator binding domain (NCBD) within the CREB binding regions (CREB). Information for the sequences is provided in the supplementary data spreadsheet on the online repository. Species silhouettes were obtained from PhyloPic (http://phylopic.org).

Figure A18

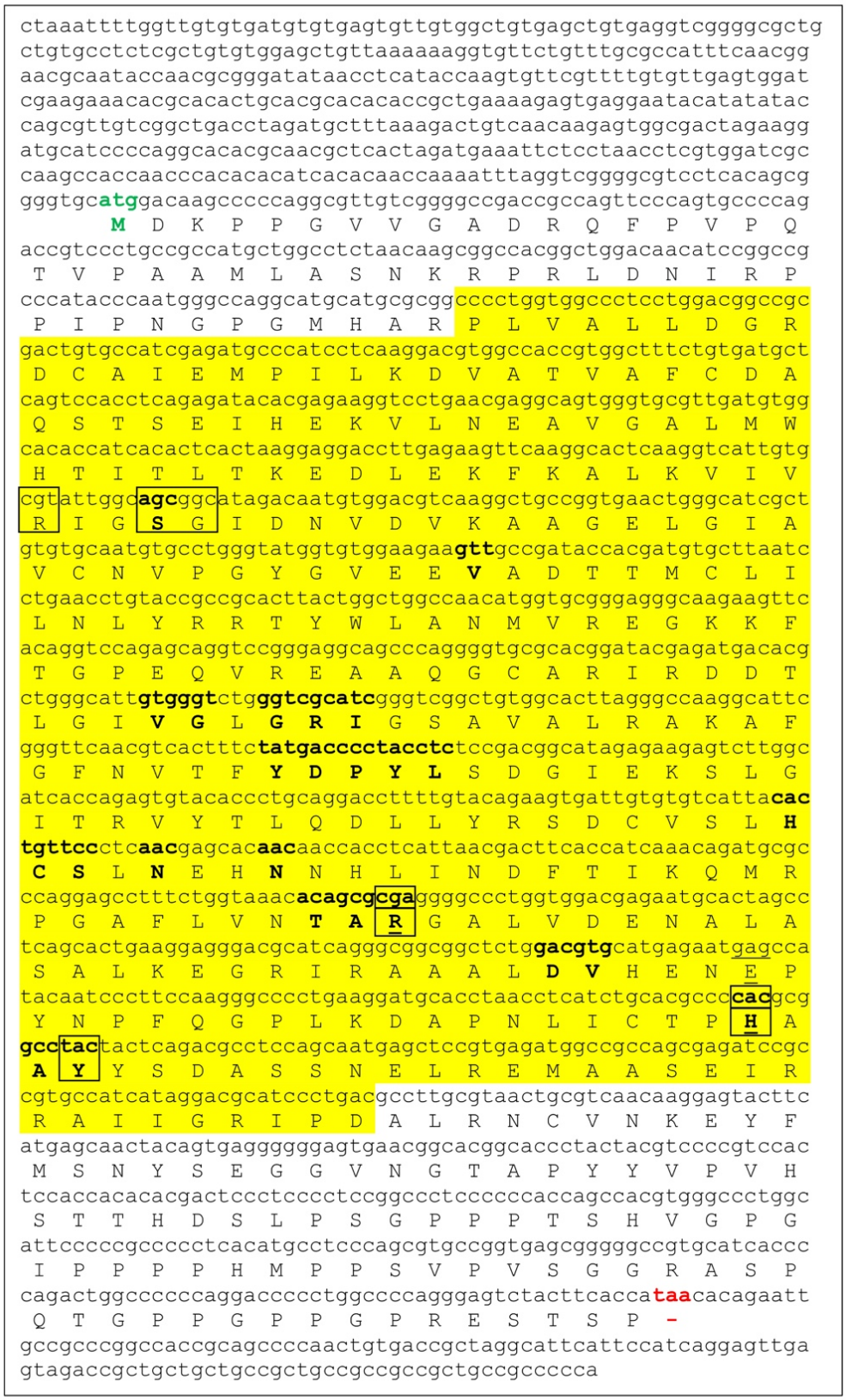
ctaaattttggttgtgtgatgtgtgagtgttgtggctgtgagctgtgaggtcggggcgctg
ctgtgcctctcgctgtgtggagctgttaaaaaaggtgttctgtttgcgccatttcaacgg
aacgcaataccaacgcgggatataacctcataccaagtgttcgttttgtgttgagtggat
cgaagaaacacgcacactgcacgcacacaccgctgaaaagagtgaggaatacatatatac
cagcgttgtcggctgacctagatgctttaaagactgtcaacaagagtggcgactagaagg
atgcatccccaggcacacgcaacgctcactagatgaaattctcctaacctcgtggatcgc
caagccaccaacccacacacatcacacaaccaaaatttaggtcggggcgtcctcacagcg
gggtgcatggacaagcccccaggcgttgtcggggccgaccgccagttcccagtgccccag
M D K P P G V V G A D R Q F P V P Q
accgtccctgccgccatgctggcctctaacaagcggccacggctggacaacatccggccg
T V P A A M L A S N K R P R L D N I R P
cccatacccaatgggccaggcatgcatgcgcggccccctggtggccctcctggacggccgc
P I P N G P G M H A R P L V A L L D G R
gactgtgccatcgagatgcccatcctcaaggacgtggccaccgtggctttctgtgatgct
D C A I E M P I L K D V A T V A F C D A
cagtccacctcagagatacacgagaaggtcctgaacgaggcagtgggtgcgttgatgtgg
Q S T S E I H E K V L N E A V G A L M W
cacaccatcacactcactaaggaggaccttgagaagttcaaggcactcaaggtcattgtg
H T I T L T K E D L E K F K A L K V I V
cgtattggcagcggcatagacaatgtggacgtcaaggctgccggtgaactgggcatcgct
R I G S G I D N V D V K A A G E L G I A
gtgtgcaatgtgcctgggtatggtgtggaagaagttgccgataccacgatgtgcttaatc
V C N V P G Y G V E E V A D T T M C L I
ctgaacctgtaccgccgcacttactggctggccaacatggtgcgggagggcaagaagttc
L N L Y R R T Y W L A N M V R E G K K F
acaggtccagagcaggtccgggaggcagcccaggggtgcgcacggatacgagatgacacg
T G P E Q V R E A A Q G C A R I R D D T
ctgggcattgtgggtctggtcgcatcgggtcggctgtggcacttagggccaaggcattc
L G I V G L G R I G S A V A L R A K A F
gggttcaacgtcactttctatgacccctacctctccgacggcatagagaagagtcttggc
G F N V T F Y D P Y L S D G I E K S L G
atcaccagagtgtacaccctgcaggacctttgtacagaagtgattgtgtgtcattacac
I T R V Y T L Q D L L Y R S D C V S L H
tgttccctcaacgagcacaacaaccacctcattaacgacttcaccatcaaacagatgcgc
C S L N E H N N H L I N D F T I K Q M R
ccaggagcctttctggtaaacacagcgccgaggggccctggtggacgagaatgcactagcc
P G A F L V N T A R G A L V D E N A L A
tcagcactgaaggagggacgcatcagggcggcggctctggacgtgcatgagaatgagcca
S A L K E G R I R A A A L D V H E N E P
tacaatcccttccaagggcccctgaaggatgcacctaacctcatctgcacgcccgcacgcg
Y N P F Q G P L K D A P N L I C T P H A
gcctactactcagacgcctccagcaatgagctccgtgagatggccgccagcgagatccgc
A Y Y S D A S S N E L R E M A A S E I R
cgtgccatcataggacgcatccctgacgccttgcgtaactgcgtcaacaaggagtacttc
R A I I G R I P D A L R N C V N K E Y F
atgagcaactacagtgaggggggagtgaacggcacggcaccctactacgtccccgtccac
M S N Y S E G G G V N G T A P Y Y V P V H
tccaccacacacgactccctcccctccggccctccccccaccagccacgtgggccctggc
S T T H D S L P S G P P P T S H V G P G
attcccccgccccctcacatgcctcccagcgtgccggtgagcgggggccgtgcatcaccc
I P P P P H M P P S V P V S G G R A S P
cagactggcccccccaggacccccctggccccagggagtctacttcaccataacacagaatt
Q T G P P G P P G P R E S T S P -
gccgcccggccaccgcagccccaactgtgaccgctaggcattcattccatcaggagttga
gtagaccgctgctgctgccgctgccgccgccgctgccgcccccca

Figure A18. Nucleotide (nt) and deduced amino acid (aa) sequence of the *G. lateralis* C-terminus binding protein contig (Y EVm005788t1) isolated from the Y-organ (YO) transcriptome. The 454 aa open reading frame (ORF) contained the C-terminal binding protein dehydrogenase (CtBP_dh) domain highlighted in yellow with the start (atg) and stop codon (taa) bolded green and red respectively. The contig included a 427 and 113 base pair (bp) 5' and 3' untranslated region (UTR) respectively. The nicotinamide adenine dinucleotide (NAD) sites were bolded, ligand binding sites boxed, and catalytic sites underlined.

Figure A19

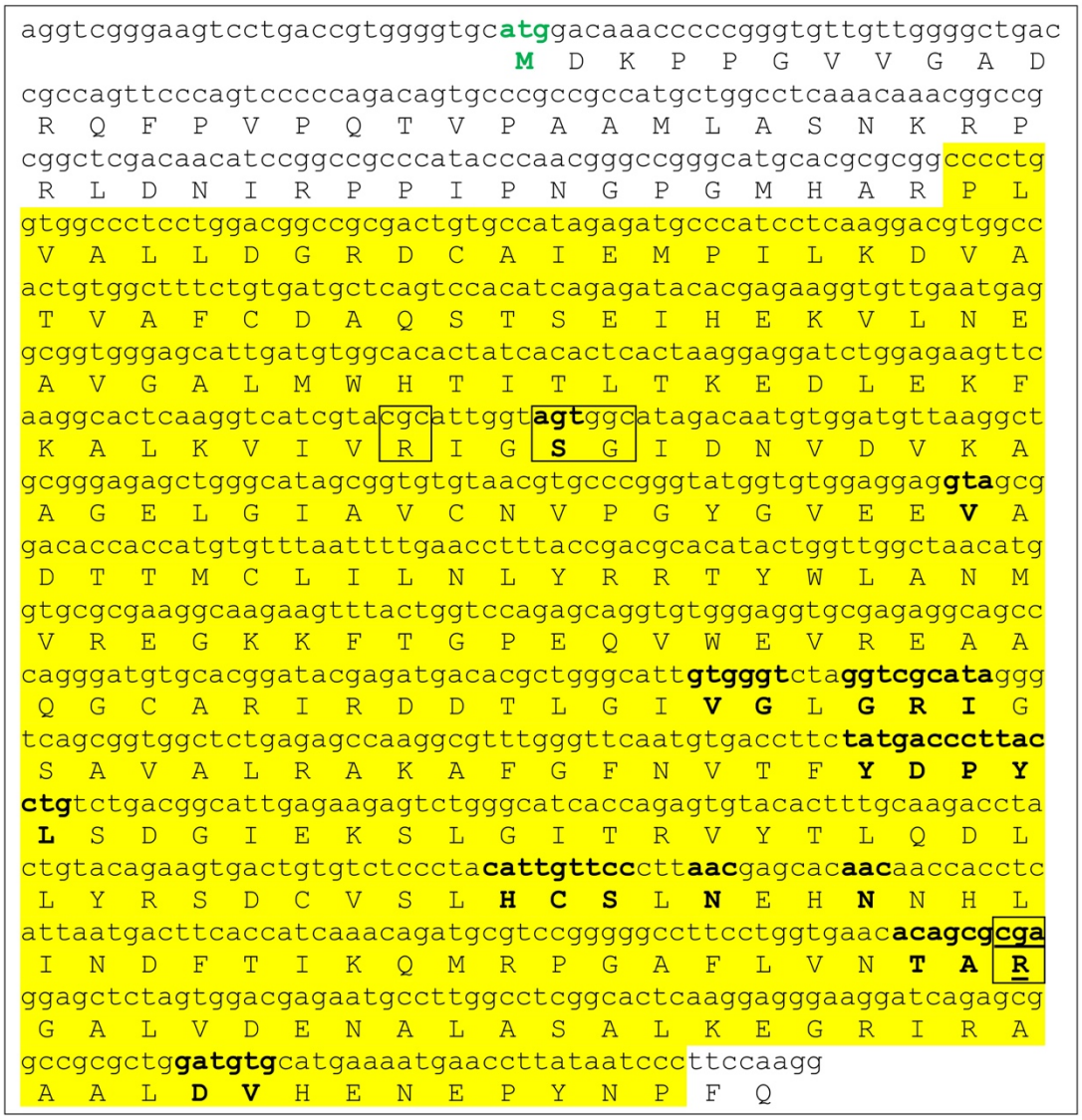

Figure A19. Nucleotide (nt) and deduced amino acid (aa) sequence of the *C. maenas* C-terminus binding protein contig (CNS EVm011952t2). The 326 aa open reading frame (ORF) contained the C-terminal binding protein dehydrogenase (CtBP_dh) domain highlighted in yellow with the start (atg) in green. The contig included a 28 base pair (bp) 5' untranslated region (UTR). The nicotinamide adenine dinucleotide (NAD) sites were bolded, ligand binding sites boxed, and catalytic sites underlined.

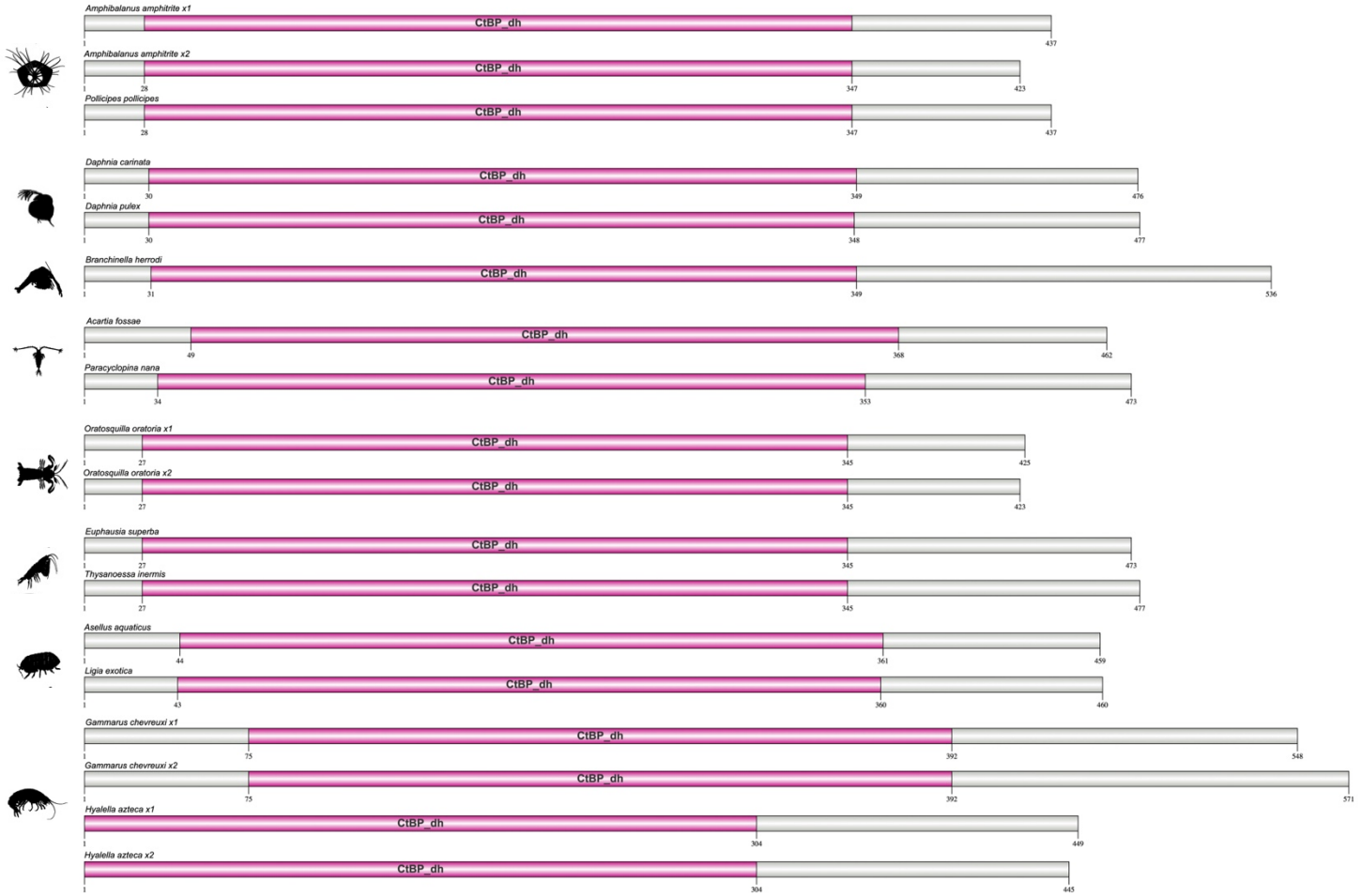

Figure A20. Domain architecture of non-decapod crustacean C-terminal binding protein (CtBP) orthologues. Domains were identified with the NCBI CD search tool and visualized with IBS 2.0 (see Materials and Methods). Information for the sequences is provided in the supplementary data spreadsheet on the online repository. Species silhouettes were obtained from PhyloPic (http://phylopic.org)

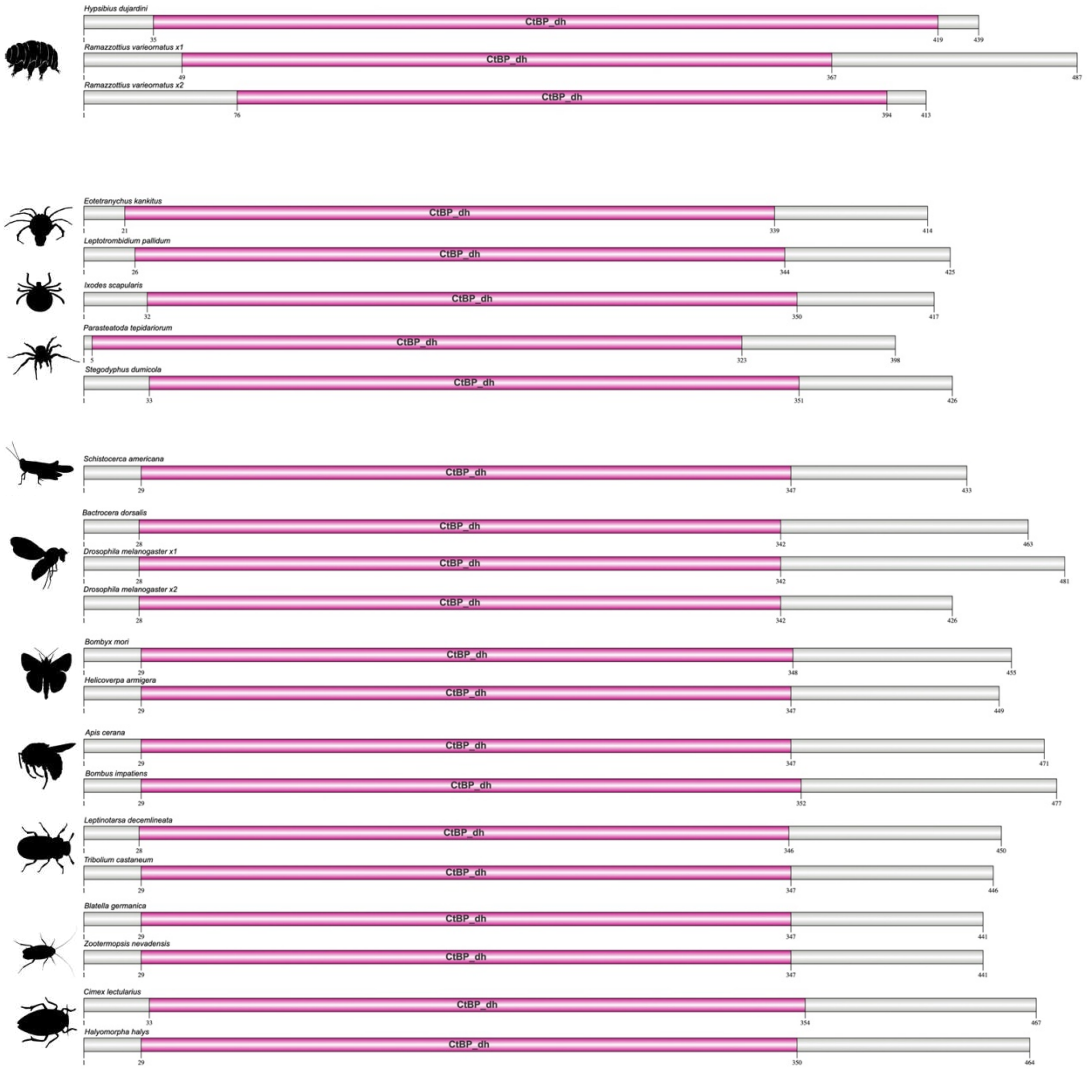

Figure A21. Domain architecture of C-terminal binding protein (CtBP) orthologs in Clade Panarthropoda (tardigrades, chelicerates, and insects). Domains were identified with the NCBI CD search tool and visualized with IBS 2.0 (see Materials and Methods). Information for the sequences is provided in the supplementary data spreadsheet on the online repository. Species silhouettes were obtained from PhyloPic (http://phylopic.org).

Figure A22

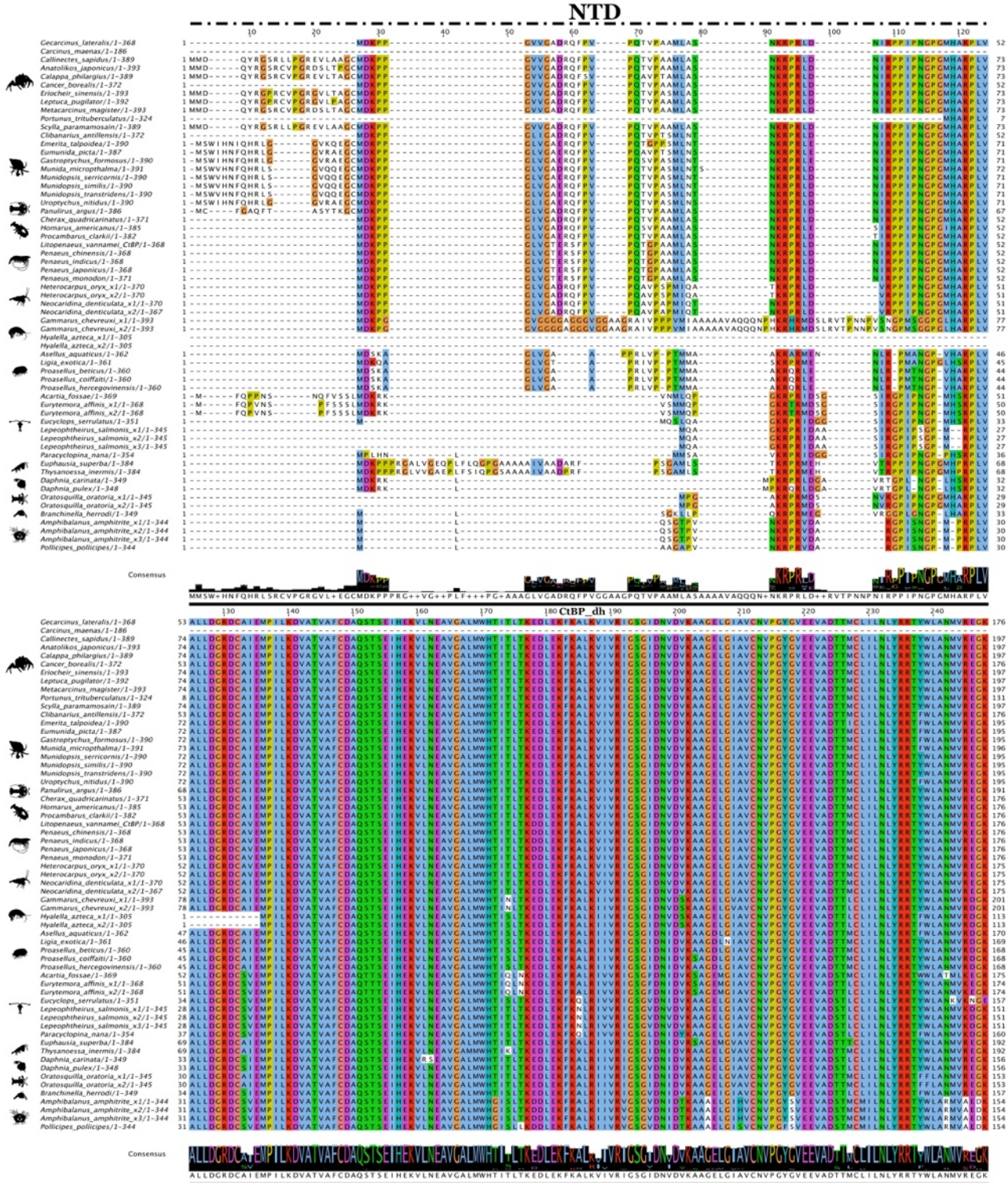

Figure A22 (continued)

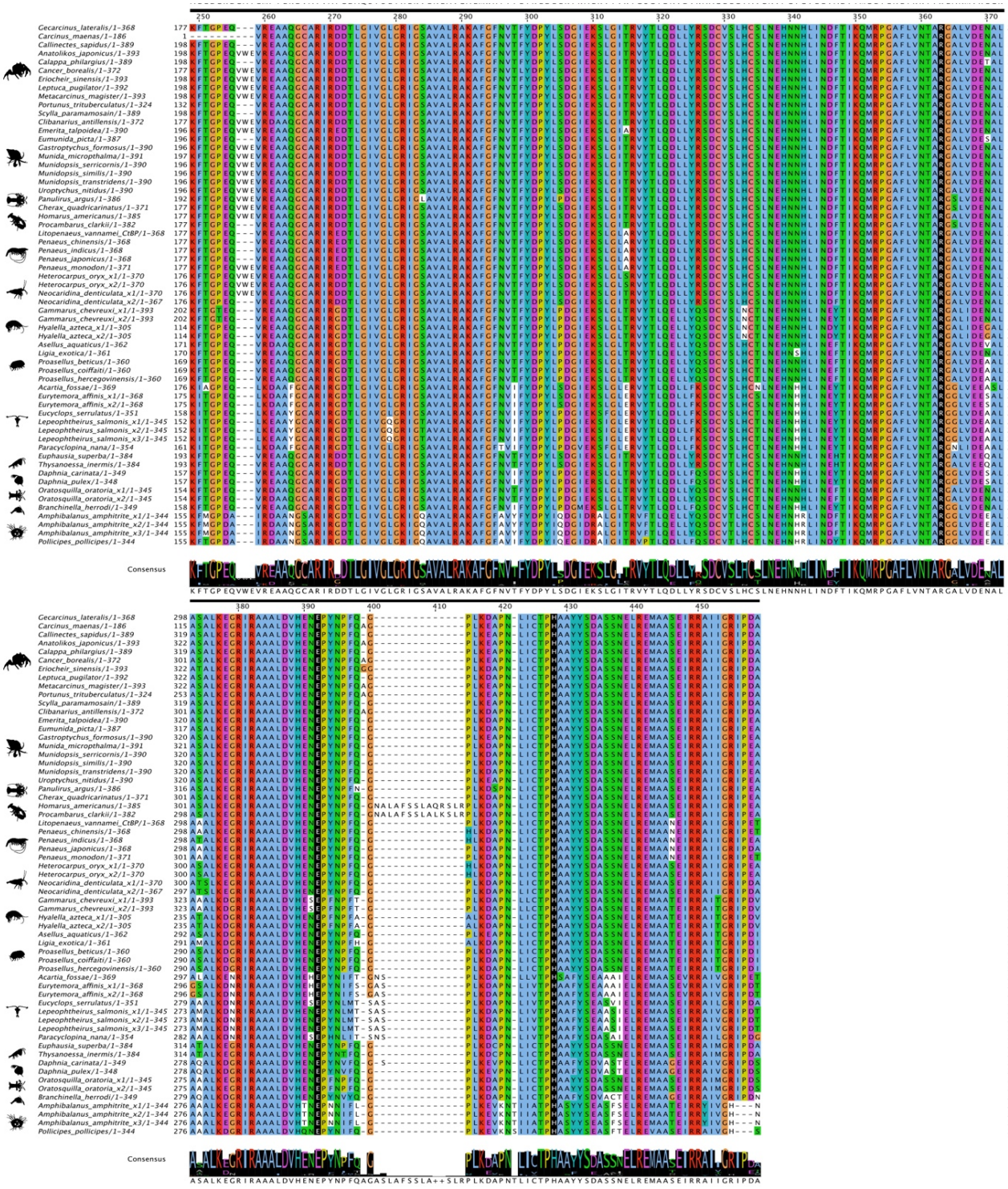

Figure A22. Multiple sequence alignment of the N-terminal region of crustacean CtBP orthologs. The sequences were aligned using the Mafft EINSI parameters, trimmed with ClipKIT, and visualized through Jalview following default Clustal coloring (see Materials and Methods). The consensus sequence is illustrated as a logo schematic. The N-terminal domain (NTD), indicated by the overhead dashed line, precedes and flanks the dehydrogenase domain (CtBP_dh), shown by the overhead solid line, which contains the R-E-H catalytic triad (highlighted in black). Sequences and databases used in the analysis are presented in the supplementary data spreadsheet on the online repository. Species silhouettes were obtained from PhyloPic (http://phylopic.org).

Figure A23

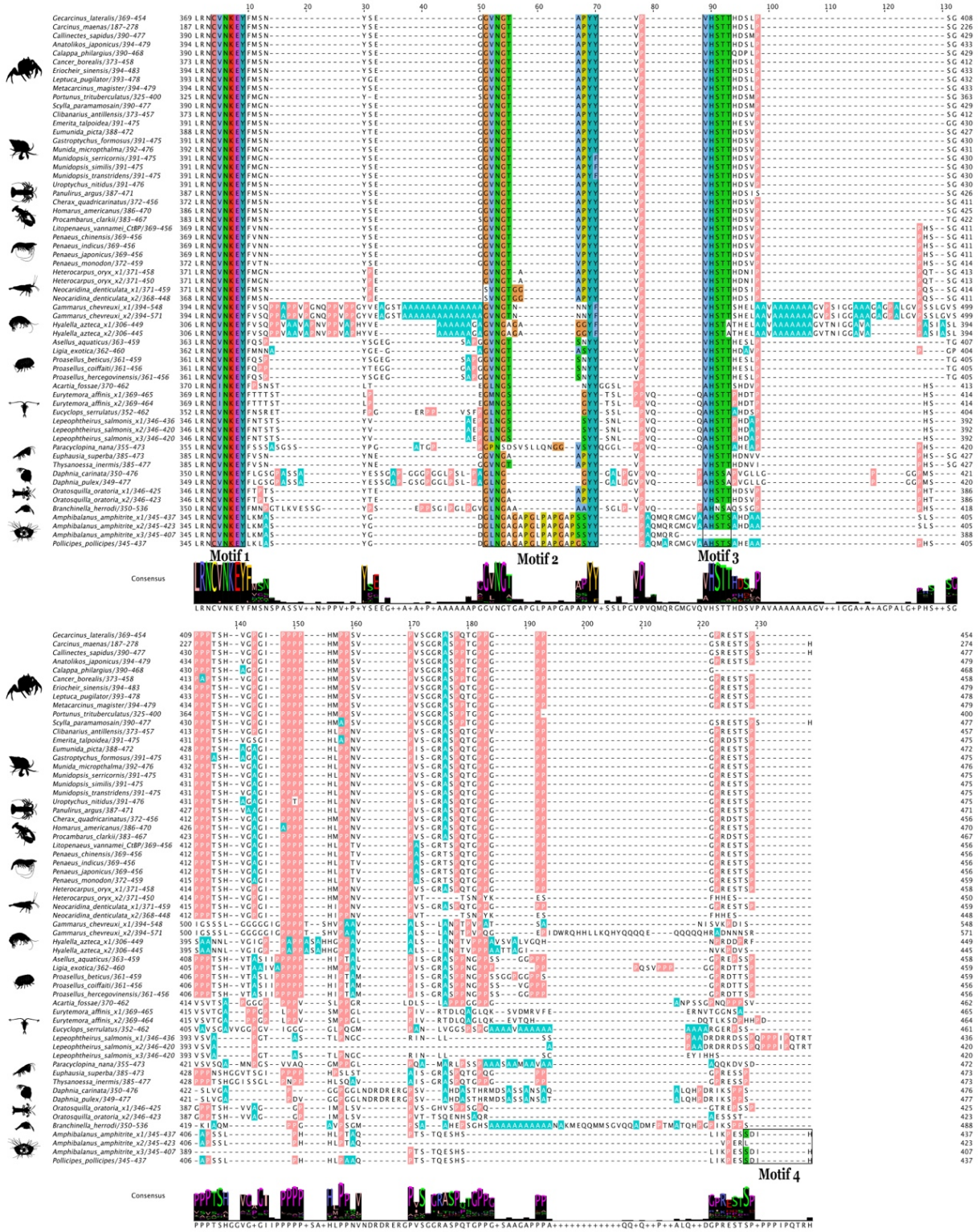

Figure A23. Multiple sequence alignment of the C-terminal domain (CTD) of crustacean CtBP orthologs. The sequences were aligned using the Mafft EINSI parameters, trimmed with ClipKIT, and visualized through Jalview following default Clustal coloring (see Materials and Methods). The CTD exhibited a disordered structure as it encompassed a proline rich region (shown in peach) along with showing sequence variability including having poly-alanine repeats (highlighted in aqua). Sequences and databases used in the analysis are presented in the supplementary data spreadsheet on the online repository. Species silhouettes were obtained from PhyloPic (http://phylopic.org).

Figure A24

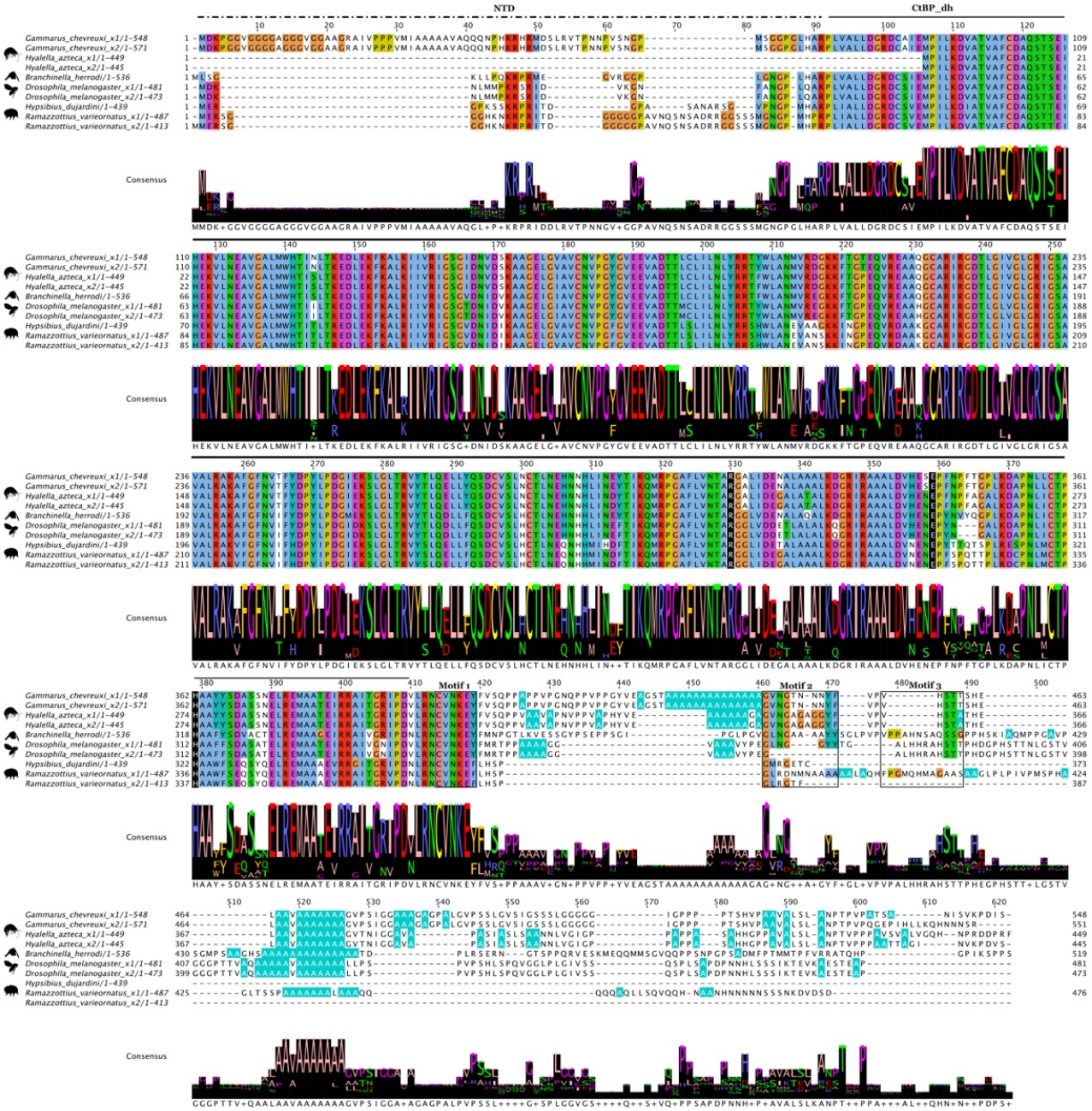

Figure A24. Multiple sequence alignment of panarthropoda CtBP orthologs. The sequences were aligned using the Mafft EINSI parameters, trimmed with ClipKIT, and visualized through Jalview following default Clustal coloring (see Materials and Methods). The consensus sequence is illustrated as a logo schematic. The N-terminal domain (NTD), indicated by the overhead dashed line, precedes and flanks the dehydrogenase domain (CtBP_dh), shown by the overhead solid line. The disordered C-terminal domain exhibited sequence variability while containing poly-alanine repeats. Sequences and databases used in the analysis are presented in the supplementary data spreadsheet on the online repository. Species silhouettes were obtained from PhyloPic (http://phylopic.org).

Figure A25

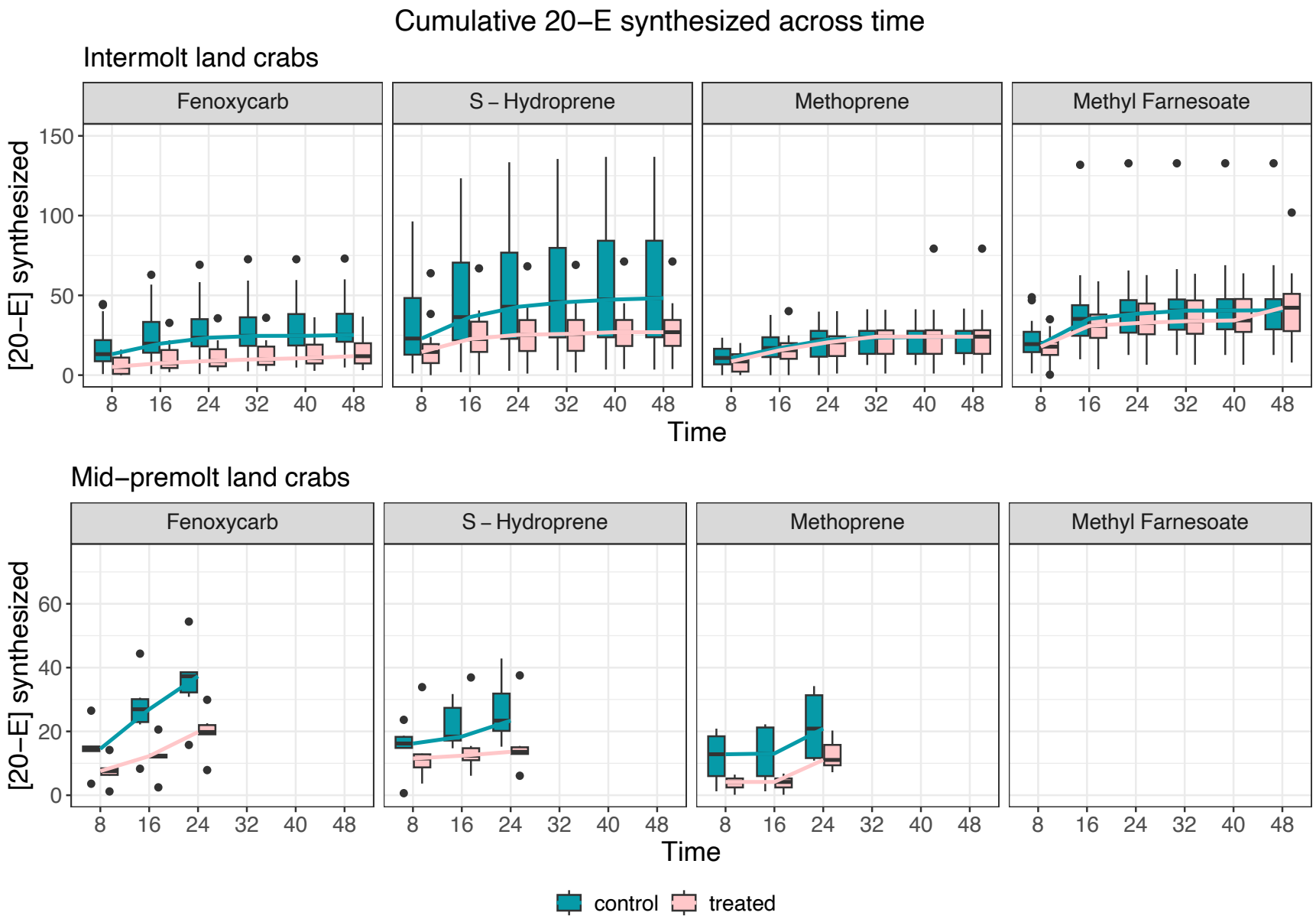
Cumulative 20−E synthesized across time
Intermolt land crabs
Fenoxycarb
S − Hydroprene
Methoprene
Methyl Farnesoate
[20−E] synthesized
150
100
50
0
8
16
24
32
40
48
Time
Mid−premolt land crabs
Fenoxycarb
S − Hydroprene
Methoprene
Methyl Farnesoate
[20−E] synthesized
60
40
20
0
8
16
24
32
40
48
Time
control
treated

Figure A25. Cumulative 20-E concentration (pg/μL) for each synthesized for blackback land crab (*G. lateralis*) YOs exposed to 10.0 μM of methyl farnesoate (MF) or a JH-mimic in each at each eight-hour interval by treatment group (fenoxycarb, S-hydropene, methoprene, and MF), control-treatment status (control and treated), and stage (intermolt or IM and mid-premolt or MP). Line for each group represents the median value for that time and stage with individual outliers indicated by dots. /

Figure A26

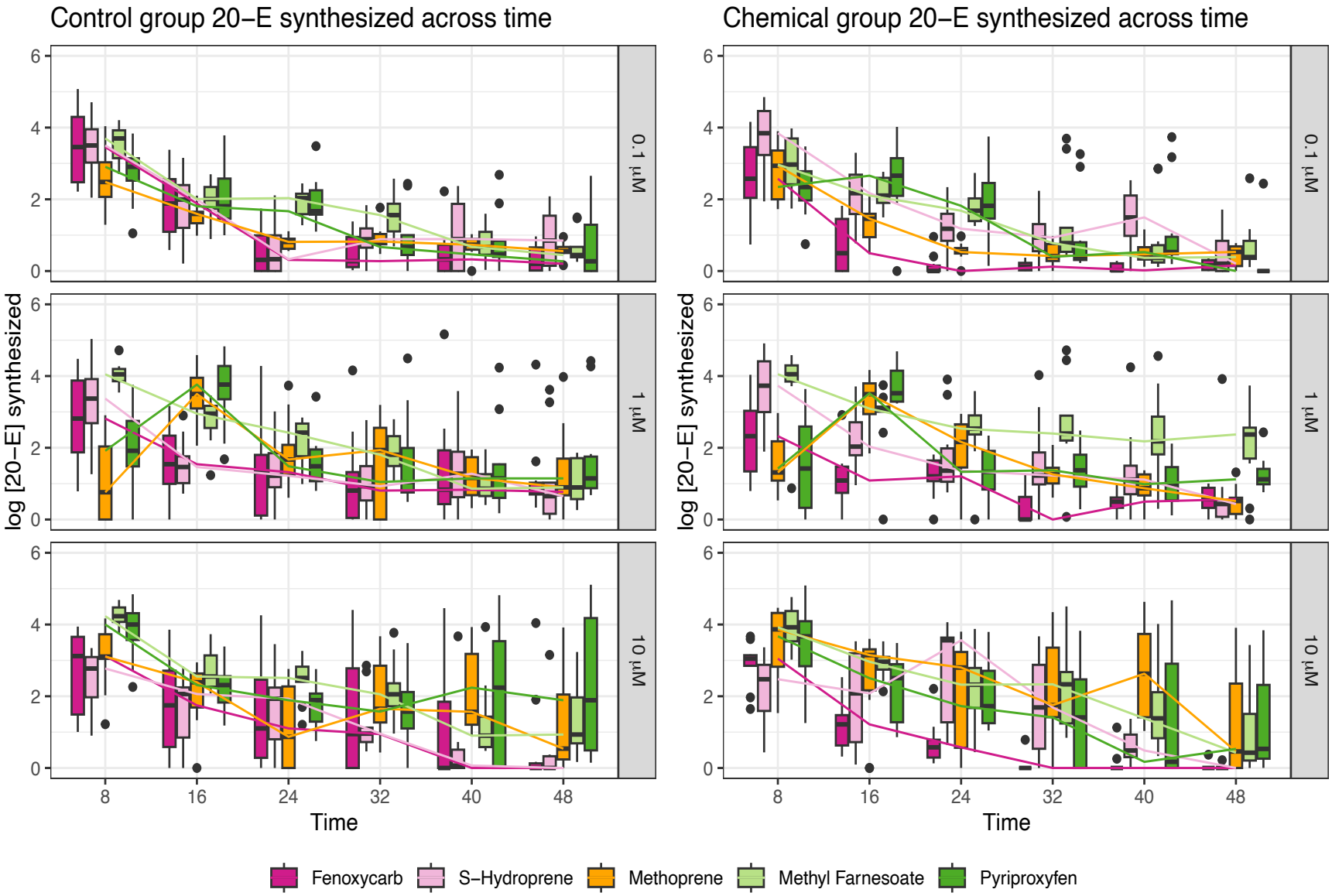
Control group 20−E synthesized across time
Chemical group 20−E synthesized across time
log [20−E] synthesized
0.1 µM
1 µM
10 µM
Time
Fenoxycarb
S−Hydroprene
Methoprene
Methyl Farnesoate
Pyriproxyfen

Figure A26. The log 20-E (log pg/μL) synthesized during each time interval for the control (left) and treated (right) green crab (*C. maenas*) Y-organs (YOs) across MF or a JH-mimic and concentration levels of 0.1 μM, 1.0 μM, and 10.0 μM. By the 24-hour mark, 20-E synthesis tends to stabilize for each concentration level. The line for each group represents the median value for the tested concentration and treatment at that time point with individual outliers indicated by dots.

Figure A27

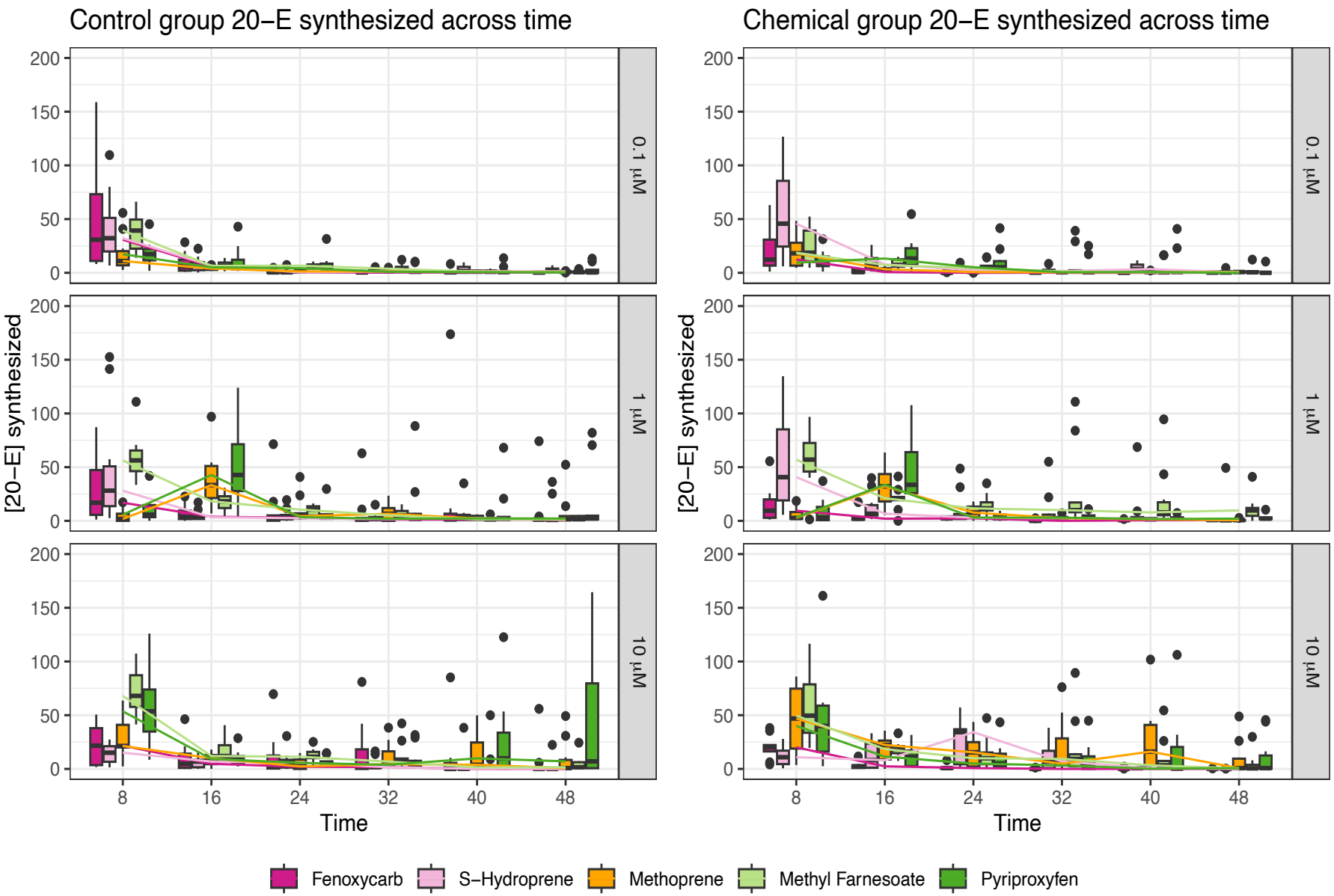
Control group 20−E synthesized across time
Chemical group 20−E synthesized across time
[20−E] synthesized
Time
0.1 µM
1 µM
10 µM
Fenoxycarb
S−Hydroprene
Methoprene
Methyl Farnesoate
Pyriproxyfen

Figure A27. Concentration of 20-E (pg/μL) synthesized during each time interval for the control (left) and treated (right) green crab *C. maenas*) YOs across MF or a JH-mimic and concentration levels of 0.1 μM, 1.0 μM, and 10.0 μM. Line for each group represents the median value for that concentration and treatment at that time point. By the 24-hour mark, 20-E synthesis tends to stabilize for each concentration level

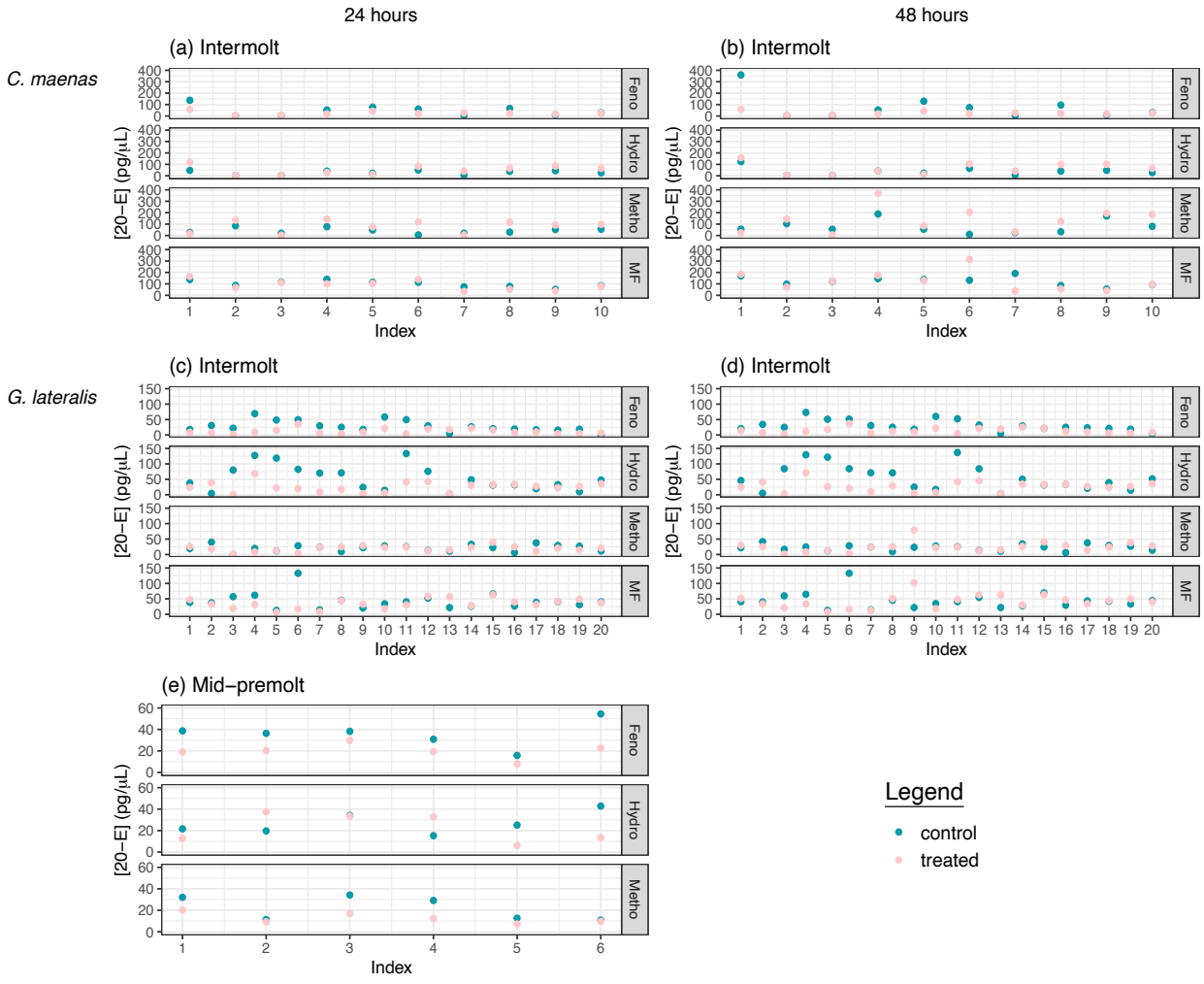

Figure A28. Cumulative 20-E concentration (pg/μL) for each Y-organ (YO) after exposure to 10.0 μM of MF or a JH-mimic and their associated untreated YO from the same host animal for intermolt (IM) green crab (*C. maenas*) along with IM and mid-premolt (MP) blackback land crab (*G. lateralis*) after 24 and 48-hours. Index refers to each animal subject from the paired YOs were harvested from. Abbreviations: Feno–fenoxycarb; Hydro–hydroprene; Metho–methoprene; and MF– methyl farnesoate.

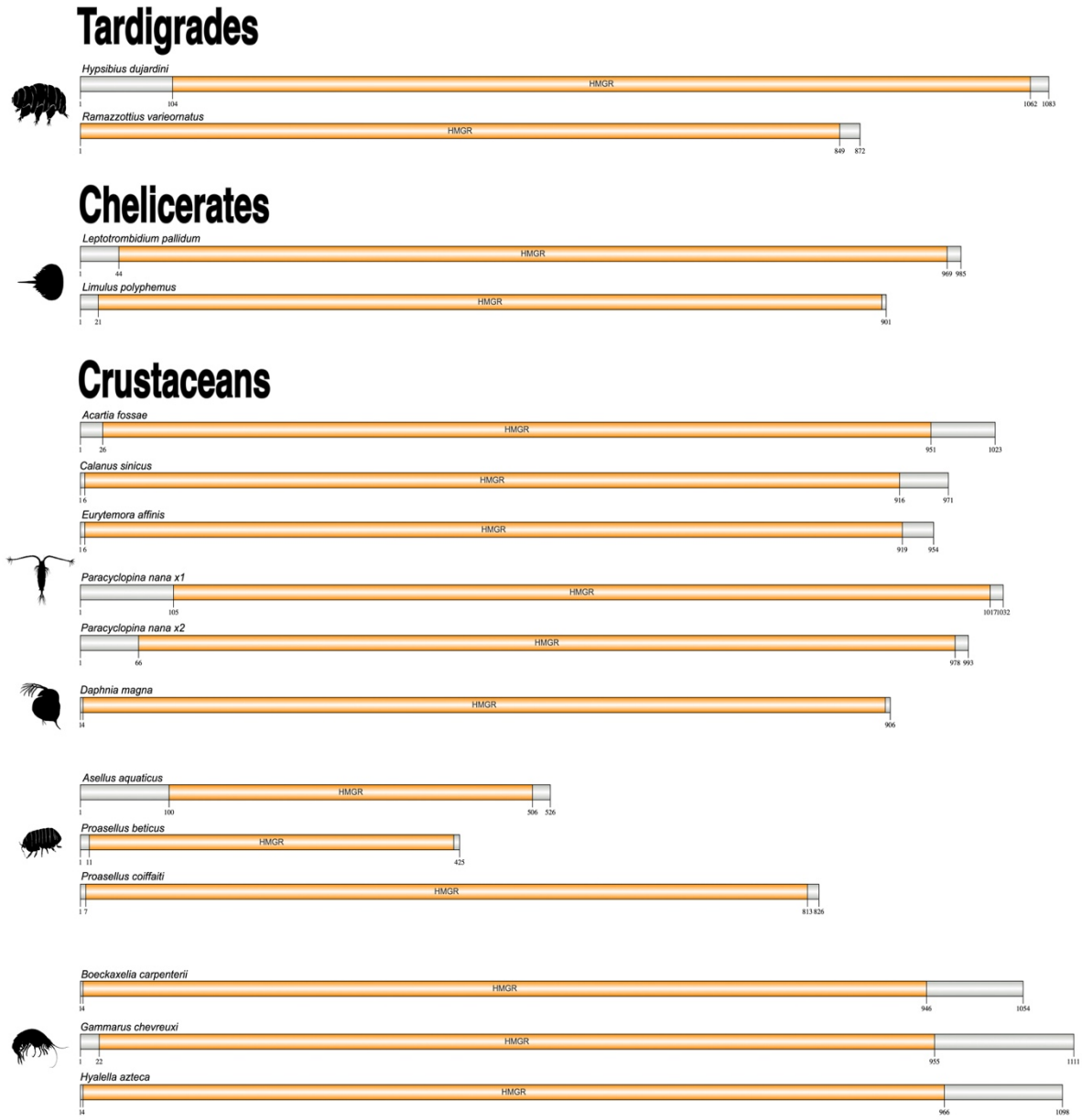

Figure B1. Domain organization of panarthropoda (tardigrades, chelicerates, and non-decapod crustaceans) 3-hydroxy-3-methyl-glutaryl-coenzyme reductase (HMGR) proteins. Domains were identified with the NCBI CD search tool and visualized with IBS 2.0 (see Materials and Methods). Information for the sequences is provided in the supplementary data spreadsheet on the online repository. Species silhouettes were obtained from PhyloPic (http://phylopic.org).

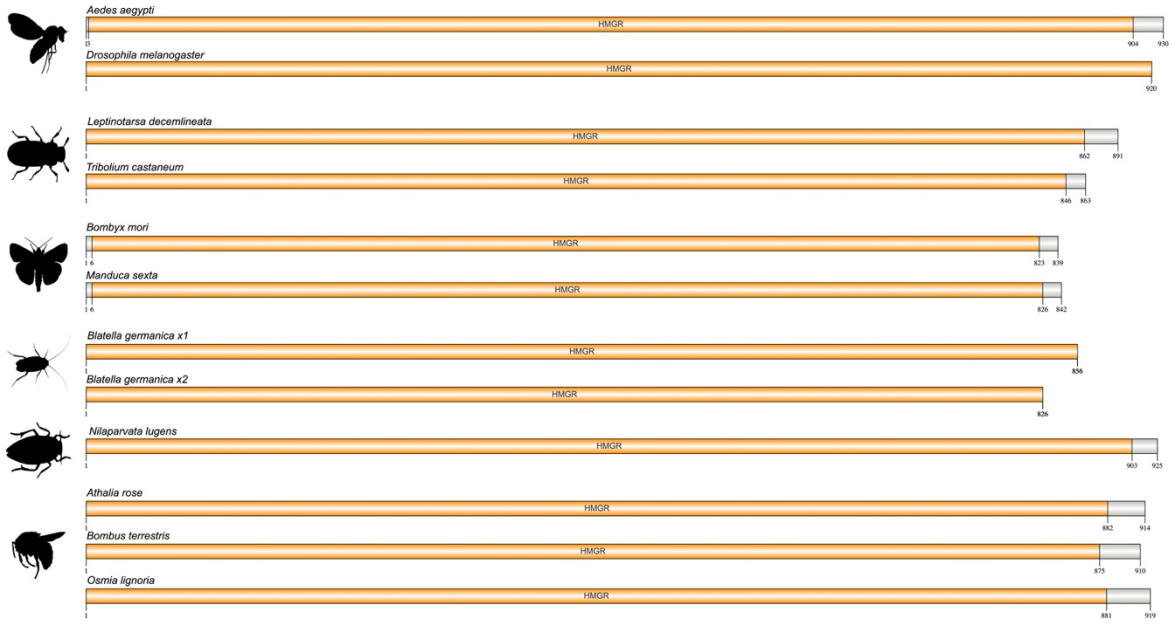

Figure B2. Domain organization of insect 3-hydroxy-3-methyl-glutaryl-coenzyme reductase (HMGR) proteins. Domains were identified with the NCBI CD search tool and visualized with IBS 2.0 (see Materials and Methods). Information for the sequences is provided in the supplementary data spreadsheet on the online repository. Species silhouettes were obtained from PhyloPic (http://phylopic.org).

Figure B3

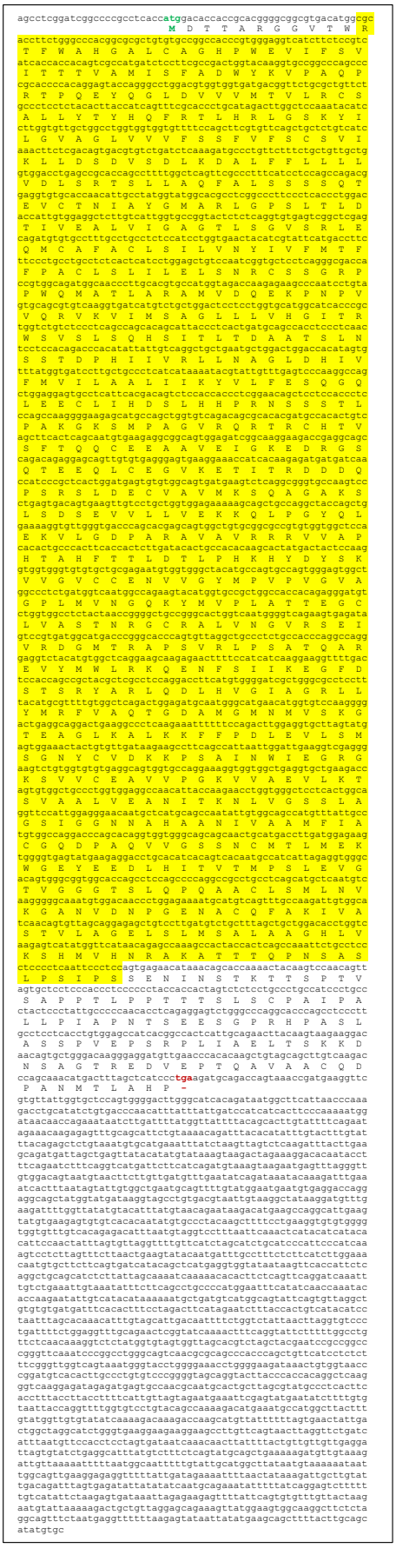

Figure B3. Nucleotide (nt) and deduced amino acid (aa) sequence of the *G. lateralis* 3-hydroxy-3-methylglutaryl-coenzyme A reductase (HMGR) contig (Y EVm001453t1) isolated from the Y-organ (YO). The contig sequence includes a 5' and 3' untranslated region (UTR) consisting of 25 and 2378 base pairs (bp) respectively; the start codon (atg) is indicated in green and stop codon (tga) in red. Within the 961 aa open reading frame (ORF) is the HMGR domain (12-858 aa) highlighted in yellow.

Figure B4

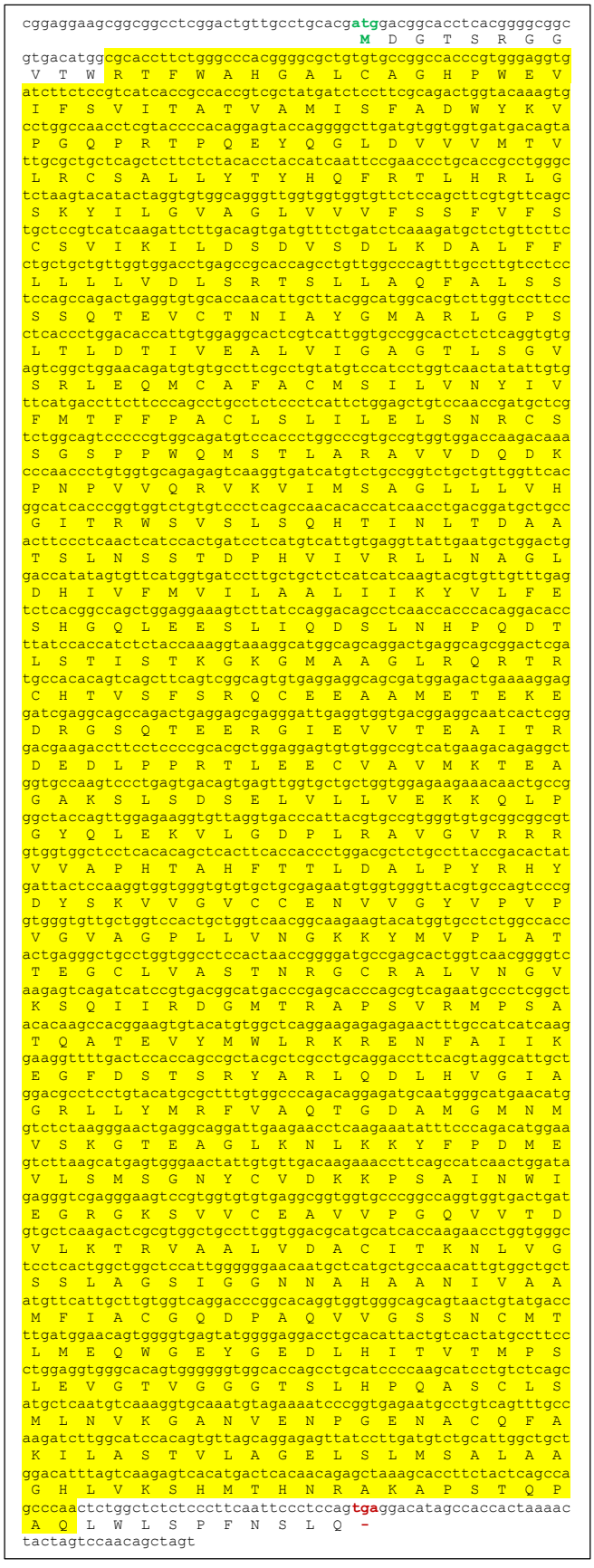
cggaggaagcggcggcctcggactgttgcctgcacgatggacggcacctcacggggcggc
M D G T S R G G
gtgacatggcgcaccttctgggcccacggggcgctgtgtgccggccacccgtgggaggtg
V T W R T F W A H G A L C A G H P W E V
atcttctccgtcatcaccgccaccgtcgctatgatctccttcgcagactggtacaaagtg
I F S V I T A T V A M I S F A D W Y K V
cctggccaacctcgtaccccacaggagtaccaggggcttgatgtggtggtgatgacagta
P G Q P R T P Q E Y Q G L D V V V M T V
ttgcgctgctcagctcttctctacacctaccatcaattccgaaccctgcaccgcctgggc
L R C S A L L Y T Y H Q F R T L H R L G
tctaagtacatactaggtgtggcagggttggtggtggtgttctccagcttcgtgttcagc
S K Y I L G V A G L V V V F S S F V F S
tgctccgtcatcaagattcttgacagtgatgtttctgatctcaaagatgctctgttcttc
C S V I K I L D S D V S D L K D A L F F
ctgctgctgttggtggacctgagccgcaccagcctgttggcccagtttgccttgtcctcc
L L L L V D L S R T S L L A Q F A L S S
tccagccagactgaggtgtgcaccaacattgcttacggcatggcacgtcttggtccttcc
S S Q T E V C T N I A Y G M A R L G P S
ctcaccctggacaccattgtggaggcactcgtcattggtgccggcactctctcaggtgtg
L T L D T I V E A L V I G A G T L S G V
agtcggctggaacagatgtgtgccttcgcctgtatgtccatcctggtcaactatattgtg
S R L E Q M C A F A C M S I L V N Y I V
ttcatgaccttcttcccagcctgcctctccctcattctggagctgtccaaccgatgctcg
F M T F F P A C L S L I L E L S N R C S
tctggcagtcccccgtggcagatgtccaccctggcccgtgccgtggtggaccaagacaaa
S G S P P W Q M S T L A R A V V D Q D K
cccaaccctgtggtgcagagagtcaaggtgatcatgtctgccggtctgctgttggttcac
P N P V V Q R V K V I M S A G L L L V H
ggcatcacccggtggtctgtgtccctcagccaacacaccatcaacctgacggatgctgcc
G I T R W S V S L S Q H T I N L T D A A
acttccctcaactcatccactgatcctcatgtcattgtgaggttattgaatgctggactg
T S L N S S T D P H V I V R L L N A G L
gaccatatagtgttcatggtgatccttgctgctctcatcatcaagtacgtgttgtttgag
D H I V F M V I L A A L I I K Y V L F E
tctcacggccagctggaggaaagtcttatccaggacagcctcaaccacccacaggacacc
S H G Q L E E S L I Q D S L N H P Q D T
ttatccaccatctctaccaaaggtaaaggcatggcagcaggactgaggcagcggactcga
L S T I S T K G K G M A A G L R Q R T R
tgccacacagtcagcttcagtcggcagtgtgaggaggcagcgatggagactgaaaaggag
C H T V S F S R Q C E E A A M E T E K E
gatcgaggcagccagactgaggagcgagggattgaggtggtgacggaggcaatcactcgg
D R G S Q T E E R G I E V V T E A I T R
gacgaagaccttcctccccgcacgctggaggagtgtgtggccgtcatgaagacagaggct
D E D L P P R T L E E C V A V M K T E A
ggtgccaagtccctgagtgacagtgagttggtgctgctggtggagaagaaacaactgccg
G A K S L S D S E L V L L V E K K Q L P
ggctaccagttggagaaggtgttaggtgacccattacgtgccgtgggtgtgcggcggcgt
G Y Q L E K V L G D P L R A V G V R R R
gtggtggctcctcacacagctcacttcaccaccctggacgctctgccttaccgacactat
V V A P H T A H F T T L D A L P Y R H Y
gattactccaaggtggtgggtgtgtgctgcgagaatgtggtgggttacgtgccagtcccg
D Y S K V V G V C C E N V V G Y V P V P
gtgggtgttgctggtccactgctggtcaacggcaagaagtacatggtgcctctggccacc
V G V A G P L L V N G K K Y M V P L A T
actgagggctgcctggtggcctccactaaccggggatgccgagcactggtcaacggggtc
T E G C L V A S T N R G C R A L V N G V
aagagtcagatcatccgtgacggcatgacccgagcacccagcgtcagaatgccctcggct
K S Q I I R D G M T R A P S V R M P S A
acacaagccacggaagtgtacatgtggctcaggaagagagagaactttgccatcatcaag
T Q A T E V Y M W L R K R E N F A I I K
gaaggttttgactccaccagccgctacgctcgcctgcaggaccttcacgtaggcattgct
E G F D S T S R Y A R L Q D L H V G I A
ggacgcctcctgtacatgcgctttgtggcccagacaggagatgcaatgggcatgaacatg
G R L L Y M R F V A Q T G D A M G M N M
gtctctaagggaactgaggcaggattgaagaacctcaagaaatatttcccagacatggaa
V S K G T E A G L K N L K K Y F P D M E
gtcttaagcatgagtgggaactattgtgttgacaagaaaccttcagccatcaactggata
V L S M S G N Y C V D K K P S A I N W I
gagggtcgagggaagtccgtggtgtgtgaggcggtggtgcccggccaggtggtgactgat
E G R G K S V V C E A V V P G Q V V T D
gtgctcaagactcgcgtggctgccttggtggacgcatgcatcaccaagaacctggtgggc
V L K T R V A A L V D A C I T K N L V G
tcctcactggctggctccattgggggggaacaatgctcatgctgccaacattgtggctgct
S S L A G S I G G N N A H A A N I V A A
atgttcattgcttgtggtcaggacccggcacaggtggtgggcagcagtaactgtatgacc
M F I A C G Q D P A Q V V G S S N C M T
ttgatggaacagtggggtgagtatggggaggacctgcacattactgtcactatgccttcc
L M E Q W G E Y G E D L H I T V T M P S
ctggaggtgggcacagtgggggtggcaccagcctgcatccccaagcatcctgtctcagc
L E V G T V G G G T S L H P Q A S C L S
atgctcaatgtcaaaggtgcaaatgtagaaaatcccggtgagaatgcctgtcagtttgcc
M L N V K G A N V E N P G E N A C Q F A
aagatcttggcatccacagtgttagcaggagagttatccttgatgtctgcattggctgct
K I L A S T V L A G E L S L M S A L A A
ggacatttagtcaagagtcacatgactcacaacagagctaaagcaccttctactcagcca
G H L V K S H M T H N R A K A P S T Q P
gcccaactctggctctctcccttcaattccctccagtgaggacatagccaccactaaaac
A Q L W L S P F N S L Q -
tactagtccaacagctagt

Figure B4. Nucleotide (nt) and deduced amino acid (aa) sequence of the *C. maenas* 3-hydroxy-3-methylglutaryl-coenzyme A reductase (HMGR) contig (Y EVm002033t1) isolated from the Y-organ (YO). The contig sequence includes a 5' and 3' untranslated region (UTR) consisting of 36 and 40 base pairs (bp) respectively; the start codon (atg) is indicated in green and stop codon (tga) in red. Within the 860 aa open reading frame (ORF) is the HMGR domain (12-850 aa) highlighted in yellow.

Figure B5. Domain organization of non-decapod crustacean farnesoic acid *O*-methyl transferase (FAMeT) proteins. Two Methyltransf_FA domains were identified in the transcripts regardless of variant length. Domains were the NCBI CD search tool and visualized with IBS 2.0 (see Materials and Methods). Information for the sequences is provided in the supplementary data spreadsheet on the online repository Species silhouettes were obtained from PhyloPic (http://phylopic.org).

Figure B6

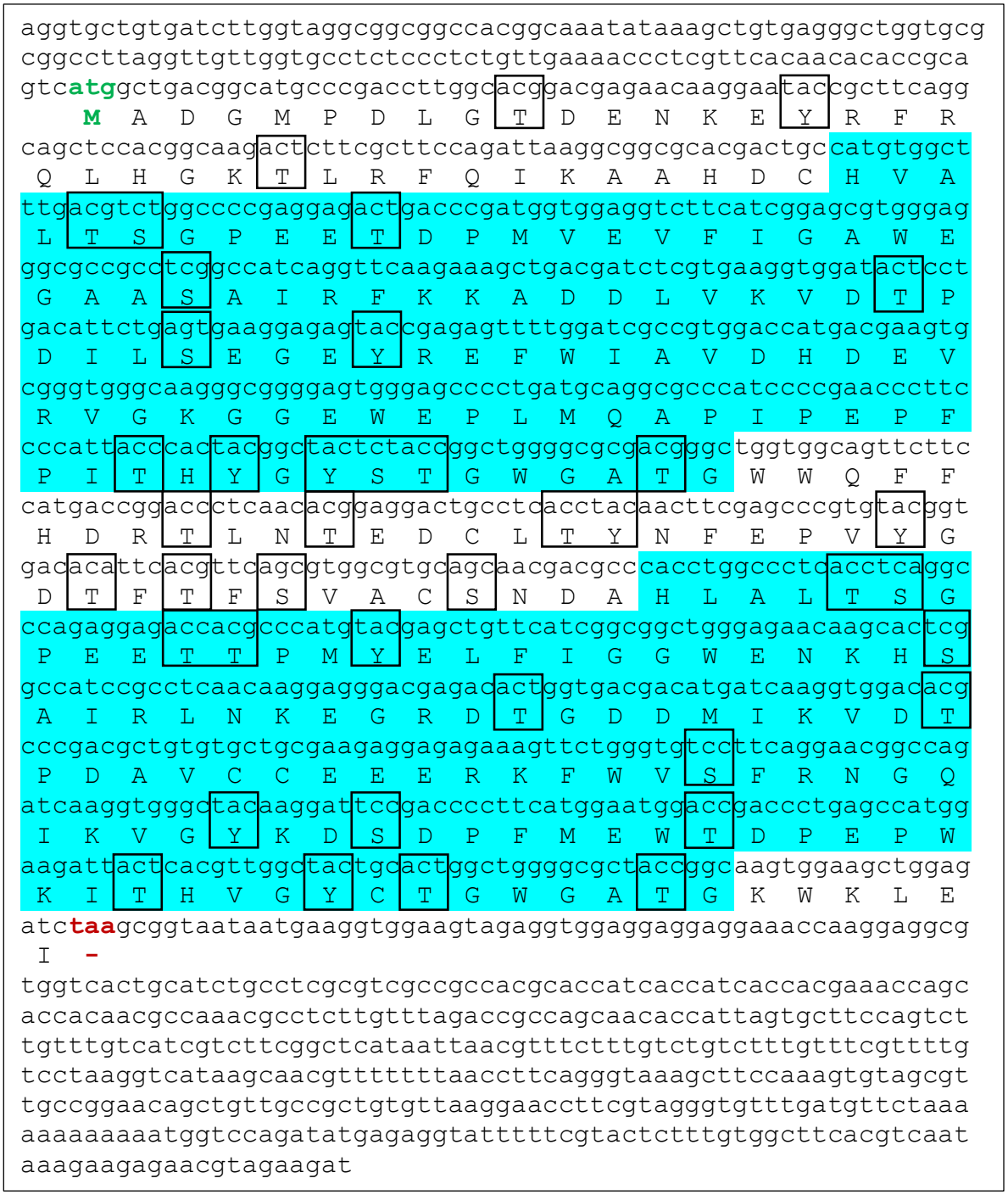
aggtgctgtgatcttggtaggcggcggccacggcaaatataaagctgtgagggctggtgcg
cggccttaggttgttggtgcctctccctctgttgaaaaccctcgttcacaacacaccgca
gtcatggctgacggcatgcccgaccttggcacggacgagaacaaggaataccgcttcagg
M A D G M P D L G T D E N K E Y R F R
cagctccacggcaagactcttcgcttccagattaaggcggcgcacgactgccatgtggct
Q L H G K T L R F Q I K A A H D C H V A
ttgacgtctggccccgaggagactgacccgatggtggaggtcttcatcggagcgtgggag
L T S G P E E T D P M V E V F I G A W E
ggcgccgcctcggccatcaggttcaagaaagctgacgatctcgtgaaggtggatactcct
G A A S A I R F K K A D D L V K V D T P
gacattctgagtgaaggagagtaccgagagttttggatcgccgtggaccatgacgaagtg
D I L S E G E Y R E F W I A V D H D E V
cgggtgggcaagggcggggagtgggagcccctgatgcaggcgcccatccccgaacccttc
R V G K G G E W E P L M Q A P I P E P F
cccattacccactacggctactctaccggctggggcgcgacgggctggtggcagttcttc
P I T H Y G Y S T G W G A T G W W Q F F
catgaccggaccctcaacacggaggactgcctcacctacaacttcgagcccgtgtacggt
H D R T L N T E D C L T Y N F E P V Y G
gacacattcacgttcagcgtggcgtgcagcaacgacgcccacctggccctcacctcaggc
D T F T F S V A C S N D A H L A L T S G
ccagaggagaccacgcccatgtacgagctgttcatcggcggctgggagaacaagcactcg
P E E T T P M Y E L F I G G W E N K H S
gccatccgcctcaacaaggagggacgagacactggtgacgacatgatcaaggtggacacg
A I R L N K E G R D T G D D M I K V D T
cccgacgctgtgtgctgcgaagaggagagaaagttctgggtgtccttcaggaacggccag
P D A V C C E E E R K F W V S F R N G Q
atcaaggtgggctacaaggattccgacccttcatggaatggaccgaccctgagccatgg
I K V G Y K D S D P F M E W T D P E P W
aagattactcacgttggctactgcactggctggggcgctaccggcaagtggaagctggag
K I T H V G Y C T G W G A T G K W K L E
atctaagcggtaataatgaaggtggaagtagaggtggaggaggaggaaaccaaggaggcg
I -
tggtcactgcatctgcctcgcgtcgccgccacgcaccatcaccatcaccacgaaaccagc
accacaacgccaaacgcctcttgtttagaccgccagcaacaccattagtgcttccagtct
tgtttgtcatcgtcttcggctcataattaacgtttctttgtctgtctttgtttcgttttg
tcctaaggtcataagcaacgtttttttaaccttcagggtaaagcttccaaagtgtagcgt
tgccggaacagctgttgccgctgtgttaaggaaccttcgtagggtgtttgatgttctaaa
aaaaaaaaatggtccagatatgagaggtatttttcgtactctttgtggcttcacgtcaat
aaagaagagaacgtagaagat

Figure B6. Nucleotide (nt) and amino acid (aa) sequence alignment of the *G. lateralis* FAMeTa contig (Y EVm0106271t1) isolated from the Y-organ (YO). The contig sequence includes a 124 and 435 base pair (bp) 5' and 3' untranslated region (UTR) with the start codon (atg) indicated in green and stop codon (tga) in red, respectively. The 280 aa open reading frame (ORF) are two farnesoic acid *O*-methyltransferase domains (Methyltransf_FA) (37 aa – 134 aa and 173 aa – 274 aa) highlighted in aqua with putative phosphorylation sites indicated in boxes.

Figure B7

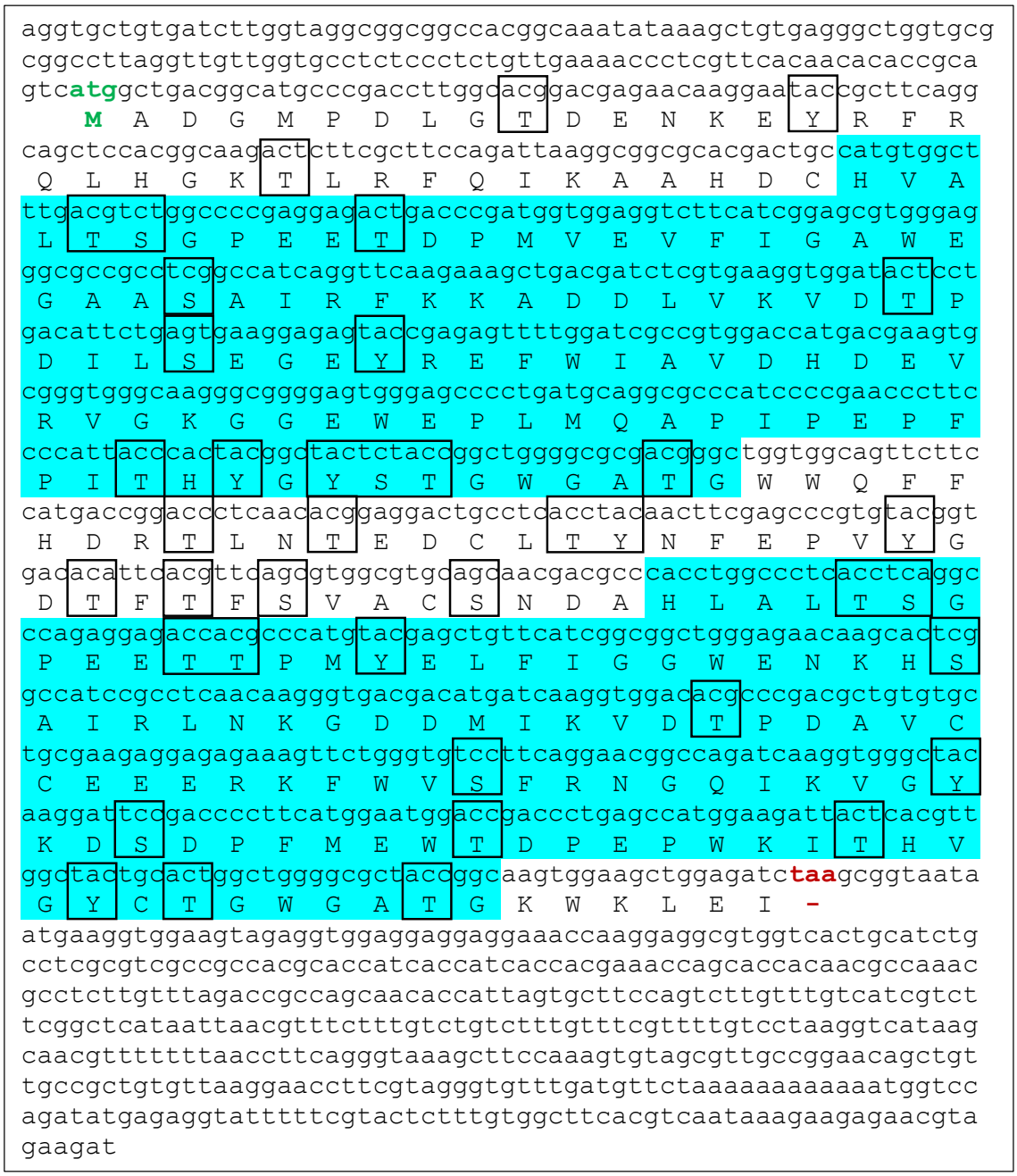
aggtgctgtgatcttggtaggcggcggccacggcaaatataaagctgtgagggctggtgcg
cggccttaggttgttggtgcctctccctctgttgaaaaccctcgttcacaacacaccgca
gtcatggctgacggcatgcccgaccttggcacggacgagaacaaggaatacccgcttcagg
M A D G M P D L G T D E N K E Y R F R
cagctccacggcaagactcttcgcttccagattaaggcggcgcacgactgccatgtggct
Q L H G K T L R F Q I K A A H D C H V A
ttgacgtctggccccgaggagactgacccgatggtggaggtcttcatcggagcgtgggag
L T S G P E E T D P M V E V F I G A W E
ggcgccgcctcggccatcaggttcaagaaagctgacgatctcgtgaaggtggatactcct
G A A S A I R F K K A D D L V K V D T P
gacattctgagtgaaggagagtaccgagagttttggatcgccgtggaccatgacgaagtg
D I L S E G E Y R E F W I A V D H D E V
cgggtgggcaagggcggggagtgggagcccctgatgcaggcgcccatccccgaacccttc
R V G K G G E W E P L M Q A P I P E P F
cccattacccactacggctactctaccggctggggcgcgacgggctggtggcagttcttc
P I T H Y G Y S T G W G A T G W W Q F F
catgaccggaccctcaacacggaggactgcctcacctacaacttcgagcccgtgtacggt
H D R T L N T E D C L T Y N F E P V Y G
gacacattcacgttcagcgtggcgtgcagcaacgacgcccacctggccctcacctcaggc
D T F T F S V A C S N D A H L A L T S G
ccagaggagaccacgcccatgtacgagctgttcatcggcggctgggagaacaagcactcg
P E E T T P M Y E L F I G G W E N K H S
gccatccgcctcaacaagggtgacgacatgatcaaggtggacacgcccgacgctgtgtgc
A I R L N K G D D M I K V D T P D A V C
tgcgaagaggagagaaagttctgggtgtccttcaggaacggccagatcaaggtgggctac
C E E E R K F W V S F R N G Q I K V G Y
aaggattccgacccttcatggaatggaccgaccctgagccatggaagattactcacgtt
K D S D P F M E W T D P E P W K I T H V
ggctactgcactggctggggcgctaccggcaagtggaagctggagatctaagcggtaata
G Y C T G W G A T G K W K L E I -
atgaaggtggaagtagaggtggaggaggaggaaaccaaggaggcgtggtcactgcatctg
cctcgcgtcgccgccacgcaccatcaccatcaccacgaaaccagcaccacaacgccaaac
gcctcttgtttagaccgccagcaacaccattagtgcttccagtcttgtttgtcatcgtct
tcggctcataattaacgtttctttgtctgtctttgtttcgttttgtcctaaggtcataag
caacgtttttttaaccttcagggtaaagcttccaaagtgtagcgttgccggaacagctgt
tgccgctgtgttaaggaaccttcgtagggtgtttgatgttctaaaaaaaaaaaatggtcc
agatatgagaggtatttttcgtactctttgtggcttcacgtcaataaagaagagaacgta
gaagat

Figure B7. Nucleotide (nt) and amino acid (aa) sequence alignment of the *G. lateralis* FAMeTb contig (Y EVm0106271t2) isolated from the Y-organ (YO). The contig sequence includes a 124 and 435 base pair (bp) 5' and 3' untranslated region (UTR) with the start codon (atg) indicated in green and stop codon (tga) in red, respectively. The 275 aa open reading frame (ORF) contains two farnesoic acid *O*-methyltransferase domains (Methyltransf_FA) (37 aa –134 aa and 173 aa – 274 aa) highlighted in aqua with putative phosphorylation sites indicated in boxes.

Figure B8

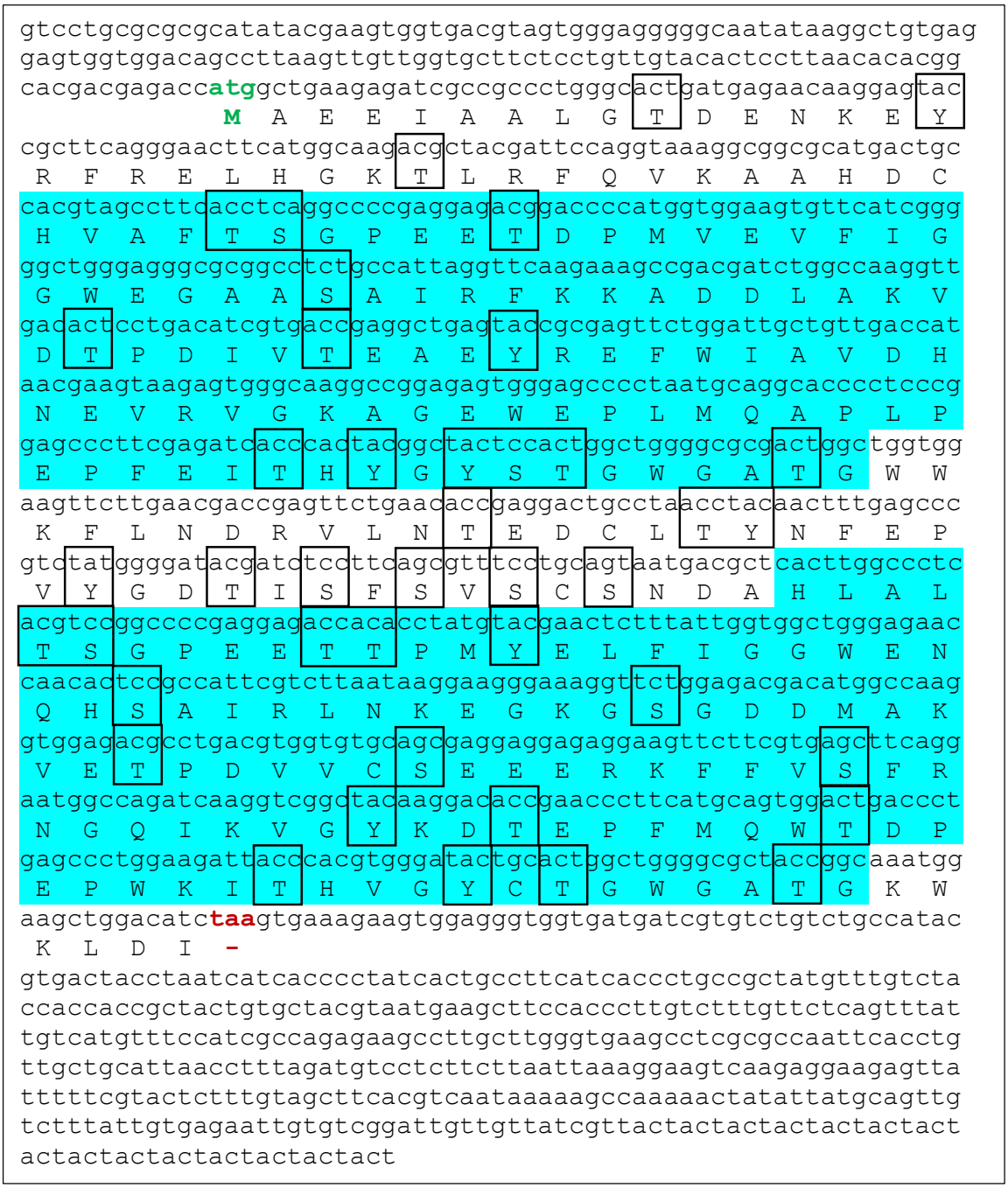
gtcctgcgcgcgcatatacgaagtggtgacgtagtgggaggggcaatataaggctgtgag
gagtggtggacagccttaagttgttggtgcttctcctgttgtacactccttaacacacgg
cacgacgagaccatggctgaagagatcgccgccctgggcactgatgagaacaaggagtac
M A E E I A A L G T D E N K E Y
cgcttcagggaacttcatggcaagacgctacgattccaggtaaaggcggcgcatgactgc
R F R E L H G K T L R F Q V K A A H D C
cacgtagccttcacctcaggccccgaggagacggaccccatggtggaagtgttcatcggg
H V A F T S G P E E T D P M V E V F I G
ggctgggagggcgcggcctctgccattaggttcaagaaagccgacgatctggccaaggtt
G W E G A A S A I R F K K A D D L A K V
gacactcctgacatcgtgaccgaggctgagtaccgcgagttctggattgctgttgaccat
D T P D I V T E A E Y R E F W I A V D H
aacgaagtaagagtgggcaaggccggagagtgggagcccctaatgcaggcacccctcccg
N E V R V G K A G E W E P L M Q A P L P
gagcccttcgagatcaccactacggctactccactggctggggcgcgactggctggtgg
E P F E I T H Y G Y S T G W G A T G W W
aagttcttgaacgaccgagttctgaacaccgaggactgcctaacctacaactttgagccc
K F L N D R V L N T E D C L T Y N F E P
gtctatggggatacgatctccttcagcgtttcctgcagtaatgacgctcacttggccctc
V Y G D T I S F S V S C S N D A H L A L
acgtccggccccgaggagaccacacctatgtacgaactctttattggtggctgggagaac
T S G P E E T T P M Y E L F I G G W E N
caacactccgccattcgtcttaataaggaagggaaaggttctggagacgacatggccaag
Q H S A I R L N K E G K G S G D D M A K
gtggagacgcctgacgtggtgtgcagcgaggaggagaggaagttcttcgtgagcttcagg
V E T P D V V C S E E E R K F F V S F R
aatggccagatcaaggtcggctacaaggacaccgaaccccttcatgcagtggactgaccct
N G Q I K V G Y K D T E P F M Q W T D P
gagccctggaagattaccacgtgggatactgcactggctggggcgctaccggcaaatgg
E P W K I T H V G Y C T G W G A T G K W
aagctggacatctaagtgaaagaagtggagggtggtgatgatcgtgtctgtctgccatac
K L D I -
gtgactacctaatcatcacccctatcactgccttcatcaccctgccgctatgtttgtcta
ccaccaccgctactgtgctacgtaatgaagcttccacccttgtctttgttctcagtttat
tgtcatgtttccatcgccagagaagccttgcttgggtgaagcctcgcgccaattcacctg
ttgctgcattaacctttagatgtcctcttcttaattaaaggaagtcaagaggaagagtta
tttttcgtactctttgtagcttcacgtcaataaaaagccaaaaactatattatgcagttg
tctttattgtgagaattgtgtcggattgttgttatcgttactactactactactactact
actactactactactactact

Figure B8. Nucleotide (nt) and amino acid (aa) sequence alignment of the *C. maenas* FAMeTa contig (Y EVm013262t1) isolated from the Y-organ (YO). The contig sequence includes a 133 and 429 base pair (bp) 5' and 3' untranslated region (UTR) with the start codon (atg) indicated in green and stop codon (tga) in red, respectively. The 280 aa open reading frame (ORF) contains two farnesoic acid *O*-methyltransferase domains (Methyltransf_FA) (37 aa – 134 aa and 173 aa – 274 aa) highlighted in aqua with putative phosphorylation sites indicated in boxes.

Figure B9

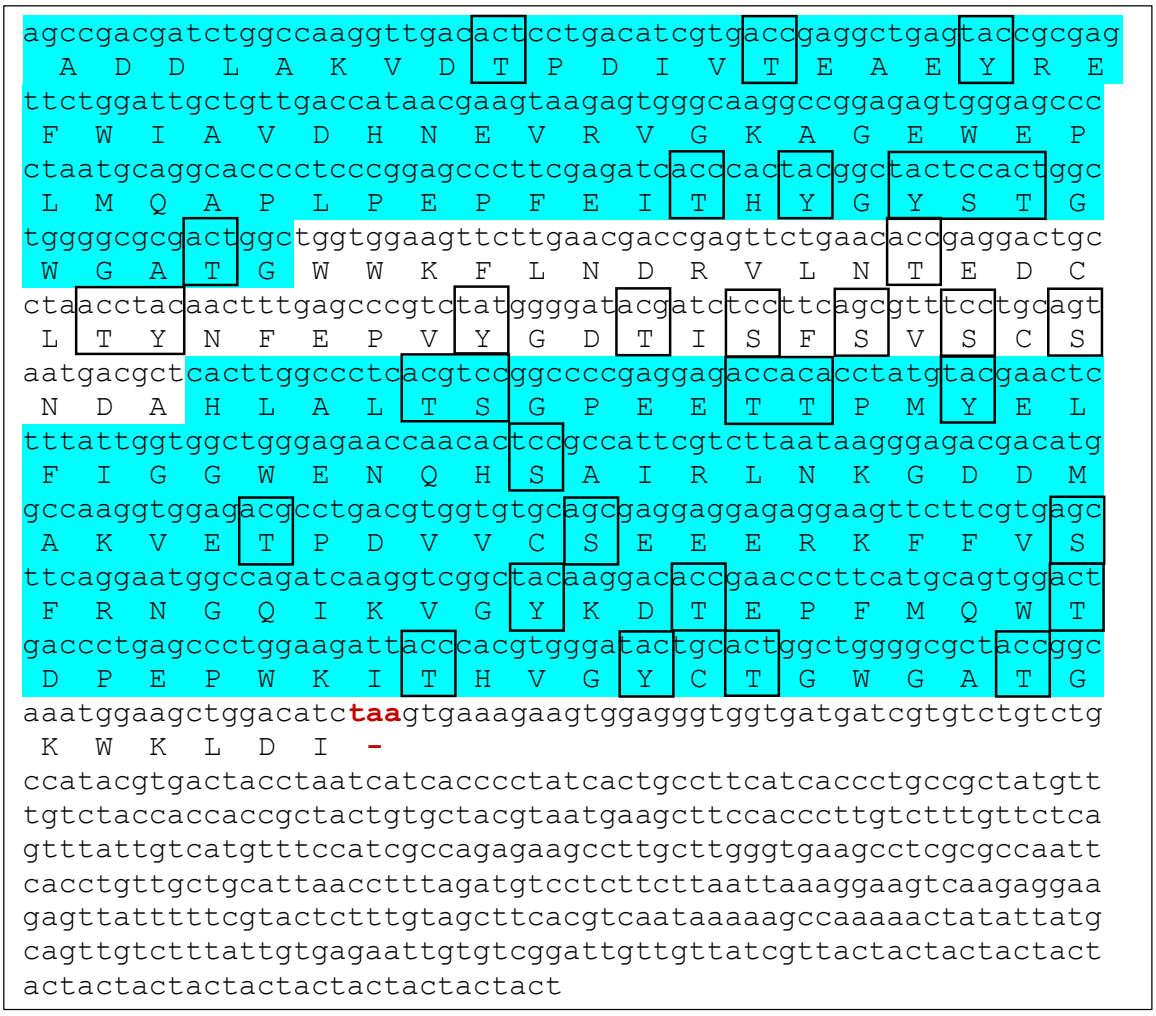
agccgacgatctggccaaggttgacactcctgacatcgtgaccgaggctgagtaccgcgag
A D D L A K V D T P D I V T E A E Y R E
ttctggattgctgttgaccataacgaagtaagagtgggcaaggccggagagtgggagccc
F W I A V D H N E V R V G K A G E W E P
ctaatgcaggcacccctcccggagcccttcgagatcacccactacggctactccactggc
L M Q A P L P E P F E I T H Y G Y S T G
tggggcgcgactggctggtggaagttcttgaacgaccgagttctgaacaccgaggactgc
W G A T G W W K F L N D R V L N T E D C
ctaacctacaactttgagcccgtctatggggatacgatctccttcagcgtttcctgcagt
L T Y N F E P V Y G D T I S F S V S C S
aatgacgctcacttggccctcacgtccggccccgaggagaccacacctatgtacgaactc
N D A H L A L T S G P E E T T P M Y E L
tttattggtggctgggagaaccaacactccgccattcgtcttaataagggagacgacatg
F I G G W E N Q H S A I R L N K G D D M
gccaaggtggagacgcctgacgtggtgtgcagcgaggaggagaggaagttcttcgtgagc
A K V E T P D V V C S E E E R K F F V S
ttcaggaatggccagatcaaggtcggctacaaggacaccgaacccttcatgcagtggact
F R N G Q I K V G Y K D T E P F M Q W T
gaccctgagccctggaagattacccacgtgggatactgcactggctggggcgctaccggc
D P E P W K I T H V G Y C T G W G A T G
aaatggaagctggacatctaagtgaaagaagtggagggtggtgatgatcgtgtctgtctg
K W K L D I -
ccatacgtgactacctaatcatcacccctatcactgccttcatcaccctgccgctatgtt
tgtctaccaccaccgctactgtgctacgtaatgaagcttccacccttgtctttgttctca
gtttattgtcatgtttccatcgccagagaagccttgcttgggtgaagcctcgcgccaatt
cacctgttgctgcattaacctttagatgtcctcttcttaattaaaggaagtcaagaggaa
gagttatttttcgtactctttgtagcttcacgtcaataaaaagccaaaaactatattatg
cagttgtctttattgtgagaattgtgtcggattgttgttatcgttactactactactact
actactactactactactactactact

Figure B9. Nucleotide (nt) and amino acid (aa) sequence alignment of the *C. maenas* FAMeTb contig (Y EVm013262t2) isolated from the Y-organ (YO). The contig sequence includes a 429 bp 3' untranslated region (UTR) with stop codon (tga) in red. The 206 aa partial open reading frame (ORF) contains two farnesoic acid *O*-methyl transferase (Methyltransf_FA) domains highlighted in aqua with putative phosphorylation sites indicated in boxes.

Figure B10

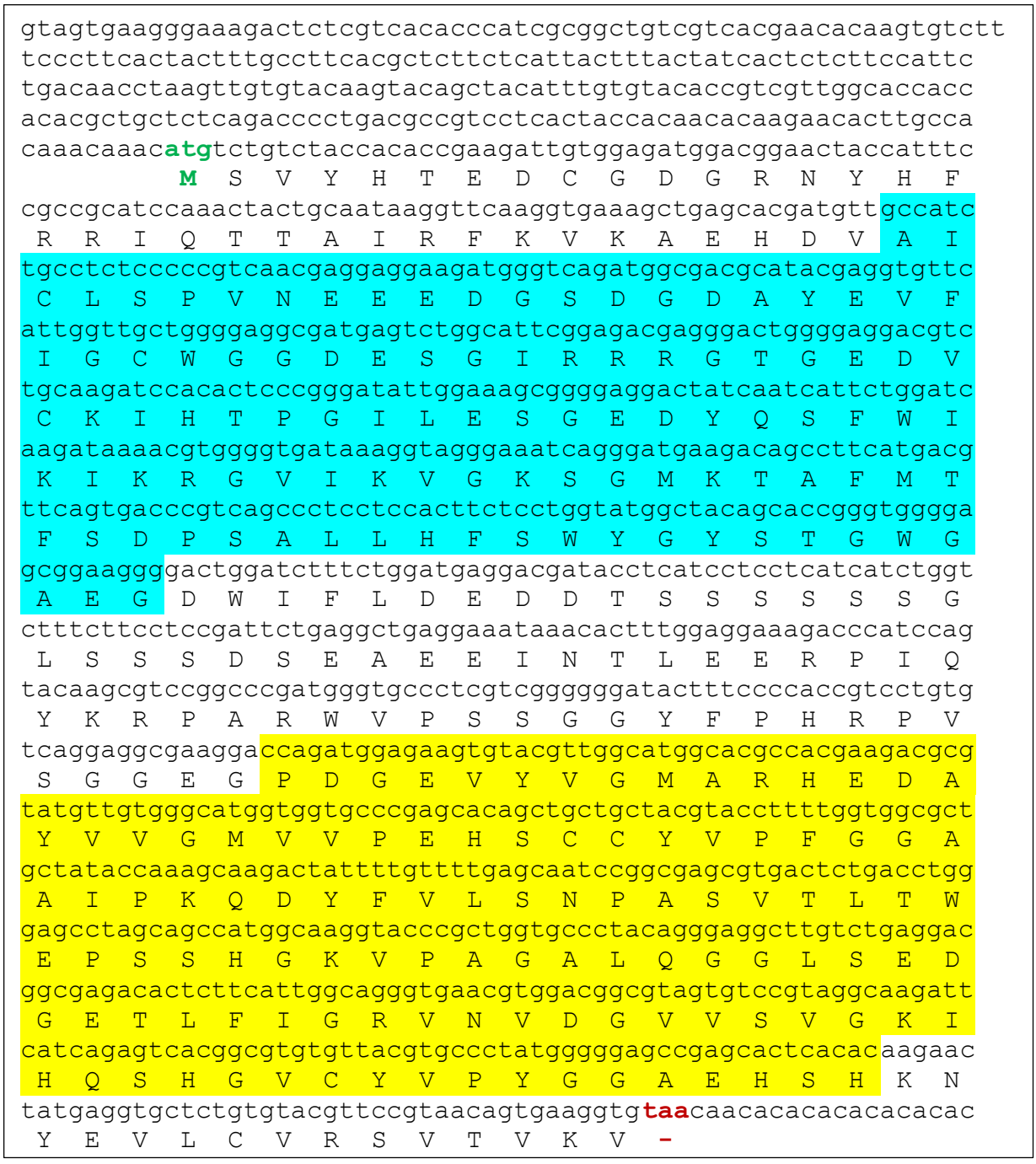
gtagtgaagggaaagactctcgtcacacccatcgcggctgtcgtcacgaacacaagtgtctt
tcccttcactactttgccttcacgctcttctcattactttactatcactctcttccattc
tgacaacctaagttgtgtacaagtacagctacatttgtgtacaccgtcgttggcaccacc
acacgctgctctcagacccctgacgccgtcctcactaccacaacacaagaacacttgcca
caaacaaacatgtctgtctaccacaccgaagattgtggagatggacggaactaccatttc
M S V Y H T E D C G D G R N Y H F
cgccgcatccaaactactgcaataaggttcaaggtgaaagctgagcacgatgttgccatc
R R I Q T T A I R F K V K A E H D V A I
tgcctctcccccgtcaacgaggaggaagatgggtcagatggcgacgcatacgaggtgttc
C L S P V N E E E D G S D G D A Y E V F
attggttgctggggaggcgatgagtctggcattcggagacgagggactggggaggacgtc
I G C W G G D E S G I R R R G T G E D V
tgcaagatccacactcccgggatattggaaagcggggaggactatcaatcattctggatc
C K I H T P G I L E S G E D Y Q S F W I
aagataaaacgtggggtgataaaggtagggaaatcagggatgaagacagccttcatgacg
K I K R G V I K V G K S G M K T A F M T
ttcagtgacccgtcagccctcctccacttctcctggtatggctacagcaccgggtgggga
F S D P S A L L H F S W Y G Y S T G W G
gcggaagggactggatctttctggatgaggacgatacctcatcctcctcatcatctggt
A E G D W I F L D E D D T S S S S S S G
ctttcttcctccgattctgaggctgaggaaataaacactttggaggaaagacccatccag
L S S S D S E A E E I N T L E E R P I Q
tacaagcgtccggcccgatgggtgccctcgtcgggggatactttccccaccgtcctgtg
Y K R P A R W V P S S G G Y F P H R P V
tcaggaggcgaaggaccagatggagaagtgtacgttggcatggcacgccacgaagacgcg
S G G E G P D G E V Y V G M A R H E D A
tatgttgtgggcatggtggtgcccgagcacagctgctgctacgtacctttggtggcgct
Y V V G M V V P E H S C C Y V P F G G A
gctataccaaagcaagactattttgttttgagcaatccggcgagcgtgactctgacctgg
A I P K Q D Y F V L S N P A S V T L T W
gagcctagcagccatggcaaggtacccgctggtgccctacagggaggcttgtctgaggac
E P S S H G K V P A G A L Q G G L S E D
ggcgagacactcttcattggcagggtgaacgtggacggcgtagtgtccgtaggcaagatt
G E T L F I G R V N V D G V V S V G K I
catcagagtcacggcgtgtgttacgtgccctatgggggagccgagcactcacacaagaac
H Q S H G V C Y V P Y G G A E H S H K N
tatgaggtgctctgtgtacgttccgtaacagtgaaggtgtaacaacacacacacacacac
Y E V L C V R S V T V K V -

Figure B10. Nucleotide (nt) and amino acid (aa) sequence alignment of the *C. maenas* FAMeT2 contig (CarmaY_EVm010974t1) isolated from the Y-organ (YO). The contig sequence includes a 251 bp and 18 bp 429 bp 5' and 3' untranslated region (UTR), respectively. The start (atg) and stop codon (tga) are bolded in green and red, respective. Within the 330 aa open reading frame (ORF) is the farnesoic acid *O*-methyl transferase (Methyltransf_FA) domain (highlighted in aqua; 37 aa – 140 aa) followed by the protein of unknown function domain, or DUF3421 (pfam11901) (highlighted in yellow; 203 aa – 315 aa).

LIST OF ABBREVIATIONS

Abbreviation	Meaning
20-E	20-Hydroxyecdysone
aa	Amino acid
Acetyl-CoA	Acetyl coenzyme A
bHLH-PAS	Basic helix-loop-helix/Period (Per) – Aryl hydrocarbon receptor nuclear
bp	Base pairs
Br-C	Broad complex
C2H2	Two cysteine (Cys) residues–two histidine (His) residues
CA	Corpora allata
CaCO3	Calcium carbonate
CC	Corpora cardiaca
CBP	Cyclic adenosine monophosphate (cAMP) response element binding
CHH	Crustacean hyperglycemic hormone
CXE	Carboxylesterase
DUF	Domain of unknown function
E93	Ecdysone inducible factor 93
ECR/RXR	Ecdysone receptor/retinoid X receptor
EP	Early premolt
ESA	Eyestalk ablation
FA	Farnesoic acid
FAMeT	Farnesoic acid *O*-methyltransferase
FPP	Farnesyl pyrophosphate
GIH	Gonad-inhibiting hormone

HAT	Histone acetyltransferase
HMG-CoA	Hydroxymethylglutharyl-CoA
HMGR	3-Hydroxy-3-methylglutarul-coenzyme A reductase
Hsp83/Hsp90	Heat shock protein (83/90)
HTH–Psq	Helix-turn-helix, pipsqueak
IGR	Insect growth regulator
ILP	Insulin-like peptide
IM	Intermolt
JH	Juvenile hormone
JHA	Juvenile hormone acid
JHAMT	Juvenile hormone acid methyltransferase
JHE (-like)	Juvenile hormone esterase (-like)
JHEH	Juvenile hormibe epoxide hydrolase
Kr-h1	Krüppel homolog-1
LP	Late premolt
Mblk-1	Mushroom body large-type Kenyon-cell protein 1
MEKRE93	Methoprene tolerant – Krüppel homolog-1 – E93
Met	Methoprene tolerant
MF	Methyl farnesoate
MFBP	Methyl farnesoate (MF)-binding proteins
MFE	Methyl farnesoate (MF) esterase
MIH	Molt-inhibiting hormone
MO	Mandibular organ
MOIH	Mandibular organ inhibiting hormone
MP	Mid premolt

mTOR	Mechanistic target of rapamycin
MVA	Mevalonate pathway
NADPH	Nicotinamide adenine dinucleotide phosphate
nt	Nucleotide
ORF	Open reading frame
PAC	PAS-associated C-terminus
PG	Prothoracic gland
PTTH	Prothroacicotropic hormone
R-index	Regeneration index
SAM	S-adenosyl-L-methionine
Src	Steroid receptor coactivator
TGF-β	Transforming growth factor β
UTR	Untranslated region
XO	X-organ, sinus gland complex
YO	Y-organ
Znf	Zinc finger